

# **New Approaches to Sustainable Terpene Modification and Application**

Zur Erlangung des akademischen Grades einer

**DOKTORIN DER NATURWISSENSCHAFTEN**

(Dr. rer. nat.)

von der KIT-Fakultät für Chemie und Biowissenschaften  
des Karlsruher Instituts für Technologie (KIT)

genehmigte

**DISSERTATION**

von

**M.Sc. Yasmin Simone Raupp**

Dekan: Prof. Dr. Manfred Wilhelm

1. Referent: Prof. Dr. Michael A. R. Meier

2. Referentin: PD Dr. Silke Behrens

Tag der mündlichen Prüfung: 10.12.2019



*Wir müssen Ausdauer und vor allem Vertrauen in uns selbst haben.  
Wir müssen glauben, dass wir begabt sind  
und dass wir etwas erreichen können.*

**Marie Curie**



Die vorliegende Arbeit wurde von Juni 2016 bis Dezember 2019 unter Anleitung von Prof. Dr. Michael A. R. Meier am Institut für Organische Chemie (IOC) des Karlsruher Instituts für Technologie (KIT) durchgeführt.

Hiermit versichere ich, dass ich die Arbeit selbstständig angefertigt, nur die angegebenen Quellen und Hilfsmittel benutzt und mich keiner unzulässigen Hilfe Dritter bedient habe. Insbesondere habe ich wörtlich oder sinngemäß aus anderen Werken übernommene Inhalte als solche kenntlich gemacht. Die Satzung des Karlsruher Instituts für Technologie (KIT) zur Sicherung wissenschaftlicher Praxis habe ich beachtet. Des Weiteren erkläre ich, dass ich mich derzeit in keinem laufenden Promotionsverfahren befinde, und auch keine vorausgegangenen Promotionsversuche unternommen habe. Die elektronische Version der Arbeit stimmt mit der schriftlichen Version überein und die Primärdaten sind gemäß der Satzung zur Sicherung guter wissenschaftlicher Praxis des KIT beim Institut abgegeben und archiviert.

Karlsruhe, 06.11.2019



# Abstract

The development of catalytic and sustainable chemical modification and polymerisation routes for renewable raw materials has become a major focus in recent years, especially in light of depleting fossil reserves and an ever-increasing emission of greenhouse gases. Among the available renewable raw materials, terpenes, which are extensively used as flavours and fragrances, are abundant and very versatile building blocks for the chemical industry. Monoterpenes, like  $\alpha$ - and  $\beta$ -pinene as well as limonene, represent inexpensive starting materials, since they are obtained as by-products from the pulp and paper industry and from the citric fruit processing industry, respectively. This thesis describes new routes for the transformation of terpenes into fine chemicals, monomers, and polymeric materials by catalytic and environmentally benign processes.

In the first part of this thesis, manganese catalysts were investigated for the liquid-phase aerobic oxidation of  $\alpha$ -pinene to afford pinene oxide. Using Mn(III) acetate as a homogeneous catalyst, the reaction conditions were optimised and pinene oxide was obtained as the main product along with smaller amounts of verbenol and verbenone. The previously optimised reaction conditions were then transferred to the oxidation reaction using a post-synthetically modified mixed-linker metal-organic framework (MOF) as manganese catalyst. The performance of this heterogeneous MOF catalyst was directly compared to its homogeneous counterpart, and while very similar activities were observed, the MOF catalyst had the advantage of being easily removable from the reaction mixture and being recyclable for at least five catalytic cycles without significant loss of activity.

In the second part of this thesis, the sustainable synthesis of a cyclic carbonate based on  $\alpha$ -pinene was investigated using an environmentally benign transesterification of *cis*- $\alpha$ -pinanediol with dimethyl carbonate as carbonyl source. Starting from  $\beta$ -pinene, hydrogen peroxide was used as a “green” oxidising agent to obtain  $\beta$ -pinene oxide which was then catalytically ring-opened to yield  $\beta$ -pinanediol *in situ* and subsequently transesterified to obtain renewable cyclic  $\beta$ -pinene carbonate.

In the last part of this thesis, the synthesis of renewable non-isocyanate poly(urethane)s (NIPUs) based on limonene was developed. The cyclic dicarbonate and diamine monomers used for these NIPUs were obtained through insertion of CO<sub>2</sub> into limonene dioxide and *via* thiol-ene reaction on the limonene double bonds using cysteamine hydrochloride, respectively. Polymerisation of the obtained monomers yielded poly(hydroxy urethane) (PHU) prepolymers with molecular weights up to 1,700 g/mol. As a proof-of-concept, the PHU prepolymers were utilised in a cross-linking reaction with epoxidised soybean oil (ESBO) to synthesise novel epoxy thermosets.

This work aims to emphasise the potential of renewable feedstocks and particularly the versatility of terpenes for the sustainable synthesis of platform chemicals and polymeric materials.



# Kurzzusammenfassung

In den letzten Jahren rückte die Entwicklung von katalytischen und nachhaltigen Prozessen zur Modifikation und Polymerisation von erneuerbaren Rohstoffen zunehmend in den Fokus der Forschung. Besonders in Hinsicht auf die zuneigehenden fossilen Reserven und die immer weiter zunehmenden Emissionen von Treibhausgasen ist weltweit ein Umdenken hin zur nachhaltigeren Produktion von Chemikalien und deren Verarbeitung notwendig, um nachhaltig die Bedürfnisse der stetig wachsenden Weltbevölkerung zu decken. Unter den erneuerbaren Rohstoffen sind Terpene, die häufig als Geruchs- und Geschmacksstoffe verwendet werden, reichlich vorhandene und vielseitige Bausteine für die chemische Industrie. Monoterpene wie z.B.  $\alpha$ - und  $\beta$ -Pinen sowie Limonen stellen preisgünstige Ausgangsstoffe dar, denn sie werden bei der Papierherstellung bzw. bei der Verarbeitung von Zitrusfrüchten als Nebenprodukte erhalten. Die vorliegende Arbeit untersucht die katalytische und umweltfreundliche Umsetzung von Terpenen zu Feinchemikalien, Monomeren und Polymerwerkstoffen.

Im ersten Teil dieser Arbeit wurde die Flüssigphasenoxidation von  $\alpha$ -Pinen durch Luftsauerstoff mit verschiedenen Mangan-Katalysatoren untersucht. Beim Einsatz von Mn(III)-acetat als homogenem Katalysator wurden Pinenoxid als Hauptprodukt und Verbenon und Verbenol als Nebenprodukte erhalten. Die für den homogenen Katalysator optimierten Reaktionsbedingungen wurden dann auf eine Oxidationsreaktion übertragen, bei der eine metallorganische Gerüstverbindung als Katalysator eingesetzt wurde. Für den Einsatz als Katalysator wurde die metallorganische Gerüstverbindung in zwei Schritten nachträglich modifiziert, sodass eine katalytisch aktive Manganspezies immobilisiert werden konnte. Die Umsätze und Selektivitäten, die durch diesen heterogenen Katalysator erreicht wurden, konnten dann mit dem homogenen Katalysator verglichen werden, wobei eine sehr ähnliche Aktivität festgestellt wurde. Darüber hinaus bot der heterogene Katalysator den Vorteil, dass er sehr leicht von der Reaktionsmischung abtrennbar war und in dieser Studie bis zu fünf Mal ohne wesentlichen Verlust der Aktivität wiederverwendet werden konnte.

Im zweiten Teil dieser Arbeit wurde eine nachhaltige Syntheseroute für die Darstellung eines auf  $\alpha$ -Pinen basierenden zyklischen Carbonats mit Hilfe einer umweltfreundlichen Umesterung von *cis*- $\alpha$ -Pinandiol mit Dimethylcarbonat entwickelt. Um auch  $\beta$ -Pinen in cyclisches  $\beta$ -Pinencarbonat zu überführen, wurde das Substrat zuerst zu  $\beta$ -Pinenoxid oxidiert, wobei Wasserstoffperoxid als „grünes“ Oxidationsmittel verwendet wurde. Das nach der Oxidation durch Ringöffnung *in situ* gebildete  $\beta$ -Pinandiol wurde anschließend

mit einem organischen Carbonat umgeestert, wodurch das nachwachsende cyclische  $\beta$ -Pinencarbonat erhalten werden konnte.

Im letzten Teil dieser Arbeit wurde die Synthese biobasierter isocyanatfreier Polyurethane ausgehend von Limonen untersucht. Das für die Herstellung der isocyanatfreien Polyurethane verwendete cyclische Dicarbonat und das Diamin, wurden durch die Reaktion von  $\text{CO}_2$  mit Limonendioxid bzw. durch eine Thiol-En-Reaktion von Limonen mit Cysteaminhydrochlorid erhalten. Die Polymerisation dieser Monomere ergab Polyhydroxyurethan-Oligomere mit Molekulargewichten bis zu 1700 g/mol. Die Polyhydroxyurethan-Oligomere wurden daraufhin für Vernetzungsreaktionen mit epoxidiertem Sojaöl verwendet, um neue Duroplaste zu erhalten.

Ziel der vorliegenden Arbeit ist es das Potential nachwachsender Rohstoffe und insbesondere die vielseitige Nutzbarkeit von Terpenen für die nachhaltige Synthese von Plattformchemikalien und Polymerwerkstoffen aufzuzeigen.

# Table of Contents

Abstract.....	I
Kurzzusammenfassung.....	III
1 Introduction .....	1
2 Theoretical Background and State-of-the-Art .....	3
2.1 Green and Sustainable Chemistry.....	3
2.1.1 The 12 Principles .....	4
2.1.2 Green Chemistry Metrics.....	11
2.2 Renewable Resources and Bio-based Plastics .....	12
2.3 Plastics and Biodegradability .....	17
2.4 Perspectives on Sustainable Catalysis.....	21
2.5 Chemical Structure of Terpenes.....	24
2.6 Terpenes as Renewable Feedstock .....	25
2.7 Catalytic Conversion of Terpenes into Fine Chemicals .....	27
2.7.1 Isomerisation of $\alpha$ -Pinene .....	28
2.7.2 Hydration of $\alpha$ -Pinene .....	29
2.7.3 Dehydroisomerisation of $\alpha$ -Pinene .....	29
2.7.4 Oxidation of $\alpha$ -Pinene.....	30
2.7.5 Isomerisation of $\alpha$ -Pinene Oxide .....	36
2.8 Sustainable Thermoplastic Polymers from Terpenes .....	38
2.8.1 Direct Polymerisation .....	38
2.8.2 Polymers from Functionalised Terpenes .....	44
2.9 Sustainable Thermosets from Terpenes.....	61
3 Aims.....	71
4 Results and Discussion .....	75
4.1 Aerobic Oxidation of $\alpha$ -Pinene Catalysed by Homogeneous and MOF-based Mn Catalysts.....	75
4.2 Follow-up Chemistry for Oxidised Terpenes.....	90
4.2.1 Cyclic and Linear Carbonates from $\alpha$ -Pinene .....	90
4.2.2 Cyclic Carbonate from $\beta$ -Pinene .....	103
4.3 Limonene-based Poly(hydroxy urethane)s .....	109
4.3.1 Monomer Synthesis .....	110
4.3.2 Poly(hydroxy urethane) Prepolymer Synthesis.....	114
4.3.3 Application of PHU Prepolymers as Hardeners for Epoxy Resins .....	123
5 Conclusion and Outlook .....	129
6 Experimental Section .....	133

6.1	Materials .....	133
6.2	Instrumentation .....	134
6.3	Experimental Procedures.....	138
6.3.1	Experimental Procedures for Chapter 4.1 .....	138
6.3.2	Experimental Procedures for Chapter 4.2 .....	144
6.3.3	Experimental Procedures for Chapter 4.3 .....	159
7	Abbreviations .....	169
8	List of Figures .....	173
9	List of Tables .....	181
10	Bibliography .....	183
11	Appendix .....	197
11.1	Publications .....	197
11.2	Conference Contributions .....	197

# 1 Introduction

More than 300 years after the necessity for sustainable development was first documented in the context of forestry,<sup>[1]</sup> and more than 30 years after the World Commission on Environment and Development (WCED) conceptualised a guiding principle for a sustainable development,<sup>[2]</sup> the need for further operationalisation and implementation is greater than ever. In contrast to the original meaning of sustainability, describing the balance between growing and felling trees, the Brundtland Report ('Our Common Future'), published by the WECD in 1987, defines sustainable development as "development that meets the needs of the present without compromising the ability of future generations to meet their own needs."<sup>[2]</sup> Starting with the Industrial Revolution, human actions have become the main driver of global environmental change.<sup>[3]</sup> Nowadays, these activities, mainly the rapidly growing reliance on fossil fuels and industrialised forms of agriculture, have reached a level that could damage Earth's regulatory capacity leading to irreversible global environmental change.<sup>[4]</sup> Consequently, a state less conducive to human development may occur.<sup>[5]</sup> As an urgent call for action and build on decades of work by countries and the UN, in 2015, the United Nations adopted the 2030 Agenda for Sustainable Development, including the 17 sustainable development goals (SDGs).<sup>[6]</sup> To achieve the ambitious goals the cooperation of all stakeholders, *i.e.* decision-makers in politics, industry, and civil society, as well as citizens, consumers and academia is required. In that way, sustainability has become a major reference point for safeguarding the future across societies worldwide and has entered practises and discourses, inter alia, in policy making, urban development and in the chemical industry.<sup>[7]</sup>

Today, modern chemistry and pharmacy contribute considerably to an improved quality of life and longevity. Moreover, chemistry is fundamental for challenges related to sustainable development, such as renewable energy, nutrition and health, environmental technology, clean air and water, efficient materials and alternative feedstocks.<sup>[7]</sup> However, the ever-increasing diversity and quantity of new chemicals and materials has downsides. The pollution of the environment with hazardous chemicals and wastes results in public health issues of global concern. In order to minimise the significant health and environmental harms caused by chemical exposure, the Strategic Approach to International Chemicals Management (SAICM) was developed at the World Summit on Sustainable Development in Johannesburg in 2002 as a global policy framework. It states that "the sound management of chemicals is essential to achieve sustainable development including the eradication of poverty and disease, the improvement of human health and the environment and the elevation and maintenance of the standard of living in countries at all levels of

development".<sup>[8]</sup> As less hazards are key to Green Chemistry, the main SAICM objectives reflect many of the 12 principles of green chemistry making them an important element of sound chemicals management.

The chemical industry and innovations in chemistry, on the one hand, enable medical advancements, adequate food supplies and comfortable living standards for a growing population and contribute to the climate change solution by improving energy efficiency and reducing greenhouse gas emission (GHGs) through advanced building materials, batteries, renewable energy sources, and lightweight plastic packaging. On the other hand, however, the chemical sector is responsible for 13% of the global industrial carbon emissions, due to its high energy demand.<sup>[9]</sup> Although the chemical sector is making progress on climate risk,<sup>[10]</sup> rapid process innovations will be required to align with the below 2-degree goal set out by the Paris Agreement.<sup>[11]</sup>

The environmental concerns, legislations and international agreements, together with depleting fossil oil reserves and economic reasons stimulate the potential for sustainable chemicals and polymeric materials derived from renewable resources. Especially, materials that have been made efficiently from natural waste and that are recyclable or biodegradable will be of increasing importance for future societies.<sup>[12]</sup>

## 2 Theoretical Background and State-of-the-Art

The following section aims to provide an overview of the theoretical background of the main aspects of this thesis. The first chapter (2.1) is an introduction to green and sustainable chemistry, including its origin, principles and several metrics. In chapter 2.2, the use of renewable resources in the chemical industry in general as well as the global bio-based and biodegradable plastics production capacity are discussed. Additionally, promising approaches towards the design of more sustainable polymers based on the different classes of renewable raw materials are highlighted. Chapter 2.3 discusses the present situation and the fate of plastics and shortly explains biodegradability. Since catalysis constitutes an indispensable part of green chemistry and is applied for synthesis procedures performed in this thesis whenever possible, chapter 2.4 presents perspectives on sustainable catalysis and discusses about elemental sustainability. Finally, the following chapters focus on terpenes, as the sustainable exploitation of this class of renewable raw material is an aim of this thesis. Therefore, chapters 2.5 and 2.6 briefly discuss about the chemical structure of terpenes and their main industrial uses. Subsequently, the state-of-the-art of the transformation of terpenes into fine chemicals, monomers and polymers is summarised. Chapter 2.7 pays special attention to the oxidation of  $\alpha$ -pinene, followed by the isomerisation of  $\alpha$ -pinene oxide. Chapters 2.8 and 2.9 provide a literature review on thermoplastic polymers and thermosets derived from the most industrially important terpenes. The examples described within these two chapters encompass direct polymerisation techniques as well as polymers from functionalised terpenes.

### 2.1 Green and Sustainable Chemistry

For a very long time chemists and chemical engineers had the freedom to synthesise, develop and design chemicals, reactions and processes without any or only few limitations, facilitating longevity and a higher quality of life.<sup>[13]</sup> Unfortunately, along with numerous success stories, an unmanageable number of unfavourable side effects surfaced, which chemists did not anticipate. A prominent example is dichlorodiphenyltrichloroethane (DDT), which was first synthesised in the second half of the 19<sup>th</sup> century. After discovering its insecticidal action, for which Paul Hermann Müller was awarded with the Nobel Prize in Physiology or Medicine in 1948, DDT was used as agricultural and household pesticide from the 1940s on. However, it was not perceived that bioaccumulation of chlorinated insecticides takes place in birds leading to nestling

failure and eggshell thinning and eventually in a dramatic decrease of bird populations. In 1962, the publication 'Silent Spring' by biologist Rachel Carson first drew attention to these adverse impacts, resulting in a public outrage and a growing environmental movement.<sup>[14]</sup> Finally, a worldwide ban of DDT was laid down in the Stockholm Convention on Persistent Organic Pollutants in 2004.<sup>[15]</sup> The convention has the aim to limit and eradicate the production and use of persistent organic pollutants (POPs). Other environmental and health problems caused by chemicals are being tackled since several years but have not been fixed, yet, and transformed to global issues. Such examples are dioxin contamination, ocean acidification, plastic pollution and climate change. Dioxin emissions of incineration plants are strictly regulated since 1990 in Germany. However, large parts of the population still have a higher intake of dioxins than recommended by the World Health Organisation (WHO) due to contaminated food, especially through meat, fish and dairy products.<sup>[16]</sup> Ocean acidification, plastic pollution and climate change are currently being addressed by the SDGs set by the UN in 2015 (SDG 3: Good health and well-being, SDG 12: Responsible consumption and production, SDG 13: Climate action, SDG 14: Life below water).<sup>[6]</sup>

In the early 1990s, the field of green chemistry emerged from the development of environmentally friendly processes and research efforts as an answer to the escalating environmental issues and increasing awareness of chemical pollution and the finite nature of resources.<sup>[17]</sup> One of the important new aspects introduced by the green chemistry movement was the focus on the prevention of pollution instead of cleaning up wastes that could have possibly been prevented.

### 2.1.1 The 12 Principles

In 1998, John Warner and Paul T. Anastas, at that time directing the Green Chemistry Program at the United States Environmental Protection Agency (US EPA), postulated a set of 12 principles as a guideline for the practice of green chemistry.<sup>[18]</sup> The authors also gave a widely accepted definition, stating that green chemistry is a framework "*based on a set of 12 principles that when used in the design, development and implementation of chemical products and processes, enables scientists to protect and benefit the economy, people and the planet*".<sup>[18]</sup> The US EPA adds that green chemistry "*applies across the life cycle of a chemical product, including its design, manufacture, use, and ultimate disposal*".<sup>[19]</sup> Therefore, the main objective of green chemistry is to reduce or eliminate the use and the generation of hazardous substances.<sup>[20]</sup> Anastas pointed out that the guiding principle to achieve this goal is the design of environmentally benign products and



processes (benign by design).<sup>[21]</sup> Moreover, the guidelines apply to raw materials and to the efficiency and safety of the transformation. The 12 principles of green chemistry are shown in Table 1:

Table 1: The 12 principles of green chemistry proposed by Anastas and Warner.<sup>[22]</sup>

Number	Principle	Description of Principle
1	Prevention	It is better to prevent waste than to treat or clean up waste after it is formed.
2	Atom Economy	Synthetic methods should be designed to maximise the incorporation of all materials used in the process into the final product.
3	Less Hazardous Chemical Synthesis	Wherever practicable, synthetic methods should be designed to use and generate substances that possess little or no toxicity to human health and the environment.
4	Designing Safer Chemicals	Chemical products should be designed to meet their desired function while minimising their toxicity.
5	Safer Solvents and Auxiliaries	The use of auxiliary substances (e.g. solvents, separation agents, etc.) should be made unnecessary wherever possible and when used, innocuous.
6	Design for Energy Efficiency	Energy requirements of chemical processes should be evaluated with regard to their environmental and economic impacts and should be minimised. If possible, synthetic methods should be conducted at ambient temperature and pressure.
7	Use of Renewable Feedstocks	A raw material or feedstock should be renewable rather than depleting whenever technically and economically practicable.
8	Reduce Derivatives	Unnecessary derivatisation (use of blocking groups, protection/deprotection, temporary modification of physical/chemical processes) should be minimised or avoided if possible, because such steps require additional reagents and generate waste.
9	Catalysis	Catalytic reagents (as selective as possible) are superior to stoichiometric reagents.
10	Design for Degradation	Chemical products should be designed so that at the end of their function they break down into innocuous degradation products and do not persist in the environment.
11	Real-Time Analysis for Pollution Prevention	Analytical methods need to be further developed to allow for real-time, in-process monitoring and control prior to the formation of hazardous substances.
12	Inherently Safer Chemistry for Accident Prevention	Substances and the form of a substance used in a chemical process should be chosen to minimise the potential for chemical accidents, including releases, explosions, and fires.

Ever since the 12 principles were first published, they have played a significant role for explaining and promoting the aims of green chemistry. Tang, Smith and Poliakoff produced

an even simpler statement on the principles in order to provide a very straightforward way to communicate them to a broad audience. They condensed the principles to a mnemonic with which they tried to capture the spirit of each principle in just three or four words, as shown in Table 2.<sup>[23]</sup>

Table 2: The 12 principles of green chemistry written in the form of a mnemonic: PRODUCTIVELY.<sup>[23]</sup>

---

P	Prevent wastes
R	Renewable materials
O	Omit derivatisation steps
D	Degradable chemical products
U	Use of safe synthetic methods
C	Catalytic reagents
T	Temperature, pressure ambient
I	In-process monitoring
V	Very few auxiliary substances
E	E-factor, maximise feed in product
L	low toxicity of chemical products
Y	Yes, it is safe

---

Indicating their timeless nature, the 12 principles have not change in the last 20 years. However, they inspired others to develop their own principles. For example, in 2013, Gałuszka, Migaszewski and Namieśnik adapted the 12 principles for a guiding framework for green analytical chemistry (GAC, see Table 3).<sup>[24]</sup> Therefore, they used four of the original principles that can be directly transferred to analytical chemistry (principles 1, 5, 6, and 8) and supplemented them with eight new principles that fully meet the needs of analytical chemistry. Generally, the goals of GAC principles are the reduction of chemical substances and energy consumption together with proper management of the analytical waste and increased safety for the operator. As already described by Anastas in 1999, the focus area of GAC is the design of new analytical procedures that generate or uses less hazardous substances.<sup>[25]</sup>

Table 3: The 12 principles of green analytical chemistry proposed by Gałuszka, Migaszewski and Namieśnik.<sup>[24]</sup>

Number	Description of Principle
1	Direct analytical techniques should be applied to avoid sample treatment.
2	Minimal sample size and minimal number of samples are goals.
3	<i>In situ</i> measurements should be performed.
4	Integration of analytical processes and operations saves energy and reduces the use of reagents.
5	Automated and miniaturised methods should be selected.
6	Derivatisation should be avoided.
7	Generation of a large volume of analytical waste should be avoided and proper management of analytical waste should be provided.
8	Multi-analyte or multi-parameter methods are preferred versus methods using one analyte at time.
9	The use of energy should be minimised.
10	Reagents obtained from renewable source should be preferred.
11	Toxic reagents should be eliminated or replaced.
12	The safety of the operator should be increased.

Anastas and Zimmerman additionally devised 12 principles for green engineering in 2003 (see Table 4).<sup>[26]</sup> These principles focus on the achievement of sustainability through science and technology and aim to have a broader applicability compared to the 12 principles of green chemistry. The authors state that “*sustainability requires objectives at the molecular, product, and system levels*”. Therefore, the principles must be likewise applicable to the design of molecular architectures needed to construct a chemical compound, to product architecture to create a car, or to urban architecture to build a city. Beyond that, the authors want the 12 principles of green engineering to be seen as a framework for necessary conversations that should take place between the designers of

molecules, components, products as well as complex systems providing them a universal method of approach.

*Table 4: The 12 principles of green engineering proposed by Anastas and Zimmerman.<sup>[26]</sup>*

---

<b>Number</b>	<b>Description of Principle</b>
1	Designers need to strive to ensure that all material and energy inputs and outputs are as inherently non-hazardous as possible.
2	It is better to prevent waste than to treat or clean up waste after it is formed.
3	Separation and purification operations should be designed to minimise energy consumption and materials use.
4	Products, processes, and systems should be designed to maximise mass, energy, space, and time efficiency.
5	Products, processes, and systems should be “output pulled” rather than “input pushed” through the use of energy and materials.
6	Embedded entropy and complexity must be viewed as an investment when making design choices on recycle, reuse, or beneficial disposition.
7	Targeted durability, not immortality, should be a design goal.
8	Design for unnecessary capacity or capability (e.g. “one size fits all”) solutions should be considered a design flaw.
9	Material diversity in multicomponent products should be minimised to promote disassembly and value retention.
10	Design of products, processes, and systems must include integration and interconnectivity with available energy and materials flows.
11	Products, processes, and systems should be designed for performance in a commercial “afterlife”.
12	Material and energy inputs should be renewable rather than depleting.

---

The systematic implementation of green chemistry principles across all scales leads to clear benefits for human health, the society, the environment and the economy, and lastly for the ultimate goal of sustainability.<sup>[26]</sup> Human health and the society profit from cleaner air and water, as well as from safer consumer products (including food) and increased safety for employees in the chemical industry. The environment in turn benefits from less pollution with toxic chemicals leading to less harm for plants and animals and less disruption of ecosystems, since green chemicals can either be recovered for further use or degrade to non-hazardous products. This also results in a lower danger for global warming, ozone layer depletion and smog formation. Economy and businesses benefit from these principles, on one hand, by saving costs through reduced energy and water consumption and reduced waste, which in return leads to the elimination of costly hazardous waste disposal, end-of-the-pipe treatments and remediation. On the other hand, plant capacity is increased by using fewer synthetic steps, potentially allowing for faster manufacturing of products and consuming smaller amounts of feedstocks, which eventually leads to higher earnings.

Although green chemistry is well defined as a formal sub-discipline of chemistry with the ultimate goal of pollution prevention, some important questions about 'green chemicals', as raised by Klaus Kümmeler, still remain: *"Can you already classify a product as green if just one of the 12 principles is fulfilled, for example, by using renewable feedstocks? Or must all 12 principles be fulfilled? How should they be weighted against each other? And what if a chemical or material meets all the 12 principles but is simply not needed?"*<sup>[27]</sup> It should be noted, that there are no "green chemicals" in general, but some chemicals are "greener" compared to other chemicals. Thus, chemicals, products and processes always need to be compared to relevant benchmarks. In general, green chemistry only rarely addresses aspects that go beyond the chemicals themselves and their technical issues. Sustainable chemistry, however, generally includes all aspects of a product related to sustainability. This includes the social and economic aspects connected to the use of resources, as well as the shareholders, the stakeholders, and the consumers (see Figure 1).<sup>[7]</sup>

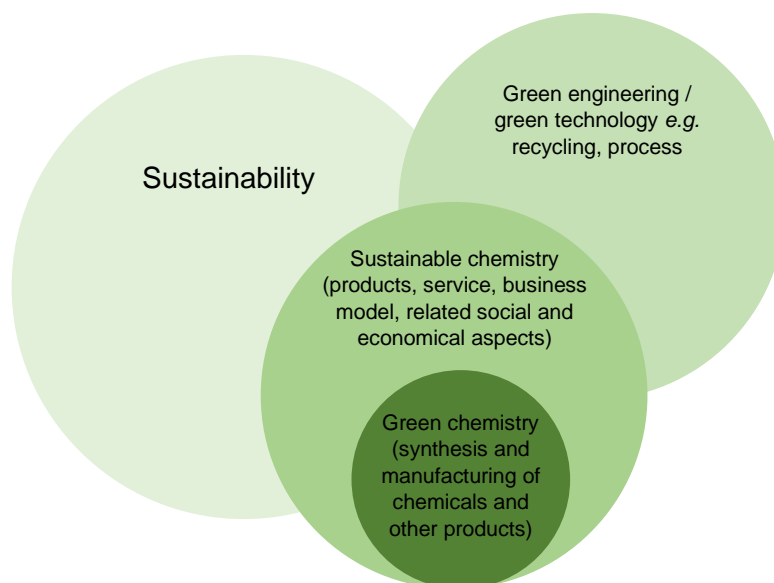


Figure 1: The relationship of sustainability, sustainable chemistry, green engineering, green technology and green chemistry.<sup>[7]</sup>

In contrast to green chemistry, sustainable chemistry has only been vaguely defined to date. Currently, it is most frequently associated with efforts to achieve resource efficiency,<sup>[28]</sup> which implies that sustainable chemistry should use resources, including energy, at a rate at which they can be regenerated naturally, and waste production should not be faster than the rate of its remediation.<sup>[13]</sup> This approach of describing sustainable chemistry is in line with the original definition of sustainability from the 18<sup>th</sup> century, when the term was first used to describe the balance between growing and felling trees. However, the German Federal Environment Agency (UBA) described sustainable chemistry as a broader concept: *“Sustainable chemistry is a process that leads to a sustainable society with regard to product design, manufacturing, consumption of resources, health and safety at work, economic success and technical innovation – not only in industrialised nations but in emerging and developing countries, too. Sustainable chemistry thus extends far beyond the application of ecological principles in chemical production.”*<sup>[29]</sup> Moreover Anastas states that the concepts, principles and methodologies of green chemistry and green engineering are fundamental to integrate sustainability throughout chemical enterprises.<sup>[30]</sup> Through the incorporation of green chemistry approaches at all stages, such as research, development, scale-up and commercialisation in industry, great steps towards sustainability can be made.

For the future, both areas, green chemistry and sustainable chemistry, offer valuable guidance that presumably will be further explored in an integrative way and harnessed to devise new approaches such as innovative business models (e.g. chemical leasing). This

ensures the comprehensive and coherent development of research, policies and practical approaches.<sup>[31]</sup>

### 2.1.2 Green Chemistry Metrics

To quantify yields or selectivity improvements, simple percentages are suitable. However, for quantifying benefits from a new technology that is introduced to change a chemical process towards improved sustainability, metrics of the potential environmental acceptability are needed. Over time, numerous metrics have been introduced and two of the most popular ones are the E factor and the atom efficiency/economy concept. The E factor was first introduced by Sheldon in 1992 and is “*the actual amount of waste produced in the process, defined as everything but the desired product*”.<sup>[32]</sup> It is obtained by calculating the mass ratio of waste to desired product and takes the chemical yield, reagents, solvent losses, all process aids and, in principle, even fuel into account.<sup>[33]</sup> To make meaningful comparisons of E factors, water is excluded from the calculation and only the inorganic salts and organic compounds contained in the water are taken into account. This is necessary, since the inclusion of water would lead to exceptionally high E factors in many cases, which is not useful for comparing processes. However, the energy that is needed for subsequent wastewater treatment should also be taken into account. As shown in Table 5, the E factors in various segments of the chemical industry are increasing drastically from oil refining and bulk chemicals to fine chemicals and pharmaceuticals. Since the ideal E factor is zero, a higher E factor indicates a higher negative environmental impact through more waste. Pharmaceuticals typically have the highest E factors as complex products often require multistep synthesis procedures and extensive purification methods.

Table 5: E factors in the chemical industry.<sup>[33]</sup>

Industry segment	Product tonnage <sup>a)</sup>	kg waste <sup>b)/kg product</sup>
Oil refining	10 <sup>6</sup> -10 <sup>8</sup>	<0.1
Bulk chemicals	10 <sup>4</sup> -10 <sup>6</sup>	<1-5
Fine chemicals	10 <sup>2</sup> -10 <sup>4</sup>	5-50
Pharmaceuticals	10-10 <sup>3</sup>	25-100

a) Typically represents annual production volume of a product at one site (lower end of range) or world-wide (upper end of range).

b) Defined as everything produced except the desired product (including all inorganic salts, solvent losses, etc.).

The atom efficiency/economy concept is, in contrast to the E factor, a theoretical number and assumes a yield of 100%, exact stoichiometry and ignores substances that are not part of the stoichiometric equation. It was first introduced by Trost and is calculated as the molecular weight of the desired product divided by the molecular weight of all substances formed in the stoichiometric equation.<sup>[34]</sup> The advantage of the atom efficiency/economy calculation is that it can be carried out without experimental results and therefore, at the very early stage of a synthesis design, one can easily find and discard low atom efficiency/economy reactions.

Another metric for the environmental acceptability of a process is the effective mass yield (EMY), introduced by Hudlicky and co-workers.<sup>[35]</sup> It is defined as the percentage of the mass of the desired product relative to the mass of all non-benign materials used in its synthesis.<sup>[7]</sup> This metric includes an attempt to recognise that not all chemicals have the same environmental impact and therefore, requires the definition of environmentally benign compounds, like for example NaCl, water, ethanol, methanol, and acetic acid, as suggested by the authors. However, it does not take into account that the environmental impact of the mentioned chemicals is quite volume-dependent, which makes it very difficult to quantify. It also does not consider that the benign compounds might be contaminated with non-benign substances after the reaction.

As a general rule, the more precise and universally applicable a metric is, the more complicated it becomes, since a lot of input data is needed. This makes life-cycle assessment (LCA) one of the most powerful but also very demanding approaches to access the overall sustainability of a product or process. LCA evaluates the environmental impacts of a product associated with all the stages of its life, from cradle-to-grave. Herein included are the extraction of raw material, materials processing, manufacturing, distribution, packaging, use, maintenance, repair and reuse, and the final disposal of a product. Besides the inputs involved in delivering the product, LCA also includes the outputs, emissions and wastes produced at all stages. The most commonly used application for LCA is the comparison of the 'total' environmental impact of a product with a comparable alternative product.<sup>[36]</sup>

## 2.2 Renewable Resources and Bio-based Plastics

Still by far the most important source of organic raw materials used by the chemical industry, not only in Germany, are fossil resources. In 2017, merely 13% of a total of 20.8 million tons of organic raw materials originated from renewable resources in



Germany, the remaining 87% were based on crude oil, natural gas and coal (see Figure 2).<sup>[37]</sup> Well-established production concepts for products based on fossil resources and affordable crude oil prices make the shift towards renewable resources seemingly unalluring. Nowadays, it is still an ongoing discussion as to how long these fossil resources will be available, however there is no doubt that fossil resources are finite.<sup>[38]</sup>

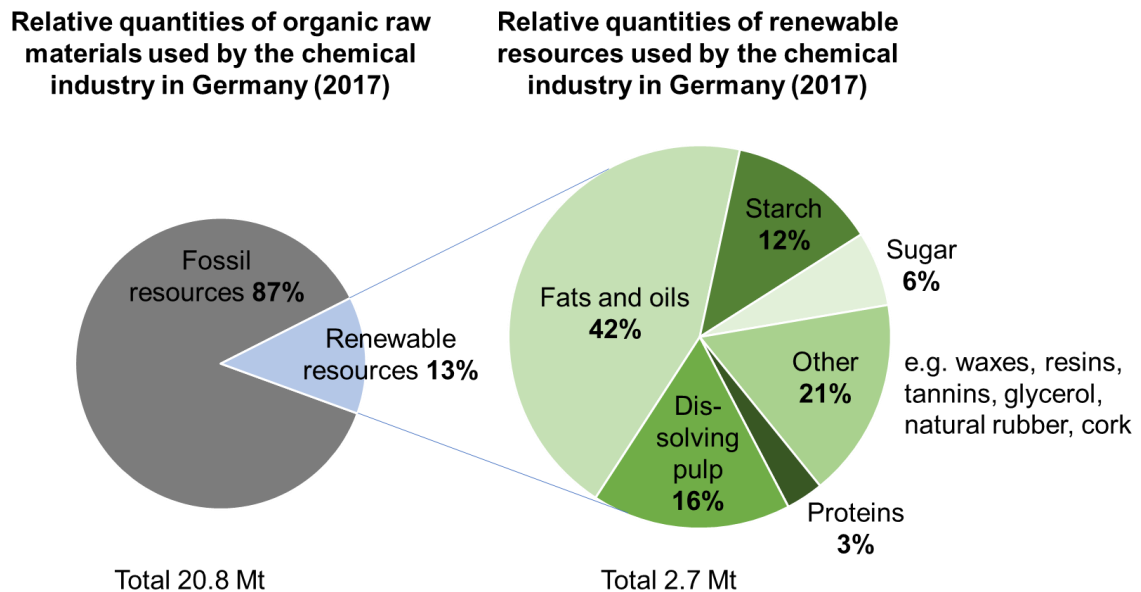


Figure 2: Relative quantities of organic raw materials used by the chemical industry in Germany in 2017.<sup>[37]</sup>

Renewable resources are generally considered as agricultural and forestry derived biomass that is not used for food or feed, but for material use, heat, electricity and fuel production. This also includes residues of the food processing industry (e.g. cashew nutshell liquid and orange peel oil) or waste products from bio-refining (e.g. rapeseed press cake and beet pulp). Renewables can be replenished through natural reproduction in a finite amount of time in a human time scale. In contrast, fossil fuels, earth minerals and metal ores are considered non-renewable, as they cannot be replaced through natural recurring processes within time frames meaningful to humans.

In Germany, fats and oils of plant and animal origin are the most used renewable raw materials (42%, see Figure 2). Dissolving pulp, which is obtained from pulpwood *via* the sulfite process or the kraft process with an acid prehydrolysis step to remove hemicellulose, yields a high cellulose content of >90% and is the second most industrially used renewable resource in Germany (16%). It is followed by carbohydrates, like starch (12%) and sugar (6%), and proteins (3%). The other renewables like waxes, resins (mainly composed of terpenes), tannins, glycerol (by-product of biodiesel production), natural

rubber (a polyterpene) and cork account for less than 3%, each. The presented numbers of organic raw materials used by the chemical industry in Germany include domestic as well as imported agricultural and forestry derived biomass. It is estimated that approximately 70% are imported from other European countries and from overseas.<sup>[37]</sup> However, compared to crude oil, which is 100% imported,<sup>[39]</sup> the further expansion of domestic renewable resources contributes to the independency of the German economy from oil-producing countries.

By performing photosynthesis, plants are able to transform water and a low-energy compound like carbon dioxide into a vast variety of high-energy organic compounds using solar energy. Natural syntheses can be readily exploited for the conversion of plant-based biomass into bulk or fine chemicals. After subsequent processing steps, a wide range of value-added products is accessible. Thermal treatment at the end of the lifetime of the product again releases, at least in principle the previously absorbed carbon dioxide, closing the idealised material cycle without adding additional greenhouse gas to the atmosphere. Therefore, the closed loop results in a reduced carbon footprint, provided that the natural reproduction occurs at a quick enough pace to keep up with consumption.<sup>[40]</sup>

The biorefinery concept is a key tool in utilising biomass in an efficient and clean way.<sup>[7]</sup> Biorefineries are ideally integrated biomass-conversion processes used to generate biofuels, bioenergy (heat and power), and bio-based chemicals and materials.<sup>[41]</sup> The concept is analogous to present-day petroleum refineries. To provide a benefit by reducing the impacts on the environment, it is necessary that biorefineries utilise low-value, locally sourced feedstocks, e.g. trees, grasses, energy crop and food crop by-products, marine resource waste, seaweed and food waste.

Renewable resources are increasingly investigated for the production of a variety of more environmentally benign materials and products such as plastics, hydrogels, flexible electronics, resins, engineering polymers and composites. However, to date, there are only few commercially successful bio-based (or partly bio-based) polymers. From the 348 Mt (including thermoplastics, poly(urethane)s, thermosets, elastomers, adhesives, coatings and sealants and PP-fibres. Not included are poly(ethylene terephthalate)-, poly(amide)- and poly(acryl)-fibers) of the global plastic production, in 2017,<sup>[42]</sup> only 2.06 Mt were bio-based or biodegradable. Nonetheless the global market is predicted to grow continuously. As of 2018, the total production capacity increased to 2.11 Mt, from which the main products were poly(ethylene terephthalate) (PET; 25.6%, 30 wt% bio-based), starch blends (18.2%, various amounts of bio-based raw material), poly(amide)s (PA; 11.6%, up to 100% bio-based), poly(lactic acid) (PLA; 10.3%, 100% bio-based),

poly(ethylene) (PE; 9.5%, 100% bio-based), poly(trimethylene terephthalate) (PTT; 9.2%, up to ~50% bio-based), poly(butylene adipate terephthalate) (PBAT; 7.2% up to ~50% bio-based), poly(butylene succinate) (PBS; 4.6%, up to 100% bio-based) and polyhydroxyalkanoates (PHA; 1.4%, 100% bio-based) (see Figure 3). A possible explanation for the low percentage of bio-based or biodegradable polymers compared to the fossil-based plastic world market are the tough criteria, which need to be met for commercially feasible sustainable polymer production.<sup>[12]</sup> Two of these challenges are that the transformation of renewable resources and the production of polymers must be highly efficient to be economically favourable, and that the new polymers must show similar or improved material properties, including thermal resistance, mechanical strength and processability, compared to the fossil-based materials. Additionally, LCA should be used to prove the benefits of the new polymers over the existing petrochemical benchmarks.

### Global bio-based/biodegradable plastics production capacity (2018)

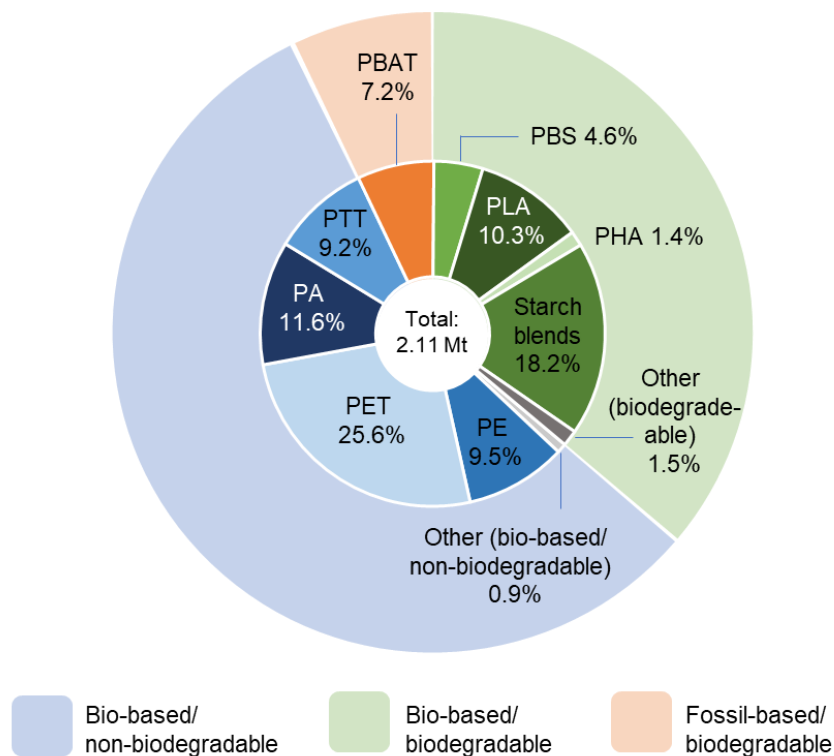


Figure 3: Global bio-based/biodegradable plastics production capacity by material in 2018.<sup>[42]</sup>

In general, there are two strategies to design polymers that are more sustainable than the currently available polymers.<sup>[12]</sup> One approach is to decrease the environmental impact of a known polymer, e.g. PET or PE, by using renewable resources to synthesise the monomers (a so-called drop in solution). The other approach aims for the preparation of new structures, like PLA, from biomass. Various opportunities that follow the described approaches for creating sustainable polymers from renewable raw materials, such as carbon dioxide, terpenes, vegetable oils and carbohydrates are shown in Figure 4. A promising approach, for example, is the copolymerisation of carbon dioxide with propylene oxide to produce propylene carbonate polyols that can be further applied for the manufacture of polyurethanes.<sup>[43]</sup> An important advantage of upcycling carbon dioxide is the possibility to use the existing infrastructure for fossil-derived polymer manufacturing, such as reactors and procedures for purification and processing.<sup>[12]</sup> Another approach is the oxidation of terpenes, such as limonene to limonene oxide and the further copolymerisation with carbon dioxide to yield poly(limonene carbonate).<sup>[44]</sup> For further details on the utilisation of terpenes as renewable feedstock for fine chemicals, thermoplastic polymers and thermosets, see chapters 2.7, 2.8 and 2.9 Triglycerides obtained from vegetable oils constitute another very promising class of renewable raw materials for the synthesis of polymers.<sup>[45]</sup> A common way of polymerising unsaturated fatty esters that are usually produced through transesterification of the triglyceride with methanol or ethanol, is by making use of the internal alkene functional groups. Methods for transforming the alkene groups to polymers are for example thiol-ene, acyclic diene metathesis, epoxidation and radical or thermal crosslinking reactions.<sup>[46]</sup> Carbohydrates, such as starch, cellulose, glucose and fructose are readily obtained from plants such as sugar cane and corn or agricultural waste and can be further transformed into monomers. Interesting monomers are lactide, succinic acid and 2,5-furandicarboxylic acid (FDCA) that can be subsequently polymerised to the corresponding polymers, namely PLA, PBS, and polyethylene furanoate (PEF), respectively. Cellulose that has been used to synthesise commercial polymers such as cellophane or cellulose acetate for more than a century, can be also used to reinforce fibre-polymer composites.<sup>[47]</sup>

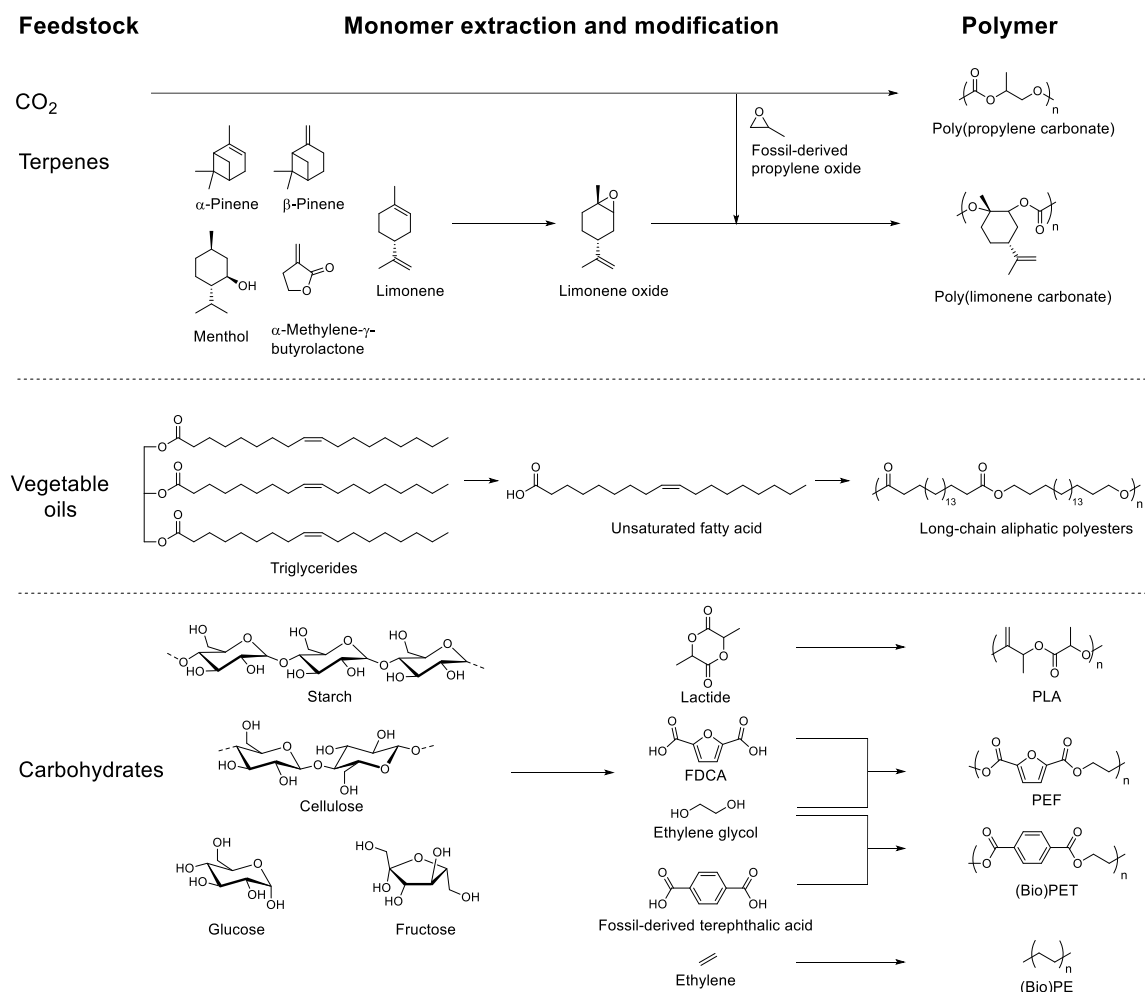


Figure 4: Options for replacing petrochemicals as raw material for polymer synthesis. Adopted from reference [12].

In conclusion, renewable raw materials have many advantages over fossil resources, including the almost unlimited availability, remarkable structural diversity and carbon footprint neutrality as well as economic benefits.<sup>[48]</sup> Thus, their contribution to a sustainable development of society will ultimately make them an inevitable part of our future.<sup>[49]</sup>

## 2.3 Plastics and Biodegradability

According to a study by Geyer, Jambeck, and Law,<sup>[50]</sup> the world plastic production increased from 2 million metric tons (Mt) in 1950 to 380 Mt in 2015, which corresponds to a compound annual growth rate of 8.4%. As a result, the total amount of plastics synthesised from 1950 to 2015 is 8300 Mt. The globally most produced non-fibre plastic is PE (including high-density PE, low-density and linear low-density PE; 36%), followed by poly(propylene) (PP; 21%), poly(vinyl chloride) (PVC; 12%), PET (<10%), poly(urethane)s

(PUR; <10%) and poly(styrene) (PS; <10%). Together with poly(ester)s, poly(amide)s, and acrylic fibres, these polymer groups account for 92% of all plastics ever made. The major share of 42% of the produced non-fibre plastics are used for packaging from which most is used for less than one year. The next largest consuming sector, using 19% of all non-fibre plastics, is the building and construction sector.

It is presumed that 30% of all plastics ever produced are currently in use (2,500 Mt), whereas, as of 2015, a total of approximately 6,300 Mt of plastic waste has been generated. Only around 9% of the plastic waste has been recycled, 12% was incinerated (with or without energy recovery) and 79% is accumulated in landfills or the natural environment (see Figure 5).

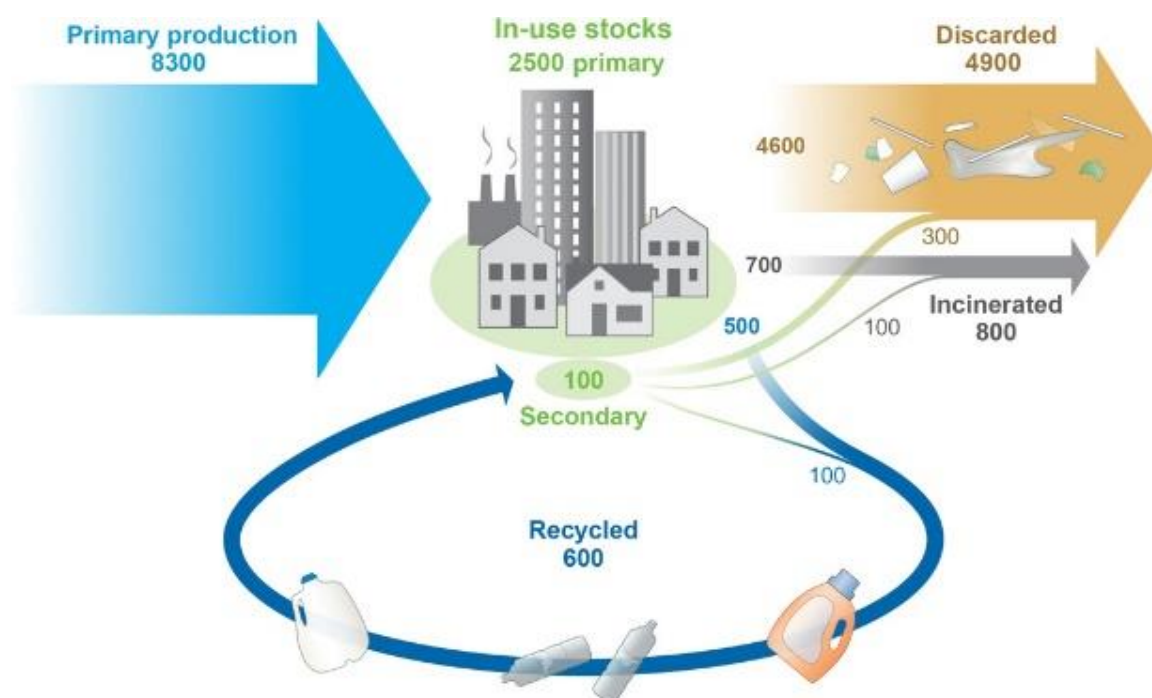


Figure 5: Global production, use, and fate of polymer resins, synthetic fibres, and additives (1950 to 2015; in Mt). This figure is reprinted from R. Geyer, J. R. Jambeck, K. L. Law, *Sci. Adv.* 2017; 3: e1700782, which is licensed under the terms of the Creative Commons Attribution Licence.<sup>[50]</sup>

Due to a functioning waste disposal system, the German numbers for plastic waste treatment are quite different compared to the worldwide average. In 2016, 5.1 Mt of plastic post-consumer waste were collected through official schemes from which 38.6% were recycled, 60.6% were incinerated for energy recovery and only 0.8% were landfilled.<sup>[42]</sup>

It is estimated that roughly 12,000 Mt of plastic waste will be discarded in landfills or the natural environment by 2050, if current production and waste management trends continue (see Figure 6).<sup>[50]</sup> Since none of the mass-produced plastics biodegrade in any meaningful

way, the increase of plastic waste in the environment further aggravates all issues related to plastic accumulation in the oceans as well as the impacts of plastic waste on land-based ecosystems of which still little is known.<sup>[51]</sup> In particular, the fragmentation into small particles (< 5 mm) *via* natural weathering processes bears numerous threats since the small size increases the probability of being ingested and accumulated in tissues of living organisms.<sup>[52]</sup> Upon ingestion, plastic additives and related chemicals (e.g. nonylphenols considered as endocrine disruptor) may leach out, leading to human health hazards.<sup>[53]</sup> Another threat is that microplastic may act as pollutant accumulator for hydrophobic POPs, such as polychlorinated biphenyls (PCBs) and dichlorodiphenyldichloroethylene (DDE), that are commonly present in the environment and ambient seawater, bringing them from the environment to organisms.<sup>[54]</sup>

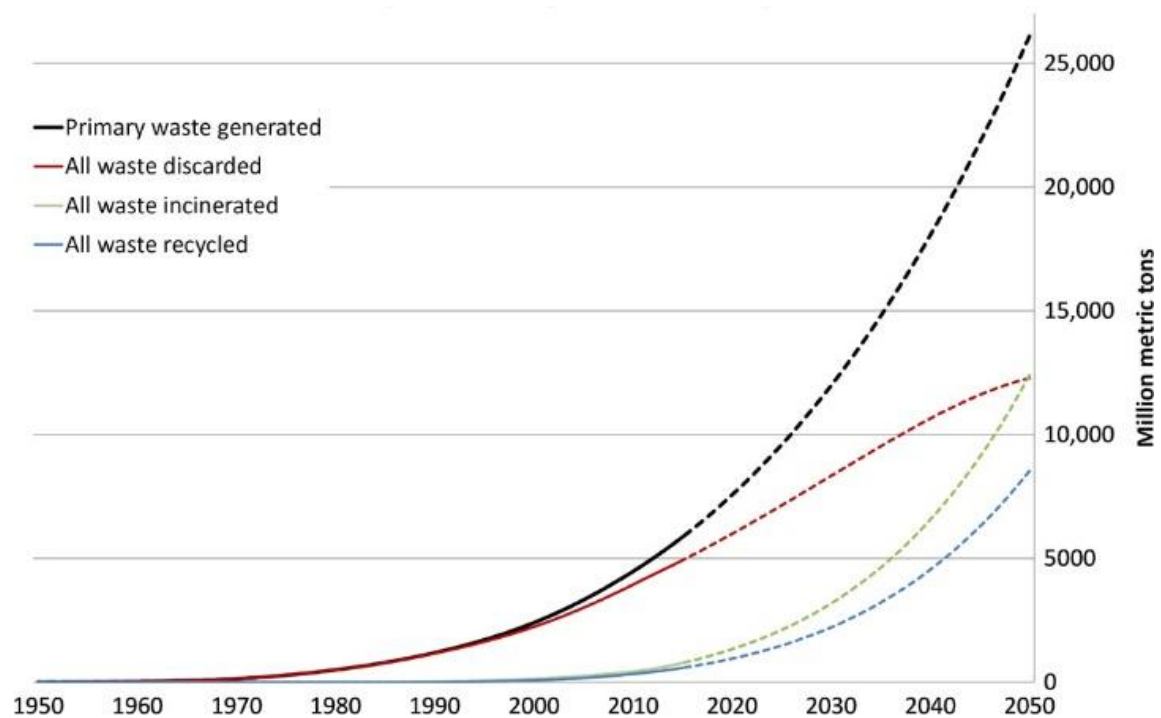


Figure 6: Cumulative plastic waste generation and disposal (in Mt). This figure is reprinted from R. Geyer, J. R. Jambeck, K. L. Law, *Sci. Adv.* 2017; 3: e1700782, which is licensed under the terms of the Creative Commons Attribution Licence.<sup>[50]</sup>

As a measure to reduce the severe impacts of plastic waste on the environment, biodegradable polymers receive more and more attention in recent years, although they have been around on an industrial scale since the end of the 1990s.<sup>[55]</sup> The global production capacity of biodegradable polymers was 0.912 Mt in 2018, corresponding to a share of approximately 0.2% of the global non-biodegradable plastic production.<sup>[42]</sup>

Biodegradable polymers are defined as polymers that can be completely converted into energy, biomass, water and carbon dioxide and/or methane by the action of microorganisms such as fungi, yeasts, algae and bacteria in their natural environment within a given period of time (e.g. in composting standards: six months).<sup>[55]</sup> This property is independent from the source of the raw material but only dependent on the chemical composition of the polymer. This is in contrast to bio-based polymers that are by definition completely or at least partially made of renewable resources.

The degradation starts with a deterioration that is cooperatively accomplished by microorganisms and abiotic factors such as ultraviolet (UV) radiation, oxidative or thermal degradation, as well as chemical hydrolysis (see Figure 7). Both factors lead to fragmentation of the bulk polymer with increasingly exposed surfaces available for biological attack.<sup>[56]</sup> Since most of the biodegradable polymers are insoluble in water and the fragments are still too large to pass the cellular membrane of the microorganisms, the biodegradation starts extracellular with enzymes, such as lipases and esterases that were secreted by the microorganism. The enzymes are too large to diffuse into the polymer, and therefore only work at the surface, making biodegradation a surface erosion process. The cleavage process of the polymer chains can be either exolytic, which directly results in small degradation products, or endolytic, which in contrast first yields oligomers and subsequently the small degradation products. The degradation products can be absorbed by the cell for further metabolisation, as soon as the molecular size has been reduced to ca. 10-50 carbon atoms.<sup>[57]</sup> The product composition is highly influenced by the oxygen level, as the microbial degradation can take place under aerobic conditions, resulting in carbon dioxide, water, energy and biomass, or anaerobic conditions, which additionally lead to the formation of methane.

In addition to the microbial degradation, abiotic processes usually take place at the same time, making the overall degradation process also dependent on humidity, light, and temperature. During the degradation process, various intermediates are formed. Depending on the nature of the surrounding, the intermediates can potentially interact with surfaces of the natural environment, such as mineral oxides, clay minerals or soil organic matter. The interaction leads to reversible or permanent bonds resulting in bound residues.<sup>[58]</sup> To be able to design biodegradable polymers that are non-hazardous during degradation and thereby decrease environmental pollution, it is of high importance to investigate the intermediates, their toxicity and their potential for bioaccumulation.



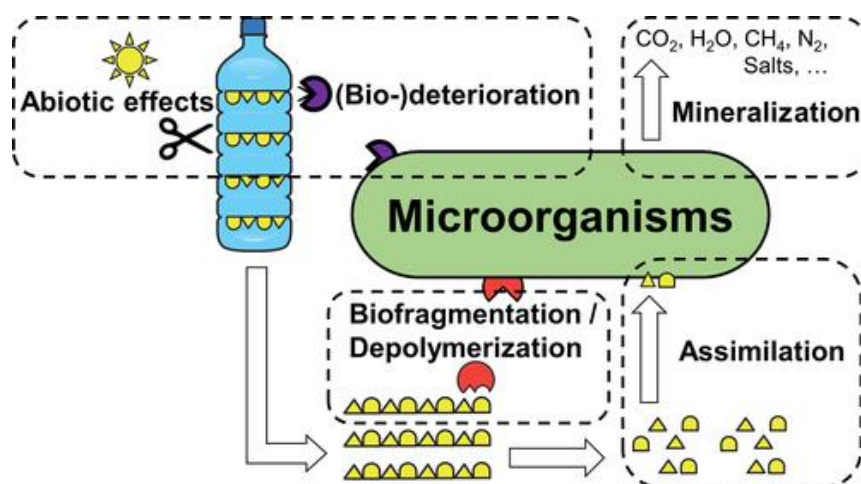


Figure 7: Schematic illustration of plastic biodegradation. This figure is reprinted from R. Wei, W. Zimmermann, *Microbial biotechnology*, 2017, 10, 1308-1322, which is licensed under the terms of the Creative Commons Attribution Licence.<sup>[56]</sup>

## 2.4 Perspectives on Sustainable Catalysis

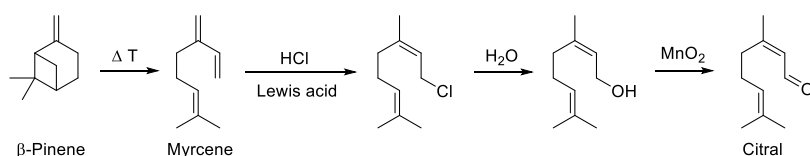
Catalysts enable alternative, energetically favourable reaction mechanisms allowing processes to be carried out more efficiently if compared the uncatalysed reaction and under industrially feasible temperatures and pressures. Nowadays, approximately 85–90% of all products of the chemical industry are produced by catalytic processes.<sup>[59]</sup> The term “catalysis” was coined by Jacob Berzelius in 1836 and later, in 1894 Friedrich Wilhelm Ostwald gave a precise definition saying: “A catalyst affects the rates of the chemical reactions without being consumed and without influencing the thermodynamic equilibrium of reactants and products”.<sup>[60]</sup>

Interestingly, the mechanisms of numerous catalytic transformations that are successfully utilised in industry are not fully known despite extensive research. Often pre-catalysts, additives and promoters (co-catalysts) are used, which form the actual catalytically active species *in situ*. Thus, the prediction of the activity of a catalyst in advance is almost impossible. This in turn makes the preparation and design of an efficient and selective catalyst challenging as the whole process requires a lot of experience and investigations.

It is especially true for oxidation reactions, that there is a huge need for green catalytic alternatives in the production of fine chemicals.<sup>[33]</sup> In contrast to reductions, oxidation reactions still largely depend on the use of stoichiometric oxidants such as chromium(VI) reagents, permanganate, manganese dioxide or periodate. However, from an economic and environmental point of view, the utilisation of clean primary oxidants, like molecular oxygen or hydrogen peroxide, is more favourable. Molecular oxygen as catalytic oxidant

is predominantly used for the production of bulk petrochemicals for economic reasons.<sup>[61]</sup> Due to the multifunctional nature of fine chemicals, the application of molecular oxygen is usually more challenging. Nonetheless, there are processes that successfully utilise molecular oxygen to produce fine chemicals on industrial scale. One example applied by BASF is a novel synthetic route for the production of citral, which is an important intermediate for the synthesis of fragrances and the vitamins A and E (see Figure 8).<sup>[62]</sup> This route starts from fossil-derived isobutene and includes a supported silver catalyst for vapour phase oxidation as a key step, instead of a stoichiometric oxidation with manganese dioxide. Compared to the classical route, starting from  $\beta$ -pinene, the new synthesis route is more atom-efficient and produces less salt waste. Thus, new route is also in accordance with more of the 12 principles of green chemistry, e.g. principle 1 (waste prevention), principle 2 (high atom economy) and principle 9 (catalysis instead of stoichiometric reagents). However, principle 7, the use of renewable feedstocks, is not fulfilled anymore, as it was for the classical route.

#### Classical route



#### New route (BASF)

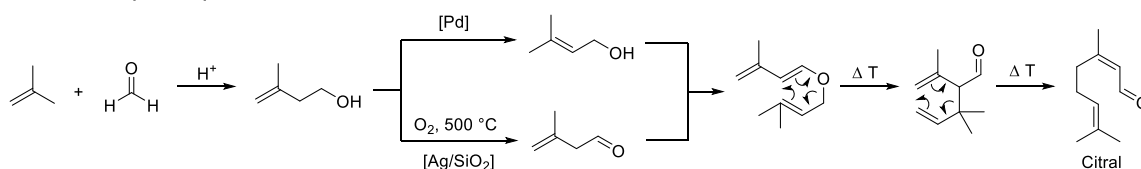


Figure 8: Classical and new routes to citral.<sup>[33]</sup>

As the availability of elements within the Earth crust is finite,<sup>[63]</sup> many elements used as catalysts today are currently regarded as critical, including silver. However, there is no universal definition for the assessment of critical elements. Therefore, diverse lists of critical elements have been generated by the European Union, United Kingdom, United States of America (USA), and a global assessment has been made by the United Nations.<sup>[64]</sup> A two-dimensional “criticality matrix”, where the two axes represent supply risk and the impact, if the supply of that element is compromised, has been developed by the National Research Council of the National Academics (NRCNA, USA). The NRCNA highlights certain elements including rare earth elements, platinum group metals and

indium, manganese and niobium as being most critical.<sup>[64]</sup> For a full assessment of “elemental sustainability” a third axis, showing the environmental impact of extraction and use of an element, is added (see Figure 9). The concept of elemental sustainability aims to guarantee that the use of an element by this generation, does not restrict its use by future generations.<sup>[65]</sup> At this point, elemental sustainability does not intend to prohibit the use of elements, but rather to promote holistic multidisciplinary strategies for extraction, manufacture, utilisation and recovery of elements.<sup>[66]</sup>

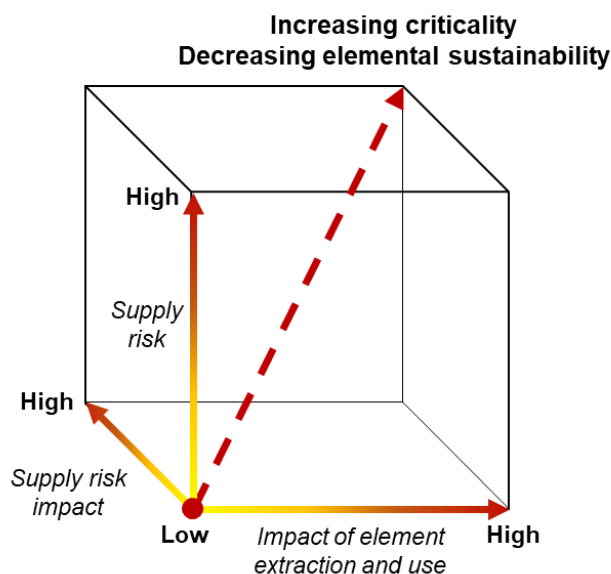


Figure 9: Diagram of criticality of elements according to A. J. Hunt et. al., Element Recovery and Sustainability, The Royal Society of Chemistry, Cambridge, 2013.<sup>[64]</sup>

For a catalyst to be regarded as sustainable, several requirements need to be fulfilled.<sup>[65]</sup> When using earth-abundant, or especially when critical elements are used as catalysts, the recovery of these catalysts must be ensured after usage and at the end of their useful life. Organic-based catalysts should be preferably produced from renewable feedstock and allow for recycling, regeneration, recovering and incineration for energy recovery at the end of life. The energy consumption for recovery and preparation should also be considered and it needs to be ensured that no hazardous substances are released into the environment through the catalyst.

In conclusion, catalysis is an important tool to meet the demands of green and sustainable chemistry. Therefore, the research on novel and efficient catalytic systems for the transformation of renewable resources into fine chemicals marks an essential milestone on the way to sustainable development.

## 2.5 Chemical Structure of Terpenes

Terpenes are a large class of organic compounds with a remarkable structural diversity. To date, about 8,000 terpenes and 30,000 terpenoids are known in the literature.<sup>[67]</sup> Although both terms are sometimes used interchangeably, terpenes are pure hydrocarbons, whereas terpenoids possess usually oxygen-containing functional groups such as alcohol-, ether-, aldehyde-, ketone-, carboxylic acid- or ester groups.<sup>[68]</sup>

The carbon skeleton of terpenes is formally derived from isoprene units that are mostly condensed head-to-tail, known as the “isoprene rule” (see Figure 10). The part of the isoprene unit, which contains the isopropyl group, is defined as “head” and the ethyl residue is defined as the “tail”. Besides head-to-tail, some examples of isoprene units connected head-to-head or tail-to-tail are also known. Depending on the number of isoprene units terpenes, are classified as hemi- ( $C_5$ ), mono- ( $C_{10}$ ), sesqui- ( $C_{15}$ ), di- ( $C_{20}$ ), sester- ( $C_{25}$ ), tri- ( $C_{30}$ ), tetra- ( $C_{40}$ ) and polyterpenes ( $C_5$ )<sub>n</sub> with  $n > 8$ .

The isoprene rule was framed by Otto Wallach in 1887, and formulated and named by Leopold Ružička in 1922.<sup>[69]</sup> In the 1950s, Ružička suggested the “biogenic isoprene rule”, which claims that all terpenes are obtained from a defined number of precursors by condensation, cyclisation and/or rearrangement, sharing a common biosynthetic pathway.<sup>[70]</sup> For their research on terpenes, both scientists were awarded the Nobel prize in Chemistry (O. Wallach 1910 and L. Ružička 1939).

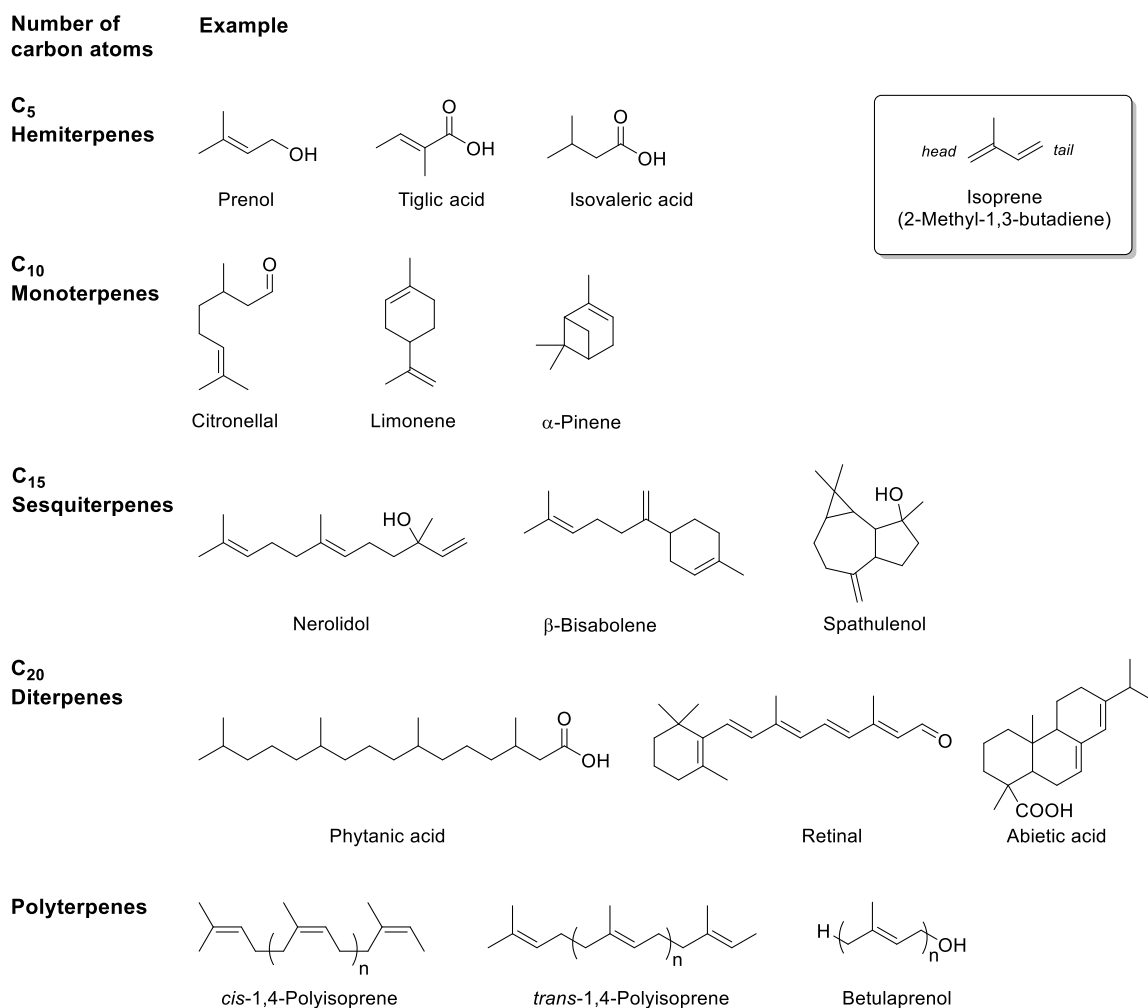


Figure 10: Isoprene unit and examples of terpenes and terpenoids with varying number of carbon atoms.

## 2.6 Terpenes as Renewable Feedstock

The term terpene originates from the resin of pine trees, the so-called “turpentine” (lat. *balsamum terebinthinae*) and was introduced by August Kekulé on a suggestion of the French chemist Marcelin Berthelot.<sup>[71]</sup> However, terpenes are not only found in the resin of pine trees but also in many other plants (see Table 6). The biological and biochemical functions of terpenes in plants are still under investigation. It is known that many plants produce volatile and less volatile terpenes to attract specific insects for pollination or to expel certain animals and to protect themselves from being eaten. Terpenes also play an important role as growth regulators and signal compounds of plants (phytohormones). After having received terpenes with their plant food, a wide range of insects metabolises them to pheromones and growth hormones.<sup>[67]</sup> Since antiquity, terpenes have been isolated and used as fragrances and flavours, which is still the most important application of pure or crude terpenes today.<sup>[72]</sup> Additionally, terpenes serve as solvents or diluting

agents for dyes and varnishes and many pharmaceutical syntheses of vitamins and insecticides start from terpenes.

Table 6: Some terpenes and the plants they can be isolated from.<sup>[73]</sup>

Substance	Plant
Pinenes	Coniferous trees, terebinth
Limonene	Citric fruits (e.g. lemon, orange)
Citronellal	Citronella, eucalyptus
Citral	Lemongrass
Geraniol	Geranium
Citronellol	Citronella
Menthol	Peppermint
Eugenol	Clove
Linalool	Lavender

Two of the most important industrial sources of terpenes are turpentine obtained from coniferous trees or terebinth, and essential oils from citric fruits.<sup>[72]</sup> Turpentine is mainly composed of  $\alpha$ -pinene (45–97%) and  $\beta$ -pinene (0.5–28%), as well as smaller amounts of other monoterpenes (see Figure 11).<sup>[74]</sup> The global production of turpentine and (*R*)-(+)-limonene, the main component of orange oil (94–96%),<sup>[75]</sup> is modest. Worldwide, approximately 300,000 tons of turpentine and 70,000 tons of limonene are produced per year.<sup>[74]</sup>

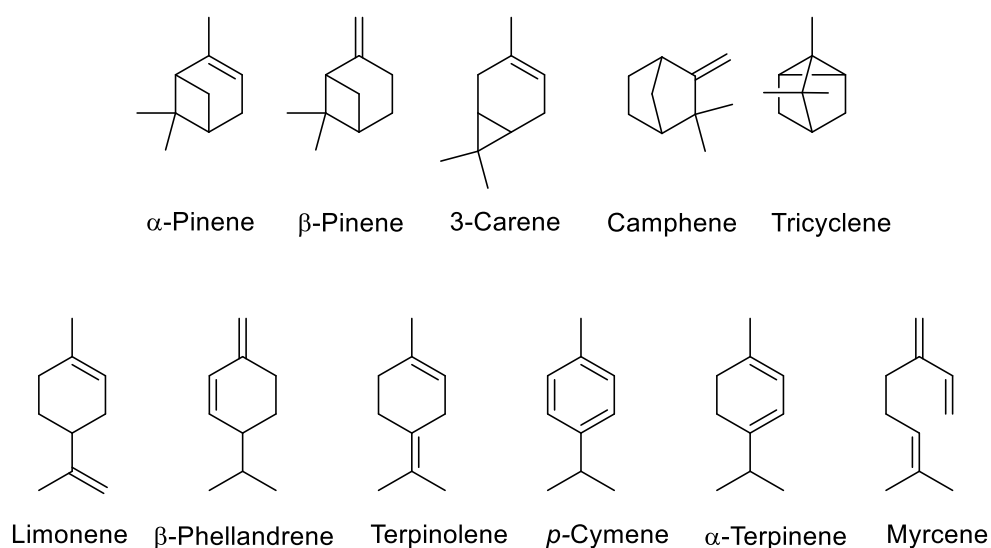


Figure 11: Structures of the most common monoterpenes found in turpentine.<sup>[76]</sup>

There are three different ways to produce turpentine:<sup>[77]</sup> first, turpentine can be obtained *via* tapping of living pine trees and subsequent steam distillation of the gum resin generated by the trees (gum turpentine). A second method to obtain turpentine is solvent extraction or destructive dry distillation of aged pine stumps, followed by purification (wood turpentine). The third route leads to turpentine as a by-product from the kraft and sulfite pulping processes that produce pulp and paper (crude sulfate or sulfite turpentine). The obtained turpentine is then distilled at 70 mbar to yield  $\alpha$ -pinene (boiling point (bp): 156 °C) and  $\beta$ -pinene (bp: 164 °C) in two different fractions and to separate them from smaller amounts of other impurities with almost no commercial value. For the further conversion of pinenes into a wide variety of chemicals for the pharmaceutical, flavour and fragrance industry, different catalytic chemical processes have been developed including reactions such as hydrogenation, oxidation, isomerisation, hydration, hydroformylation, condensation, cyclisation, ring contraction, *etc.* (see Chapter 2.7 for further details).

Essential orange oil, distilled for the flavour and fragrance industry since the late 1800s, contains along with (*R*)-(+)-limonene over 140 different chemical compounds. Nowadays, orange oil is produced as a by-product of citric fruit processing.<sup>[75]</sup> The oil is obtained either by steam distillation or by a cold process that involves centrifugation and leads to high quality orange oil due to the minimisation of oxidation reactions that take place at higher temperatures. (*R*)-(+)-limonene can be extracted from orange oil by distillation.

Recently, Luque, Clark and co-workers reported a novel cascade-type valorisation approach to extract (*R*)-(+)-limonene,  $\alpha$ -terpineol, pectin, sugars and a form of mesoporous cellulose from waste orange peel using a single-step, low-temperature hydrothermal microwave treatment.<sup>[78]</sup> The industrial potential of this approach is emphasised by already available continuous microwave processors that operate at several tonnes per hour.

## 2.7 Catalytic Conversion of Terpenes into Fine Chemicals

Due to the large number of terpenes and corresponding transformation reactions, a vast literature on catalytic transformations of terpenes into fine chemicals is available. This chapter focuses on the reactions related to pinenes and with a particular attention to the oxidation of  $\alpha$ -pinene. An in depth overview of recent studies comprising other important terpenes and catalytic transformation reactions, can be found in the literature.<sup>[73, 79-81]</sup>

To date, many different reactions for the conversion of pinenes into valuable compounds have been developed. An overview of these conversions is presented in Figure 12.

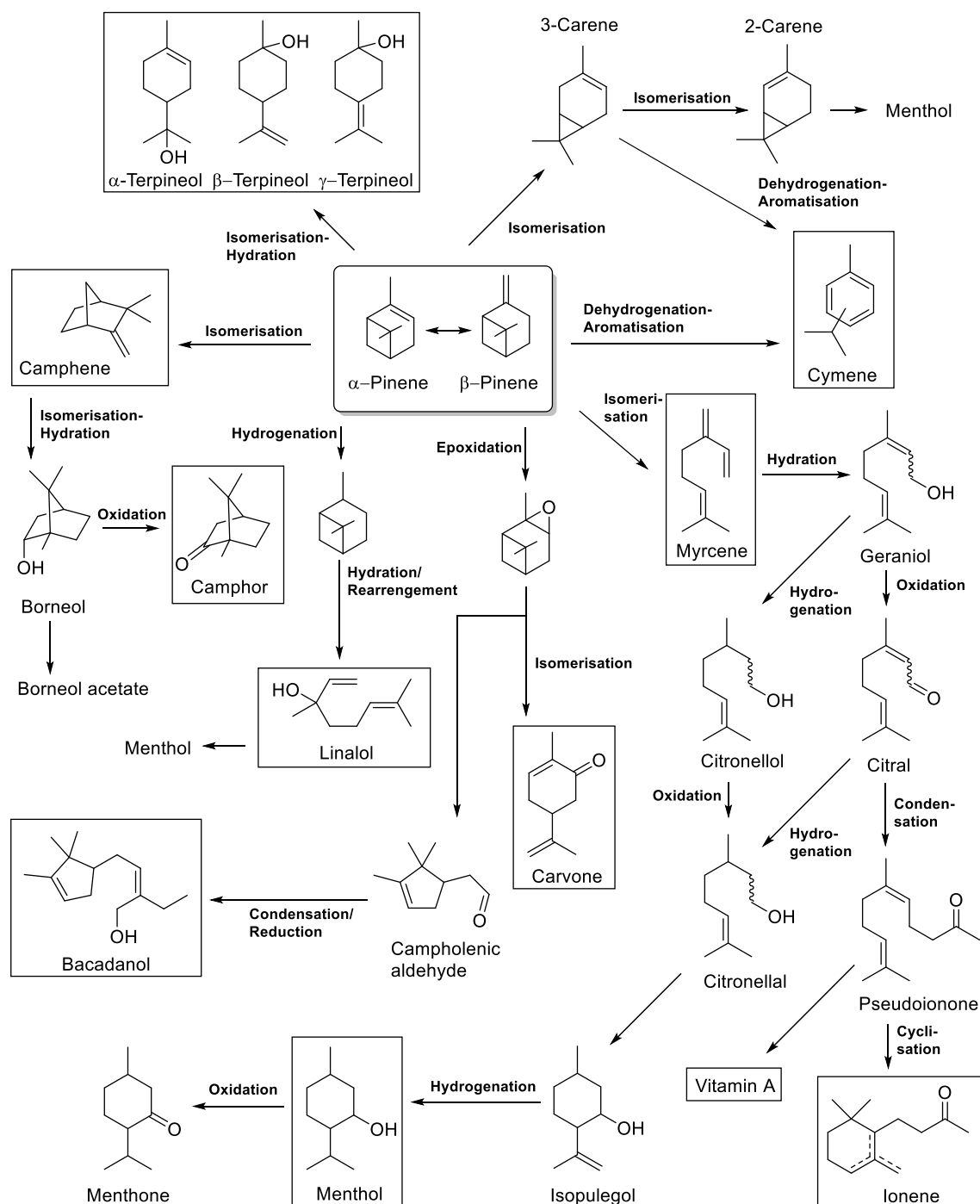


Figure 12: Overview of valuable compounds obtained from  $\alpha$ - and  $\beta$ -pinene, adopted from reference [72].

### 2.7.1 Isomerisation of $\alpha$ -Pinene

The industrial isomerisation of  $\alpha$ -pinene occurs at temperatures above 373 K and under normal pressure in closed systems over  $\text{TiO}_2$  catalysts that have been treated with acids to form a layer of titanate acid on the catalyst surface.<sup>[82]</sup> In the presence of acid catalysts, the isomerisation starts by protonation of the double bond and subsequent formation of a pinylium ion intermediate, which can rearrange into a complex mixture of mono-,



bi- and tricyclic products *e.g.* *via* Wagner-Meerwein rearrangement.<sup>[83]</sup> The overall yield of the main products camphene and limonene, and of by-products ( $\beta$ -pinene, tricyclene, *p*-cymene, terpinenes, terpinolenes, phellandrenes, etc.) is around 75-80%. However, the isomerisation rate is relatively low, which increases the interest in finding novel catalysts with higher activity and selectivity to camphene and/or limonene. Generally, the selectivity and conversion depend on the nature of the catalyst. Camphene is an industrially important intermediate for the synthesis of camphor, which is used as insect repellent, as cough suppressant and decongestant, and in the manufacture of films, plastics, lacquers, and explosives.<sup>[72]</sup> The investigated catalysts are usually acidic materials, like clays,<sup>[84]</sup> zeolites<sup>[85]</sup> or carbon.<sup>[86]</sup>

### 2.7.2 Hydration of $\alpha$ -Pinene

The hydration of  $\alpha$ -pinene results in complex mixtures containing  $\alpha$ -terpineol, limonene and terpinolene as main products and oligomers, while other terpineols, terpinenes, borneol, *etc.* can be formed minor by-products.<sup>[72]</sup>  $\alpha$ -Terpineol is the most important monocyclic monoterpene alcohol and, owing to its typical lilac odour, is mainly used as fragrant. A common industrial preparation of  $\alpha$ -terpineol is the hydration of  $\alpha$ -pinene with aqueous mineral acids, yielding crystalline *cis*-terpin hydrate. The hydration is followed by partial dehydration to give the desired product (see Figure 13). Acid-activated silica gel or weak acids are suitable catalysts for the hydration reaction. It is also possible to use organic acids, such as acetic acid, to convert  $\alpha$ -pinene into terpinyl esters, which can be further hydrolysed to terpineol, sometimes *in situ*.<sup>[87]</sup>

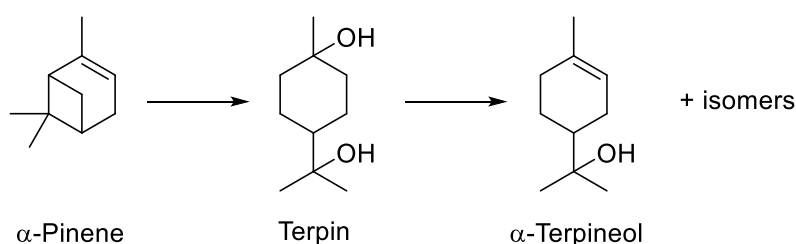


Figure 13: Industrial  $\alpha$ -terpineol synthesis via the hydration of  $\alpha$ -pinene.<sup>[87]</sup>

### 2.7.3 Dehydroisomerisation of $\alpha$ -Pinene

Dehydroisomerisation of  $\alpha$ -pinene,<sup>[88]</sup> 3-carene<sup>[89]</sup> or limonene<sup>[90]</sup> can be applied to produce *p*-cymene which is used as solvent for dyes and varnishes, as an additive in fragrances, in musk perfume, and as a masking odour for industrial products.<sup>[72]</sup> Palladium or platinum supported on silica, alumina, and zeolites have proven to be useful catalysts for the

dehydroisomerisation of  $\alpha$ -pinene.<sup>[91]</sup> For this reaction, the catalyst has a dual functionality: the acid sites of the carrier material are responsible for the isomerisation, whereas the metal sites carry out the hydrogenation/dehydrogenation. The reaction cascade starts with the isomerisation of  $\alpha$ -pinene into camphene and terpinolene. Camphene subsequently isomerises into terpinolenes, which isomerise to give terpinenes. In the next step, the terpinenes are dehydrogenated to give *p*-cymene or partially hydrogenated to yield menthenes and carvomenthenes (see Figure 14).<sup>[72]</sup>

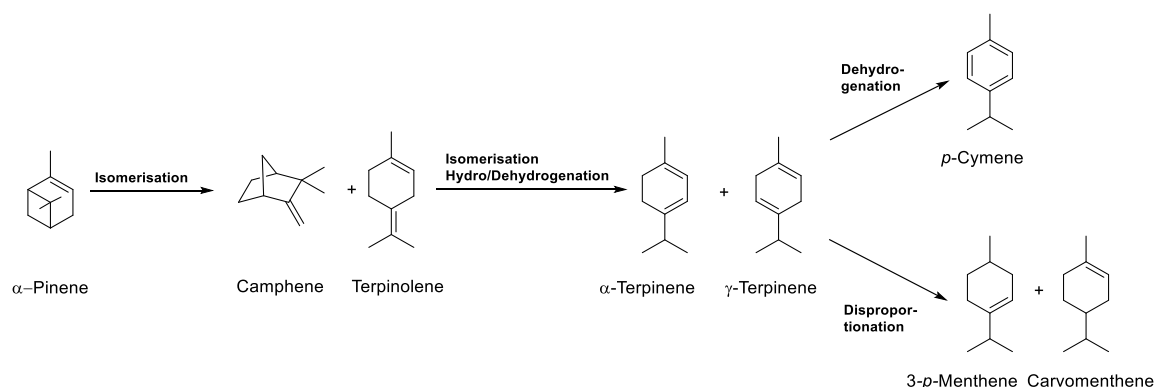


Figure 14: Possible pathways and products resulting from dehydroisomerisation of  $\alpha$ -pinene.

#### 2.7.4 Oxidation of $\alpha$ -Pinene

A common approach towards commercially important intermediates for pharmaceuticals, flavours, fragrances and chiral building blocks based on monoterpenes is the epoxidation of the respective double bond and the subsequent rearrangement of the resulting epoxide ring-system under the influence of various catalysts. The main products of the selective oxyfunctionalisation, which is followed by a rearrangement, are usually alcohols, carbonyl compounds and skeletally rearranged products.<sup>[73]</sup>

The autoxidation of pinenes is known for more than two centuries and has been extensively described in the literature.<sup>[92]</sup> The epoxidation of  $\alpha$ -pinene with various oxidants and catalysts usually yields a complex mixture of different products, since competitive reactions, such as isomerisation, hydration, hydrogenation and dehydrogenation can occur simultaneously.<sup>[72]</sup> Verbenol, verbenone and  $\alpha$ -pinene oxide, which can be isomerised to campholenic aldehyde, are the most important oxidation products. The oxygenated  $\alpha$ -pinene derivatives can be used as flavour chemicals and as precursors for fine chemicals such as citral, menthol, sandalwood-like fragrances, vitamin A and E, and paclitaxel.<sup>[87, 93, 94]</sup>

Despite great industrial and academic interest, the basic chemistry behind the autoxidation process is not completely understood. The radical chain mechanism proposed by early studies has been investigated in detail in 2010 by Hermans *et al.*, who combined experimental findings with quantum chemical calculations to gain a quantitative insight into the reaction mechanism of the aerobic oxidation of  $\alpha$ -pinene.<sup>[95]</sup> The oxidation was studied at 363 K and 1 bar of pure oxygen and already at conversions as low as 2%, a multitude of products was formed (see Figure 15).

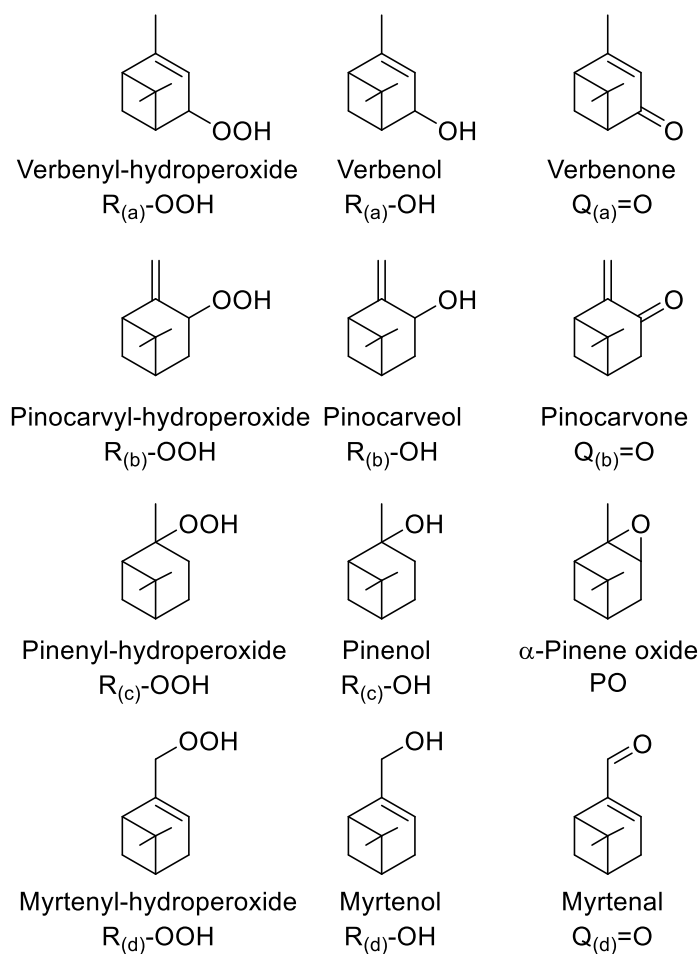


Figure 15: Main products observed during the thermal oxidation of  $\alpha$ -pinene.<sup>[95]</sup>

The large number of products can be explained by the fact that radicals are able to abstract hydrogen atoms from different carbon atoms of the  $\alpha$ -pinene molecule: The two most reactive positions are denoted a and d (see Figure 16, left). To date, it remains unclear how the first radicals are generated. It has been proposed that traces of impurities, such as ROOH, induce the initial reaction.<sup>[95]</sup>

In case the radical abstracts the hydrogen atom from the a-site, a resonance-stabilised radical is formed, from which verbenyl as well as pinenyl products can emerge (see Figure

16). The abstraction of an hydrogen atom from the d-site leads to another resonance-stabilised radical resulting in pinocarvyl and myrtenyl products (see Figure 16). Radicals that arise from the abstraction of other hydrogen atoms are not resonance-stabilised or contain a lot of ring strain which makes them less relevant.

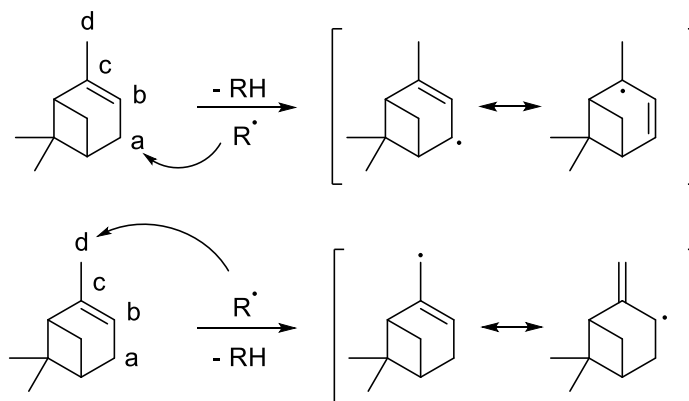


Figure 16: Four different oxidation sites (denoted a – d) in  $\alpha$ -pinene and the resulting resonance-stabilised radicals formed upon abstraction of an hydrogen atom at the a- and d-sites (top and bottom, respectively).<sup>[95]</sup>

In a next step, the resonance-stabilised alkyl radicals react with molecular oxygen resulting in the following four different types of chain-carrying peroxy radicals:  $R_{(a)}\text{-OO}^\bullet$ ,  $R_{(b)}\text{-OO}^\bullet$ ,  $R_{(c)}\text{-OO}^\bullet$  and  $R_{(d)}\text{-OO}^\bullet$ . The peroxy radicals then give rise to the various allylic oxidation products found in the reaction mixture. To yield the also observed  $\alpha$ -pinene oxide molecule, peroxy radicals add to the C=C double bond of  $\alpha$ -pinene. This is followed by a unimolecular ring-closure leading to the elimination of alkoxy radicals ( $\text{RO}^\bullet$ ) and resulting in  $\alpha$ -pinene oxide as product (see Figure 17).<sup>[95]</sup>

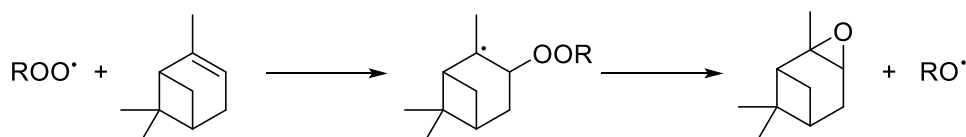


Figure 17: Epoxidation of  $\alpha$ -pinene under autoxidation conditions.<sup>[95]</sup>

The addition of molecular oxygen to the radical adduct, which arose from the peroxy radical and  $\alpha$ -pinene (see Figure 18), competes with the conversion of  $\alpha$ -pinene to pinene oxide shown in Figure 17. However, the addition of molecular oxygen to the radical adduct is likely diffusion-controlled and therefore cannot compete with the epoxidation mechanism under 1 bar oxygen pressure.<sup>[95]</sup>

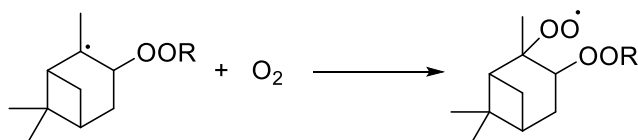


Figure 18: Addition of molecular oxygen to a radical adduct; a reaction that can potentially compete with the epoxidation shown in Figure 17.<sup>[95]</sup>

Hermann *et al.* also investigated the primary and secondary nature of the main reaction products pinene oxide, verbenyl-hydroperoxide ( $R_{(a)}\text{-OOH}$ ), verbenol ( $R_{(a)}\text{-OH}$ ) and verbenone ( $Q_{(a)}\text{=O}$ ). They found that strikingly all products appeared to be predominantly primary in origin. Based on the epoxidation mechanism, this can readily be explained for pinene oxide and  $R_{(a)}\text{-OOH}$  (see Figure 17). The epoxidation mechanism co-produces alkoxy radicals ( $\text{RO}\cdot$ ), which can rapidly (much more than peroxy radicals) abstract allylic hydrogen atoms. This leads to the formation of the alcohol  $R_{(a)}\text{-OH}$  having a primary character. However, the ketone seems to be predominantly of primary origin as well. Herman *et al.* observed an initial linear correlation of the concentrations of  $R_{(a)}\text{-OH}$  and  $Q_{(a)}\text{=O}$  with the epoxide, indicating that both the alcohol and the ketone arise from the same species, the alkoxy radicals. The abstraction of the weakly bonded  $\alpha$ -hydrogen atom by molecular oxygen from the alkoxy radical appears to be a likely mechanism for the formation of the ketone (see Figure 19). The  $\text{HO}_2\cdot$  radicals that are also produced during this reaction mainly react with the hydroperoxide products, converting them in turn into peroxy radicals for further reactions.<sup>[95]</sup>

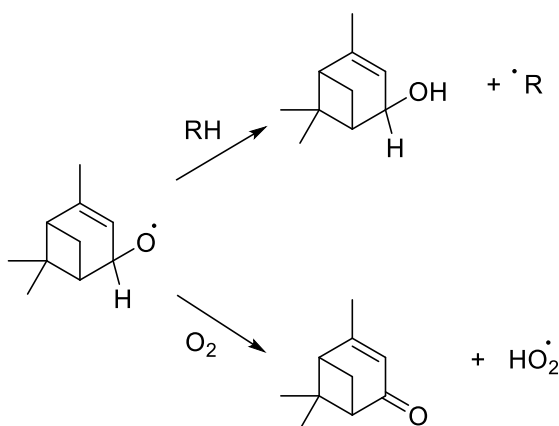


Figure 19: Proposed fate of the  $R_{(a)}\text{-O}\cdot$  radicals.<sup>[95]</sup>

The autoxidation mechanism results in several different products and is nonselective towards a specific species. To enhance the efficiency and the selectivity, considerable efforts have been made in developing catalysts, mainly based on transition metals. Wang

*et al.* recently investigated a metal-free catalytic system based on carbon nanotubes (CNTs) and nitrogen-doped CNTs (NCNTs).<sup>[96]</sup> For the liquid-phase oxidation of  $\alpha$ -pinene with molecular oxygen as oxidising agent, a conversion of 54.5% and selectivities up to 37.8% for pinene oxide after 4 h were achieved. Wang *et al.* also proposed a plausible mechanism for the metal-free catalytic oxidation based on the results and theoretical calculations (see Figure 20). Pathways I, II and IV are similar to the previously described autoxidation process. Pathway I and II result in equimolar amounts of epoxidation product and allylic oxidation products. However, the autoxidation process usually yields more allylic oxidation products than epoxidation products caused by the additive allylic product contribution of pathway IV. The higher epoxide selectivity achieved by the carbon-catalysed oxidation is explained by the radical stabilisation abilities of CNTs. Thus, the stability of ROR• radicals formed by the interaction of alkoxy radicals and  $\alpha$ -pinene in pathway III might increase. The additionally obtained pinene oxide then leads to the observed selectivity towards the epoxidation product.

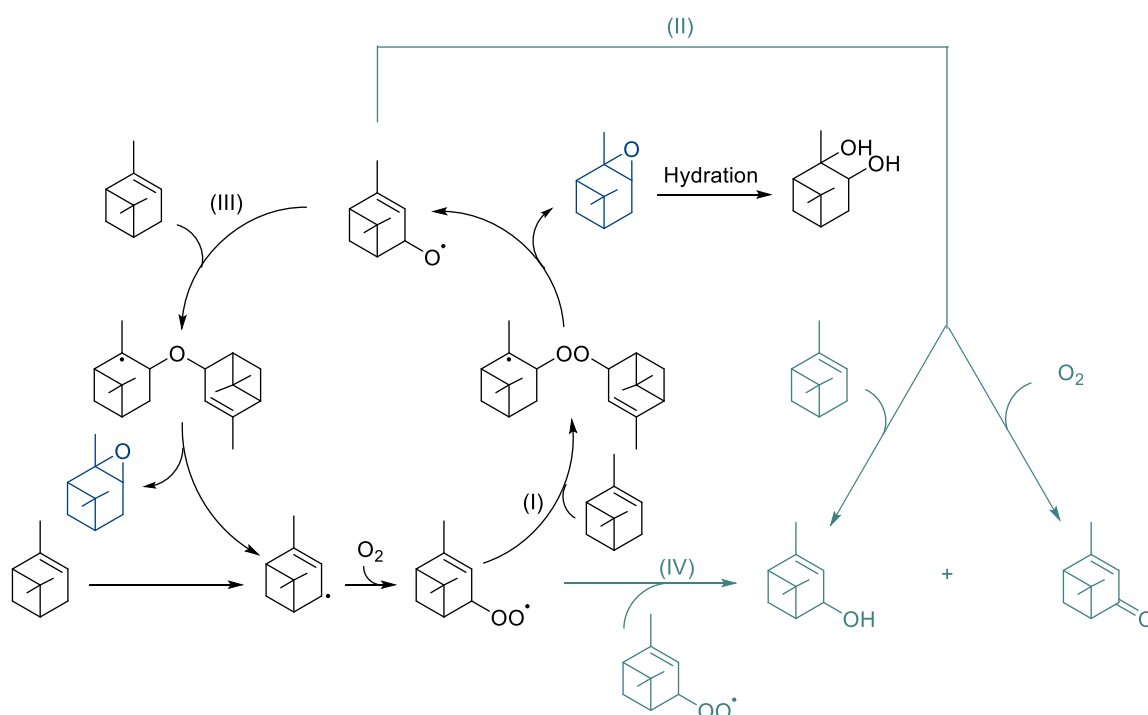


Figure 20: Proposed reaction pathways of the NCNT-catalysed oxidation of  $\alpha$ -pinene.<sup>[96]</sup>

Transition metals as catalysts in autoxidation reactions of alkenes are more widespread than metal-free catalytic systems. The role of the metal ions is generally explained in terms of catalysis by the decomposition of allylic hydroperoxide intermediates facilitating the initiation of the free radical chain mechanism.<sup>[97]</sup> In the literature, numerous approaches to harness transition metals, such as cobalt, chromium, iron, manganese, *etc.* for the

oxidation of pinenes have been reported. However, a direct comparison of the catalytic performance is rarely possible since these systems differ in many aspects, such as oxidising agent (e.g. molecular oxygen, hydrogen peroxide (H<sub>2</sub>O<sub>2</sub>), *tert*-butyl hydroperoxide (TBHP)), homogeneous or heterogeneous catalysis, as well as reaction conditions (solvent, temperature, pressure, reaction time).

Nardello-Rataj *et al.* performed the epoxidation of various terpenes with eco-friendly solvents (cyclopentyl methyl ether (CPME) and 2-methyl tetrahydrofuran (2-MeTHF)) and amphiphilic polyoxometalate nanoparticles using H<sub>2</sub>O<sub>2</sub> as oxidant.<sup>[98]</sup> Employing  $\alpha$ -pinene as substrate and CPME as solvent, a conversion of 58% with an  $\alpha$ -pinene oxide selectivity of 32% was obtained after 3 h at 65 °C. Moreover, the authors showed that the polyoxometalate nanoparticles could be easily reused.

In some other studies, catalytic systems for the oxidation of terpenes that do not require the use of any solvent were developed. For example, Lajunen and coworkers performed the aerobic oxidation of olefins under solvent-free conditions using a Co(II)-pyridine complex as catalyst and, in contrast to several previous papers,<sup>[99]</sup> without co-oxidant.<sup>[100]</sup> After 22 h at 50 °C with continuous oxygen flow through the reaction mixture, a conversion of 77% was achieved, while 14% pinene oxide, 14% verbenol, 32% verbenone and 17% other products were formed. However, this procedure shows the typical environmental and economical drawbacks of homogeneous catalytic systems as the complexity of catalyst separation hinders the recycling and leads to product contamination with traces of metal ions.<sup>[101]</sup>

Gusevskaya *et al.* also performed the reaction under solvent-free conditions with molecular oxygen, but promoted by heterogeneous chromium containing mesoporous molecular sieves MCM-41.<sup>[102]</sup> A reaction time of 6 h at 1 atm and 3.5 h at 5 atm oxygen pressure at 60 °C resulted in a substrate conversion of 40%. The main product was verbenol with a selectivity of 33%, followed by verbenone (26%), along with smaller amounts of pinene oxide (8%) and campholenic aldehyde (4%). Additionally, no metal leaching of the catalyst was observed, which made catalyst recovery easy and enabled its recycling without any special treatment.

Kholdeeva and colleagues explored the potential of the iron- and chromium-based metal-organic frameworks (MOFs) MIL-100 and MIL-101 for the solvent-free oxidation of alkenes.<sup>[103, 104]</sup> The applied reaction conditions were rather mild (1 bar of O<sub>2</sub>, 40 – 60 °C, TBHP as initiator) and afforded mainly the allylic oxidation products with an  $\alpha$ -pinene conversion of 26% after 16 h. The authors also investigated the heterogeneous nature of the catalysis and found that Fe-MIL-101 only behaves as heterogeneous catalyst at

temperatures lower than 50 °C, otherwise iron leaches into the solution which drastically limits the potential of the heterogeneous catalyst for liquid-phase oxidations.<sup>[105]</sup>

Over the last twenty years, various Mn(III) acetate-mediated oxidative free-radical reaction protocols have been developed for inter- or intramolecular reactions:<sup>[106, 107]</sup> Usually, Mn(III) acetate is used for oxidative free-radical cyclisations<sup>[108]</sup> and for  $\alpha$ -keto-acetoxylation.<sup>[109]</sup> Some studies also utilised Mn(III) acetate for allylic oxidation reactions. One example was reported by Bégué *et al.* who used Mn(III) acetate as a catalyst for the aerobic epoxidation of various olefins including limonene with pivalaldehyde as sacrificial aldehyde in fluoruous solvents.<sup>[110]</sup> Likewise, Shing *et al.* applied Mn(III) acetate for allylic oxidations of simple and complex olefins while using TBHP in decane as co-oxidant.<sup>[111]</sup> The authors also implemented the catalytic system for  $\alpha$ -pinene. For this, 3 Å molecular sieves and ethyl acetate as solvent were applied. After degassing the solution, filling it with pure oxygen and stirring at room temperature for 48 h, pinene oxide was obtained in a yield of 63%. Manganese has also been employed for the heterogeneously catalysed epoxidation of alkenes with air as oxidant. For instance, Raja *et al.* designed redox molecular sieve catalysts for the selective oxidation of  $\alpha$ -pinene among other alkenes and used benzaldehyde as sacrificial aldehyde.<sup>[112]</sup>

### 2.7.5 Isomerisation of $\alpha$ -Pinene Oxide

The isomerisation of  $\alpha$ -pinene oxide yields different compounds depending on the utilised type of acid catalyst. Brönsted acid catalysts favour the formation of *trans*-carveol, *trans*-sobrerol, isopinocampone and *p*-cymene, while mild Lewis acids tend to facilitate the formation of campholenic aldehyde and pinocarveol.<sup>[72]</sup>



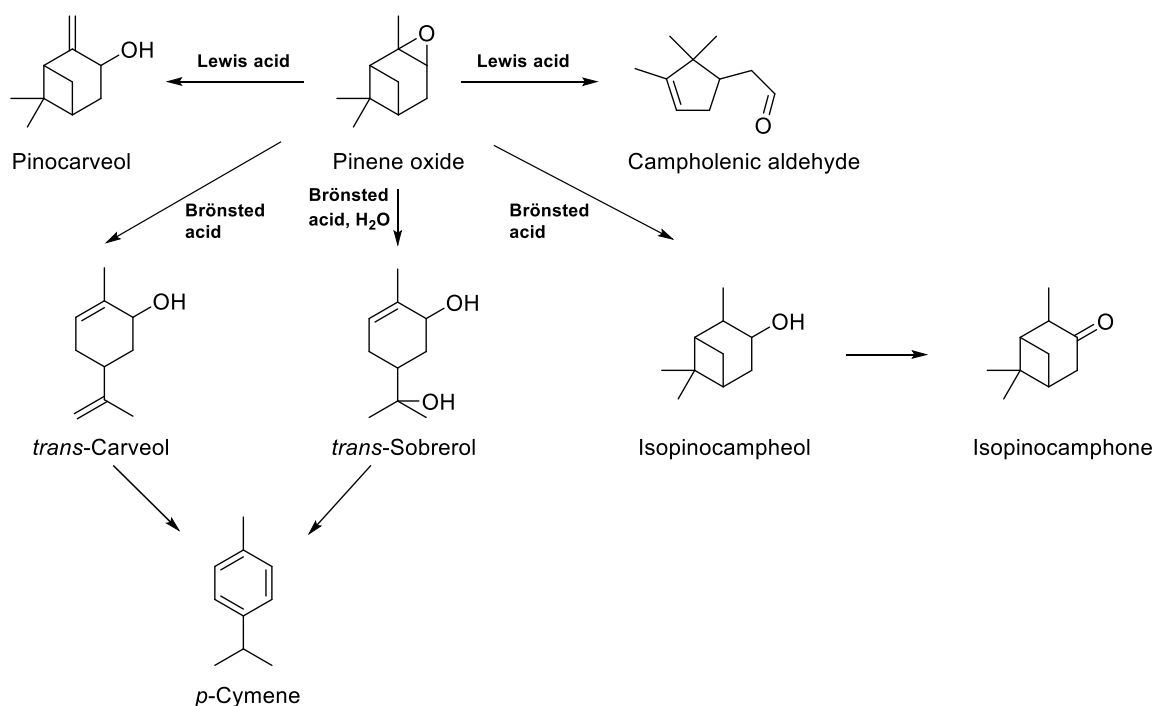


Figure 21: Compounds obtained from isomerisation of  $\alpha$ -pinene.<sup>[72]</sup>

From an industrial point of view, the most important product coming from pinene oxide is campholenic aldehyde. The most active and selective catalysts for the isomerisation of pinene oxide into campholenic aldehyde are the homogenous Lewis acid catalysts  $\text{ZnCl}_2$  and  $\text{ZnBr}_2$ .<sup>[113]</sup> However, the use of zinc halides has several drawbacks. The low reaction rates (turn over numbers lower than 20)<sup>[114]</sup> and the fast deactivation require a high catalyst to substrate ratio. Additionally, the aqueous extraction of the catalyst produces a considerable amount of heavy metal contaminated waste.<sup>[72]</sup> Zeolites, zeotype materials and MOFs have also been explored as Lewis acids and proved to be promising heterogeneous catalytic materials for overcoming the mentioned drawbacks.<sup>[115-117]</sup>

In conclusion, terpenes constitute a very versatile class of natural products that can be transformed into a wide range of commercially valuable products, e.g. for fragrances, flavours, pharmaceuticals, chiral building blocks and useful synthetic intermediates. The reactions applied for these transformations comprise reactions, such as isomerisation, hydration, condensation, hydroformylation, hydrogenation, cyclisation, oxidation, rearrangement, and ring contraction/enlargement.

## 2.8 Sustainable Thermoplastic Polymers from Terpenes

Since  $\alpha$ -pinene,  $\beta$ -pinene, myrcene and limonene are relatively easy to isolate at low cost and show high abundance, they are, despite the vast number of different terpenes available, the most widely studied terpenes for polymerisation applications.<sup>[118]</sup> This chapter will therefore focus on these terpenes as renewable raw materials for polymers.

### 2.8.1 Direct Polymerisation

#### 2.8.1.1 Homopolymers of $\beta$ -pinene

It was in 1798, when Bishop Watson published the possibly first report of a polymerisation of  $\beta$ -pinene. He recorded that the addition of a drop of sulfuric acid to turpentine resulted in the formation of a sticky resin. However, it took another one and a half centuries before the first systematic studies of polymerisations based on terpenes were reported.<sup>[119]</sup> Early research mainly focused on  $\beta$ -pinene instead of  $\alpha$ -pinene because it has a sterically more accessible exocyclic double bond. In addition, it has two alkyl groups with electron donating effects at the double bond, stabilising the carbenium ion that is formed during cationic polymerisation. Roberts and Day carried out the first studies of the cationic homopolymerisation of  $\beta$ -pinene in 1950 using Friedel-Crafts conditions (see Figure 22, A).<sup>[120]</sup> Used as a catalyst, aluminium trichloride forms a strong proton donor after reacting with water and subsequently protonates the double bond. The formed carbenium ion rearranges to a *para*-menthene type carbenium ion which starts and propagates the reactions. The polymerisation is driven by the high reactivity of the exomethylene double bond, the breaking of the highly strained fused cyclobutane ring and the formation of the relatively stable *para*-menthene carbenium ion, leading to a solid polymer with a molecular weight of around 2 kDa.<sup>[118]</sup>

Lu *et al.* presented the first example of a living cationic polymerisation based on  $\beta$ -pinene in 1997.<sup>[121]</sup> Using  $\alpha$ -chlorodiethyl ether as initiator and titanium trichloride isopropoxide ( $\text{TiCl}_3(\text{O}i\text{Pr})$ ) as activator in the presence of tetrabutylammoniumchloride ( $n\text{Bu}_4\text{NCl}$ ) in dichloromethane at temperatures between  $-40$  to  $-78$  °C, molecular weights of up to 5 kDa and a narrow dispersities of  $\mathcal{D} = 1.1$  to 1.2 were achieved. The authors confirmed the living nature of the system with the linear increase of  $M_n$  with monomer conversion.

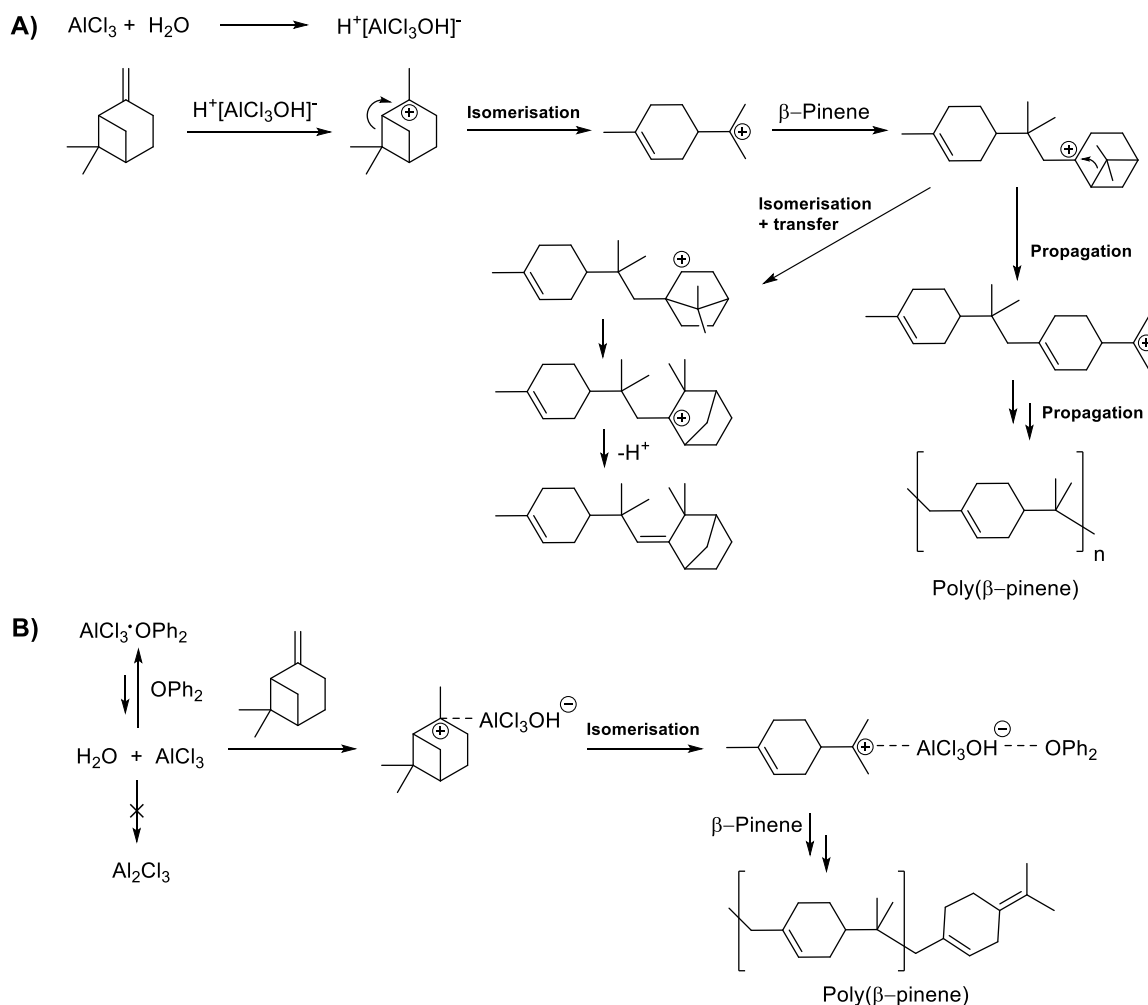


Figure 22: Cationic polymerisation of  $\beta$ -pinene: A) General mechanism catalysed by  $\text{AlCl}_3$ .<sup>[120]</sup> B) Proposed mechanism using  $\text{H}_2\text{O}/\text{AlCl}_3\text{OPh}_2$  as initiating system.<sup>[122]</sup>

In order to decrease the relative kinetic contribution of the transfer reaction with respect to chain propagation, the polymerisation reaction needs to be carried out at low temperatures, such as  $-78\text{ }^\circ\text{C}$ , to be able to obtain polymers with higher molecular weights.<sup>[118]</sup> However, such temperatures are incompatible with industrial requirements.

Yu *et al.* aimed to overcome these issues by applying Schiff-base nickel complexes in conjunction with methylaluminoxane (MAO).<sup>[123]</sup> The catalytic system was employed at  $40\text{ }^\circ\text{C}$  and polymers with a molecular weight of  $M_n = 11\text{ kDa}$  were obtained.

More recently, Satoh and co-workers established a synthesis protocol for a high molecular weight hydrogenated poly( $\beta$ -pinene) with useful properties such as good processability, high optical transparency, non-hygroscopicity, high mechanical strength, and excellent thermal properties.<sup>[124, 125]</sup> The polymerisation was achieved by using ethylaluminium dichloride ( $\text{EtAlCl}_2$ )/diethyl ether in a solvent mixture of dichloromethane and *n*-hexane and a halide as the initiator at  $-78\text{ }^\circ\text{C}$  and resulted in a molecular weight of  $M_n > 40\text{ kDa}$ .

The post-modification hydrogenation was performed in order to increase the durability, optical properties and thermal resistance. It yielded a conversion > 99% using *n*-hexane at 1 MPa hydrogen pressure with a Pd/aluminium oxide (Al<sub>2</sub>O<sub>3</sub>) species as a catalyst and resulted in a material possessing mechanical strength (> 70 MPa) comparable to commercial polymers.

To overcome synthesis procedures that involve cryogenic temperatures and catalysts such as Schiff-base nickel complexes, which are not commercially available but need a multistep synthesis and expensive MAO activators, Kukhta *et al.* investigated commercially available aluminium chloride etherates (AlCl<sub>3</sub>OPh<sub>2</sub>) for room-temperature polymerisation of β-pinene (see Figure 22, B).<sup>[122]</sup> The obtained polymers possessed a molecular weight in the range of 9-14 kDa and glass transition temperatures (*T*<sub>g</sub>) of 82-87 °C, demonstrating that it is possible to synthesise homopolymers of β-pinene at ambient temperatures and with inexpensive catalyst systems. One important factor for the achievement of higher molecular weight was thought to be the *in situ* generation of a weakly nucleophilic counter anion through the interaction of AlCl<sub>3</sub>OH<sup>-</sup> with diphenyl ether that leads to the suppression of chain transfer reactions (see Figure 22, B).<sup>[122]</sup>

### 2.8.1.2 Homopolymers of α-Pinene

In contrast to β-pinene, α-pinene possesses a sterically shielded and thermodynamically more stable endocyclic double bond, instead of a reactive exocyclic one. Since this double bond is obstructed and consequently chain growth is slower, polymerisation attempts for α-pinene have not been as successful as for β-pinene, yielding only oligomers. Despite the lack of reactivity, many approaches for the polymerisation of α-pinene have been reported, on account of α-pinene being the most naturally abundant terpene.<sup>[118]</sup> The first polymerisation was published by Roberts and Day in 1950. However, using a Lewis acid resulted in very low yield and only oligomer formation.<sup>[120]</sup> Other groups improved the cationic polymerisation approach by combining Lewis acids with antimony trichloride (SbCl<sub>3</sub>) as activator.<sup>[126]</sup> The polymerisation was carried out in toluene at -15 °C using aluminium chloride and SbCl<sub>3</sub> as catalyst system yielding poly(α-pinene) with a molecular weight of *M*<sub>n</sub> = 1.1 kDa. SbCl<sub>3</sub> is able to co-catalyse the polymerisation by stabilising the growing carbenium ion, favouring propagation. Interestingly, the addition of SbCl<sub>3</sub> to a polymerisation of β-pinene is rather detrimental concerning reaction rate and molecular weight. The mechanism for the polymerisation of α-pinene involves two different pathways (see Figure 23). The first forms a *para*-menthene intermediate, as obtained during the β-pinene polymerisation mechanism, whereas the second pathway involves the

isomerisation into a saturated secondary bornane isomer.<sup>[127]</sup> The main chain of the resulting poly( $\alpha$ -pinene) contains both repeating units.

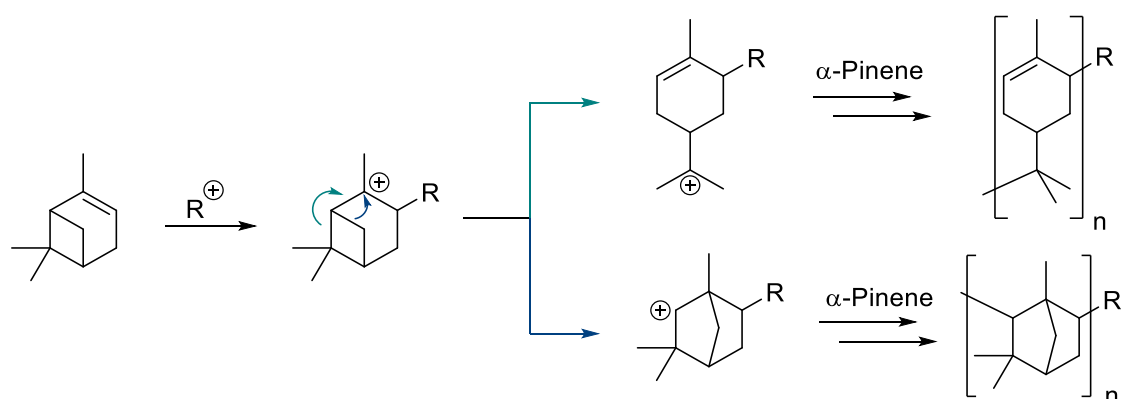


Figure 23: Two proposed mechanisms for the polymerisation of  $\alpha$ -pinene.<sup>[118]</sup>

### 2.8.1.3 Polymerisation of Limonene and Myrcene

For the polymerisation of limonene, different cationic polymerisation procedures have been described, including the application of a Ziegler-type catalyst. However, only low-molecular weight polymers have been achieved.<sup>[120, 128]</sup> Brum *et al.* recently studied the cationic polymerisation of limonene in more detail using  $AlCl_3$  and obtained a molecular weight around of 0.5 kDa and low conversion, which was attributed to chain termination *via*  $\beta$ -elimination.<sup>[129]</sup>

It is generally assumed that cyclic monoterpenes do not undergo radical homopolymerisation due to their high reactivity and ability to act as chain transfer agents.<sup>[119]</sup> Although there are a few studies that report radical homopolymerisation using azobisisobutyronitrile (AIBN), the obtained products are only oligomers ( $M_n \sim 0.9$  kDa).<sup>[130, 131]</sup> To achieve higher molecular weight and useful properties based on free-radical polymerisation of monoterpenes, they are used as co-monomers in the polymerisation of auxiliary synthetic monomers. In this context, many radical co-polymerisations of limonene with methacrylates,<sup>[132, 133]</sup> acrylonitrile,<sup>[134]</sup> styrene<sup>[135]</sup> and *N*-vinyl pyrrolidone<sup>[136]</sup> have been reported. One example was described by Kamigaito and co-workers who co-polymerised limonene and maleimides *via* radical polymerisation (see Figure 24).<sup>[137, 138]</sup>

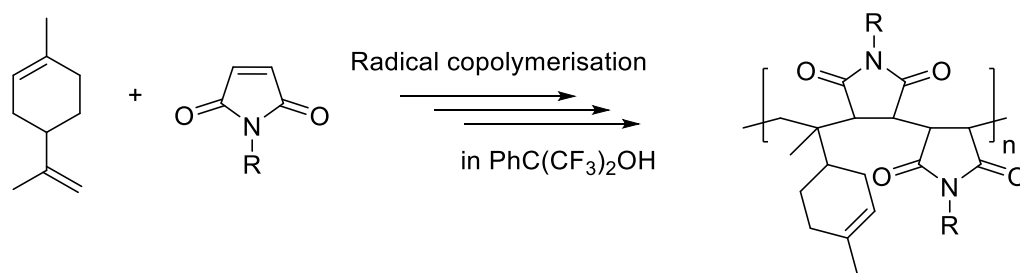


Figure 24: Copolymers obtained by sequence-regulated radical copolymerisation of limonene and functionalised maleimide derivatives.<sup>[138]</sup>

The polymerisation was conducted in 1,1,1,3,3,3-hexafluoro-2-phenyl-2-propanol and resulted in a 1:2 (limonene-maleimide) statistical copolymer with molecular weights ( $M_n$ ) up to 16.9 kDa.

While the introduction of synthetic co-monomers into the monomer feed increases the molecular weight and the material properties, it reduces at the same time the sustainability of the obtained polymers.

The acyclic monoterpene myrcene can be readily obtained by pyrolysis of  $\beta$ -pinene or from the essential oils of various plants.<sup>[139]</sup> Its three double bonds make myrcene an attractive candidate for cationic or radical polymerisation. Recently, Sarkar and Bhowmick introduced an environmentally benign emulsion polymerisation technique for the preparation of polymyrcene (see Figure 25, A).<sup>[140]</sup> The polymerisation was initiated by ammonium persulfate (APS) and resulted in high molecular weights (up to 93 kDa) and a very low glass transition temperature of -73 °C. Additionally, the polymer exhibited shear thinning behaviour, making it a promising candidate in the field of bio-based elastomers. More recently, Hilschmann and Kali presented the first approach to polymerise myrcene in a controlled way by applying reversible addition-fragmentation chain-transfer (RAFT) polymerisation (see Figure 25, B).<sup>[141]</sup> Using AIBN as initiator and ethyl 2-[(ethylthio)thiocarbonylthio]propionate as chain transfer agent, the polymerisation was run in bulk at 65 °C for three days. The obtained polymer showed low dispersities between 1.1 and 1.4 and exhibited a glass transition temperature of -60 °C. Nuclear magnetic resonance (NMR) spectroscopy validated that the polymer consisted of 96% 1,4 units, both *cis* and *trans*.

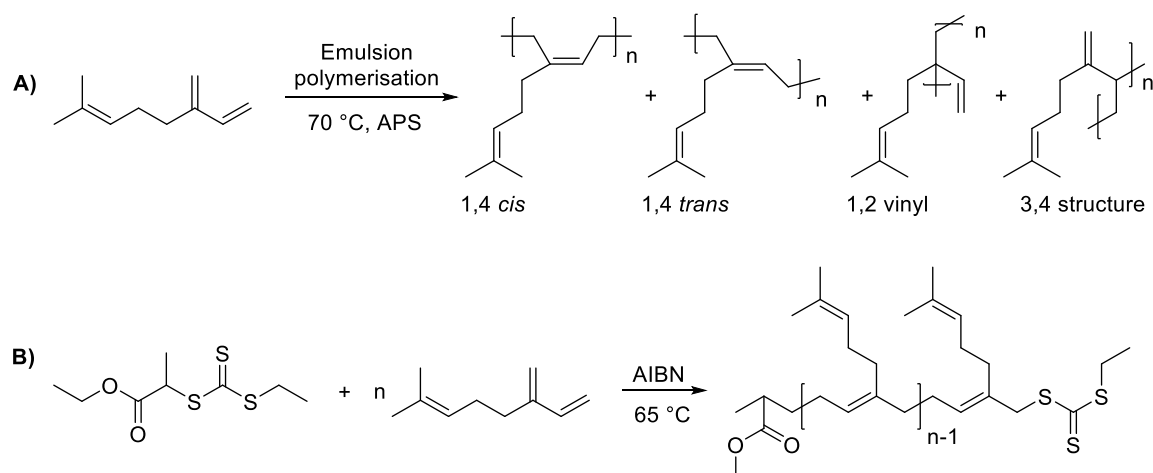


Figure 25: Two polymerisation procedures for the synthesis of polymyrcene: A) Emulsion polymerisation,<sup>[140]</sup> B) RAFT polymerisation.<sup>[141]</sup>

In 2014, a way of utilising myrcene for the synthesis of thermoplastic elastomers (TPEs) was presented by the group of Hillmyer and Hoye.<sup>[142]</sup> The authors synthesised an ABA triblock co-polymer by living anionic polymerisation (see Figure 26). Besides myrcene,  $\alpha$ -methyl-*p*-methylstyrene (AMMS) was used as the second co-monomer. AMMS can be obtained from limonene *via* a one-step dehydrogenation reaction applying Wacker-type reaction conditions.<sup>[143]</sup> For the synthesis of the triblock co-polymer, myrcene (MYR) was sequentially added to a solution of living poly( $\alpha$ -methyl-*p*-methylstyrene) (PAMMS-Li) to yield living PAMMS-PMYR-Li. Then, dichlorodimethylsilane, which served as a coupling agent, was added to the solution leading to PAMMS-PMYR-PAMMS triblocks. The resulting bio-renewable thermoplastic elastomer showed ultimate elongation of up to 1300%, low energy loss recovery attributes and competitive tensile strength compared to petroleum-derived styrenic TPEs. Additionally, the upper service temperature is about 70 °C higher than for current styrenic TPEs, making it attractive for high-temperature applications.

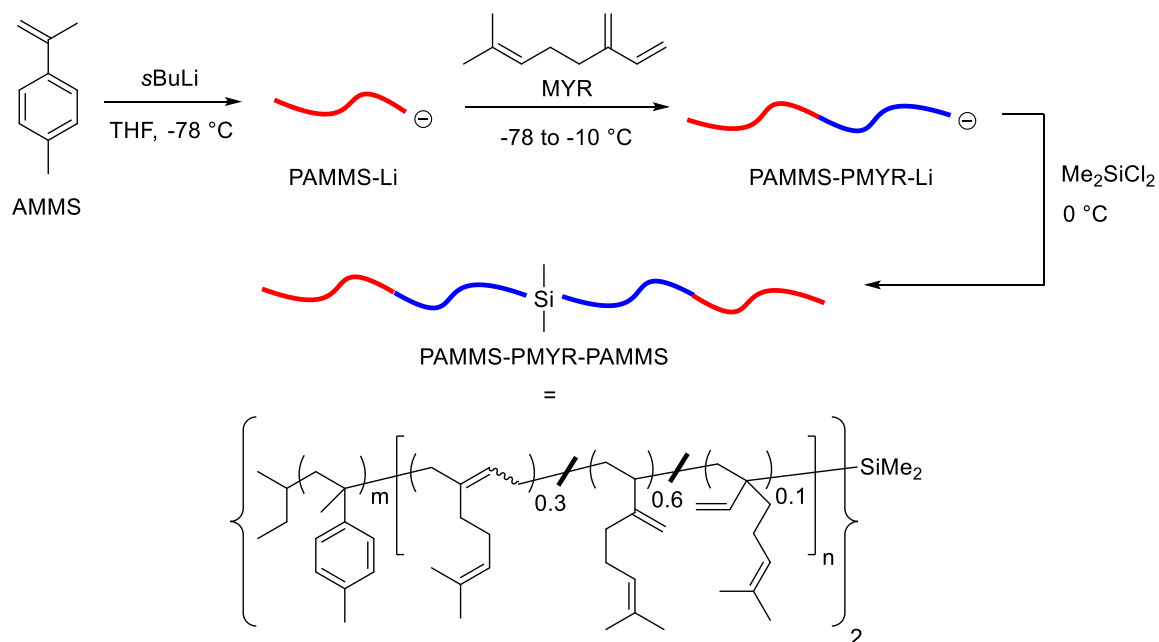


Figure 26: Synthesis of PAMMS-PMYR-PAMMS triblock copolymer by sequential anionic polymerisation of  $\alpha$ -methyl-*p*-methylstyrene (AMMS) and myrcene (MYR) and subsequent coupling with dichlorodimethylsilane.<sup>[142]</sup>

In conclusion, most of the direct polymerisation approaches of terpenes resulted in polymers that do not meet the requirements of commercially used plastics since they often lack the necessary properties. In this case the path of polymerising terpenes directly is futile even if the utilisation of renewable raw material is very desirable. For that reason, new approaches for the polymerisation of terpenes are highly appreciated.

## 2.8.2 Polymers from Functionalised Terpenes

Apart from the discussed direct polymerisation of terpenes, much research is focused on the controlled and sustainable functionalisation of terpenes to transform them into monomers for renewable polymers that can compete with current plastics. The following chapters show selected examples for the functionalisation of the terpenes  $\alpha$ - and  $\beta$ -pinene, limonene, myrcene, carvone and menthol; including the subsequent polymerisation methods.

### 2.8.2.1 $\alpha$ - $\beta$ -Pinene and Limonene

In order to establish a different way to polymerise unreactive  $\alpha$ -pinene by radical polymerisation techniques, Satoh and Kamigato quantitatively converted  $\alpha$ -pinene into pinocarvone under visible-light irradiation. Pinocarvone possesses a reactive exo-methylene group conjugated to the ketone moiety (see Figure 27).<sup>[144]</sup> The bicyclic vinyl



ketone was then homopolymerised *via* radical ring-opening polymerisation. After a reaction time of 18 h in hexafluoroisopropanol (HFIP) and with AIBN as initiator, a polymer with a high molecular weight of 26 kDa and a high glass transition temperature of 162 °C was obtained. The resulting polymer contained chiral six-membered rings with conjugated ketone units in the main chain and exhibited optical activity dependent on the number of ring-opened units.

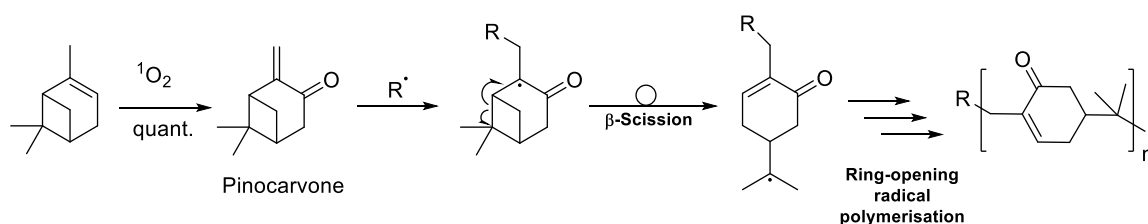
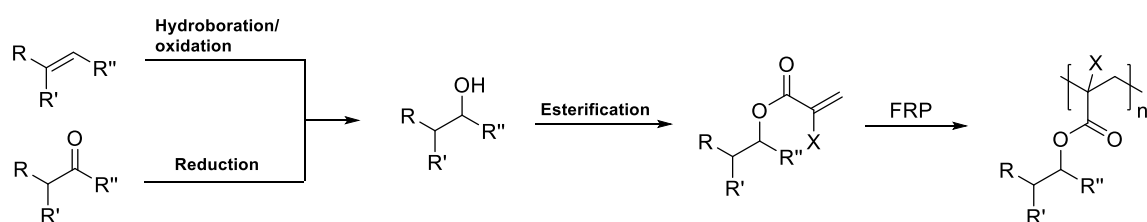


Figure 27: Selective ring-opening radical polymerisation of  $\alpha$ -pinene-derived pinocarvone.<sup>[144]</sup>

Recently, Howdle and Stockmann *et al.* developed new pinene- and limonene-based monomers through the addition of acrylate and methacrylate functionalities that can undergo free-radical polymerisation (FRP) (see Figure 28). Starting from  $\alpha$ - and  $\beta$ -pinene and limonene, the terpenes were transformed into alcohol derivatives by a hydroboration and oxidation sequence. In the case of (*R*)-(-)-carvone, reduction of the ketone functionality to the alcohol was achieved by lithium aluminium hydride. Considering the 12 principles of green chemistry, both procedures are unfavourable, since stoichiometric amounts of by-products are formed, resulting from the use of boranes and lithium aluminium hydride. The introduced alcohol functionality was then esterified using acryloyl or methacryloyl chloride with triethylamine as a base yielding (meth)acrylate monomers. In order to make the reaction “greener” and more sustainable by avoiding the use of toxic acryloyl and methacryloyl chloride, the authors established a reaction protocol using acrylic and methacrylic acid, which might become commercially available from renewable resources in the near future.<sup>[118]</sup> The esterification was then promoted by propyl phosphonic anhydride, only resulting in an environmentally benign, water-soluble triphosphate by-product. The monomers were polymerised by FRP with AIBN as initiator yielding polymers with molecular weights up to 24 kDa and glass transition temperatures ranging between 12 and 142 °C. By varying the terpene and acrylic acid starting material, the properties of the resulting polymer were tuned, making the approach an interesting candidate for useful polymers from renewable resources.

## Monomer synthesis and free-radical polymerisation (FRP)



## Monomers

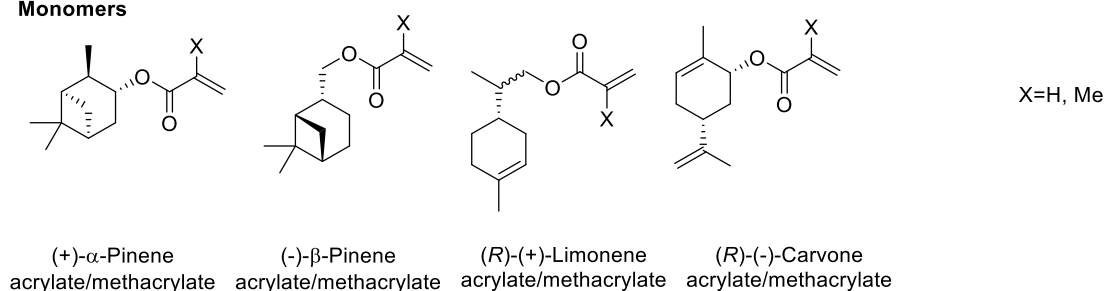


Figure 28: Synthesis of acrylate and methacrylate monomers based on various terpenes followed by free-radical polymerisation.<sup>[145]</sup>

To overcome the two-step synthesis of the monomers, the authors also introduced a more efficient one-step synthesis protocol for the methacrylic monomer based on  $\beta$ -pinene. The new catalytic protocol incorporates acrylates at allylic positions using C-H oxidation. The best conditions were found to be two equivalents of benzoquinone (BQ) and 2 mol% palladium(II) acetate in air at 50 °C, yielding 82% product. However, the use of stoichiometric amounts of BQ also leads to considerable amounts of waste which significantly decreases the sustainability of the reaction.

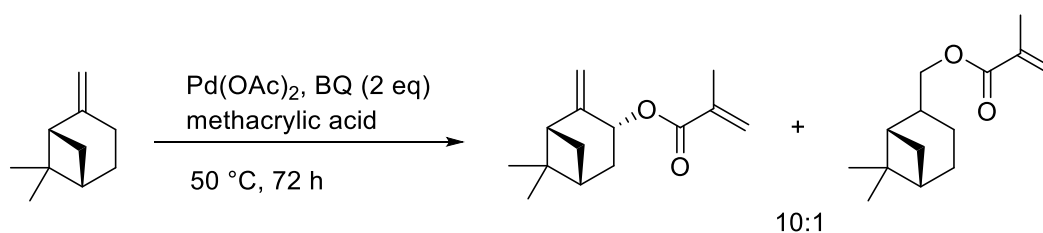


Figure 29: Catalytic C-H oxidation/coupling of  $\beta$ -pinene with methacrylic acid in a one-step procedure.<sup>[145]</sup>

Coates and co-workers used limonene oxide for the co-polymerisation with anhydrides.<sup>[146]</sup> The catalyst chosen was a highly active  $\beta$ -diiminate (BDI) zinc acetate catalyst that was previously shown to be highly active for the co-polymerisation of epoxides with CO<sub>2</sub> (see below (Figure 32)).<sup>[147]</sup> In the case of limonene oxide and maleic anhydride, the resulting novel aliphatic polyesters exhibited a molecular weight of  $M_n = 12$  kDa, narrow dispersity of 1.1 and a glass transition temperature of 62 °C. In 2011, Thomas *et al.* reported a new

strategy for the synthesis of alternating polyesters from dicarboxylic acids and epoxides based on tandem catalysis (see Figure 30).<sup>[148]</sup> The authors found that commercially available salen complexes were efficient catalysts for the cyclisation of dicarboxylic acids with commercially available dialkyl dicarbonates. When full conversion was indicated by NMR spectroscopy after a reaction time between 0.5 and 10 h at 40 °C in tetrahydrofuran (THF), volatile by-products were removed, and the resulting monomers polymerised without further purification. For the polymerisation step, the epoxide was added in toluene and the reaction was conducted at elevated temperatures. Tested epoxides include the terpene-based pinene oxide and limonene oxide, which gave molecular weights of up to  $M_n = 8.4$  kDa and  $M_n = 27$  kDa, respectively. Inspired by the work of Coates *et al.*, Duchateau and co-workers investigated the copolymerisation of limonene oxide and phthalic anhydride, using metal salen catalysts.<sup>[149]</sup> The authors found that chromium and aluminium catalysts in combination with the onium salt  $\text{PPN}^+\text{Cl}^-$  performed best. Additionally, the authors investigated the application of various mono-, di-, and trifunctional chain transfer agents including alcohols, acids and amines to afford (poly)-functionalised polyesters.

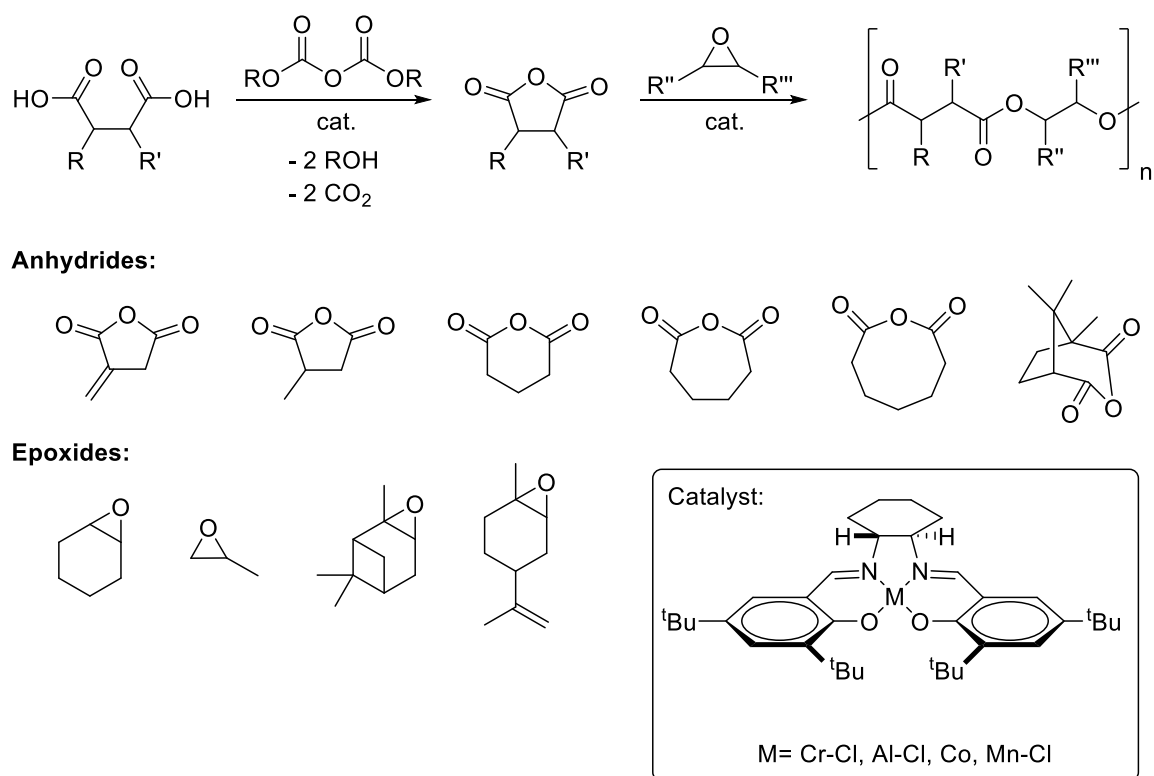


Figure 30: Tandem synthesis of aliphatic polyesters from epoxides and anhydrides. Salen-complexes are efficient catalysts for the cyclisation of dicarboxylic acids and the subsequent polymerisation of the resulting anhydride with epoxides.<sup>[148]</sup>

In 2015, Coates and co-workers similarly described the alternating copolymerisation of propylene oxide with terpene-based cyclic anhydrides catalysed by chromium, cobalt and aluminium salen complexes (see Figure 31).<sup>[150]</sup> The anhydride monomers were synthesised by Diels-Alder reaction of maleic anhydride with 1,3-cyclohexadiene,  $\alpha$ -phellandrene and  $\alpha$ -terpinene, respectively. The authors found a high dependency of the polymerisation conditions and the choice of catalyst on the molecular weight distribution, the glass transition temperature and the relative stereochemistry of the diester units along the chain. When the Diels-Alder adduct of  $\alpha$ -terpinene and maleic anhydride was co-polymerised with propylene oxide, catalysed by an aluminium salen complex, the resulting polymer exhibited a high molecular weight of  $M_n = 55.4$  kDa, narrow dispersity ( $\mathcal{D} = 1.3$ ) and a high glass transition temperature of 109 °C. The low cost of the monomer and the high bio-content make these polyesters an interesting alternative to fossil-based high- $T_g$  polymers.

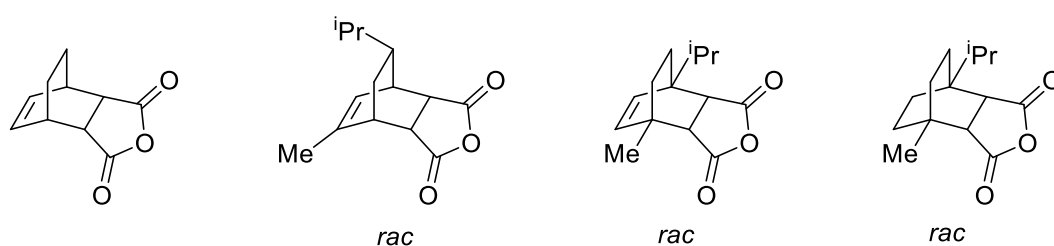


Figure 31: Cyclic anhydride comonomers: The first three were obtained by reacting 1,3-cyclohexadiene,  $\alpha$ -phellandrene and  $\alpha$ -terpinene, respectively, with maleic anhydride in a Diels-Alder reaction. The fourth was obtained by catalytic hydrogenation of the third one.<sup>[150]</sup>

Another promising approach for the transformation of limonene into bio-based and potentially bio-degradable polymers is the ring-opening copolymerisation (ROCOP) of limonene oxide with CO<sub>2</sub> to produce linear polycarbonates. Coates and co-workers utilised BDI zinc acetate complexes for the polymerisation on account of their high activity known from prior research on the co-polymerisation of petroleum-based cyclohexene oxide and CO<sub>2</sub> (see Figure 32).<sup>[151]</sup> The authors studied the effect of temperature, pressure and various ligands on the molecular weight and the dispersity of the resulting polymers.<sup>[152]</sup> Under optimised conditions of 0.2 mol% catalyst over 24 h at 25 °C and 7 bar CO<sub>2</sub>, a high molecular weight regio- and stereoregular alternating polycarbonate ( $M_n = 25$  kDa), with a narrow dispersity of  $\mathcal{D} = 1.16$  was obtained. At higher temperatures (50 °C), the copolymerisation yielded the regioirregular poly(limonene carbonate) with a broadened molecular weight distribution ( $\mathcal{D} = 1.34$ ) and 13% *cis*-isomer in the co-polymer. The drawback of this polymerisation technique is the superior selectivity to the *trans*-limonene

isomer compared towards the *cis*-isomer, leading to a considerable amount of unreacted starting material.

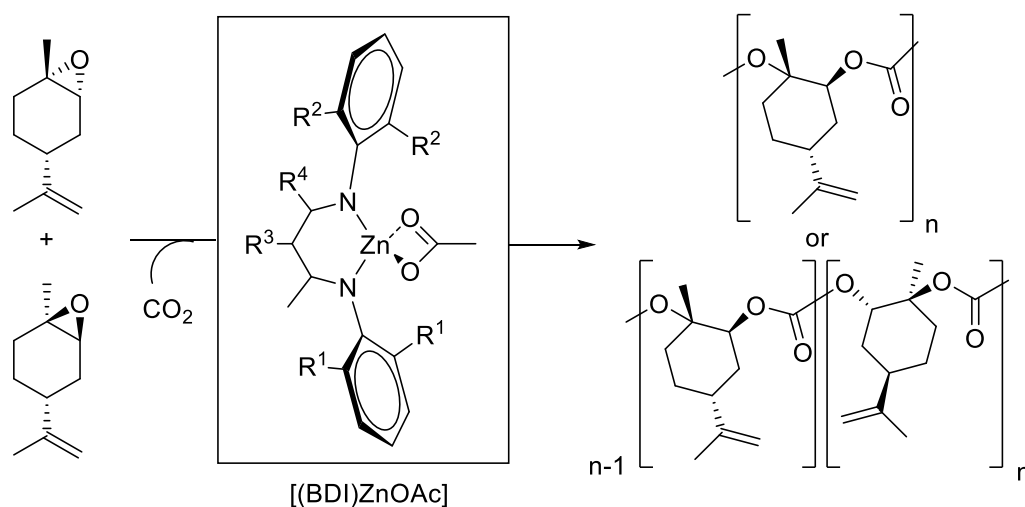


Figure 32: Copolymerisation of *trans*- and *cis*-(*R*)-limonene oxide and  $\text{CO}_2$  using  $\beta$ -diimine zinc acetate complexes as catalyst.<sup>[152]</sup>

In order to overcome this disadvantage, Greiner *et al.* established a synthesis protocol for the stereoselective synthesis of *trans*-limonene oxide without hydroxy impurities (see Figure 33).<sup>[44]</sup> The synthesis protocol starts with a slightly modified procedure of the two-step synthesis of *trans*-limonene oxide from (*R*)-limonene developed by Gurudutt and coworkers.<sup>[153]</sup> The first step involves the synthesis of the *endo*-cyclic bromohydrin (regio and stereoselective for limonene) with *N*-bromosuccinimide (NBS) in aqueous acetone. In a second step, the bromohydrin is transformed into the corresponding epoxide by the addition of aqueous sodium hydroxide (see Figure 33, A). However, the obtained product contained impurities with hydroxyl groups that could neither be removed by simple distillation nor by chromatographic methods, but act as chain transfer agent and lower the molecular weight in polymerisations. Therefore, the hydroxyl groups were masked through *O*-methylation *via* Williamson ether synthesis with sodium hydride as deprotonating agent and methyl iodide as *O*-methylating moiety (see Figure 33, B). The methylated mixture was then fractionally distilled resulting in 85% *trans*-limonene oxide and mainly *cis*-limonene oxide as by-product. The monomer synthesis and the subsequent copolymerisation were conducted in kilogram-scale and yielded 1.2 kg poly(limonene carbonate) with a very high molecular weight of 109 kDa and a low dispersity ( $\mathcal{D} = 1.13$ ). To remove the  $\beta$ -diimine zinc acetate catalyst from the polymer without precipitation, which would require considerable amounts of solvent, amide coupled ethylenediaminetetraacetic acid (EDTA) on silica was applied. EDTA on silica was easily filtered from the solution reducing the amount of organic solvents employed by a factor 10,

compared to standard precipitation methods. The high glass transition temperature of 130 °C, which is close to that of bisphenol A (BPA)-based polycarbonate, and the transparency make the obtained poly(limonene carbonate) a promising candidate for bio-based coating materials. Albeit efficient, a less hazardous masking agent than iodomethane has yet to be reported for such reactions.

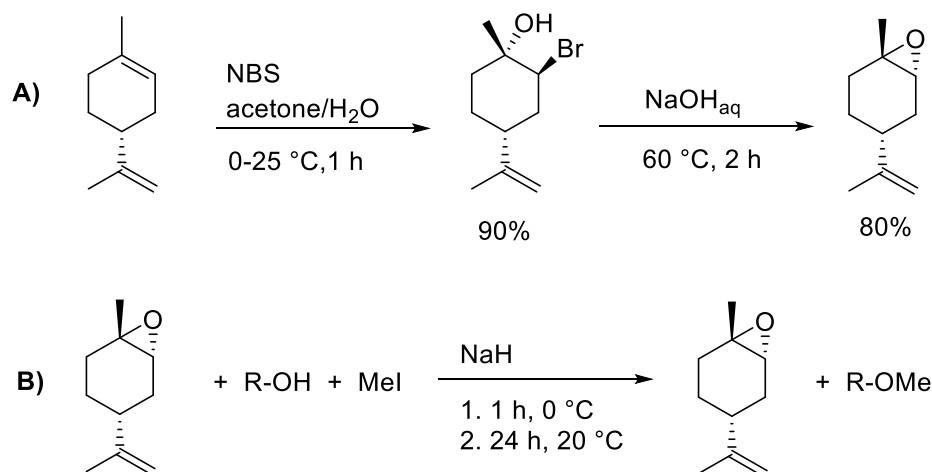


Figure 33: A) Stereoselective synthesis of trans-limonene oxide via the corresponding trans-bromohydrin and subsequent ring-closing by the addition of a base; B) O-Methylation of OH-impurities with sodium hydride and methyl iodide.<sup>[44]</sup>

Greiner *et al.* showed that the double bond, which poly(limonene carbonate) possesses in every repeating unit, can be exploited for further chemical modifications.<sup>[154]</sup> Thiol-ene reactions proved to be a versatile technique for introducing hydrophilicity, pH-dependent solubility or antibacterial activity (by functionalisation with quaternary amines) to the polymer. By addition of butyl-3-mercaptopropionate, the thermoplastic poly(limonene carbonate) was turned into a rubbery material. The authors also demonstrated a synthetic route to obtain the saturated counterpart of poly(limonene carbonate), which has a lower reactivity and therefore exhibits improved heat processability which is important for extrusion and injection moulding. Kleij and co-workers, post-synthetically modified poly(limonene carbonate) to synthesise poly(limonene dicarbonate) (PLDC) in two steps.<sup>[155]</sup> In the first step, the double bonds of poly(limonene carbonate) were epoxidised to obtain poly(limonene-8,9-oxide carbonate) using *meta*-chloroperoxybenzoic acid (*m*CPBA). Then, in the second step, the epoxy groups of poly(limonene-8,9-oxide carbonate) were reacted with CO<sub>2</sub> applying an air-stable Al(III) complexes as catalyst. The obtained PLDC exhibited molecular weights of up to 15.3 Da and tuneable and very high *T<sub>g</sub>* values of up to 180 °C. Another way to obtain PLDC was demonstrated by Sablong *et al.* by polymerising limonene dioxide with CO<sub>2</sub> using a zinc β-diiminate complex as

catalyst.<sup>[156]</sup> The obtained poly(limonene-8,9-oxide carbonate)s showed glass transition temperatures up to 135 °C and were subsequently converted into PLDC by CO<sub>2</sub> insertion catalysed by lithium bromide. Additionally, the authors demonstrated the modification of the epoxy groups present in these polycarbonates using thiols or carboxylic acids in combination with lithium hydroxide or tetrabutylphosphonium bromide as catalysts, respectively. The molecular weight of the functionalised polycarbonates ranged between 11.8 and 14.2 kDa. Kleij and Martín further exploited the double bond of limonene in polycarbonates *via* thiol-ene cross-linking.<sup>[157]</sup> For this, the authors prepared terpolymers derived from non-functional cyclohexene oxide, functional limonene oxide and CO<sub>2</sub> using a binary combination of an Al<sup>III</sup>(aminotriphenolate) complex (see below, Figure 48) and bis(triphenylphosphine)iminium chloride (PPNCl) as catalytic system. The obtained polycarbonates featured a controllable number of olefinic groups in their terpolymer backbone, which were subsequently crosslinked through thiol-ene reactions with dithiols such as 1,2-ethanedithiol. After crosslinking, the networks showed improved thermal properties and glass transition temperatures of up to 150 °C. Koning and Williams *et al.* also investigated the thiol-ene crosslinking reactions of low molecular weight poly(limonene carbonate) ( $M_n = 4.2$  kDa) obtained with the aforementioned binary catalytic system.<sup>[158]</sup> The low molecular weight was targeted to minimise the melt viscosity with regard to the desired coating applications. For the cross-linking reaction, the commercial trithiol trimethylolpropane tris(3-mercaptopropionate) was used in the presence of a photo-initiator. The resulting thermosets were evaluated as coatings, showing promising properties in terms of scratch and solvent resistance.

In 2015, Coates *et al.* synthesised enantiomerically pure, regioregular isotactic poly((*R*)-limonene carbonate) as the first example of an amorphous, enantiomerically pure polymer that became crystalline *via* stereocomplexation with its complementary enantiomer poly((*S*)-limonene carbonate).<sup>[159]</sup> As with other biodegradable stereocomplex polymers, the authors suggested biomedical uses, such as drug delivery, tissue engineering and nanostructured surfaces as potential applications.

Photoinitiated cationic ring-opening polymerisation constitutes another method for the utilisation of limonene oxide and  $\alpha$ -pinene oxide as renewable raw material for polymers. Crivello *et al.* investigated the reactivity of these monomers for cationic polymerisation using diaryliodonium salts and triarylsulfonium salts as photoinitiators.<sup>[160]</sup> The study showed that  $\alpha$ -pinene oxide is more reactive than limonene oxide, since it is able to simultaneously undergo ring-opening reaction of the epoxide group and of the cyclobutane ring, however, it also undergoes undesirable side reactions. Due to the competing side reactions, the cationic ring-opening polymerisations of limonene oxide and  $\alpha$ -pinene oxide

result in low-molecular weight polymers, limiting the use of these monomers for the production of homopolymers. However, as demonstrated by the authors, these bio-sourced terpene epoxide monomers are highly beneficial as co-monomers in photoinitiated cationic crosslinking polymerisations (see Figure 34). The benefits of adding these monomers to crosslinking photocopolymerisations with multifunctional epoxide and oxetane monomers included lowered viscosity, polymerisation rate enhancement and shortening of the induction periods.

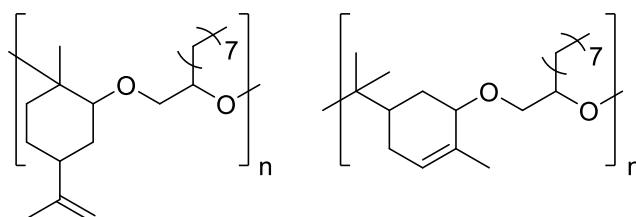


Figure 34: Structural elements of the co-polymers derived from limonene oxide and  $\alpha$ -pinene oxide with 1,2-epoxydecane.<sup>[160]</sup>

Thiol-ene additions are known to proceed either through a free-radical addition mechanism when initiated by light, heat or radical initiators or a Michael addition mechanism when catalysed by a base or a nucleophile (see thia-Michael addition). Radical thiol-ene additions represent an interesting reaction type for the efficient introduction of functional groups into terpene monomers, as well as for their polymerisation. The reaction between an aliphatic thiol and an alkene leads to *anti*-Markownikow addition products and has been extensively used over the past century.<sup>[161]</sup> Due to the tolerance of various functional groups, regioselectivity, compatibility with water and oxygen, generally high yields and reaction rates, together with a high atom efficiency, thiol-ene reactions can in some cases be considered as “click” reactions, when they comply with most of the “click” features.<sup>[162, 163]</sup> Although the thiol-ene addition can start *via* self-initiation,<sup>[164]</sup> it is usually performed with a radical initiator such as AIBN or 2,2-dimethoxy-2-phenylacetophenone (DMPA). In the first step, a radical provided from the radical initiator reacts with the thiol to form a thiyl radical (see Figure 35). Then, the alkene reacts with the thiyl radical resulting in a secondary carbon radical. This reaction step is reversible and thus *cis/trans* isomerisation is possible.<sup>[165]</sup> The secondary carbon radical, in turn, undergoes an irreversible chain transfer reaction with another thiol, yielding the desired addition product and a new thiyl radical, starting the reaction cycle again.



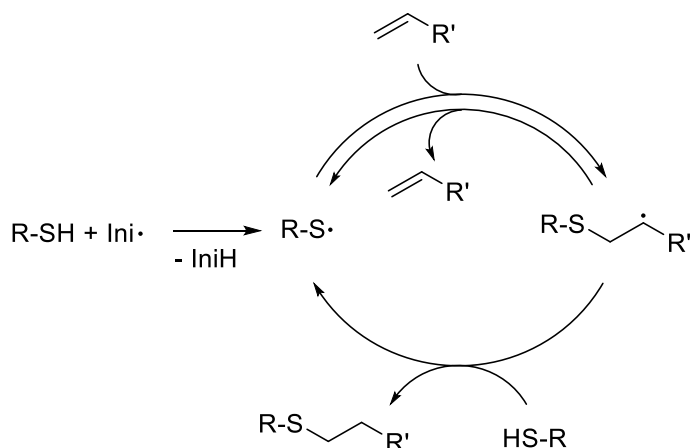
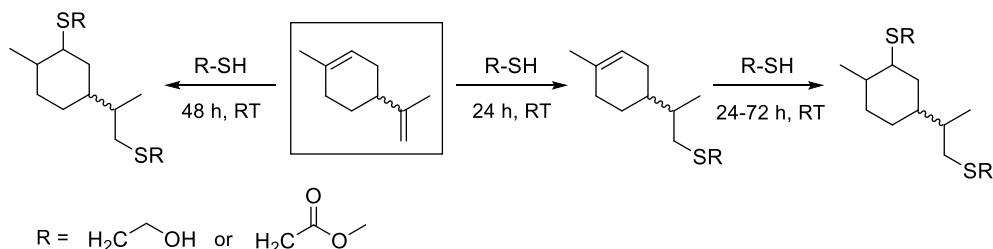


Figure 35: General mechanism of thiol-ene additions.<sup>[166]</sup>

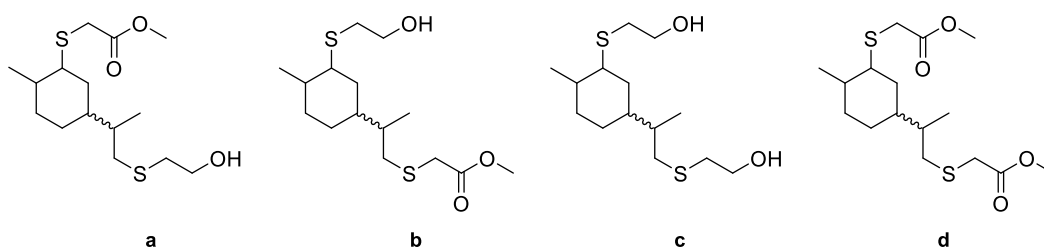
Radical thiol-ene reactions can be applied either as a polymerisation technique for AA- or AB-type monomers, or to introduce polymerisable functional groups into monomers for the subsequent polymerisation. In 2011, the Meier working group chose the latter approach to synthesise various difunctional and heterodifunctional monomers for polyester synthesis (see Figure 36).<sup>[167]</sup> The two double bonds in limonene (exocyclic and endocyclic) possess considerable differences in reactivity. Therefore, it was possible to selectively functionalise the more reactive exocyclic one and leave the endocyclic double bond unreacted to introduce another thiol with a different functional group in a second reaction step. This led to heterodifunctional limonene monomers. For the introduction of methyl ester and alcohol groups, limonene was reacted with 2-mercaptoethanol and methyl thioglycolate in the absence of solvent and radical initiator at room temperature. The authors optimised the terpene to thiol ratios for the diaddition product, resulting in two difunctional monomers, containing either two alcohol groups or two methyl ester groups. Furthermore, the ratios for the monoaddition were optimised and the products were obtained in good yields after column chromatography. Subsequently, the monofunctionalised products were subjected to a second thiol addition, yielding two heterodifunctional monomers containing both a methyl ester and an alcohol functionality. The polycondensations were conducted at 120 °C under reduced pressure with 5 mol% 1,5,7-triazabicyclo[4.4.0]dec-5-ene (TBD) as transesterification catalyst. Even though TBD has a high transesterification activity, the copolymerisation between the diester and the diol only resulted in oligomers. In contrast, the homopolymerisation of the heterodifunctional monomers produced polyesters with low molecular weights between 7.7 and 10.5 kDa and dispersities from 1.65 to 1.89. The low molecular weight was attributed to the steric hindrance of the bulky cyclic structure of the terpene preventing the catalyst from accessing the reactive centres. Therefore, when long-chain fatty ester-based diols and diesters derived from castor oil were used as co-

monomers for the difunctional limonene monomers, polyesters with  $M_n$  up to 25 kDa were obtained. In this case, long-chain fatty ester-based diols and diesters served as long-chain spacers, reducing the effect of the steric hindrance of the bulky limonene molecule.

### A) Monomer synthesis



### B) Monomers



### C) Polymerisation

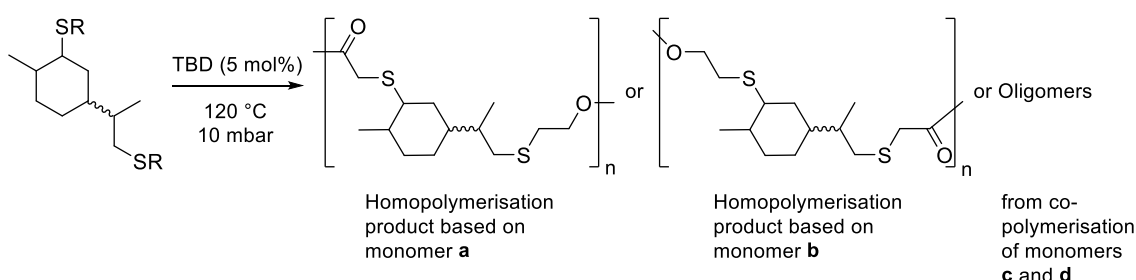
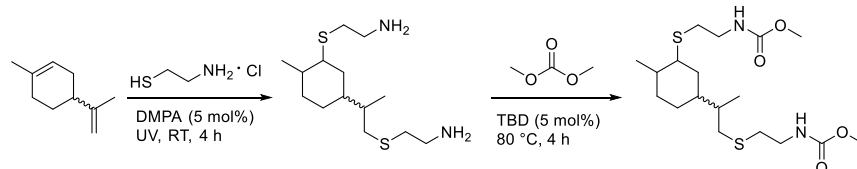


Figure 36: A) Monomer synthesis via diadditions or mono- and subsequent diadditions of thiols to limonene; B) resulting monomers; C) homopolymerisation of heterodifunctional monomers **a** and **b**, respectively, and copolymerisation of difunctional monomers **c** and **d** (yielding oligomers).<sup>[167]</sup>

More recently, in 2013, the Meier working group established a synthesis protocol for polyamides and isocyanate-free polyurethanes based on a limonene-derived diamine, dicarbamate and diol obtained *via* thiol-ene reactions (see Figure 37).<sup>[168]</sup> To synthesise the diamine, limonene was reacted with cysteamine hydrochloride. The thiol-ene addition was performed under UV irradiation using DMPA as photoinitiator and a small amount of ethanol as a solvent. After column chromatography, the diaddition products of (*R*)-(+)-limonene and (*S*)-(-)-limonene were obtained in 84 and 81% yield, respectively. In a second step, the diamines were further transformed in order to introduce a carbamate functionality. For the methoxycarbonylation of the diamines, dimethyl carbonate in

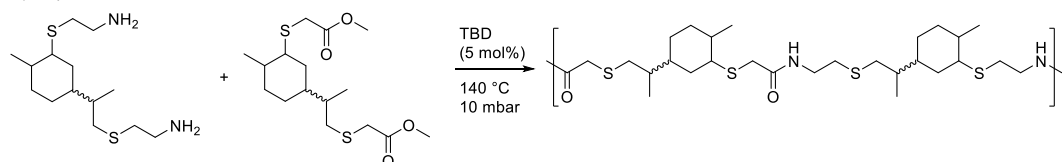
combination with TBD as an organocatalyst was used, instead of toxic phosgene or chloroformates. After 4 h at 80 °C in bulk, the limonene-derived carbamates were purified *via* column chromatography and received in 82 and 79% yield, respectively. Finally, limonene-based diamines and the aforementioned limonene-based diesters were copolymerised in a polycondensation reaction, catalysed by TBD at 140 °C and reduced pressure. The resulting polyamides exhibited low molecular weights up to 7.8 kDa. Through the combination of the limonene-based diamine monomers with less bulky, long-chain fatty acid derived diesters or hexamethylenediamine and dimethyl adipate (Nylon 6,6), higher molecular weights up to 12 kDa were achieved. In a second approach, the limonene-derived dicarbamates were employed for polycondensation reactions with several renewable diols, including the formerly discussed limonene-based diol. The obtained linear isocyanate-free polyurethanes were obtained at molecular weights between 6.1 and 12.6 kDa.

#### Monomer synthesis



#### Polymerisations

##### A) Polyamides



##### B) Polyurethanes

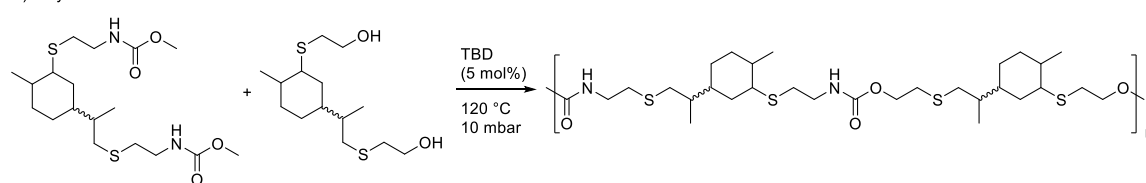
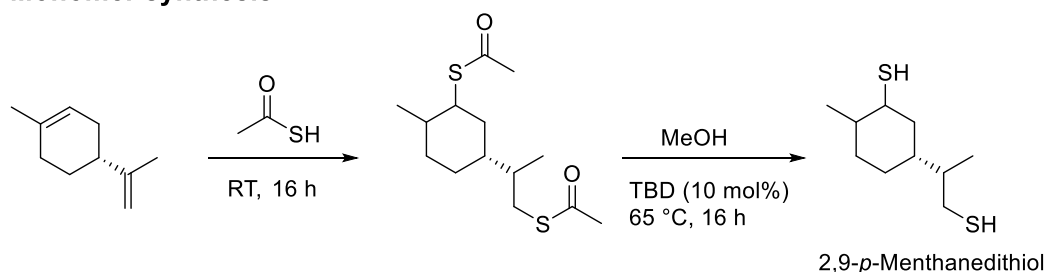


Figure 37: Synthesis of limonene-derived diamine and dicarbamate monomers for the synthesis of A) polyamides; and B) polyurethanes.<sup>[168]</sup>

Additionally, in 2013, Meier, Metzger and co-workers, reported the application of dithiol-functionalised limonene and a bio-based monomer from castor oil for thiol-ene copolymerisations (see Figure 38). 2,9-*p*-Menthanedithiol is a commercially available product, however, it was easily synthesised in high yield (90%) by thiol-ene addition of thioacetic acid to limonene and subsequent TBD-catalysed saponification of the resulting thioester. The synthesis procedure was adapted and slightly modified from a protocol reported by Marvel and Olsen.<sup>[169]</sup> The thiol-ene copolymerisation of the limonene-based

dithiol and castor oil-derived di-10-undecenyl ether (obtained *via* GaBr<sub>3</sub>-catalysed reduction of 10-undecenyl 10-undecenoate) was photochemically initiated with DMPA in bulk resulting in a high molecular weight polymer ( $M_n = 31.8$  kDa).

### Monomer synthesis



### Polymerisation

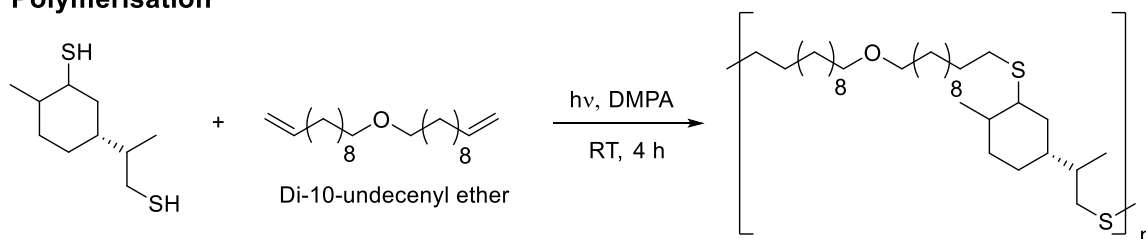


Figure 38: Synthesis of a limonene-based dithiol monomer and subsequent co-polymerisation with a castor oil-derived diene via thiol-ene reaction.<sup>[170]</sup>

Exploiting a similar concept as Meier *et al.*, Zhang and co-workers used the limonene-based diol, resulting from the thiol-ene diaddition of 2-mercaptoethanol to limonene, for the synthesis of elastomers.<sup>[171]</sup> For this purpose, the authors reacted the limonene-based diol with several diacids, such as sebacic acid, succinic acid, itaconic acid and maleic anhydride, as comonomers in the presence of tetra-*n*-butyltitanate as catalyst and under constant vacuum (200 mbar) *via* melt polycondensation. Apart from the polyester based on maleic anhydride ( $M_n = 186$  kDa,  $\bar{D} = 4.6$ ), molecular weights between 3.1 and 8.7 kDa and dispersities between 2.1 and 4.1 were achieved. To further process the obtained elastomers, the products were mixed with dicumyl peroxide resulting in cross-linked elastomers.

In order to synthesise a bio-based analogue of a plastic that is already in use, Colonna *et al.* produced the commodity monomer terephthalic acid from limonene and butanediol from bio-succinic acid (see Figure 39).<sup>[172]</sup> After polymerisation, high molecular weight poly(butylene terephthalate) (PBT,  $M_n = 44$  kDa) with thermal properties ( $T_m = 222$  °C) very close to those of commercial PBT ( $T_m = 223$  °C) was obtained. However, this synthesis protocol of bio-based poly(terephthalic acid) cannot be considered as green due to the use stoichiometric amounts of oxidising agents leading to increased waste formation.

This shows that merely utilising a renewable resource for the synthesis of a polymer does not necessarily lead to a commercially viable or sustainable route to a polymeric material.

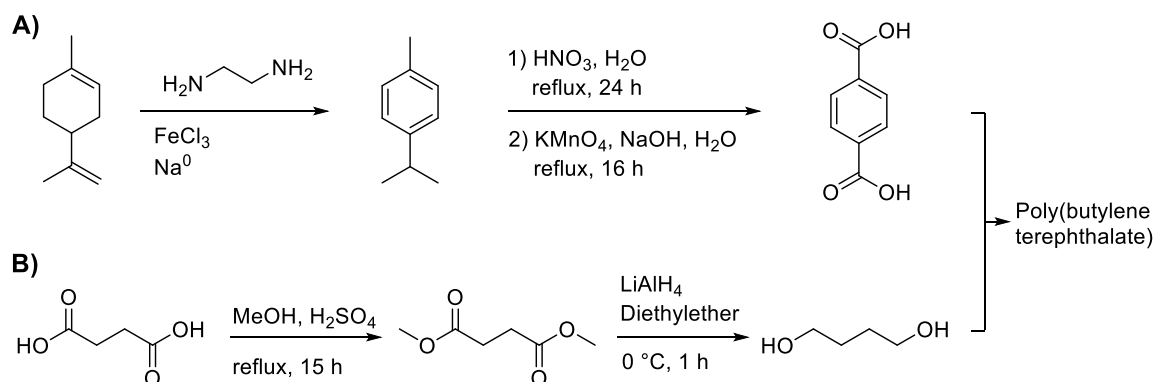


Figure 39: A) Synthesis of terephthalic acid from limonene; B) Butanediol synthesis from succinic acid; and terephthalate polyester synthesis.<sup>[172]</sup>

### 2.8.2.2 Myrcene

Hillmyer, Hoyer and co-workers utilised ring-closing metathesis (RCM) for the synthesis of 3-methylenecyclopentene from myrcene (see Figure 40).<sup>[173]</sup> Cationic polymerisation of 3-methylenecyclopentene afforded regiopure 1,4-poly-3-methylenecyclopentene with a molecular weight of up to 22 kDa and a narrow molecular weight distribution ( $\mathcal{D} = 1.21$ ). The polymerisation was initiated by a *i*-BuOCH(Cl)Me/zinc chloride/Et<sub>2</sub>O system in toluene at -40 °C and showed excellent control of the molecular weight. The end groups were identified as exploitable 1,3-cyclopentadienyl groups. However, drawbacks of this procedure are the low yield of the RCM (45%) and the use of an expensive ruthenium metal catalyst.

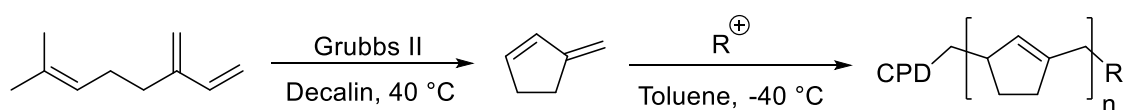


Figure 40: Ring-closing metathesis of myrcene to 3-methylenecyclopentene and subsequent cationic polymerisation with *i*-BuOCH(Cl)Me/Lewis Acid/Et<sub>2</sub>O in toluene.<sup>[173]</sup>

### 2.8.2.3 Carvone and Menthol

(4*S*)-(+)-Carvone is the main constituent of caraway (*Carum carvi*) and dill (*Anethum graveolens*) seed oil, whilst (4*R*)-(+)-carvone is the main constituent of spearmint (*Mentha spicata*).<sup>[174]</sup> Dihydrocarvone can be produced by the hydrogenation of carvone or by the oxidation of limonene. Hillmyer, Tolman and co-workers oxidised dihydrocarvone to the

corresponding epoxy lactone using *m*CPBA (see Figure 41).<sup>[175]</sup> The resulting epoxy lactone was applied as multifunctional monomer and cross-linker for ring-opening polymerisations (ROP). However, homopolymerisations using diethyl zinc or tin(II) 2-ethylhexanoate resulted in low molecular weight oligomers with apparent  $M_n$  values of less than 2.5 kDa. Co-polymerisations between  $\epsilon$ -caprolactone and 0.3 to 50% of the epoxy lactone, in turn, yielded cross-linked materials with shape memory properties. In another study by Hillmyer, Tolman and co-workers, the authors chose Oxone<sup>®</sup> as the oxidant for the Baeyer-Villiger reaction to avoid the epoxidation of the terminal double bond of dihydrocarvone (see Figure 41).<sup>[176]</sup> The obtained dihydrocarvide was polymerised by ROP in bulk at 100 °C using diethyl zinc as a catalyst and benzoyl alcohol as the initiator. In a second approach, dihydrocarvone was first hydrogenated by using Wilkinson's catalyst to give carvomenthone, which was transformed into carvomenthide using *m*CPBA for the Baeyer-Villiger reaction. Carvomenthide was also polymerised *via* ROP. The resulting aliphatic polyesters exhibited a high molecular weight of  $M_n = 62.3$  kDa, a narrow molecular weight distribution ( $\mathcal{D} = 1.16$ ) and a  $T_g$  of -27 °C in the case of the poly(carvomenthide), while for poly(dihydrocarvide) a lower  $M_n$  of 10.5 kDa, a dispersity of  $\mathcal{D} = 1.24$  and a  $T_g$  of -20 °C was reported. Additionally, both monomers were co-polymerised and the double bonds in poly(dihydrocarvide) were modified by post-polymerisation reactions, such as radical-induced crosslinking and epoxidation. It should, however, be noted that the synthesis of the polymerizable monomers using of oxidising agents, such as Oxone<sup>®</sup> and *m*CPBA cannot be considered as sustainable, since stoichiometric amounts of waste is formed during the reaction.

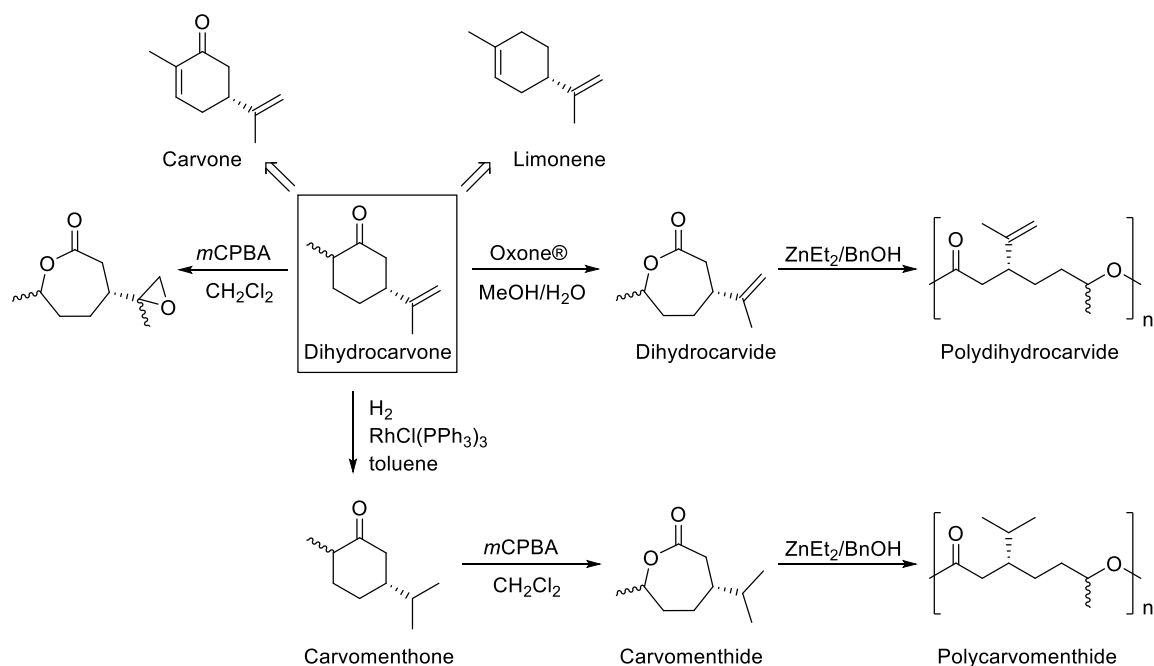


Figure 41: Retrosynthesis of dihydrocarvone and synthesis of dihydrocarvone-based lactones followed by polymerisation to polydihydrocarvide and polycarvomenthide.<sup>[175, 176]</sup>

Menthol is commercially available in its oxidised form, known as menthone. Similar to the previously mentioned ROP of dihydrocarvone-based monomers, Tolman, Hillmyer *et al.* transformed menthone into the lactone monomer menthide *via* Baeyer-Villiger oxidation using *m*CPBA.<sup>[177]</sup> Subsequently, menthide was polymerised by ROP using a highly active zinc alkoxide catalyst, which allowed to perform the reaction at room temperature for 8.5 h. The molecular weight of the resulting polyester was tuned by adjusting the monomer-to-catalyst ratio and ranged from 3 to 91 kDa with  $\bar{D}$  values below 1.6.

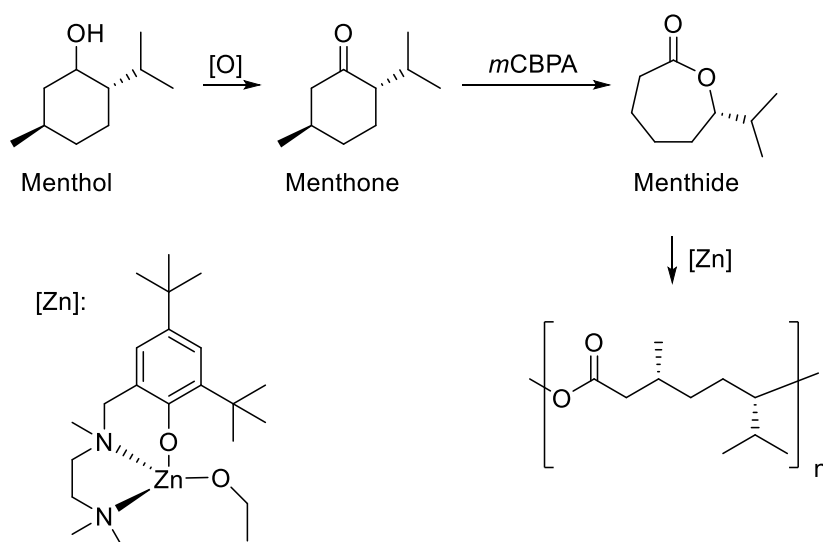


Figure 42: Synthesis of menthone from menthol followed by Baeyer-Villiger oxidation to give menthide and polymerisation of menthide using a defined Zn alkoxide catalyst.<sup>[177]</sup>

The same group also synthesised thermoplastic elastomers based on renewable triblock copolymers that contain polymenthide (PM).<sup>[178]</sup> This was achieved by ROP of menthide in the presence of diethylene glycol followed by termination with water, affording  $\alpha,\omega$ -dihydroxy polymenthide (HO-PM-OH).<sup>[179]</sup> The obtained telechelic polymer was treated with triethylaluminium, which resulted in the corresponding aluminium alkoxide macroinitiator. The macroinitiator was used for the controlled polymerisation of lactide to yield polylactide-*b*-polymenthide-*b*-polylactide triblock copolymers (PLA-PM-PLA). Later, a new method for the synthesis of PLA-PM-PLA triblock co-polymers, which show promise as hydrolytically degradable pressure-sensitive adhesives, was reported by the same group.<sup>[180]</sup> In another study, HO-PM-OH was functionalised *via* esterification with 2-bromoisobutyryl bromide to give bromo-terminated polymenthide.<sup>[181]</sup> The latter was used as macroinitiator for atom transfer radical polymerisation (ATRP) with methylene butyrolactone (MBL). The obtained triblock co-polymer (PMBL-PM-PMBL) was proposed to serve as a useful candidate for renewable high-performance thermoplastic elastomers.

Using a similar approach as for the ROP of carvone- and menthone-based lactones, the Beckmann rearrangement can be utilised to produce lactams from menthone for subsequent ROP. It is known that menthone can be transformed into its oxime followed by the transformation into the corresponding lactam.<sup>[182-184]</sup> The second regioisomeric lactam has been reported.<sup>[185]</sup> In 2014, Rieger *et al.* synthesised both lactams starting from menthone *via* oxime and Beckmann rearrangement.<sup>[186]</sup> The authors also reported the ROP of these lactams using anionic or acid-catalysed conditions. The use of potassium as initiator and benzoyl chloride as co-initiator, however, resulted in alkyl-substituted and stereocenter-containing oligoamides ( $M_n$  approximately 0.5 kDa). An acid-catalysed hydrolytic procedure at 230 °C also resulted in oligomerisation, but only for lactam **a** (see Figure 43). Lactam **b** was not converted, due to the steric hindrance of the bulky isopropyl group next to the amino group. More recently, the Rieger working group developed a regioselective one-step synthesis route from menthone to lactam **b**, using hydroxylamine-*O*-sulfonic acid (HOSA).<sup>[187]</sup> The procedure also proceeds *via* Beckmann rearrangement, but without any necessary isolation of oxime species. Again, acid induced and neutral ROP, this time induced by benzoylated caprolactam, produced only oligoamides. In another approach, the free amino acid, which can be obtained by treatment of lactam **b** with sulfuric acid/H<sub>2</sub>O, was first isolated and then polymerised. However, polycondensation resulted in oligomerisation, although monomer was still present. These findings were assumed to be due to precipitation from bulk. In 2016, Winnacker and Rieger *et al.* improved the ROP of menthone-derived lactams by using sodium hydride or potassium *tert*-butoxide as initiator instead of elemental potassium.<sup>[188]</sup> These changes



allowed to perform the synthesis on a larger scale and gave materials with  $M_n$  values of 1.4 to 1.9 kDa with dispersities between 2.0 and 3.0 and high melting temperatures of around 300 °C.

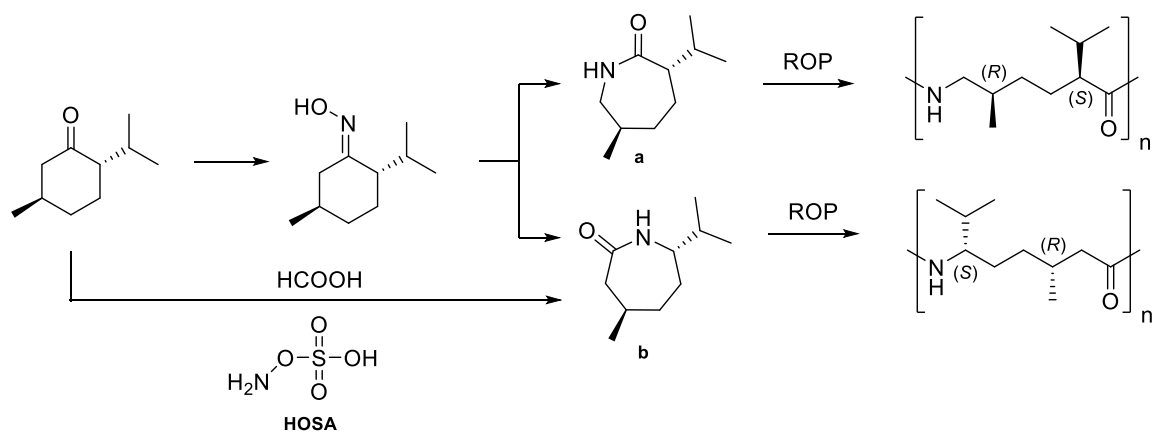


Figure 43: Menthone-based synthesis of lactams **a** and **b**, via oxime, or direct and regioselective synthesis of lactam **b** with hydroxylamine-O-sulfonic acid (HOSA) followed by ROP.<sup>[187]</sup>

In conclusion, the functionalisation of terpenes prior to polymerisation has enabled the use of polymerisation techniques other than radical and cationic polymerisations. It allowed to apply methods such as condensation and ring-opening polymerisations achieving the synthesis of novel polyesters, polyamides, polyurethanes and polycarbonates with useful properties. However, only a limited amount of the examples were completely “green” approaches. Indeed, the applied procedures for the functionalisation of the monomers often do not meet the requirements of green and sustainable chemistry e.g. by using stoichiometric amounts of reagents, toxic reagents or non-biobased co-monomers. This finding further emphasises that the renewability of the monomers is not enough to achieve “green” polymers. Therefore, the research on catalytic routes in combination with mild and solvent-free conditions is an important step for the design of sustainable polymeric materials.

## 2.9 Sustainable Thermosets from Terpenes

Thermosetting polymers are prepolymers in a viscous or soft solid state, that can be irreversibly transformed into an insoluble, infusible polymer network by curing. The curing of a thermosetting polymer or monomers can be induced through suitable radiation and/or heat, and after curing the thermosetting polymer is called thermoset.<sup>[189]</sup> A necessary requirement for the production of a thermoset *via* step-growth polymerisation is that one

or more of the monomers bears three or more reacting groups per molecule. Then, a three-dimensional, cross-linked network is formed, which cannot be reshaped, once the chemical reaction takes place. In industry, a large variety of thermosets is used, however, thermoset materials represent only 20% of the global plastic production.<sup>[190]</sup> Well-known examples are phenolic and urea formaldehyde resins, unsaturated polyesters and epoxy resins.

A commercial application for terpenes in epoxy resins is the use of limonene oxide and dioxide as reactive diluents.<sup>[190]</sup> As shown by Mathers *et al.*, monoterpenes can also be utilised to control the degree of crosslinking during ring-opening metathesis polymerisations (ROMP).<sup>[191]</sup> The authors investigated the influence of  $\beta$ -pinene, carvone, limonene, limonene oxide and myrcene on the physical properties and thermal stability of the ROMP of dicyclopentadiene (DCPD). As a result, the  $T_g$  values of poly(DCPD) could be adjusted between 65 and 150 °C by adding various amounts of  $\beta$ -pinene. By adding 5 wt% of  $\beta$ -pinene, the crosslinking density was decreased, leading to a decrease in  $T_g$  and storage modulus. However, when 10-20 wt% were added, covalently bound side chains and noncovalently bound oligomers were formed, the latter acting as plasticiser in the thermoset, further lowering the  $T_g$  values.

Another strategy is to use terpenes as hardeners for epoxy materials that either carry amine or phenol groups. One example is the use of menthane diamine to decrease the exotherm during the curing reaction of an epoxy resin (see Figure 44).<sup>[192]</sup> Another way of exploiting terpenes as hardeners was achieved by using terpene diphenol, which has already been utilised to synthesise a bio-based polycarbonate through the reaction with diphenyl carbonate (see Figure 44).<sup>[193]</sup> It was also shown that it is possible to use limonene for the synthesis of steric epoxy monomers by alkylation with naphthol with a Friedel-Crafts catalyst.<sup>[194]</sup> After introducing a methylene linkage between the naphthalene rings, an epoxy resin was obtained by epoxidation with epichlorohydrin in the presence of sodium hydroxide and poly(ethylene glycol). The epoxy resin was then cured with different curing agents and showed a higher  $T_g$ , lower coefficient of thermal expansion, higher thermal stability, better moisture resistance and dielectric property compared to that of bisphenol A diglycidyl ether (DGEBA).

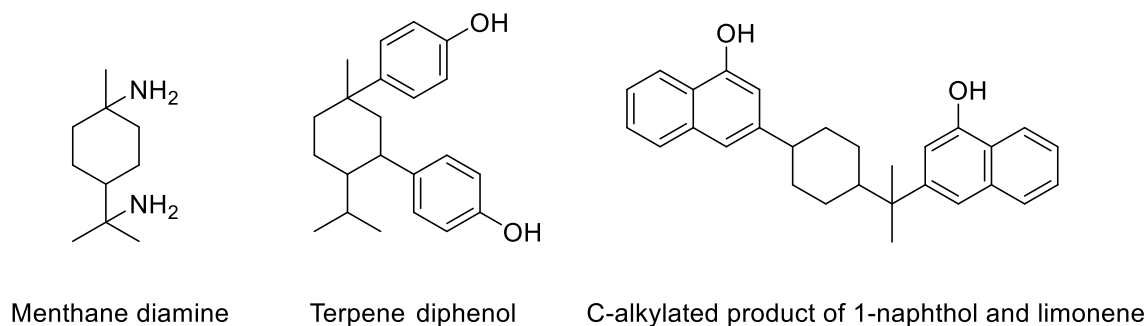


Figure 44: Formula of menthane diamine and terpene diphenol that can be used as hardeners for epoxy resins and formula of the C-alkylated product of 1-naphthol and limonene that can be transformed into an epoxy resin.

Another concept to produce terpene-containing prepolymers is the reaction of 1,1'-(methylenedi-4,1-phenylene)bismaleimide (BMI) with limonene or myrcene at 150 °C, as reported by Shibata and Asano.<sup>[195]</sup> The curing reaction was achieved *via* compressing (5 MPa) at 250 °C and produced cross-linked myrcene/BMI and limonene/BMI thermosets.

Sibaja and co-workers exploited limonene and myrcene as co-monomers for the cationic co-polymerisation with tung oil, initiated by boron trifluoride.<sup>[196]</sup> Dynamic mechanical analysis revealed the thermosetting behaviour of the copolymers. By increasing the myrcene content, the  $T_g$  increased. Increased limonene content led to an almost linear decrease of the  $T_g$ . The Young's modulus ranged from 33.8 to 4.7 MPa for all tested thermosets.

As described above, some cationic polymerisations of terpenes result in oligomers or low-molecular-weight polymers. Along with other terpene monomers, these oligomers can be further modified to synthesise epoxy resins and polyols.<sup>[197]</sup> Wu *et al.* started their synthesis protocol by adding maleic anhydride to  $\alpha$ -terpinene and hydrogenated the adduct in an autoclave to obtain hydrogenated terpinene-maleic anhydride (HTMA) (see Figure 45).<sup>[198]</sup> HTMA was further reacted with epichlorohydrin resulting in hydrogenated terpinene-maleic ester type epoxy resins (HTME). To prepare polyols with different hydroxyl values, HTME was functionalised with three kinds of secondary amines (diethylamine, *N*-methylethanolamine and diethanolamine). These polyols were then reacted with polyisocyanates, catalysed by the tertiary amine groups included in the polyol, resulting in cross-linked epoxy-urethane polymers with good chemical- and thermal resistance properties, good impact strength and flexibilities.<sup>[199]</sup> The new crosslinked thermosets combine the flexibility and resilience of polyurethanes with the rigidity and weathering resistance of saturated alicyclic terpinene epoxy resins.

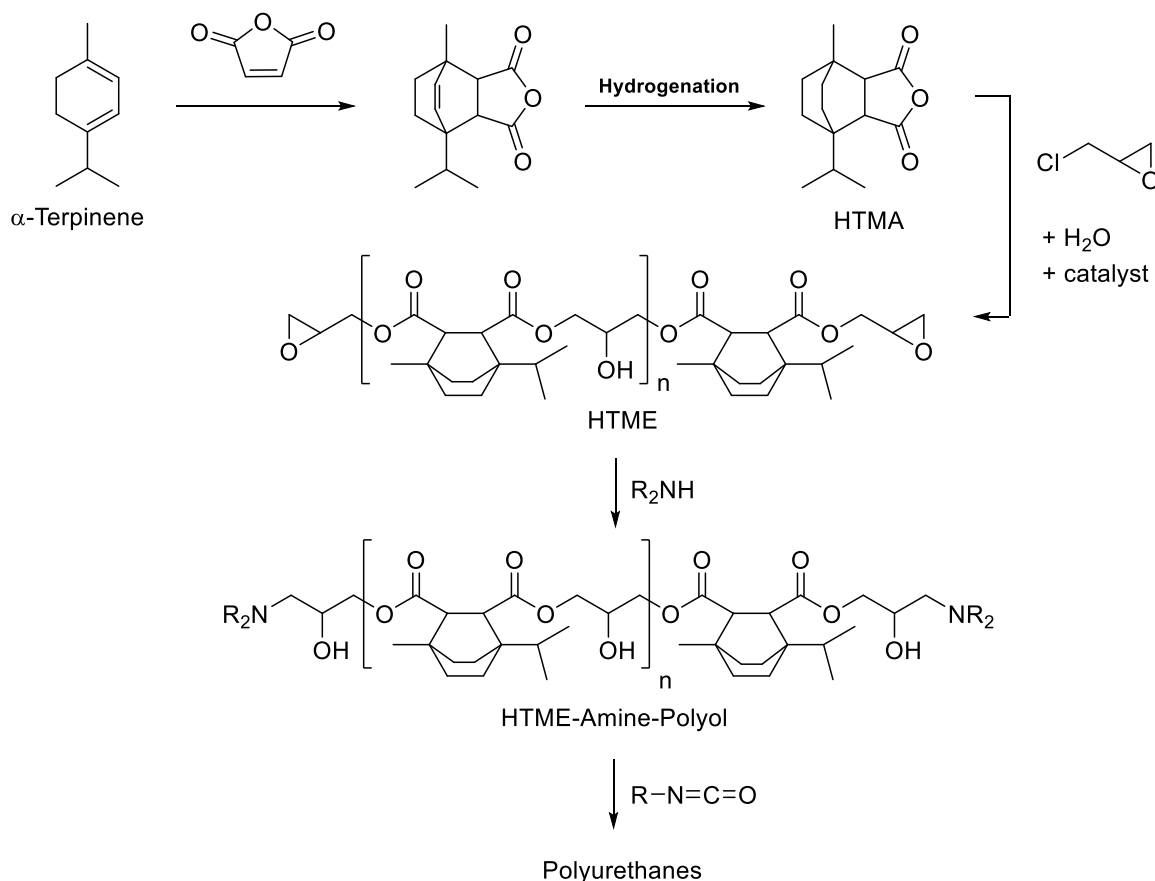
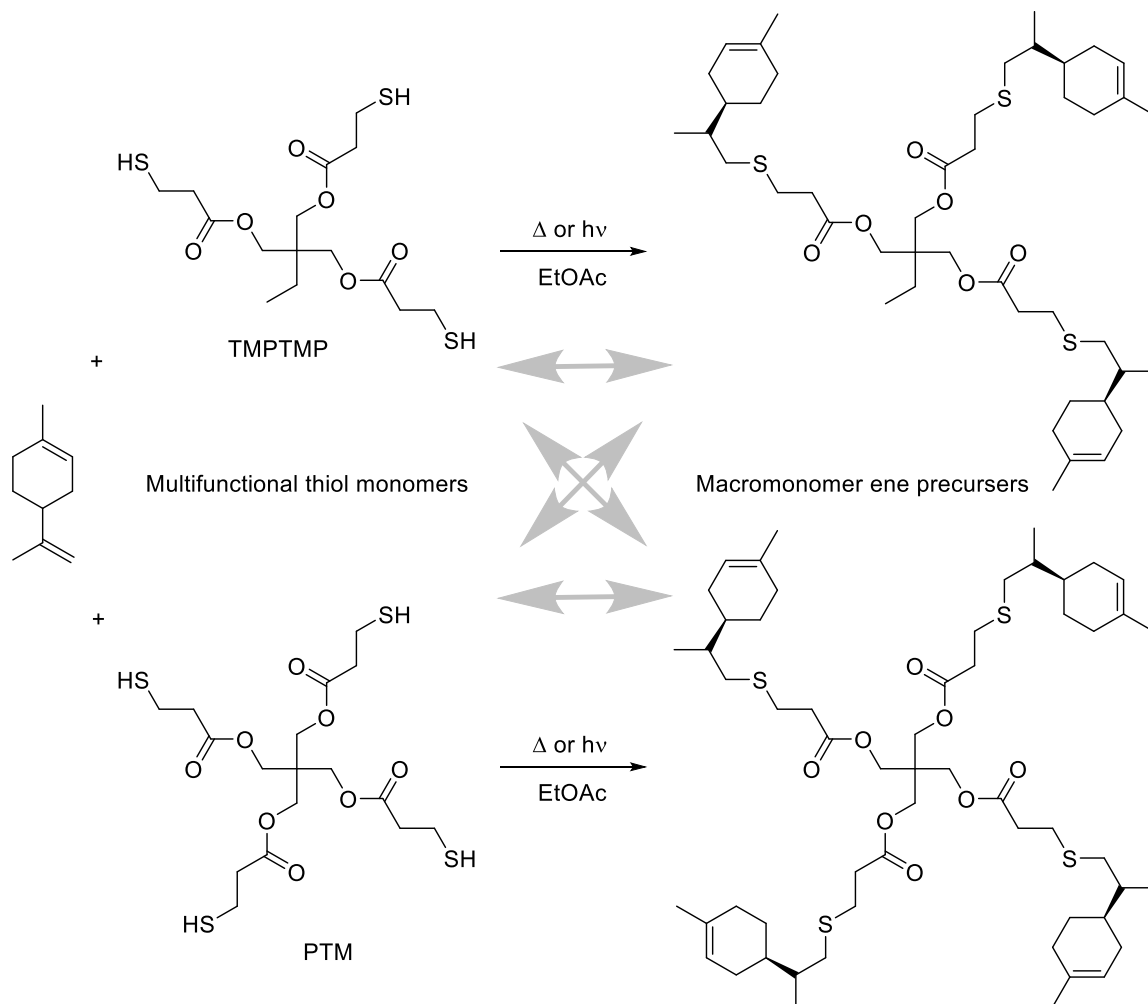


Figure 45: Synthesis of polyols and polyurethanes from hydrogenated terpinene-maleic ester type epoxy resin (HTME).<sup>[198]</sup>

Johansson and co-workers utilised limonene directly as a co-monomer in combination with free-radical thiol-ene coupling reactions to obtain permanent networks.<sup>[200]</sup> After having investigated the kinetics of free-radical thiol-ene photo-additions between limonene and thiols that possess a propionate ester moiety, the authors found that the reaction taking place at the *exo*-olefinic bond is about 6.5 times faster than at the endocyclic one.<sup>[201]</sup> The first step in the synthesis protocol for limonene-based thermosets makes use of this intrinsic difference in reactivity to produce branched macromonomer ene precursors by reacting limonene with two different thiols (either tri- or tetrafunctional, see Figure 46). Although an excess of limonene facilitates the formation of well-defined macromolecular precursors, an initial thiol-ene ratio of 1:0.5 was chosen, since the low vapour pressure of limonene hampers its removal *via* evaporation after the macromonomer formation. In a second step, the macromonomer ene precursors were crosslinked with equimolar multifunctional alkyl ester 3-mercaptopropionates, yielding amorphous, highly sticky and flexible elastomers. The final poly(thioether) network showed tuneable thermo-mechanical properties depending on the amount of unreacted thiol occluded within the thermoset that works as a plasticiser. In addition, Johansson *et al.* developed a fundamental kinetic

platform for the design of thiol-ene systems based on limonene and alkyl ester 3-mercaptopropionates.<sup>[202]</sup>

### A) Synthesis of the limonene-terminated precursors



### B) Network formation

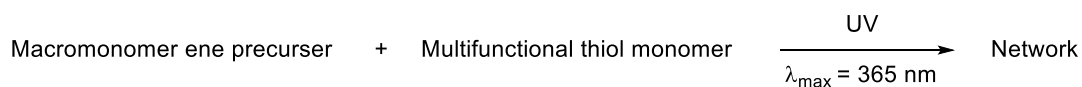


Figure 46: A) Synthesis route for the limonene-terminated precursors. Bidirectional grey arrows denote thiol-ene coupling between multifunctional thiols and macromonomers. B) Network formation based on equimolar amounts of multifunctional groups.<sup>[200]</sup>

Another example for network polymers composed solely of limonene and a polythiol co-monomer was reported by Hearon *et al.*<sup>[203]</sup> The authors reported a method for the recycling of polystyrene by synthesising new poly(thioether) networks based on limonene. First, a beverage-contaminated expanded polystyrene waste cup was dissolved in limonene ( $M_w \approx 396 \text{ kDa}$ ). Through basic extraction and filtration, a purified solution of

polystyrene in limonene was obtained. The reclamation of poly(styrene) was then accomplished by addition of DMPA as photoinitiator and trimethylolpropane tris(3-mercaptopropionate) (TMPTMP) as co-monomer. The mixture was heated to 140 °C for homogeneous dissolution and poured into a preheated mould that was irradiated with UV light. With proceeding formation of the elastomeric poly(thioether) network, phase separation of poly(styrene) occurred, leading to polystyrene micro- and nanophases throughout the network. To demonstrate the processability of the new material, a prototype of a protective cover for a mobile phone was fabricated.

Yan *et al.* used limonene-based 2,9-*p*-menthanedithiol, for the synthesis of thiourethane thermoset coatings.<sup>[204]</sup> The coatings were produced *via* thermal thiol-ene reactions between sucrose soya ester and multifunctional thiols, including 2,9-*p*-menthanedithiol, followed by the reaction with hexamethylene diisocyanate trimer or isophorone diisocyanate trimer. All the coatings exhibited low chemical resistance and mechanical properties due to the softness of the fatty acid chains in the sucrose soya ester.

Morinaga and Sakamoto also used thiol-ene reactions for network formations derived from limonene, however, thiol-ene reactions were only used for the synthesis of multifunctional epoxides, that were subsequently cured with branched poly(ethylenimine).<sup>[205]</sup> For the synthesis of the multifunctional epoxides, limonene oxide was reacted with polyhydric thiols such as 1,2-ethanedithiol, TMPTMP, and pentaerythritol tetrakis(3-mercaptopropionate) (PTM) resulting in di-, tri-, and tetra-epoxides. The cured epoxy resins were obtained in high yields and exhibited relatively high thermal resistance.

In 2012, Mülhaupt and co-workers investigated the catalytic conversion of limonene dioxide with CO<sub>2</sub> to synthesise cyclic limonene dicarbonate and presented the first approach for the preparation of non-isocyanate poly(hydroxyurethanes) (NIPUs) derived from limonene dicarbonate.<sup>[206]</sup> For this purpose, limonene dioxide was carbonated with CO<sub>2</sub> in the presence of either homogeneous tetrabutylammonium bromide or heterogeneous silica-supported 4-pyrrolidinopyridinium iodide (SiO<sub>2</sub>-I) (see Figure 47). Despite the advantages of a heterogeneous catalyst in terms of easy removal, TBAB at 140 °C and 30 bar CO<sub>2</sub> pressure was preferred over SiO<sub>2</sub>-I (78% epoxy conversion after 120 h), since it showed better activity and full conversion was achieved after 55 h. In the preliminary study, the authors applied the obtained limonene dicarbonate without any purification directly for NIPU preparation, although NMR analysis revealed olefinic as well as aldehyde by-products. First, a set of linear NIPU prepolymers possessing molecular weights ( $M_n$ ) between 0.43 and 1.84 kDa and dispersities between 1.2 and 1.5 were obtained by reacting limonene dicarbonate with commercial diamines, such as 1,4-butane

diamine, 1,6-hexamethylene diamine, isophorone diamine or 1,8-octamethylene diamine. Additionally, the limonene carbonate to diamine ratio was varied to gain control over the end groups of the prepolymers. In a second approach, limonene carbonate was cured with tri- and polyfunctional amines like citric acid aminoamides, tris(*N*-2-aminoethyl)amine and amine-terminated hyperbranched poly(ethylenimines) resulting in novel thermosets.

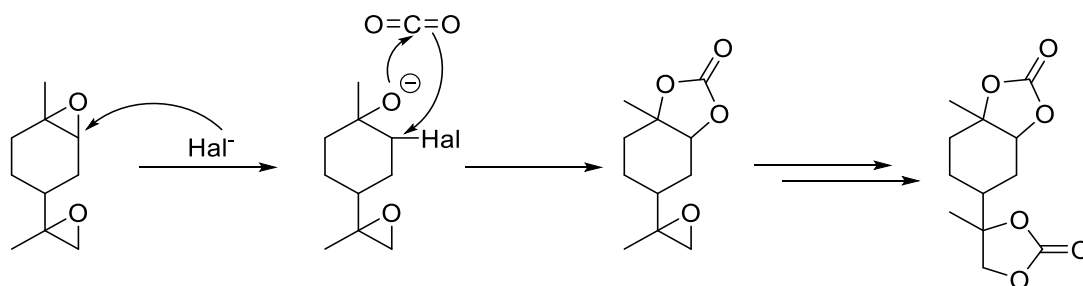


Figure 47: Conversion of limonene dioxide to limonene dicarbonate.<sup>[206]</sup>

Recently, Kleij *et al.* reported another synthesis procedure for the coupling of CO<sub>2</sub> and highly substituted acyclic as well as cyclic terpene epoxides, including limonene dioxide (see Figure 48).<sup>[207]</sup> The authors used Lewis acidic Al<sup>III</sup>(aminotriphenolate) complexes<sup>[208, 209]</sup> as catalysts together with PPNCI as a nucleophilic additive. The reaction was usually conducted in methyl ethyl ketone for 66 h, at 85 °C with 1.0 MPa of CO<sub>2</sub> pressure and after chromatographic purification resulted in isolated yields in the range of 50-60% in most cases. In general, cyclic substrates exhibited good chemoselectivity towards the cyclic carbonate, whereas acyclic terpene oxides showed lower selectivity due to unwanted polyether side product formation and epoxide rearrangement reactions.

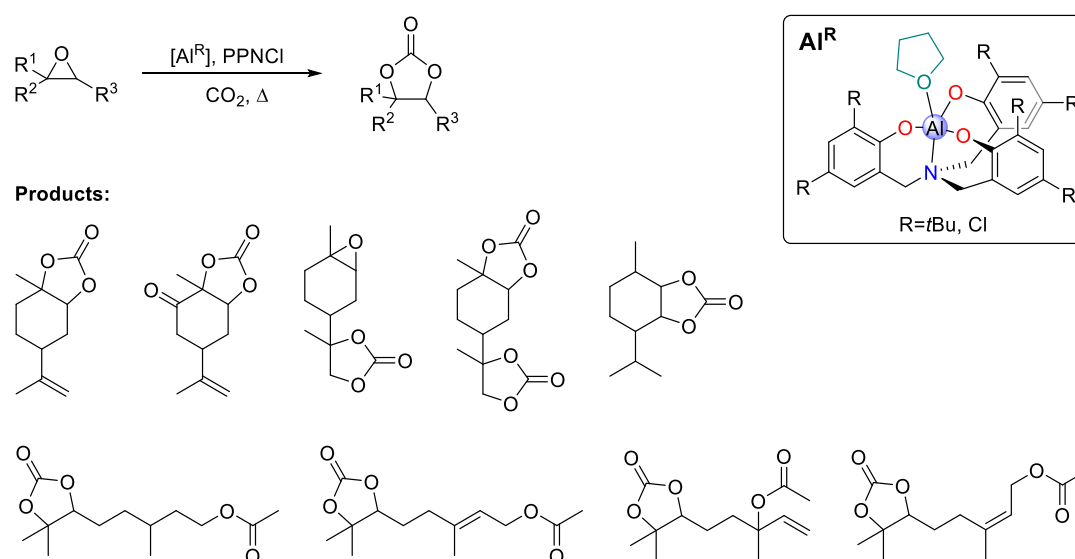


Figure 48: Coupling of terpene-based epoxides with CO<sub>2</sub> catalysed by Al(aminotriphenolate) complexes and product scope.<sup>[207]</sup>

More recently, Mülhaupt *et al.* reported the synthesis of limonene dicarbonate *via* TBAB-catalysed carbonation of limonene dioxide with significantly improved purity and without chromatographic separation.<sup>[210]</sup> The purification was achieved by crystallisation and resulted in a mixture of crystalline *cis/trans*-limonene dicarbonate after the first recrystallisation and isomerically pure *trans*-limonene dicarbonate after the second recrystallisation. Subsequently, the crystalline limonene carbonate was used for the melt-phase polyaddition with a commercially available dimer fatty acid-based diamine (Priamine 1074) in excess, resulting in a low molecular weight diamine-terminated prepolymer ( $M_n = 4.3$  kDa) (see Figure 49). To increase the molecular weight, carbonated 1,4-butanediol diglycidyl ether (BDGC) was added as a chain extender, since BDGC has a much higher reactivity compared to limonene dicarbonate. The resulting NIPU thermoplastics were fully bio-based and had a molecular weight of  $M_n = 22.8$  kDa at 21.3 wt% limonene dicarbonate content. Besides limonene dicarbonate-derived NIPU thermoplastics, the authors also reported a synthesis protocol for limonene dicarbonate-based NIPU thermosets (see Figure 49).

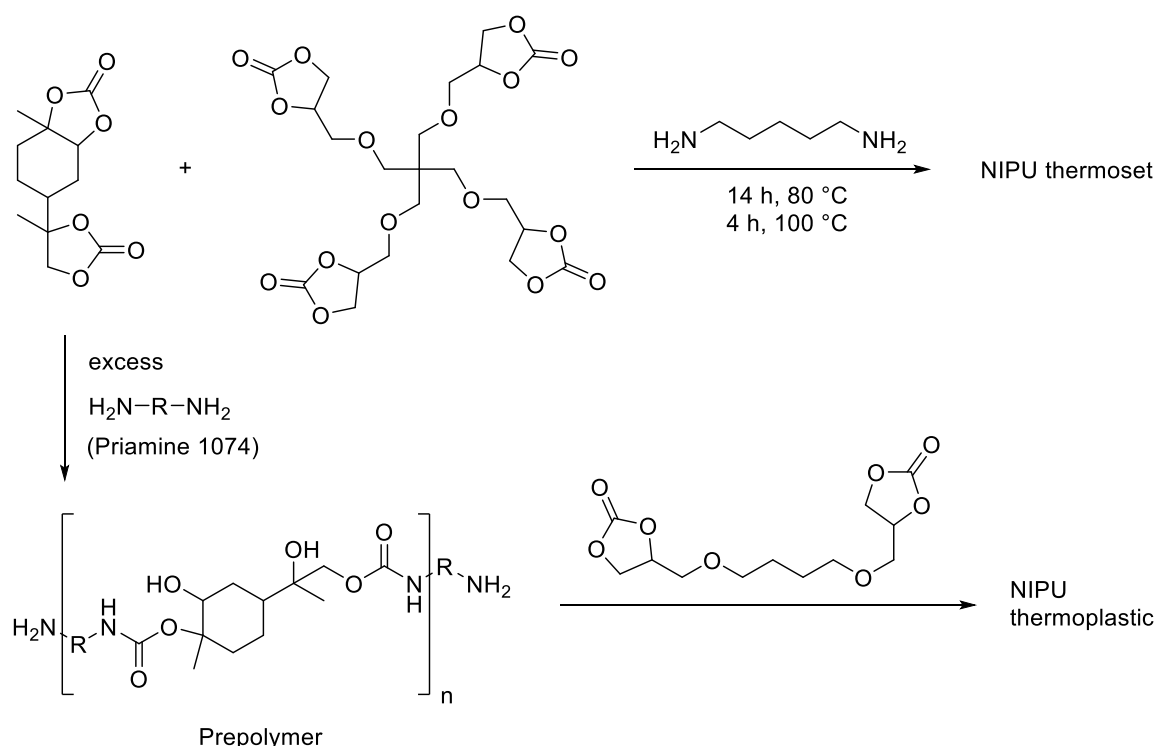


Figure 49: Synthesis of fully bio-based NIPU thermosets from carbonated pentaerythritol glycidyl ether/limonene dicarbonate blends cured with 1,5-diaminopentane and synthesis of thermoplastic NIPU copolymers via prepolymers based on limonene dicarbonate and Priamine 1074 with subsequent chain extension by using carbonated 1,4-butanediol diglycidyl ether.<sup>[210]</sup>



For this purpose, limonene dicarbonate was blended with pentaerythritol glycidyl ether and then cured with bio-based 1,5-diaminopentane, gained from lysine. The incorporation of 23 wt% of the rather rigid limonene dicarbonate building block into the NIPU thermoset leads to an increase of the glass transition temperature, of the tensile strength and of the Young's modulus. However, embrittlement was observed at limonene dicarbonate contents higher than 38 wt%, which was attributed to the rigidity of the limonene unit.

In conclusion, the utilisation of terpenes in thermosets comprises the direct application as reactive diluents or as co-monomers as well as the application of functionalised terpenes. After functionalisation, the terpene monomers can be applied as hardeners for epoxy resins, as polyepoxides that can be cured to form networks or as co-monomers for other thermosetting polymers. Although the methods of applying terpenes in thermosets are very versatile, fully terpene-based thermosets are rare.

All in all, the above described examples for the transformation of terpenes into polymeric materials, show that these building blocks fulfil all requirements, such as abundance, (relatively) low cost and functionality, to be a highly applicable renewable feedstock. Although terpenes are widely used as renewable fine chemicals, they have been neglected for the synthesis of sustainable polymers and advanced materials for a long time. This was mainly due to the difficulties of precisely controlling the molecular and macromolecular structures, as it is well established for polymeric materials derived from petrochemicals. However, the interest in terpenes as starting material for polymers has increased in the last decade, encouraged by recent accomplishments in the field of controlled polymerisation and post-polymerisation modification techniques.

The present production of terpenes is not sufficient to synthesise commodity materials on a large scale, but there is the potential to increase the production of terpenes by exploiting waste streams, if the demand is rising.<sup>[118]</sup> The chemically diverse nature of terpenes makes them very promising candidates for the synthesis of low-volume speciality materials that are directly obtainable from the renewable feedstock. To be successful in producing sustainable polymers and fine chemicals with valuable and tuneable properties, the polymerisation processes and the procedures for the modification of the terpenes needs to be efficient and "green". Catalysis plays a fundamental role for the development or adaption of new technologies that fulfil these requirements. Especially in the case of fine chemicals production, catalysis is often the key to enable benign reaction conditions and to achieve the necessary selectivity.<sup>[73]</sup>

The present demand towards more sustainability, in both society and research, urges the scientific community to ensure that there are suitable solutions for environmental needs

available. In this regard, the development of collaborations across all scientific disciplines and industry is imperative to be able to provide sustainable polymeric materials and fine chemicals.<sup>[118]</sup> With continuous efforts to improve their synthesis and polymerisation technologies, and with conscientious understanding among the public, renewable chemicals and polymers will play an ever-increasing role for future generations and a sustainable society.

In this thesis, terpenes are assessed for their potential as renewable starting materials to produce sustainable fine chemicals, monomers and polymers.

### 3 Aims

In the previous chapters (chapter 2.7, 2.8 and 2.9), the general synthetic procedures to obtain terpene-derived chemicals described in the literature as well as industrial uses were outlined. These approaches also apply petrochemicals, toxic reagents and non-sustainable reaction pathways. In light of the European Commission's initiative for a Circular Economy<sup>[211]</sup> and a general perception that "renewability is not enough",<sup>[212]</sup> the development of renewable platform chemicals in a sustainable and green fashion is of high interest. Therefore, this thesis aims for novel strategies towards the transformation of terpenes into valuable fine chemicals and polymeric materials using green and sustainable reaction procedures and applying the 12 principles of green chemistry as guideline in all synthetic steps.

In particular, the field of catalytic systems used to convert terpenes into valuable chemicals is extremely fertile for the development of new ideas, since there is a constant interest for novel catalysts exhibiting higher activity, stability and selectivity to the desired products. Lately, a lot of effort has been made to substitute conventional homogeneous catalysts with heterogeneous ones to simplify catalyst separation and regeneration. In the first part of this thesis (chapter 4.1), the use of Mn(III) acetate as a homogeneous catalyst for the oxidation of  $\alpha$ -pinene is thus studied and compared to the performance of a novel Mn-containing metal-organic framework catalyst. The focus is laid on a more environmentally benign reaction procedure by avoiding stoichiometric reagents, such as organic hydroperoxides, which are generally toxic and hazardous and lead to the formation of considerable amounts of waste. Instead the aim is to adapt the reaction conditions in such a way that oxygen from air can be used as the sole oxidant. Furthermore, different reaction conditions are investigated in detail for the homogeneous model catalyst, Mn(III) acetate in order to find optimised conditions while focussing on high conversion in combination with a high selectivity. For the purpose of "greener" reaction conditions, commonly employed organic solvents are substituted by "greener" alternatives, e.g. diethyl carbonate. Furthermore, to benefit from the advantages of heterogeneous catalysis, such as easy recyclability and thus conservation of resources, a new strategy for the preparation of a heterogeneous Mn catalyst is explored. Therefore, Mn complexes are immobilised in a novel metal-organic framework which is synthesised *via* two-step post-synthetic modification of MIXMIL-53-NH<sub>2</sub>(50) with maleic anhydride and Mn(III) acetate. With the aim to directly compare the efficiency of both catalysts, the reaction conditions developed for the homogenous model catalyst are transferred to the liquid-phase oxidation of  $\alpha$ -pinene using the Mn-containing MOF as heterogeneous catalyst. Finally, the

heterogeneous nature of the catalytic system is assessed to ensure that no metal-leaching takes place which substantially limits the recyclability and leads to a metal contamination of the organic phase including the product.

Among the selective oxyfunctionalisation of olefins, which is an important step in the chemical chain as readily available substances can be converted into a wide variety of valuable products, the sustainable production of cyclic carbonates is a valuable synthetic target. Cyclic carbonates are useful as inert media, *e.g.* as solvent or electrolytes, and as reactive intermediates for polymers, plasticisers and lubricants. However, the synthesis of the starting epoxides mainly used for the production of cyclic carbonates involves petrochemicals, powerful oxidants, and procedures that produce waste. Within the second part of this thesis (chapter 4.2), the formation of renewable cyclic carbonates is targeted using  $\alpha$ - and  $\beta$ -pinene as substrates and applying “greener” reaction conditions. Therefore,  $\text{CO}_2$  as a readily available and non-toxic carbonyl source is assessed for the insertion into the epoxide functionality of  $\alpha$ -pinene oxide to directly obtain the  $\alpha$ -pinene-based cyclic carbonate. To profit from the mild reaction conditions of the TBD-catalysed transesterification reaction, a strategy introducing the carbonyl functionality *via* transesterification of 1,2 diols with linear organic carbonates is investigated for  $\alpha$ - and for  $\beta$ -pinane diol. With the aim to obtain  $\beta$ -pinandiol *via* an environmentally benign oxidation protocol followed by the epoxide ring-opening with water instead of a dihydroxylation reaction using highly toxic osmium tetroxide, a procedure applying hydrogen peroxide as benign oxidising agent and methyltrioxorhenium as catalyst was employed. Finally, the synthesis protocol for the catalytic transesterification of  $\alpha$ - and  $\beta$ -pinandiol is compared to existing literature procedures in order to prove the advantages of the new protocol regarding the environmental sustainability.

Besides being useful for the preparation of platform and fine chemicals, terpenes are also very interesting candidates for the synthesis of advanced polymers. Polyurethanes (PUs) are indispensable in daily life, however, PUs are commercially synthesised from highly toxic isocyanates. Non-isocyanate polyurethanes (NIPUs), on the other hand, are available by polymerising cyclic carbonates with amines to yield poly(hydroxy urethane)s (PHUs). Inspired by the work of Mülhaupt *et al.*, who used cyclic limonene dicarbonate as monomer for non-isocyanate oligo- and polyurethanes (NIPU) for the first time,<sup>[206, 210]</sup> the synthesis of fully limonene-based NIPUs and their application as hardeners for epoxy thermosets is investigated in chapter 4.3. Therefore, cyclic limonene dicarbonate and limonene diamine are synthesised and subsequently applied as homo-bifunctional monomers for the preparation of poly(hydroxy urethane)s. To establish green and sustainable reaction conditions, various reaction temperatures, solvents and catalysts are

evaluated. Moreover, the influence of the amine to cyclic carbonate molar ratio on the molecular weight and on the end groups of the prepolymer is investigated to enable the further application as hardener for epoxy resins. To prove the concept, the novel poly(hydroxy urethane) prepolymers are used as renewable alternatives to petrochemical-based curing agents in the synthesis of renewable epoxy thermosets based on soybean oil.

Overall, this work aims to develop novel and environmentally benign routes to renewable fine chemicals, monomers and polymers based on terpenes. It thereby paves the way for the implementation of more sustainable routes towards the replacement of fossil-based materials with renewable feedstocks.



## 4 Results and Discussion

### 4.1 Aerobic Oxidation of $\alpha$ -Pinene Catalysed by Homogeneous and MOF-based Mn Catalysts

Parts of this chapter and the associated parts in the experimental section were published before: Y. S. Raupp, C. Yildiz, W. Kleist, M. A. Meier, *Appl. Catal., A*, **2017**, *546*, 1-6.<sup>[213]</sup> This project has been started during this PhD candidates master thesis<sup>[214]</sup> and was continued in the PhD thesis. Footnotes in the experimental section mark the respective reactions that were carried out during the master thesis and provide detailed differentiation between master and PhD thesis.

The aerobic oxidation of  $\alpha$ -pinene was performed as a collaboration project with the working group of Prof. Wolfgang Kleist. The catalytic oxidation reactions were performed by Yasmin Raupp, whereas the synthesis of the MOF-based Mn catalyst was performed by Ceylan Yildiz. The catalytic oxidation reactions as well as the synthesis of the heterogeneous MOF catalyst will be discussed within this chapter with a detailed focus on the catalysis as it was carried out by the author. Footnotes in the experimental part mark the reactions and characterisations that have been carried out by the cooperation partner and provide detailed differentiation.

Within this chapter, Mn-based catalysts were investigated for the oxidation of  $\alpha$ -pinene (see Figure 50). In particular Mn(III) acetate was used homogeneous catalyst and compared to the performance of a novel Mn-containing MOF catalyst. The heterogeneous MOF catalyst allowed to benefit from the advantages of heterogeneous catalysis, such as easy recovery and straightforward reusability of the catalyst facilitating waste prevention and conservation of resources. To establish environmentally benign reaction conditions, the use of stoichiometric reagents such as organic hydroperoxides, which produce considerable amounts of waste and are generally toxic and hazardous, was avoided by utilising oxygen from air as the oxidant. Additionally, diethyl carbonate, which is considered a more sustainable alternative to conventional solvents, was employed as reaction medium.

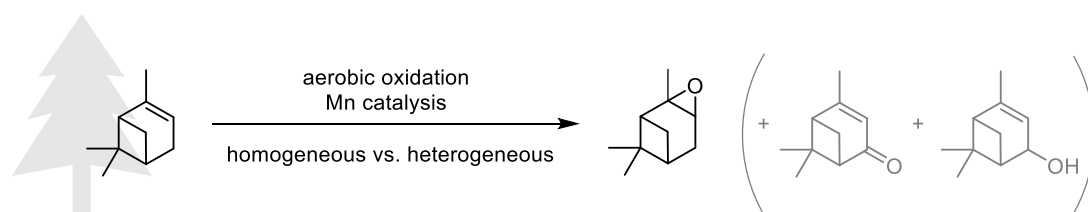


Figure 50: Graphical abstract for the aerobic oxidation of  $\alpha$ -pinene catalysed by homogeneous and MOF-based Mn catalysts yielding pinene oxide as main product and verbenone and verbenol as side-products.

The investigations on the manganese-catalysed aerobic oxidation of  $\alpha$ -pinene were started by determining optimal reaction conditions for Mn(III) acetate as a homogeneous counterpart to the metal-organic framework MIXMIL-53-NH<sub>2</sub>(50)-Mal-Mn that was subsequently applied as a heterogeneous oxidation catalyst. Conversion, yield and selectivity were optimised by variation of one reaction parameter at a time (reaction time, solvent composition, catalyst concentration, temperature, oxidant flow rate). Reaction products were identified using gas chromatography-mass spectrometry (GC-MS) by comparison with authentic samples and quantified by gas chromatography (GC) techniques (for details see experimental part 6.3.1). In the first set of experiments, the oxidation of  $\alpha$ -pinene was monitored at 130 °C for 24 h with continuous air flow through the solution (50 mL min<sup>-1</sup>) and a 50:50 mixture of toluene/DMF as solvent. The solvent mixture toluene/DMF was chosen on the basis of reports on aerobic epoxidations of olefins without radical initiators or sacrificial aldehydes using DMF as solvent.<sup>[215-220]</sup> In these reports, the use of DMF was essential for the progress of the catalytic reaction and the following mechanism was suggested: a metal-DMF complex is produced that coordinates molecular oxygen to form a superoxo species, which then transfers the molecular oxygen to the olefin. On that account, the suitability of DMF was tested first. For practical reasons,



the addition of a lower boiling solvent was required to achieve adequate reflux conditions. Since toluene has been widely used for the aerobic oxidation of alcohols at least 50% toluene were added as co-solvent.<sup>[221]</sup>

Applying the above-mentioned conditions, the reaction gave pinene oxide as the main product together with verbenone and verbenol as minor side-products (see Figure 50).

First, the impact of the reaction time was studied. An increase in reaction time from 6 to 24 h improved the  $\alpha$ -pinene conversion from 30 to 51%. In contrast, only a slight increase of the pinene oxide yield was observed, resulting in a remarkable decrease of the selectivity from 60 to 36% (see Figure 51). This observation is in accordance with the studies of Jasra *et al.*<sup>[216]</sup> and Yu *et al.*<sup>[96]</sup>, who explained this observation by the high reactivity of epoxides and thus the conversion of pinene oxide into isomeric products. Therefore, longer reaction times were not favourable for the formation of pinene oxide.

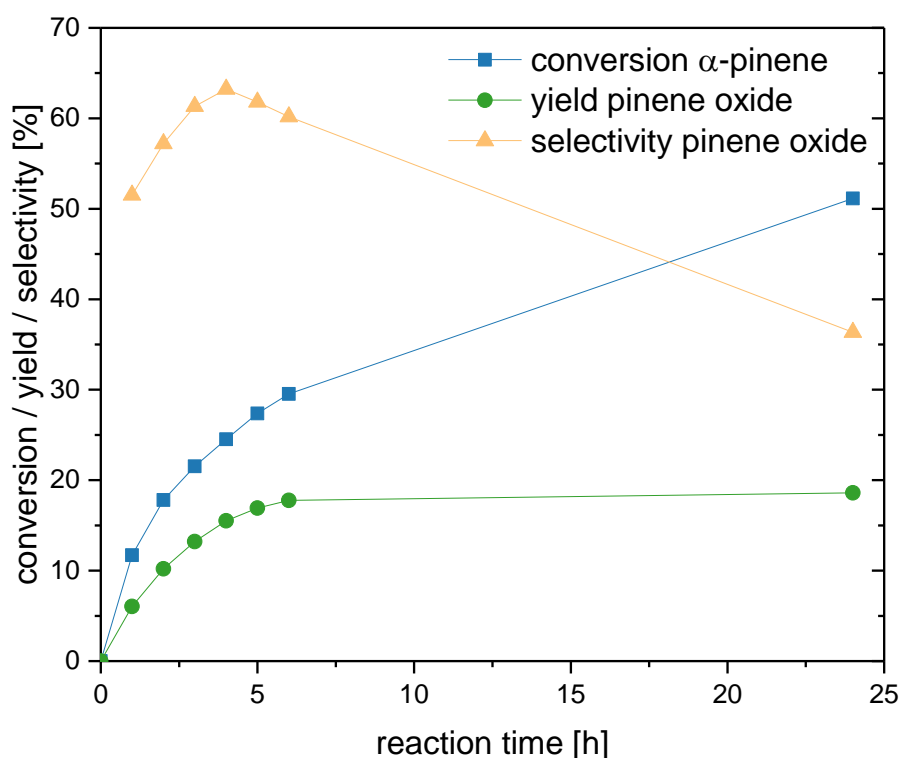


Figure 51: Conversion, yield and selectivity of aerobic  $\alpha$ -pinene oxidation catalysed by Mn(III) acetate. Reaction conditions:  $\alpha$ -pinene (1.00 mmol), catalyst (1.00 mol% Mn), toluene/DMF (50:50, 30 mL), compressed air (50 mL min<sup>-1</sup>), 130 °C.

Next, the influence of the solvent was subject of investigation. Thus, the toluene/DMF ratio was varied (50:50, 60:40, 70:30, 80:20, 90:10), proving the 90:10 mixture to be the most

efficient solvent system. This observation might be explained by a lower concentration of amines, which are formed by DMF decomposition at high temperature and can block the free metal sites of the catalyst and thus limit the oxidation reaction. However, a certain amount of DMF seems to have a positive impact on the conversion and yield of pinene oxide, as the latter dropped if only toluene was used. This observation was also made in earlier studies, when Baiker and co-workers discovered that the STA-12(Co)-catalysed epoxidation of (*E*)-stilbene did not occur in toluene, whereas mixtures of toluene and DMF permitted some catalytic activity,<sup>[222]</sup> most likely due to a solvent co-oxidation mechanism. A strong indication for this theory was the detection of *N*-formyl-*N*-methylformamide (FMF) as a by-product by GC–MS, which was also found in this study. This is in accordance with the studies of Baiker *et al.*, who reported that olefin transformation can be accompanied by significant DMF oxidation, leading to FMF formation.<sup>[221, 223]</sup> In this case, the intermediate *N*-(hydroperoxymethyl)-*N*-methylformamide derived from DMF can act as an oxygen-transfer agent, forming FMF as result. The autoxidation of amides is accelerated by transition metal ions and thus by the presence of the catalyst.<sup>[224]</sup> However, also the oxidation of the olefin mediated by a transition metal peroxo species and the following regeneration of the catalyst through oxidation of the solvent could explain the strong influence of the solvent and its oxidation.<sup>[222]</sup>

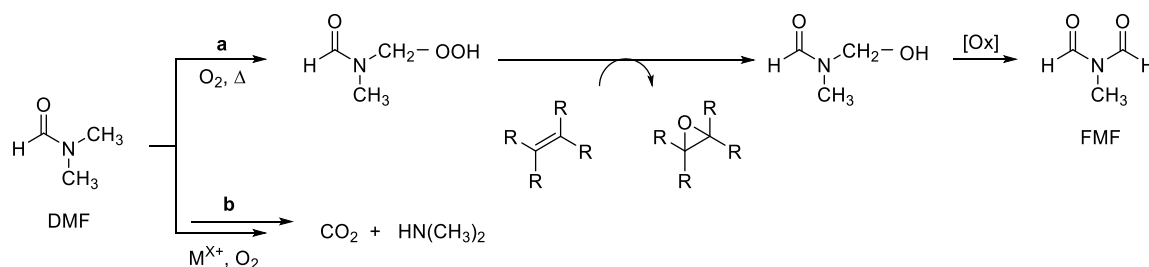


Figure 52: Autoxidation of DMF: a: thermal oxidation of DMF including the epoxidation of alkenes in DMF and the formation of *N*-formyl-*N*-methylformamide (FMF); b: metal ion-catalysed oxidation of DMF.<sup>[223]</sup>

Ensuing investigations were focused on the effect of five different catalyst concentrations on the conversion and selectivity. The results of the performed reactions with catalyst amounts varying between 2.00 and 0.250 mol% are summarised in Table 7. A reaction without catalyst was performed as blank test (Table 7, entry 6). The blank test gave 5% conversion with only 2% product formation, conforming that the successful formation of pinene oxide in the other reactions was truly induced by the catalyst.

Interestingly, the best conversion (62%) and yield of pinene oxide (40%) were achieved by the lowest amount of catalyst (0.250 mol%). Conversion, yield and selectivity observed for the reactions containing 1.50, 1.00 and 0.500 mol% catalyst were in a similar range but

slightly lower. The reaction with the highest amount of catalyst (2.00 mol%) resulted in only 46% conversion. These findings are in accordance with the study of Lajunen *et al.*, who applied Co(II) complexes for the aerobic oxidation of  $\alpha$ -pinene. The authors also reported that the oxidation with the largest catalyst amount was slower and produced fewer product than the reactions with less catalyst.<sup>[100]</sup> A possible explanation might be a bimolecular catalyst deactivation mechanism.

Table 7: Effect of catalyst concentration on conversion and selectivity. Reaction conditions:  $\alpha$ -pinene (1.00 mmol), Mn(III) acetate (as indicated), toluene/DMF (90:10, 30 mL), compressed air (50 mL min<sup>-1</sup>), 130 °C, 6 h.

Entry	Catalyst conc. [mol/%]	Conversion [%]	Selectivity (yield) [%]		
			Pinene oxide	Verbenone	Verbenol
1	2.00	46	67 (31)	4 (2)	5 (2)
2	1.50	53	67 (35)	8 (4)	6 (3)
3	1.00	53	66 (35)	5 (3)	4 (2)
4	0.50	52	66 (34)	7 (3)	5 (3)
5	0.25	62	65 (40)	7 (4)	5 (3)
6	0 (blank test)	5	52 (2)	8 (0.4)	6 (0.3)

In further experiments, the dependency of conversion and yield on the reaction temperature was investigated (see Figure 53).  $\alpha$ -Pinene conversion and pinene oxide yield increased at higher temperatures. By increasing the temperature from 100 to 130 °C, conversion and pinene oxide yield almost tripled from 19 and 13% to 53 and 36%, respectively. As expected, the increase of the reaction temperature led to an increased reaction rate but did not result in a significant difference in selectivity, as only a marginal decrease from 69 to 67% was detected for the pinene oxide selectivity.<sup>[225]</sup>

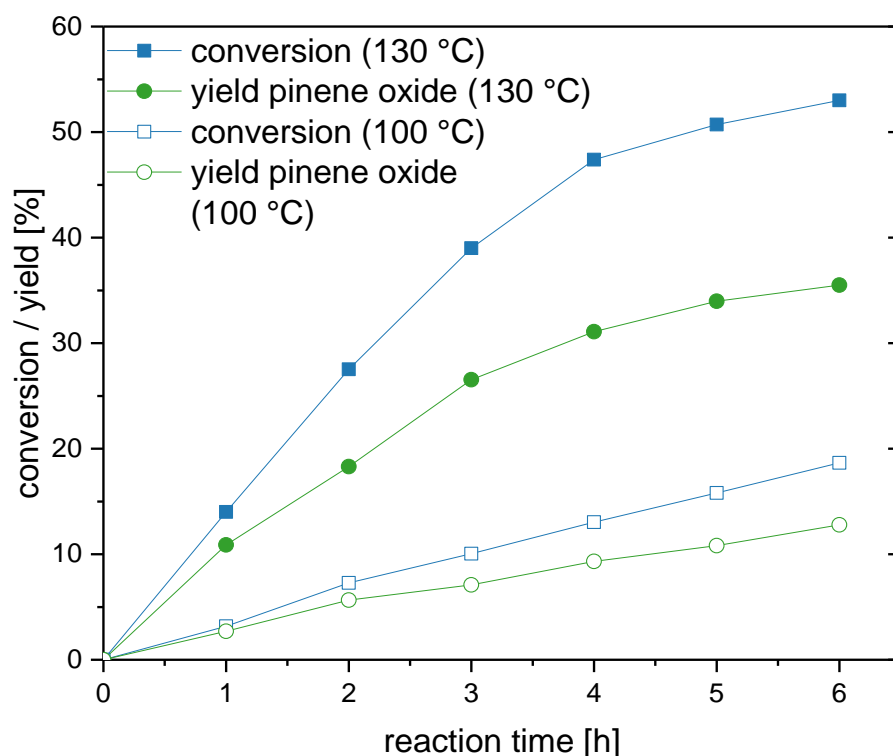


Figure 53: Dependency of reaction temperature on conversion and yield. Reaction conditions:  $\alpha$ -pinene (1.00 mmol), Mn(III) acetate (1.00 mol%), toluene/DMF (90:10, 30 mL), compressed air (50 mL min<sup>-1</sup>).

Next, the applied air flow rates were varied from 25 to 100 mL min<sup>-1</sup> (see Figure 54). The analysis showed that high flow rates were advantageous for the overall conversion. By doubling the oxidant flow rate from 25 to 50 mL min<sup>-1</sup>, the conversion increased from 36 to 54% and also the yield of pinene oxide increased to 35%. However, an increase in flow rate from 50 to 100 mL min<sup>-1</sup> did not result in further enhancement of conversion, yield and selectivity to pinene oxide. The selectivity, which amounted almost 70% in all three experiments, did not depend on the flow rate. Thus, it can be concluded that a high oxygen availability is crucial to this reaction, although an upper limit for the positive impact was discovered. Another cause of the benefits from high oxidant flow rates might be assigned to the faster removal of volatile catalyst poisons, such as dimethylamine, that could be generated by DMF degradation.

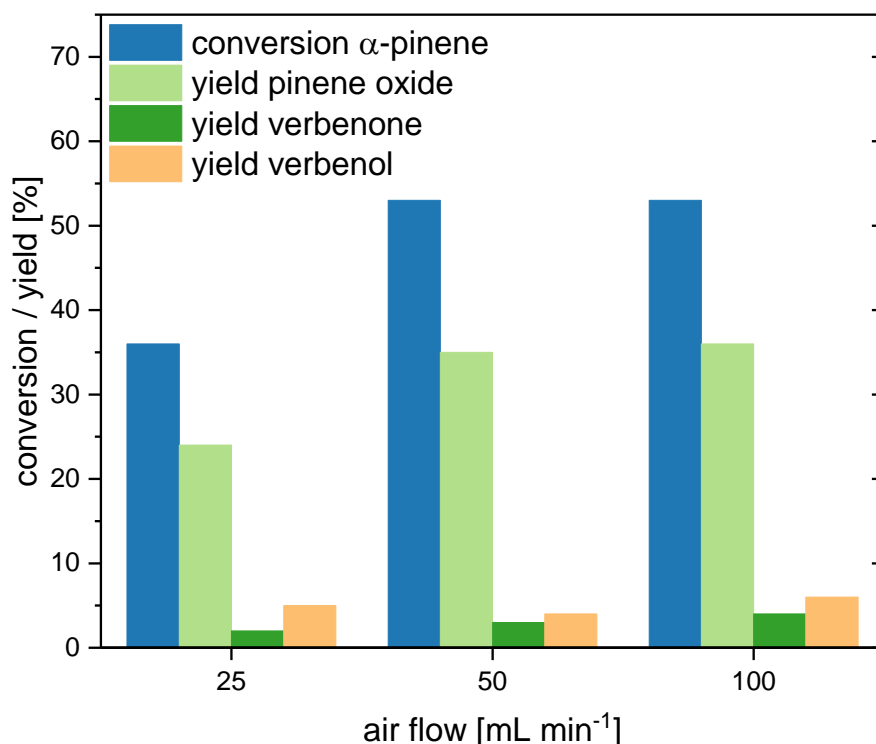


Figure 54: Influence of air flow rate on conversion and yield for the catalytic oxidation of  $\alpha$ -pinene. Reaction conditions:  $\alpha$ -pinene (1.00 mmol), catalyst (0.500 mol% Mn), toluene/DMF (90:10, 30 mL), compressed air (flow as indicated), 130 °C, 6 h.

Combining the findings of the performed screening reactions, a reaction time of 6 h, toluene/DMF (90:10) as solvent mixture, 130 °C, 0.250 mol% catalyst concentration and an air flow of 50 mL min<sup>-1</sup> gave the best result for the aerobic  $\alpha$ -pinene oxidation catalysed by Mn(III) acetate. With the optimised reaction conditions, an  $\alpha$ -pinene conversion of 62% and a pinene oxide yield of 40% were achieved, resulting in a turnover number (TON =  $[n_{\text{product}}/n_{\text{catalyst}}]$ ) of 166 and a selectivity of 65%.

Although, Anastas and Warner recommend solvent-free procedures in their 12 principles of Green Chemistry in this case the use of a solvent is inevitable to dissolve the catalyst.<sup>[22]</sup> As reviewed by Mallat and Baiker, the involvement of organic solvents in redox reactions is rarely considered, although the ‘sacrificial’ solvent may take over the role of the actual oxidising agent leading to false mechanistic interpretations of the results.<sup>[221]</sup> Moreover, the formation of solvent-derived by-products that do not belong to the actual oxidation mechanism effects the atom economy and increases the E factor. In particular, sulfoxides (e.g. DMSO), nitriles (e.g. acetonitrile) and amides (e.g. DMF) are known to act as sacrificial solvents. Caps *et al.* also identified methylcyclohexane as an active part in the

epoxidation mechanism of *trans*-stilbene.<sup>[226]</sup> Considering these studies, the choice of an appropriate reaction medium represents a demanding task.

In this regard, both DMF and toluene are not ideal solvents for this reaction, although DMF turned out to be an essential component for the epoxidation mechanism. In addition to the by-product formed by DMF oxidation, GC–MS analysis of the reaction mixture also revealed that toluene was not an inert solvent under the applied reaction conditions, leading to considerable amounts of benzyl alcohol and benzaldehyde as by-products. To find a more sustainable alternative for toluene, dimethyl carbonate (DMC) and diethyl carbonate (DEC) were evaluated as co-solvents under the same reaction conditions (see Table 8). The 90:10 mixture of DMC and DMF resulted in the lowest conversion (7%) and yield of pinene oxide (1%), which might be caused by the lower boiling point (90 °C) compared to toluene (111 °C) and DEC (126 °C). The 90:10 mixture of DEC and DMF gave an  $\alpha$ -pinene conversion of 38% and a pinene oxide yield of 23%. This mixture should be preferred over toluene/DMF for sustainability reasons (see safety (S), health (H) and environment (E) scores by CHEM21 selection guide: toluene: S = 5, H = 6, E = 3, overall ranking = problematic; DMC: S = 4, H = 1, E = 3, overall ranking = recommended),<sup>[227]</sup> even if the conversion was slightly lower (compare Table 8, entries 1 and 3). Although these data are for DMC (data for DEC is not available), they suggest a better sustainability for the latter. Moreover, no additional by-products related to solvent oxidation were produced (i.e. carbonates were inert solvents under these conditions). However, as already experienced for toluene as the sole solvent, DEC without addition of DMF gave poor conversion and yield. Moreover, if only a stoichiometric amount of DMF (Table 8, entry 4) was used (in relation to  $\alpha$ -pinene), both conversion (20%) and pinene oxide yield (9%) were low compared to the reaction using larger amounts of DMF (Table 8, entry 3).

Table 8: Solvent effect in the aerobic epoxidation of  $\alpha$ -pinene. Reaction conditions:  $\alpha$ -pinene (1.00 mmol), Mn(III) acetate (1.00 mol%), solvent (30 mL), compressed air (50 mL min<sup>-1</sup>), 130 °C, 6 h.

Entry	Solvent	Conversion [%]	Selectivity (yield) [%]		
			Pinene oxide	Verbenone	Verbenol
1	Toluene/DMF (90:10)	53	66 (35)	5 (3)	4 (2)
2	DMC/DMF (90:10)	7	14 (1)	6 (0.4)	5 (0.3)
3	DEC/DMF (90:10)	38	59 (23)	5 (2)	4 (1)
4	DEC/DMF (99.5:0.5)	20	43 (9)	7 (1)	8 (2)
6	DEC	11	14 (2)	4 (0.4)	5 (0.3)

After having investigated appropriate reaction conditions for the aerobic  $\alpha$ -pinene oxidation with Mn(III) acetate as a homogeneous catalyst, these reaction conditions were subsequently applied for the reaction using a novel Mn-containing MOF as heterogeneous counterpart.

Recently, a lot of effort has been made to replace conventional homogeneous catalytic systems by their heterogeneous equivalents to benefit from the possibility of catalyst regeneration. This substitution contributes to avoid or simplify steps, such as catalyst separation, *etc.* For this purpose, various strategies for the immobilisation of redox-active elements in a solid matrix have been investigated. For instance, isomorphous substitution in the crystallographic positions of an inorganic framework, deposition of metal compounds onto surfaces, tethering metal complexes to the surface *via* a spacer ligand, encapsulation into a solid matrix, *etc.* proved to be suitable approaches.<sup>[228]</sup> Recently, metalorganic frameworks have been considered as promising and effective catalysts for various types of oxidations in the liquid phase (*e.g.* alcohol oxidation,<sup>[229-231]</sup> epoxidation,<sup>[101, 222, 232, 233]</sup> hydrocarbon oxidation,<sup>[104]</sup> *etc.*). Advantageously, the well-distributed and well-defined isolated metal centres of MOFs enable them to potentially combine the advantages of heterogeneous and the efficiency of homogeneous catalysts.<sup>[234, 235]</sup>

In this regard, a novel Mn-containing MOF MIXMIL-53-NH<sub>2</sub>(50)-Mal-Mn was developed and implemented for a more sustainable catalytic process. The heterogeneous catalyst also enabled a direct comparison to the performance of the homogeneous Mn(III) acetate catalyst. For this purpose, a mixed-linker metal-organic framework with MIL-53(Al)

structure containing equal amounts of terephthalate and 2-aminoterephthalate linkers was synthesised in a modified two-step post-synthetic modification (PSM) that has been previously reported for the generation of MOF-based single-site Pd catalysts (see Figure 55).<sup>[235]</sup> First, the amine groups of the organic linker molecules were covalently modified using maleic anhydride, resulting in a chelating side group at the linkers that was subsequently used for the immobilisation of manganese complexes.

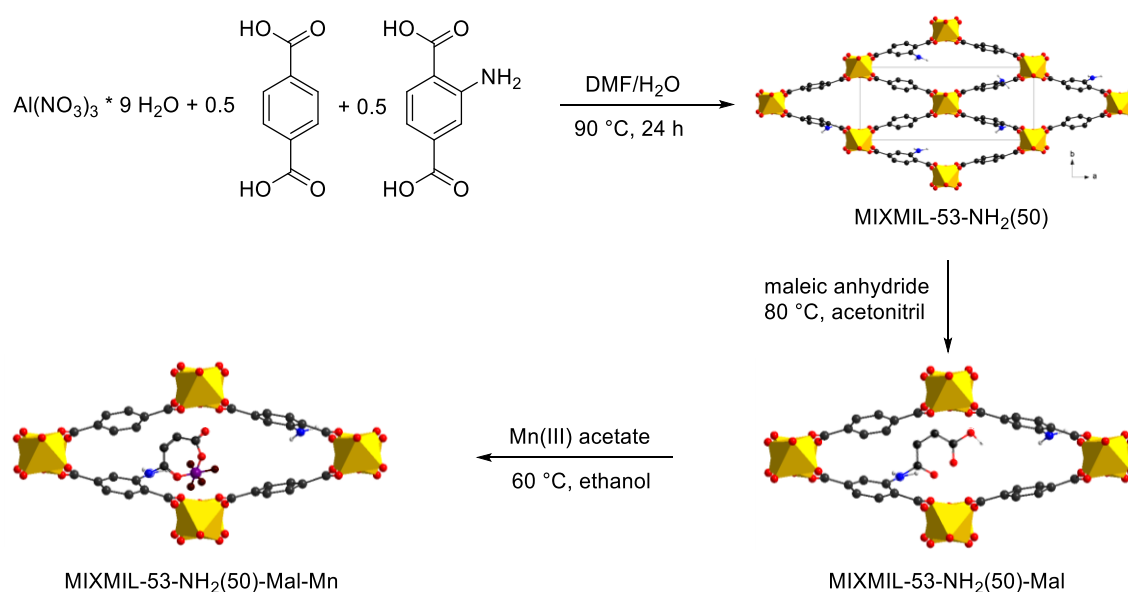


Figure 55: Synthesis procedure for MIXMIL-53-NH<sub>2</sub>(50) and subsequent two-step post-synthetic modification to immobilise manganese complexes.

The XRD pattern (see Figure 56) of the resulting catalyst revealed a crystalline structure that is very similar to the simulated diffractogram for MIL-53(Al) with minor deviations that can be explained by a breathing behaviour of the pores after the introduction of the immobilized guest species in the pore structure.<sup>[236]</sup>



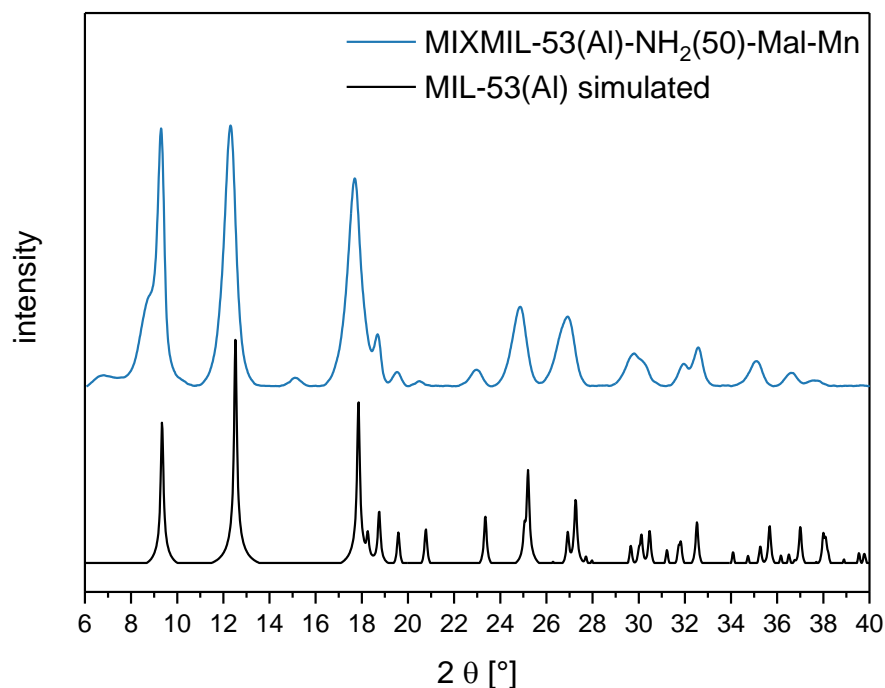


Figure 56: XRD patterns of simulated MIL-53(Al) and MIXMIL-53(Al)-NH<sub>2</sub>(50)-Mal-Mn.

Attenuated total reflection (ATR) IR spectra (see Experimental Part, Chapter 6.3.1, Figure 94 - Figure 96) were recorded to exclude residual free acid (C=O band expected around 1685 cm<sup>-1</sup>) or solvent molecules (DMF; C=O band expected around 1650 cm<sup>-1</sup>) in the pores of the frameworks. The N-H stretching vibrations of the amine functionalities (around 3500 cm<sup>-1</sup> and 3389 cm<sup>-1</sup>), the OH stretching vibrations of the Al-OH-chains (around 3621 cm<sup>-1</sup>) and the OH stretching vibrations of the maleate side group (around 3692 cm<sup>-1</sup>) were observed. <sup>1</sup>H NMR spectra of the MOF before and after immobilisation of the Mn species proved the presence of the two linker molecules in the desired ratio (1:1) and revealed a modification degree of ~6% of the amine groups. Results from physisorption experiments (see Table 9) proved that the catalyst still featured a high specific surface area and accessible micropore volume after the PSM reaction. The manganese content of the catalyst was determined by atomic absorption spectroscopy (AAS), resulting in a loading of 0.9 wt% (see Table 9, entry 3).

Table 9: Specific surface areas and micropore volumes of modified MIL-53(Al) materials obtained from nitrogen physisorption measurements. Mn content of MIXMIL-53-NH<sub>2</sub>(50)-Mal-Mn determined by AAS measurements.

Entry	Material	S <sub>BET</sub> [m <sup>2</sup> g <sup>-1</sup> ]	Micropore volume [cm <sup>3</sup> g <sup>-1</sup> ]	Mn content [wt%]
1	MIXMIL-53-NH <sub>2</sub> (50)	840	0.23	-
2	MIXMIL-53-NH <sub>2</sub> (50)-Mal	480	0.21	-
3	MIXMIL-53-NH <sub>2</sub> (50)-Mal-Mn	380	0.15	0.9

In a first attempt, the Mn-containing MOF catalyst showed notable activity for the aerobic oxidation of  $\alpha$ -pinene in a solvent mixture of DEC and DMF with a continuous feed of air into the reaction mixture for 6 h at 130 °C. Pinene oxide was detected as the major product by GC–MS and comparison with authentic samples (see Figure 57). Additionally, the formation of the side-products verbenone and verbenol was observed.

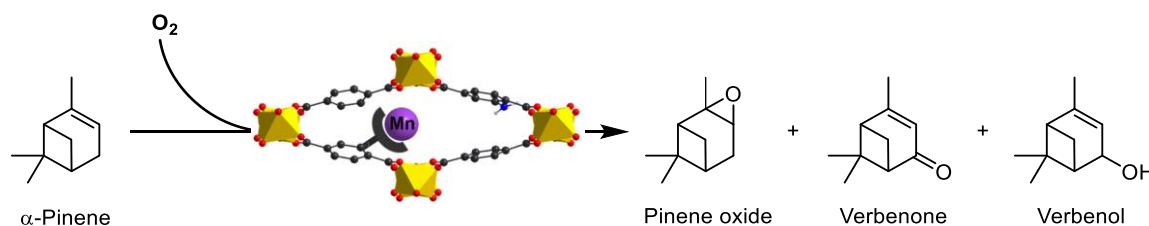


Figure 57: Catalytic oxidation of  $\alpha$ -pinene by MIXMIL-53-NH<sub>2</sub>(50)-Mal-Mn resulting in pinene oxide, verbenone and verbenol as the main products (conversion: 31%, selectivities: 54, 8 and 3%, respectively). Reaction conditions:  $\alpha$ -pinene (1.00 mmol), MIXMIL-53-NH<sub>2</sub>(50)-Mal-Mn (0.500 mol% Mn), DEC/DMF (90:10, 30 mL), compressed air (50 mL min<sup>-1</sup>), 130 °C, 6 h.

Subsequently, the catalytic performance of the MOF-based catalyst was compared to the homogeneously dissolved Mn salt (see Figure 58). The heterogeneous catalyst exhibited a good activity and showed similar results as achieved with 0.500 mol% Mn(III) acetate under the same conditions. Indeed, after 6 h, the conversion was 31% both for the homogeneous system and the MOF-containing catalyst. The selectivities of Mn(III) acetate and the MOF-containing catalyst to pinene oxide (55% and 54%, respectively), verbenone (7% and 8%, respectively) and verbenol (6% and 3%, respectively) were also similar. The mass balances accounted for 68% and 65%, respectively. The remainder of the converted  $\alpha$ -pinene could be assigned to pinene oxide isomerisation products since the

chromatogram showed several, very small peaks in the same region as the main oxidation products pinene oxide, verbenol and verbenone. GC–MS analysis indicated the additional formation of campholenic aldehyde, pinocarvone and carveol in low concentrations.

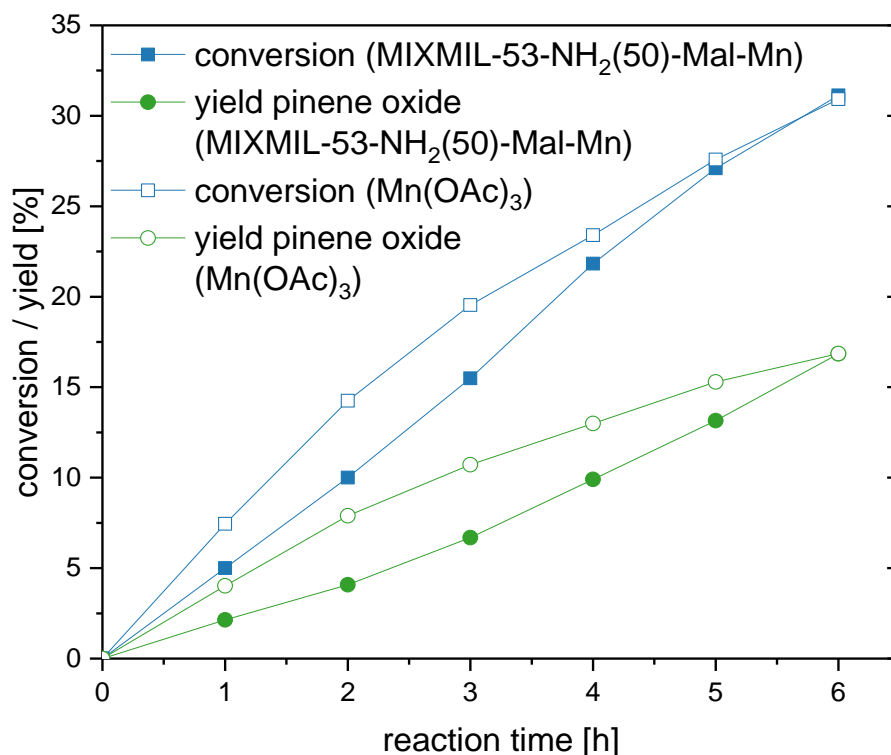


Figure 58: Conversion and yield of aerobic  $\alpha$ -pinene oxidation catalysed by MIXMIL-53-NH<sub>2</sub>(50)-Mal-Mn and homogeneous Mn(III) acetate, respectively. Reaction conditions:  $\alpha$ -pinene (1.00 mmol), catalyst (0.500 mol% Mn), DEC/DMF (90:10, 30 mL), compressed air (50 mL min<sup>-1</sup>), 130 °C.

To benefit from the main advantages of heterogeneous catalysis, the Mn-containing MOF must be easily recoverable from the reaction medium and allow for a straightforward regeneration. If these criteria are fulfilled, heterogeneous catalysis facilitates waste prevention and conservation of resources. Therefore, the stability of the catalyst under the applied reaction conditions has to be ensured. For the assessment of its stability, the reusability of the MOF-based catalyst was tested by using it in five successive catalytic reactions. After each catalytic reaction, the catalyst was filtered from the reaction mixture, washed, dried at room temperature and reused in another  $\alpha$ -pinene oxidation reaction under the same conditions. The results of the recycling test showed that the catalyst was active for at least five reaction cycles without significant loss of activity (see Figure 59).

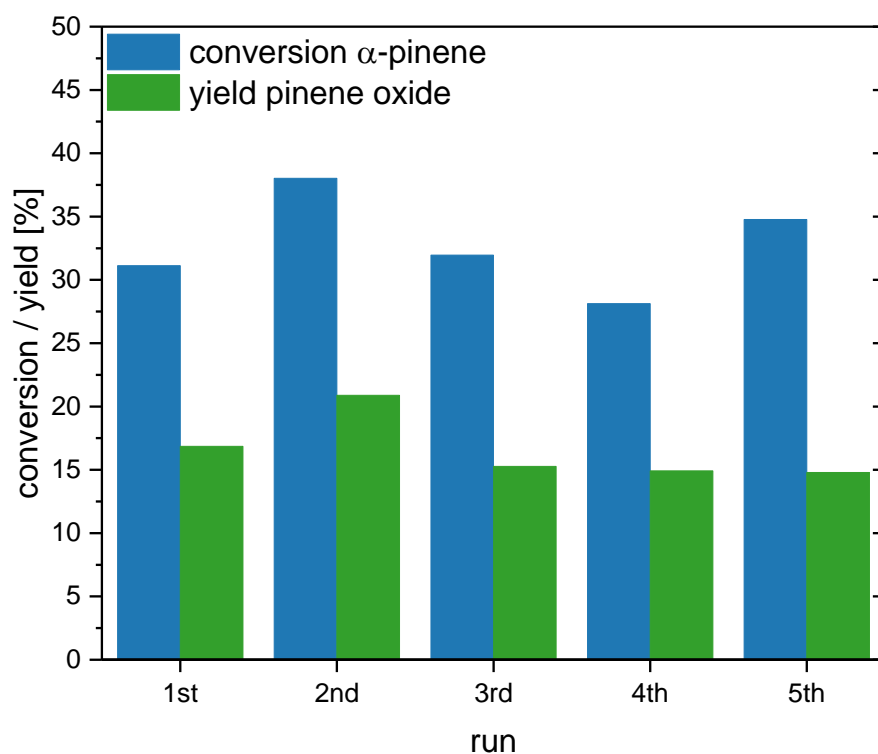


Figure 59: Catalytic performance of MIXMIL-53-NH<sub>2</sub>(50)-Mal-Mn in five cycles of  $\alpha$ -pinene epoxidation. Reaction conditions:  $\alpha$ -pinene (1.00 mmol), MIXMIL-53-NH<sub>2</sub>(50)-Mal-Mn (0.500 mol% Mn), DEC/DMF (90:10, 30 mL), compressed air (50 mL min<sup>-1</sup>), 130 °C, 6 h.

The successful reuse of MIXMIL-53-NH<sub>2</sub>(50)-Mal-Mn may be interpreted as a first indication that the catalytically active sites of the catalyst neither became inactive during the reaction nor that significant amounts of Mn leached out of the catalyst. However, a truly heterogeneous reaction pathway can only be asserted by a heterogeneity test as proposed by Sheldon and Schuchardt et al.<sup>[105]</sup> Therefore, a hot filtration test was carried out by filtering the catalyst from the hot reaction mixture after 3 h and continuing the reaction for another 5 h. At the same time, a control experiment was conducted, in which the catalyst remained in the reaction mixture. In the case of exclusive heterogeneous catalysis, conversion and yield should remain constant after catalyst removal. In the experiments, the conversion and yield of pinene oxide further increased slightly after removal of the MIXMIL-53-NH<sub>2</sub>(50)-Mal-Mn catalyst (see Figure 60). However, in comparison to the control experiment, the reaction rate was remarkably lower, indicating that the reaction was mainly catalysed heterogeneously.

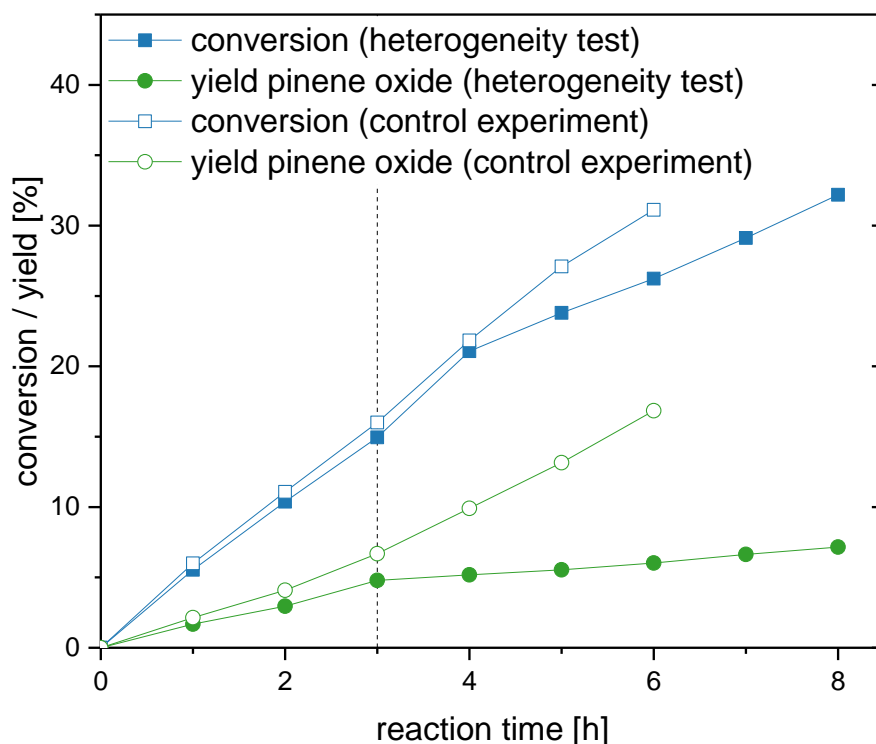


Figure 60: Comparison of conversion and yield of  $\alpha$ -pinene epoxidation with and without catalyst removal after 3 h (as indicated by vertical line). Reaction conditions:  $\alpha$ -pinene (1.00 mmol), MIXMIL-53-NH<sub>2</sub>(50)-Mal-Mn (0.500 mol% Mn), DEC/DMF (90:10, 30 mL), compressed air (50 mL min<sup>-1</sup>), 130 °C.

The observed activity despite catalyst filtration might arise from solid catalyst particles that were too small to be removed by the filter, although minor amounts of homogeneous species cannot be completely ruled out as an additional catalytically active species. In summary, the recycling experiments demonstrated the reusability of the catalyst and the advantages of a heterogeneous system. In the five consecutive runs, an overall TON of 166 was obtained.

Despite significant constraints due to the necessity of DMF as a sacrificial reductant, this work provides evidence that the Mn-containing MOF MIXMIL-53-NH<sub>2</sub>(50)-Mal-Mn can be considered a promising solid catalyst for aerobic oxidation reactions.

## 4.2 Follow-up Chemistry for Oxidised Terpenes

### 4.2.1 Cyclic and Linear Carbonates from $\alpha$ -Pinene

Within this chapter, oxidised pinenes are evaluated as renewable starting materials for the synthesis of cyclic and linear carbonates. For the design of new synthesis protocols, the focus lies with the development of green and sustainable reaction procedures. Before discussing results, the properties, applications and production of organic carbonates in general are briefly introduced, elucidating the motivation for the presented studies.

Among linear and cyclic carbonates, dimethyl, diphenyl, ethylene and propylene carbonate are prominent examples, which are produced on industrial scale with increasing growth rates.<sup>[237]</sup> Organic carbonates are particularly relevant as intermediates in the manufacturing of fine chemicals<sup>[238-241]</sup> and as monomers for the production of isocyanate-free polyurethanes, polycarbonates and other polymers.<sup>[242-245]</sup> In addition, they can be used as components of electrolytes in lithium ion rechargeable batteries,<sup>[246]</sup> industrial lubricants,<sup>[247]</sup> additives to gasoline<sup>[248]</sup> and components in cosmetics and paints.<sup>[249, 250]</sup> Due to their high solubilising power, relatively low toxicity, good biodegradability, high boiling and flash points, and low odour and evaporation rates, organic carbonates are well suited as aprotic polar green solvents, capable of replacing conventional hazardous solvents, such as toluene or dichloromethane.<sup>[251]</sup>

The conventional route to linear carbonates is a two-step process starting with the formation of phosgene from carbon monoxide and chlorine gas, followed by the reaction with alcohols (see Figure 61, A). Due to the high toxicity of phosgene and co-produced hydrogen chloride, several alternative routes to linear carbonates were established. Since the middle 1980s, a single-step process based on the copper salt catalysed oxidative carbonylation of methanol was commercialised for the production of dimethyl carbonate (DMC) (see Figure 61, B).<sup>[252]</sup> Another alternative route to linear carbonates is the insertion of CO<sub>2</sub> into an epoxide, such as ethylene oxide, resulting in cyclic carbonate, which is subsequently reacted with an alcohol, e.g. methanol. This route is nowadays mainly used for the production of dimethyl carbonate.<sup>[253]</sup> However, it generates ethylene glycol as by-product and involves toxic and explosive ethylene oxide as starting material (see Figure 61, C). From an environmental point of view, the direct formation of dimethyl carbonate from CO<sub>2</sub> and methanol is the most efficient and straightforward process (see Figure 61, D). The dehydrative condensation is carried out at elevated temperatures and high pressures using organostannanes, titanium or zirconium alkoxides as catalysts and acetals as dehydrating agents.<sup>[254]</sup> Another approach, which is also carried out on industrial

scale, is the transesterification of urea with methanol. Here, only ammonia is formed as a by-product which, in principle, can be recycled for urea synthesis with CO<sub>2</sub>.<sup>[255]</sup>

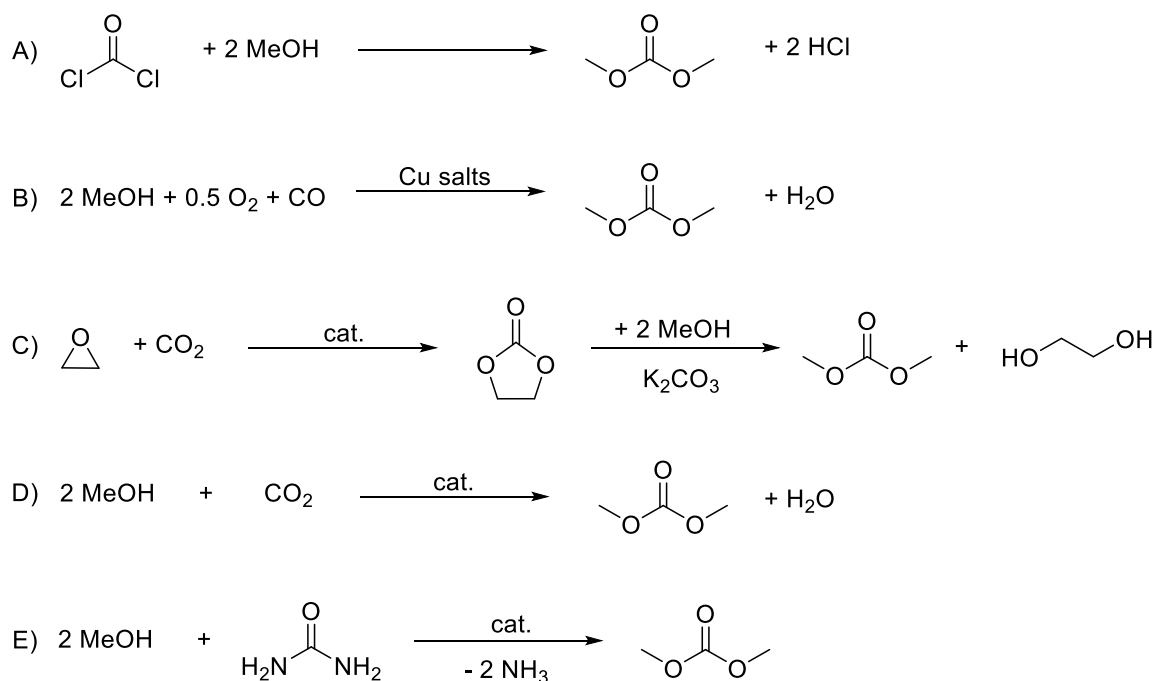


Figure 61: Synthesis routes for the production of linear carbonates exemplified by dimethyl carbonate. A) via phosgene; B) by catalytic oxidative carbonylation of methanol, C) by CO<sub>2</sub> insertion into oxirane; D) dehydrative condensation of methanol and CO<sub>2</sub>; and E) by transesterification of urea with methanol.

It is worth noting that dimethyl carbonate, depending on the reaction conditions and the applied nucleophile, can either be used as a methoxycarbonylation or methylation agent and therefore allows replacing toxic and carcinogenic substances such as dimethyl sulfate, methyl halides, and phosgene.<sup>[256]</sup> Its remarkably versatile reactivity arises from the two different pathways, in which nucleophiles can react with DMC. In the first pathway (see Figure 62, left), the nucleophile attacks the carbonyl carbon group resulting in transesterification, while methanol is released. The second pathway (see Figure 62, right), leads to the alkylation of the nucleophile by attacking at the methyl group of DMC. The preferred reaction pathway depends on the reaction conditions and on the type of nucleophile according to the HSAB theory. Aliphatic amines and alcohols, classified as hard nucleophiles, predominantly attack the carbonyl carbon group at low temperatures leading to reversible transesterification. At temperatures higher than the reflux temperature of 90 °C hard nucleophiles also undergo alkylation as side reaction. Soft nucleophiles such as anilines, phenols and carboxylates are irreversibly alkylated, while CO<sub>2</sub> is released, which can be useful in polymer foam production. If the temperature exceeds 150 °C, both

hard and soft nucleophiles attack the soft electrophilic site of the two methyl groups resulting irreversible alkylation.<sup>[237]</sup>

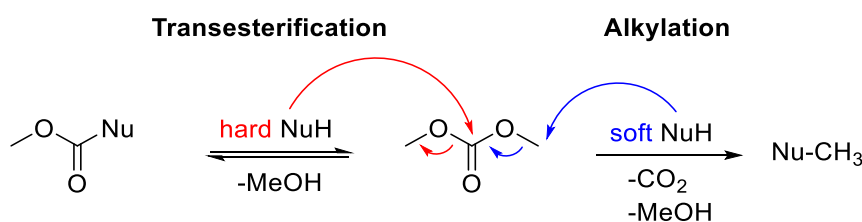


Figure 62: Reactivity of dimethyl carbonate according to the HSAB theory: transesterification (left) and alkylation (right).<sup>[257]</sup>

Since their commercialisation in the mid-1950s, cyclic carbonates are valuable synthetic targets with a wide range of applications (see Figure 63).<sup>[254]</sup> Particularly cyclic carbonates with a five-membered ring are not only useful as inert media, but also as reactive intermediates, e.g. as alkylating agents for aromatic amines, phenols and thiols at high temperatures.<sup>[258]</sup> Figure 63 shows various phosgene free, CO<sub>2</sub> based synthetic routes to five-membered cyclic carbonates using carbon dioxide and their possible applications.

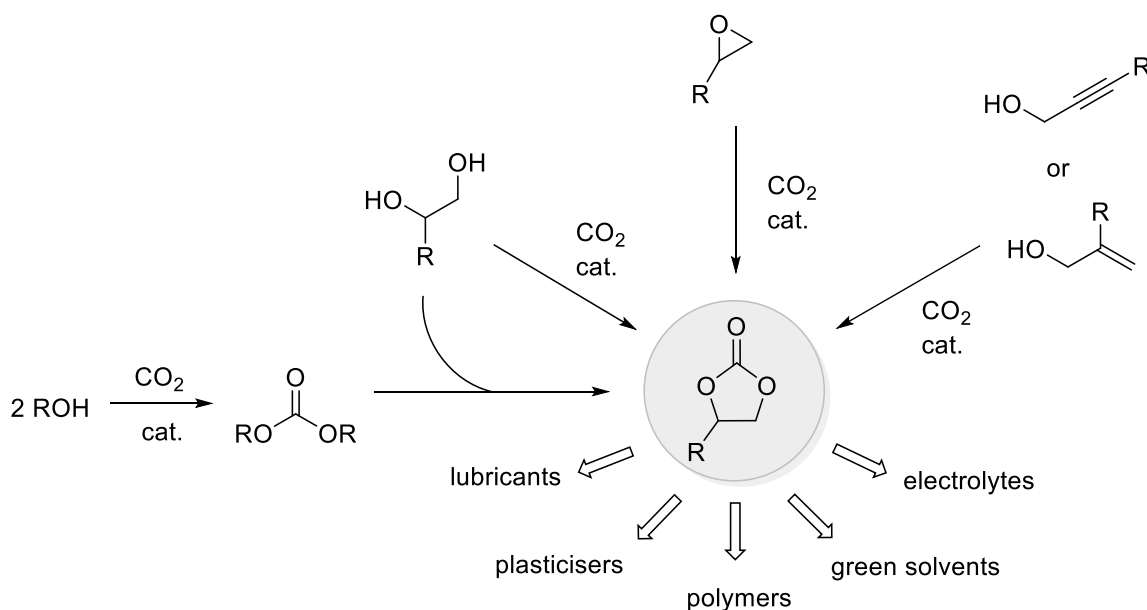


Figure 63: Synthetic routes to five-membered cyclic carbonates and various fields of application.

The synthesis procedures exploit the reaction of carbon dioxide with activated alkenes or alkynes, oxiranes and diols, and the reaction of diols with dialkylcarbonates. On an industrial scale, the synthesis of cyclic carbonates is usually achieved *via* CO<sub>2</sub> and oxiranes using Lewis acids or bases as catalysts at high temperatures and pressures. However, the harsh reaction conditions are the limiting factor due to the excessive energy



consumption resulting in high energy costs and high indirect carbon dioxide emission associated with the energy production which reduces the overall sustainability of the process. Therefore, there is a great demand for new, commercially viable catalysts that enable reactions to proceed at room temperature and at atmospheric CO<sub>2</sub> pressure. In the literature, numerous catalytic systems have been investigated for the coupling of CO<sub>2</sub> and epoxides. These catalysts include transition metals,<sup>[259]</sup> alkali metal salts,<sup>[260]</sup> carbenes,<sup>[261]</sup> quaternary ammonium<sup>[262]</sup> or phosphonium salts,<sup>[263]</sup> functional polymers<sup>[264]</sup> and ionic liquids.<sup>[265]</sup>

The mechanism postulated for the formation of five-membered cyclic carbonates by catalytic conversion of epoxides with CO<sub>2</sub> involves the ring-opening of the epoxide *via* nucleophilic attack at the less hindered carbon atom by the anion X<sup>-</sup> (see Figure 64). The thereby formed alcoholate then reacts with CO<sub>2</sub>, resulting in another anion which yields the cyclic product upon ring-closure.

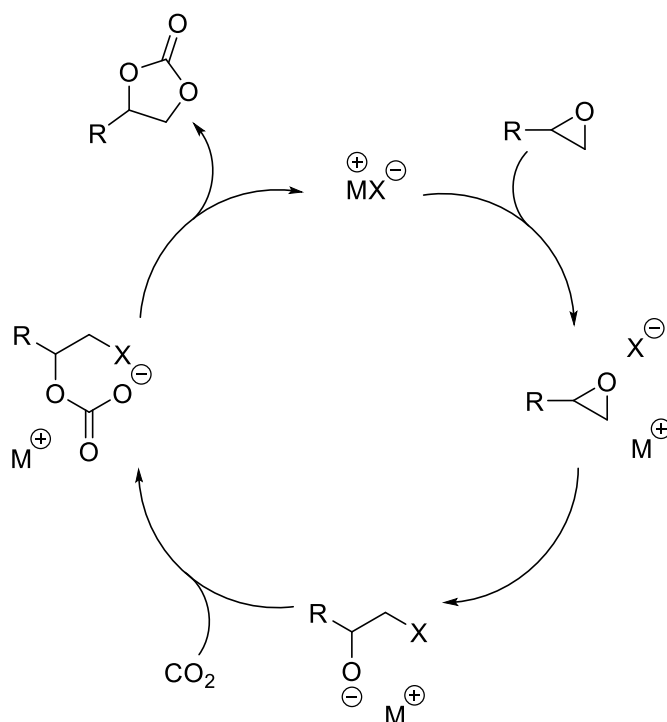


Figure 64: Proposed reaction mechanism for the synthesis of five-membered cyclic carbonates via direct chemical fixation of CO<sub>2</sub> with epoxides.<sup>[266]</sup>

The chemical fixation of CO<sub>2</sub> into commodity chemicals has been proposed as part of the solution to mitigate the effects of the increased concentration of CO<sub>2</sub> in the atmosphere by capture and sequestration. This, together with the wide availability, renewability and non-toxicity puts the utilisation of CO<sub>2</sub> as a C<sub>1</sub> feedstock in the spotlight of academic research.

#### 4.2.1.1 Coupling of $\alpha$ -Pinene Oxide and $\text{CO}_2$

With the aim to synthesise linear and cyclic carbonates based on pinenes, various approaches were investigated within this chapter. Due to the aforementioned advantages related to chemical fixation of  $\text{CO}_2$ , synthesis protocols involving the coupling reaction between epoxides and  $\text{CO}_2$  were tested first. To begin with, commercially available  $\alpha$ -pinene oxide was chosen as substrate (see Figure 65). To date, no reaction procedure was reported that proved to be capable of transforming  $\alpha$ -pinene oxide into the corresponding cyclic carbonate using  $\text{CO}_2$ . Pescarmona and co-workers reported the attempt to transform  $\alpha$ -pinene oxide and limonene oxide into the corresponding cyclic carbonate *via*  $\text{CO}_2$  insertion using a novel iron pyridylamino-bis(phenolate) catalyst. However, the presence of a methyl group on the epoxide ring imposed a significant steric barrier for the nucleophilic attack and therefore no conversion was achieved.<sup>[259]</sup>

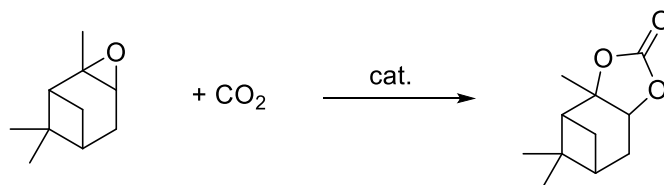


Figure 65: Theoretical coupling reaction between  $\alpha$ -pinene oxide and  $\text{CO}_2$  yielding  $\alpha$ -pinene cyclic carbonate.

In order to find reaction conditions that enable the conversion of  $\alpha$ -pinene oxide with  $\text{CO}_2$ , several promising literature-known procedures for the coupling of  $\text{CO}_2$  with other epoxy substrates were transferred to the reaction of  $\text{CO}_2$  with  $\alpha$ -pinene oxide. However, since in the literature a vast amount of catalytic systems for the cyclic carbonate formation from epoxides (other than  $\alpha$ -pinene oxide) can be found, the search for a suitable catalytic system needed to be specified. Employed criteria were commercial availability of the catalyst as well as the potential co-catalyst, and in ideal case, proved activity for internal, bulky epoxides. With these criteria in mind, four different catalytic systems were selected (see Figure 66). The first system tested was established by Werner and Tenhumberg in 2014 (see Figure 66, A).<sup>[267]</sup> The authors combined simple amines and especially amino alcohols with catalytically active potassium iodide for the cyclic carbonate formation from epoxides and  $\text{CO}_2$ . It was stated that the enhanced catalytic activity originates from synergistic effects of the potassium iodide/triethanolamine system. This was explained by the known ability of amino alcohols to complex alkali metal halides, which potentially allows triethanolamine to act as a phase transfer catalyst increasing the solubility of the salt. Additionally, the hydroxyl function of the amino alcohol can activate the epoxide through

hydrogen bonding. Furthermore, it was assumed that CO<sub>2</sub> is activated by the amino alcohol in close approximation to the activated epoxide. By applying the catalytic system for the coupling of different epoxides, including cyclohexene oxide as an internal epoxide, with CO<sub>2</sub>, the authors proved its activity. However, in the case of cyclohexene oxide 2 mol% potassium iodide, 2 mol% triethanolamine, 90 °C, and 10 bar CO<sub>2</sub> pressure for two hours under solvent-free conditions resulted in a yield of only 2%. Therefore, the authors increased temperature, pressure and time to 120 °C and 50 bar for six hours, which led to a better result of 27% yield after column chromatography.

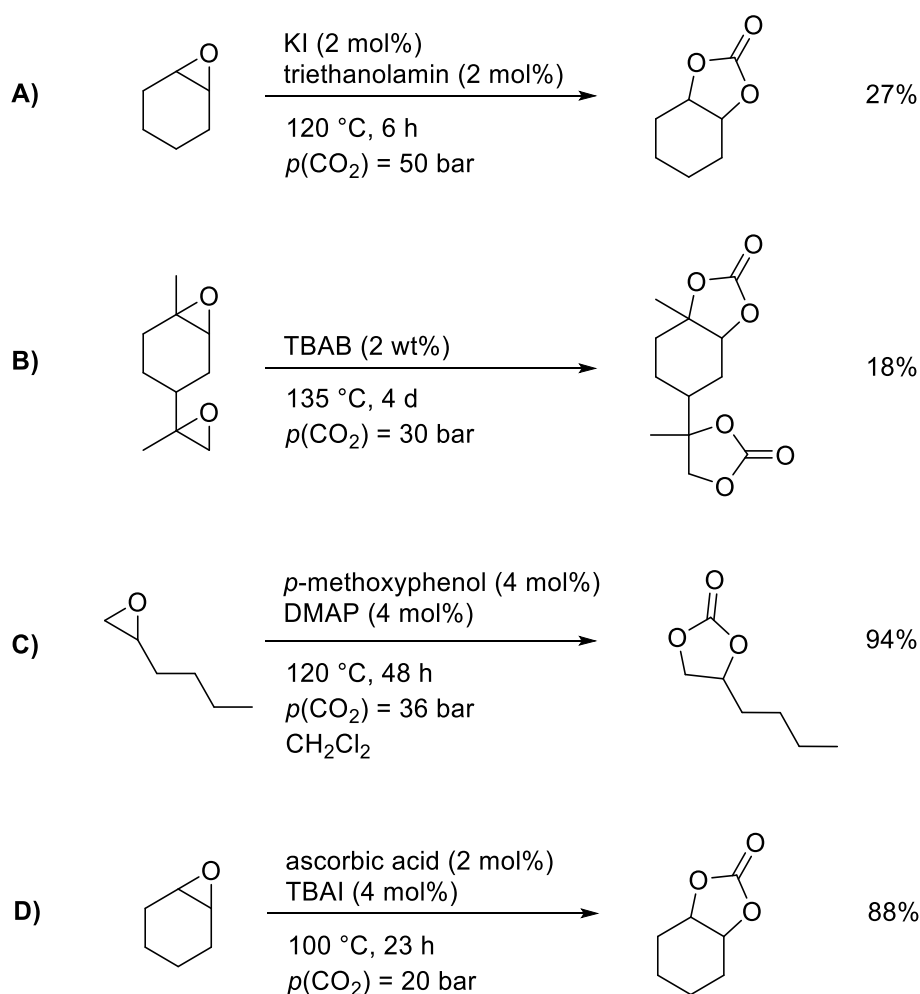


Figure 66: Literature procedures for the coupling reaction between epoxides and CO<sub>2</sub>. A) Werner and Tenhumberg,<sup>[267]</sup> B) Mülhaupt et al.,<sup>[210]</sup> C) Shi et al.<sup>[268]</sup> and D) D'Elia et al.<sup>[269]</sup>

Since these reaction conditions seemed promising also for internal epoxides, they were transferred to  $\alpha$ -pinene oxide. Therefore, a stainless-steel high-pressure-reactor with PTFE inset was charged with 25.0 mmol of the substrate, 2 mol% triethanolamine and 2 mol% potassium iodide. Additionally, 10 mol% hexadecane were added as internal standard for GC analysis. Due to the layout of the available high pressure equipment, it

was not possible to reach 50 bar CO<sub>2</sub> pressure as used by Werner and Tenhumberg. Instead, 35 bar CO<sub>2</sub> pressure were applied. After a reaction time of six hours, the vessel was allowed to cool down to room temperature. Subsequently, a GC sample was taken. However, when compared with an authentic sample and the internal standard, the obtained chromatogram revealed that no conversion took place. It is assumed that steric hindrance of the bicyclic  $\alpha$ -pinene skeleton does not allow the catalyst and the co-catalyst to activate and open the epoxide ring for CO<sub>2</sub> insertion.

In a second approach, tetrabutylammonium bromide (TBAB) was evaluated as catalyst for the coupling of  $\alpha$ -pinene oxide and CO<sub>2</sub> based on preliminary studies by Mülhaupt *et al.* (see Figure 66, B).<sup>[210]</sup> The authors showed that it was possible to transform limonene dioxide into the corresponding dicarbonate with CO<sub>2</sub> in the presence of TBAB. It was proposed that the halide opens the epoxy ring resulting in an alkoxide ion. The alkoxide ion, in turn, attacks the CO<sub>2</sub> yielding a five-membered cyclic carbonate after ring-closure. The authors applied 2 wt% of TBAB at 135 °C and 30 bar of CO<sub>2</sub> pressure for four days and obtained limonene dicarbonate in 18% yield after recrystallisation. However, transferring these reaction conditions to  $\alpha$ -pinene did not result in any conversion.

Animated by the readily available catalytic system established by Shi and co-workers, a third attempt for the synthesis of  $\alpha$ -pinene carbonate from CO<sub>2</sub> was carried out using a combination of a phenol and an organic base, *i.e.* *N,N*-dimethylpyridin-4-amine (DMAP) (see Figure 66, C).<sup>[268]</sup> As assumed by the authors, the amine and the phenol (through hydrogen bonding) serve as Lewis base and Lewis acid, respectively, which together co-catalyse the reaction. In the proposed reaction mechanism, the Lewis base and the Lewis acid work together to open the epoxy ring followed by CO<sub>2</sub> insertion and recyclisation. Unlike the aforementioned studies, the authors evaluated the catalytic system only by the reactions of terminal epoxides with CO<sub>2</sub>. The established reaction conditions of 4 mol% *p*-methoxyphenol, 4 mol% DMAP in dichloromethane at 120 °C and 36 bar CO<sub>2</sub> pressure for 48 h were directly applied for  $\alpha$ -pinene oxide as a substrate. Most likely due to the same reason as in reaction protocols above, no conversion was observed by GC analysis.

In a last approach, ascorbic acid was evaluated as an environmentally benign hydrogen bond donor in combination with tetrabutylammonium iodide (TBAI) as nucleophilic co-catalyst for the coupling of  $\alpha$ -pinene oxide and CO<sub>2</sub> (see Figure 66, D). D'Elia *et al.* recently showed that the binary catalytic system ascorbic acid/TBAI has remarkable activity also for internal epoxides.<sup>[269]</sup> This was supported by density functional theory (DFT) calculations proving the cooperative role of the different hydroxyl moieties (enediol, ethyldiol) of the ascorbic acid scaffold for lowering the activation barrier of CO<sub>2</sub>. As

reported, 2 mol% ascorbic acid and 4 mol% TBAI at 100 °C and 20 bar CO<sub>2</sub> pressure for 23 h resulted in 88% yield of cyclohexene carbonate from cyclohexene oxide determined by <sup>1</sup>HNMR spectroscopy. After directly transferring the reported reaction conditions to  $\alpha$ -pinene oxide, GC analysis revealed that five different products were formed during the reaction. However, as analysed by comparison with an authentic  $\alpha$ -pinene carbonate sample (retention time: 8.4 min), carbonate formation did not take place. The obtained product peaks (3.3 – 4.9 min) are in the region of the retention time of the starting material (3.5 min) implying isomerisation. Also prolonged reaction times of 48 h instead of 23 h did not lead to cyclic carbonate formation. Again, steric hindrance caused by the bicyclic  $\alpha$ -pinene skeleton might be the strongest reason for the obtained isomerisation instead of product formation. Thus, harsh conditions are required, but these lead to the typically observed side-reactions for terpenes, such as isomerisation.

#### 4.2.1.2 $\alpha$ -Pinene Carbonate Synthesis via $\alpha$ -Pinnediol

To overcome the issues related to the sterically hindered CO<sub>2</sub> insertion of  $\alpha$ -pinene oxide, a new synthesis strategy was applied. The new strategy aims to circumvent the CO<sub>2</sub> insertion step by introducing the carbonyl functionality *via* transesterification. Therefore, it is necessary to introduce a diol functionality into the substrate to obtain  $\alpha$ -pinnediol. In the literature, three different procedures for the synthesis of  $\alpha$ -pinene carbonate are known - all starting from  $\alpha$ -pinnediol (see Table 10). In 1969, Richards *et al.* reported the cyclic carbonate formation using ethyl chloroformate, pyridine and a pinene based diol as substrate with 47% yield.<sup>[270]</sup> However, due to the toxicity of ethyl chloroformate and its production from phosgene, this procedure must be considered as problematic for environmental reasons. Another synthesis protocol for the transformation of *cis*- $\alpha$ -pinnediol into the corresponding cyclic carbonate was published by Beller and co-workers in 2016.<sup>[271]</sup> The authors used urea as sustainable carbonylation agent and FeBr<sub>2</sub> as catalyst. As reported, after a reaction time of 18 h in 1,4-dioxane at 150 °C,  $\alpha$ -pinene carbonate was obtained in 93% yield. A major drawback of this procedure are the relatively harsh reaction conditions of 150 °C.

For the dihydroxylation of double bonds that can be used to transform  $\alpha$ -pinene into *cis*- $\alpha$ -pinnediol procedures using osmium tetroxide are known.<sup>[272]</sup> Another way to achieve the introduction of a diol functionality, although in *trans* configuration, is the epoxidation of a double bond followed by the ring-opening of the epoxy ring with water. However, since the butane ring in  $\alpha$ -pinene oxide possesses high ring-strain, which tends to be relieved, there are no reports in the synthetic organic chemistry literature that describe the production of anti-pinnediols from the hydrolysis of epoxides of  $\alpha$ -pinene. Nevertheless, the hydrolysis

of  $\alpha$ -pinene oxide results in valuable products, such as sobrerol, campholenic aldehyde and carveol. Especially sobrerol is an interesting substrate, since its two hydroxy groups could be used to introduce polymerisable functional groups *via* transesterification. Ellrod and Bleier studied the hydrolysis of  $\alpha$ -pinene oxide under neutral and acidic condition in great detail using  $D_2O$  as reaction medium.<sup>[273]</sup> However, the authors did not investigate basic conditions. To directly compare the influence of the pH value on the product distribution of the hydrolysis of  $\alpha$ -pinene oxide, the hydrolysis was performed using acidic, basic and neutral conditions. For the acid-catalysed reaction, 0.1 g  $\alpha$ -pinene oxide were dissolved in 5 mL dioxane and subsequently 1 mL water and 0.03 mL concentrated sulfuric acid were added. Then, the reaction mixture was stirred for 24 h at room temperature. The crude reaction mixture was analysed by GC showing that full conversion into three main products and various by-products was achieved. GC-MS analysis showed that campholenic aldehyde was formed as main product at 3.8 min along with smaller amounts of unidentified by-products. The base-catalysed hydrolysis of  $\alpha$ -pinene oxide was conducted in the same scale and same solvent as the acid-catalysed hydrolysis and 0.9 mL of aqueous one molar solution of sodium hydroxide under reflux conditions (115 °C) for 16 h. GC analysis revealed extremely low conversion and only small peaks around the peak of the substrate. In contrast, the hydrolysis performed without acid or base catalysis gave full conversion into various products, from which the main product at 6.3 min was found to be sobrerol (see Figure 67). After evaporation of the solvent and drying over sodium sulfate, the crude product was purified by column chromatography to obtain the pure main product as white solid in 29% yield.

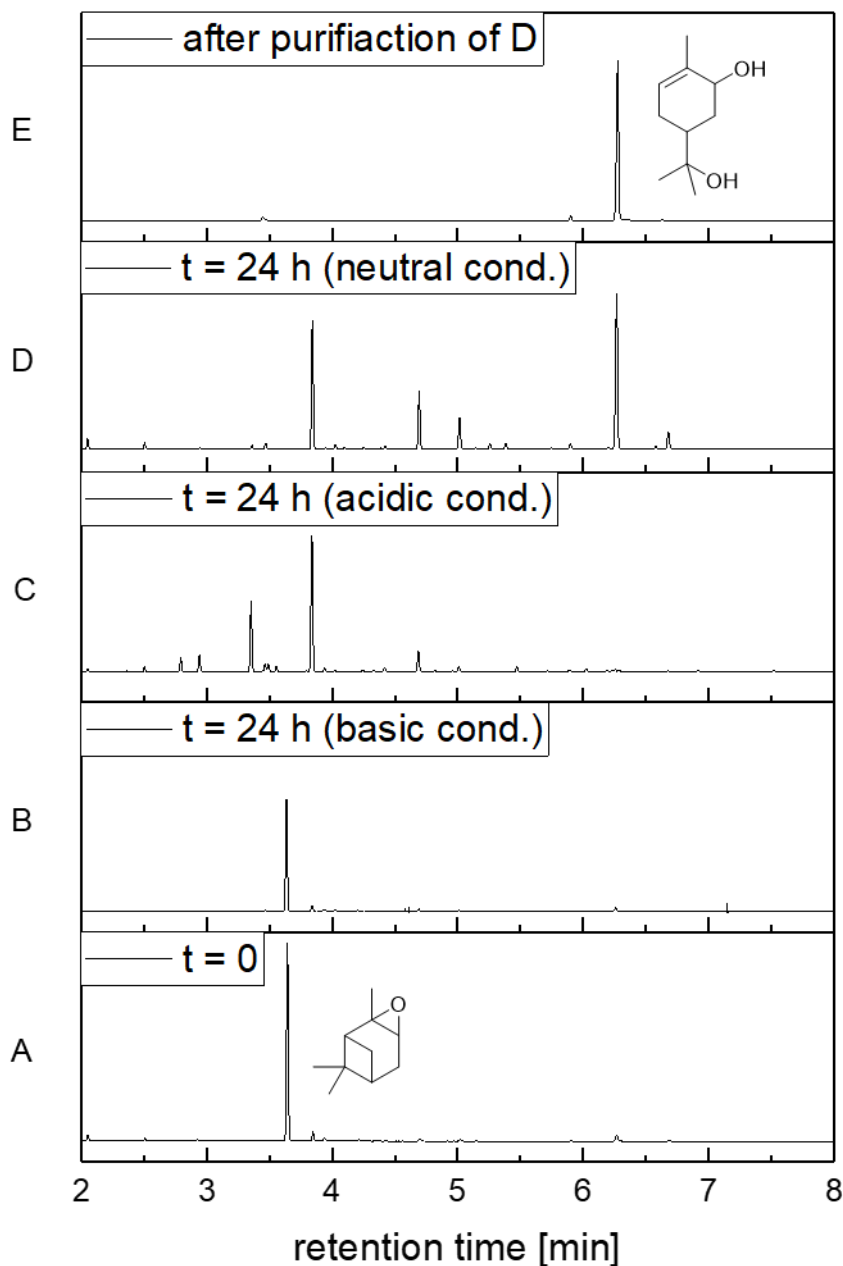


Figure 67: GC chromatograms of  $\alpha$ -pinene oxide hydrolysis under neutral conditions. A:  $t = 0$  h, B: crude reaction mixture under basic conditions after 24 h. C: crude reaction mixture in acidic medium after 24 h. D: crude reaction mixture in neutral medium after 24 h, E: pure product after purification via column chromatography. Reaction conditions: B:  $\alpha$ -pinene oxide (100 mg), water (1.00 mL), dioxane (5.00 mL), 1M-sodium hydroxide solution (0.9 mL), 115 °C, 24 h. Reaction conditions C:  $\alpha$ -pinene oxide (100 mg), water (1.00 mL),  $H_2SO_4$  (0.03 mL), dioxane (5.00 mL), RT, 24 h. D:  $\alpha$ -pinene oxide (100 mg), water (1.00 mL), dioxane (5.00 mL), 115 °C, 24 h.

Thorough NMR analysis proved the formation of sobrerol (5-(2-hydroxypropan-2-yl)-2-methylcyclohex-2-en-1-ol) (see Figure 68). In the  $^1\text{NMR}$  spectrum two distinct peaks at 4.00 ppm and 4.5 ppm are observed belonging to the two hydroxy groups since they do not show any coupling to carbon atoms in the HSQC NMR spectrum. Furthermore, the typical chemical shift for the vinyl proton is observed at 5.44 – 5.38 ppm. Also, the chemical shifts of the vinyl carbon atoms obtained at 134.88 ppm and 123.79 ppm in the  $^{13}\text{C}$  NMR spectrum confirm the presence of the double bond. Additionally, the mass of sobrerol (calculated: 170.1307 m/z) was confirmed *via* mass spectrometry (HRMS-EI, found: 170.1307 m/z). Sobrerol is well known to be formed in Brønsted acid catalysed isomerisation reactions of  $\alpha$ -pinene oxide (see Chapter 2.7.1). Interestingly, this product is already formed as main product without the addition of any acid catalyst. The product formation might be explained by water acting as a weak acid catalyst. Then, one water molecule forms a bond with the epoxide oxygen atom acting as the general acid by using one of its acidic hydrogen atoms. In the next step, a second water molecule attacks this water-epoxide species acting as a nucleophile. Finally, the first water molecule is released, and the hydrolysis product is formed. This observation is in accordance with the studies of Elrod and Bleier, who also discovered that  $\alpha$ -pinene oxide added to  $\text{D}_2\text{O}$  additionally results in the isomerisation products campholenic aldehyde and *cis*- and *trans*-carveol.<sup>[273]</sup> The addition of sulfuric acid in high concentration, in contrast, did not result in sobrerol as product (see Figure 67, C). At higher acid concentrations, campholenic aldehyde as confirmed by GC-MS and pinol are observed to form in higher yield, as reported by Elrod and co-workers.<sup>[273]</sup> With the help of computational thermodynamics calculations, the authors also showed that the relief of ring-strain in the bicyclic  $\alpha$ -pinene oxide molecule, which is a large enthalpic driving force, most likely is the reason that no product with the retained bicyclic carbon skeleton was observed.

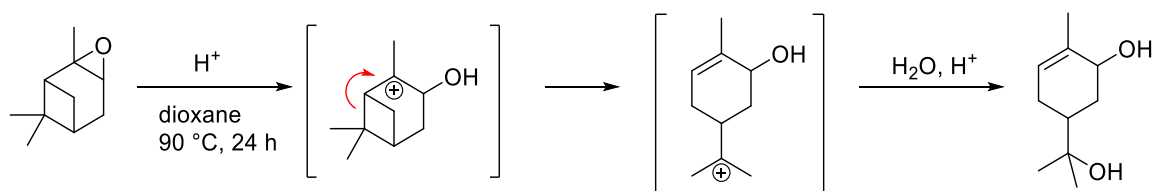


Figure 68: Proposed reaction mechanism for the acid-catalysed synthesis of sobrerol from  $\alpha$ -pinene oxide.<sup>[273]</sup>

To evaluate the reactivity of the two different hydroxyl groups, the obtained sobrerol was transesterified with dimethyl carbonate (see Figure 69). The reaction was carried out on 50.0 mg-scale in a pressure tube using DMC as reagent and as solvent. Since TBD is known to be a selective transesterification catalyst with high activity also at low



temperatures,<sup>[274]</sup> 5 mol% TBD were chosen as catalyst in a first try. After a reaction time of 20 h at 60 °C, DMC was evaporated under reduced pressure and the crude product was purified *via* column chromatography. <sup>1</sup>H, <sup>13</sup>C and 2D NMR spectroscopy revealed that only the secondary hydroxy group of sobrerol was esterified in 84% yield, whereas the tertiary hydroxy group remained unmodified. Changing the catalyst from TBD to 1,8-diazabicyclo[5.4.0]undec-7-ene (DBU), TBAB and potassium carbonate (K<sub>2</sub>CO<sub>3</sub>), respectively, did not lead to any product formation. Also, the variation of the reaction conditions for the reaction catalysed by TBD from a pressure tube to microwave irradiation in a closed vessel did only lead to the formation of the monofunctionalised product. To shift the reaction equilibrium to the product side and to promote the transesterification of the tertiary hydroxyl group, the reaction was also run while constantly removing methanol from the reaction mixture under reduced pressure. Therefore, the reaction mixture was heated to 60 °C at the rotary evaporator at 300 mbar. However, again, only the monofunctionalised-carbonate was obtained. Most probably due to the steric hindrance, the tertiary hydroxyl group was not esterified under the applied conditions.

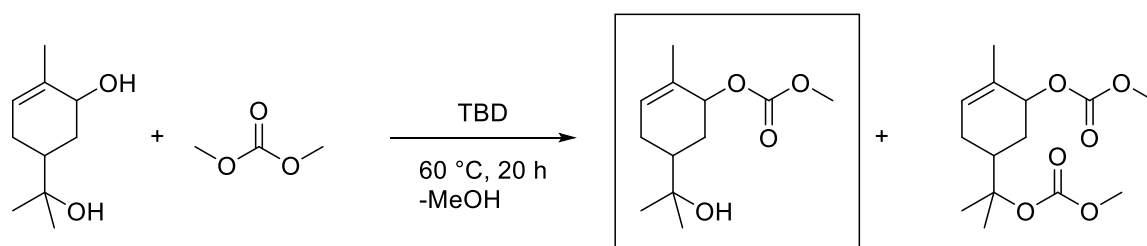


Figure 69: Transesterification of sobrerol with DMC showing both theoretically possible products.

Since it was not possible to obtain *trans*- $\alpha$ -pinanediol *via* epoxide ring-opening reaction with water, in a next step, commercially available *cis*- $\alpha$ -pinanediol ((1*R*,2*R*,3*S*,5*R*)-(-)-pinanediol) was subsequently evaluated as substrate for the formation of the cyclic carbonate. *Cis*- $\alpha$ -pinanediol was converted in the same manner as sobrerol using DMC as reagent and solvent, and TBD as transesterification catalyst for 17 h at 60 °C (see Figure 70).

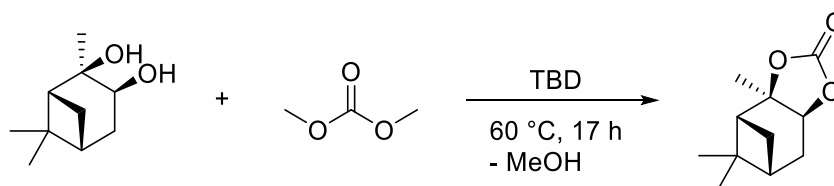


Figure 70: TBD-catalysed transesterification of *cis*- $\alpha$ -pinanediol with DMC yielding  $\alpha$ -pinene carbonate.

Then, DMC was evaporated under reduced pressure and the crude product was washed with water to obtain pure  $\alpha$ -pinene carbonate in a yield of 86%. Subsequently, the product was analysed *via*  $^1\text{H}$ ,  $^{13}\text{C}$ , COSY, HSQC and HMBC NMR spectroscopy and the mass of  $\alpha$ -pinene carbonate (calculated: 196.1099 m/z) was confirmed *via* mass spectrometry (HRMS-EI, found: 196.1101 m/z). The presence of the cyclic carbonate functionality was proven by the presence of a quaternary carbon atom with a chemical shift of 154.51 ppm, which is typical for carbonate functionalities and by the vanishing of the signals belonging to the hydroxyl groups. Due to the mild and safe reaction conditions and the simple workup, together with the renewable origin of the non-hazardous reagents, this catalytic reaction procedure clearly fulfils the 12 principles of green chemistry. Further advantages are the relatively high yield and the good atom economy of 75.4% (see Table 10). As recently reported for the cyclic carbonate formation from erythritol by Meier and Dannecker, it is possible to recycle a reaction mixture containing excess DMC and TBD up to eight times.<sup>[275]</sup> The product erythritol bis(carbonate) precipitated from the reaction mixture during the reaction and was filtered and washed with DMC to remove the catalyst and to obtain the pure product in high yields. The mother liquor and the DMC used for washing were then reused for the next reaction proving that the catalyst is stable under the applied reaction conditions. The reaction conditions of 5 mol TBD at 60 °C, as applied by the authors, are quite similar to the ones used for the cyclic carbonate formation from *cis*- $\alpha$ -pinanediol herein and therefore indicate that recycling of excess DMC and might also be possible for the herein investigated reaction. In this case, DMC needs to be evaporated from the reaction mixture to allow  $\alpha$ -pinene carbonate to precipitate and to enable subsequent washing with water to remove the catalyst. The possibility to recycle and reuse the excess of DMC which is serving as solvent and as reagent at the same time could drastically decrease the E factor of this procedure.

Only recently, Kim and co-workers applied diphenyl carbonate as carbonyl source in the combination with TBD for the synthesis of sterically demanding carbonates including  $\alpha$ -pinene carbonate.<sup>[276]</sup> As reported, the reaction was conducted at 30 °C for 12 h using 2-methyltetrahydrofuran as solvent and the product was obtained in a yield of 91% after purification *via* column chromatography. 2-Methyltetrahydrofuran (2-MeTHF) is considered an eco-friendlier alternative to tetrahydrofuran, since it can be produced from renewable resources, *i.e.* furfural, and is less toxic. However, it is still ranked as “problematic” in the CHEM21 solvent selection guide due to health and safety issues.<sup>[227]</sup> In contrast, DMC is ranked as “recommended”. Furthermore, the atom economy of DMC as reagent is 75.4%, whereas the atom economy of diphenyl carbonate is only 51.0%, due to the formation of phenol as by-product instead of methanol. It is also less sustainable

compared to DMC since it is industrially produced from fossil-based phenol. Table 10 provides a detailed comparison of the literature procedures and the new procedure reported herein, clearly demonstrating the advantages.

Table 10: Comparison of literature procedures and the new procedure for the synthesis of  $\alpha$ -pinene carbonate.

	<b>Richards et al.<sup>[270]</sup></b>	<b>Beller et al.<sup>[271]</sup></b>	<b>Kim et al.<sup>[276]</sup></b>	<b>New procedure</b>
Carbonyl source	Ethyl chloroformate	Urea	Diphenyl carbonate	DMC
Solvent	Pyridine & ethyl chloroformate	1,4-Dioxane	2-MeTHF	DMC
Reaction temperature and conditions	RT	150 °C, Ar atmosphere	30 °C	60 °C
Reaction time	N/A	18 h	12 h	17 h
Stoichiometric by-products	HCl, EtOH	NH <sub>3</sub>	Phenol	MeOH
Workup	Distillation	Column chromatography	Column chromatography	Washing with water
Catalyst	Pyridine	FeBr <sub>2</sub>	TBD	TBD
Reagent in excess	Ethyl chloroformate, recycling not possible	Diol, recycling <i>via</i> column chromatography in theory possible	Diol, recycling <i>via</i> column chromatography in theory possible	DMC, recycling <i>via</i> distillation in theory possible
Atom economy	70.4%	85.2%	51.0%	75.4%
Yield	47%	93%	91%	86%

#### 4.2.2 Cyclic Carbonate from $\beta$ -Pinene

Subsequently, also  $\beta$ -pinene was evaluated as a substrate for the cyclic carbonate formation applying the reaction procedure established above. Analogous to the hydrolysis of  $\alpha$ -pinene oxide there appear to be no reports in the literature that describe the formation of  $\beta$ -pinanediol from the hydrolysis of  $\beta$ -pinene. However, it is reported that  $\beta$ -pinanediol

can be achieved starting from  $\beta$ -pinene *via* selective epoxidation with hydrogen peroxide catalysed by methyltrioxorhenium (MTO) and followed by the likewise catalysed *in situ* epoxide ring-opening reaction (see Figure 71).<sup>[277]</sup>

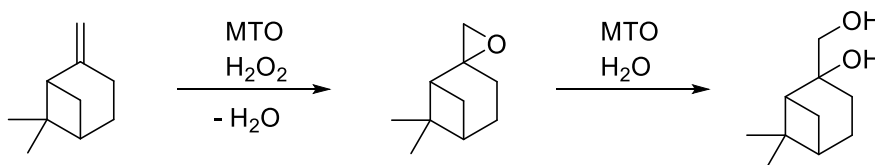


Figure 71: MTO-catalysed epoxidation of  $\beta$ -pinene followed by the MTO-catalysed epoxide ring-opening reaction with water yielding  $\beta$ -pinenediol.

The catalytic reaction cycle starts with the multistep formation of a hydroperoxo complex by the reaction of MTO with hydrogen peroxide. This complex then serves as oxidising agent transforming the alkene into the epoxide. The subsequently catalysed ring-opening reaction with water can be suppressed by adding a base co-catalyst, such as pyridine.<sup>[278]</sup> Following the reaction procedure without the addition of pyridine, as reported by Herrmann *et al.*, the reaction was started by adding  $\beta$ -pinene at 5 °C to a solution of MTO in *tert*-butanol and hydrogen peroxide. The mixture of *tert*-butanol and hydrogen peroxide was previously dried over magnesium sulfate. After addition of  $\beta$ -pinene, the reaction mixture was allowed to warm-up to room temperature, while stirring overnight. For the decomposition of excess hydrogen peroxide, manganese(IV) oxide was added followed by filtration of the suspension and evaporation of the solvent at reduced pressure. The crude product was analysed by GC and purified *via* column chromatography, yielding a fraction with two product species (see Figure 72). GC analysis showed that full conversion was achieved, since the peak of the starting material at 2.5 min completely vanished.

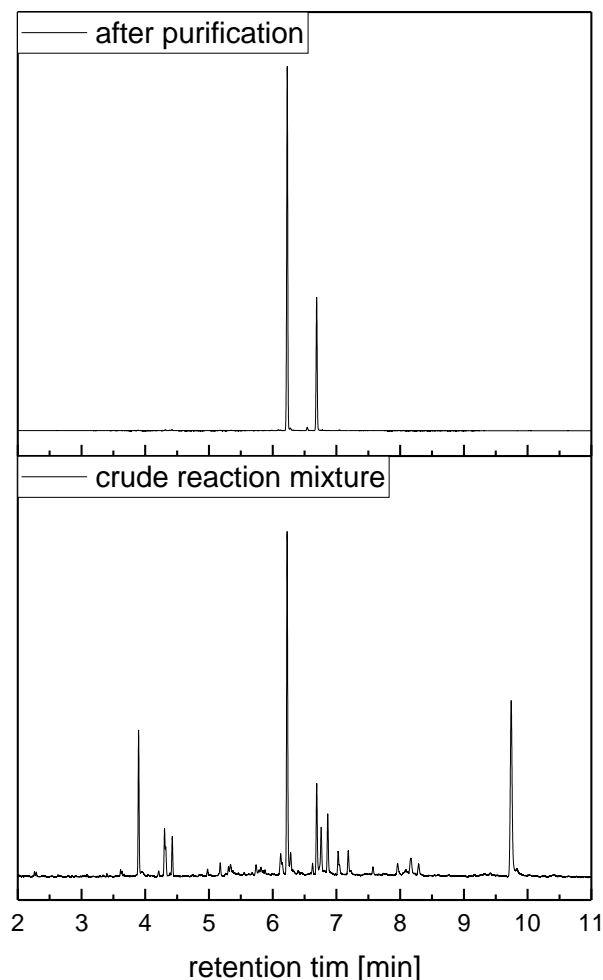


Figure 72: GC chromatograms of the MTO catalyzed epoxidation and ring-opening reaction of  $\beta$ -pinene. Bottom: crude reaction mixture. Top: fraction containing two species after column chromatography.

However, it was not possible to separate the main product from a minor by-product by column chromatography due to equal retention times. Therefore, NMR analysis of the obtained fraction containing two product species (GC retention times: 6.2 min and 6.7 min) was difficult. Comparison of the measured  $^{13}\text{C}$  NMR spectrum with a  $^{13}\text{C}$  NMR spectrum of  $\beta$ -pinanediol reported in the literature<sup>[279]</sup> showed that the signals with the lower intensity have similar shifts as the signals of the authentic  $\beta$ -pinanediol sample. This indicates that the species at 6.7 min corresponds to  $\beta$ -pinanediol. To prove this assumption, the fraction containing both species, of which one corresponds to  $\beta$ -pinanediol, was further transformed with diallyl carbonate to obtain either the  $\beta$ -pinene based cyclic carbonate or other allylated products *via* transesterification (see Figure 73).

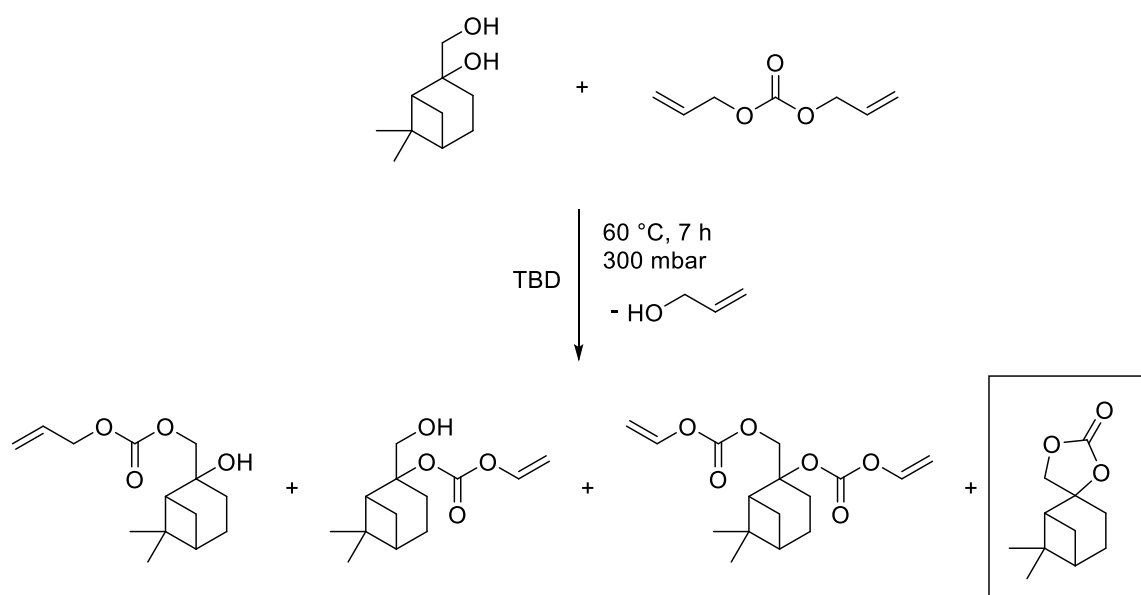


Figure 73: Transesterification reaction of  $\beta$ -pinenediol showing all theoretically possible products.

The reaction was carried out at 60 °C and 300 mbar for 7 h using TBD as catalyst and diallyl carbonate as reagent and solvent. Subsequently, the crude reaction mixture was purified *via* column chromatography and  $\beta$ -pinene carbonate was obtained as pure product as confirmed by  $^1\text{H}$ ,  $^{13}\text{C}$  and 2D NMR spectroscopy. This proved that  $\beta$ -pinenediol was present in the product mixture obtained from the MTO catalysed epoxidation and ring-opening reaction of  $\beta$ -pinene. However, it was not possible to calculate a yield, since a mixture of two substrates, from which one could not be identified, was used as starting material. In the literature, the formation of  $\beta$ -pinene carbonate was only reported by Richards *et al.* in 1969. The authors reacted  $\beta$ -pinenediol with diethyl carbonate and sodium as base catalyst. However, no detailed analysis of the product is provided. To complement the available characterisation data of  $\beta$ -pinene carbonate, detailed NMR analysis including the exact assignment of all signals was performed using 2D NMR techniques (see Figure 74 and Figure 75). In the  $^1\text{H}$  NMR spectrum, the two protons  $\text{CH}_2^{10}$  adjacent to the oxygen atom exhibit the most upfield shift at 4.39 ppm. Since these protons are different in a stereoisomeric manner, the coupling results in two doublets. As typically for the methylene protons present in the cyclobutane ring of the  $\alpha$ -pinene skeleton, the signals of the protons  $H^{7a}$  and  $H^{7b}$  are widely split and obtained at 2.30 – 2.09 ppm and 1.36 ppm, respectively, which is confirmed by the HSQC NMR spectrum. The  $^{13}\text{C}$  NMR shows a strong upfield shift for the tertiary carbon  $\text{C}_q^{11}$  at 153.91 ppm. Thus,  $\text{C}_q^{11}$  can be assigned as the carbonyl carbon present in the cyclic carbonate. As confirmed by the HSQC NMR spectrum, no hydroxy groups are present in the obtained molecule further proving the formation of a cyclic carbonate instead of a linear carbonate.

In summary, the successful synthesis of the cyclic carbonates based on the sterically demanding substrates  $\alpha$ - and  $\beta$ -pinene was demonstrated. In the case of  $\alpha$ -pinene, commercially available *cis*-pinanediol was used as starting material to establish a sustainable and benign reaction procedure for the cyclic carbonate formation *via* transesterification. Starting from  $\beta$ -pinene, the substrate was first transformed into the corresponding epoxide using hydrogen peroxide as environmentally friendly oxidising agent followed by *in situ* catalysed ring-opening to obtain  $\beta$ -pinanediol. The diol was then successfully transesterified to yield the desired cyclic  $\beta$ -pinene carbonate.

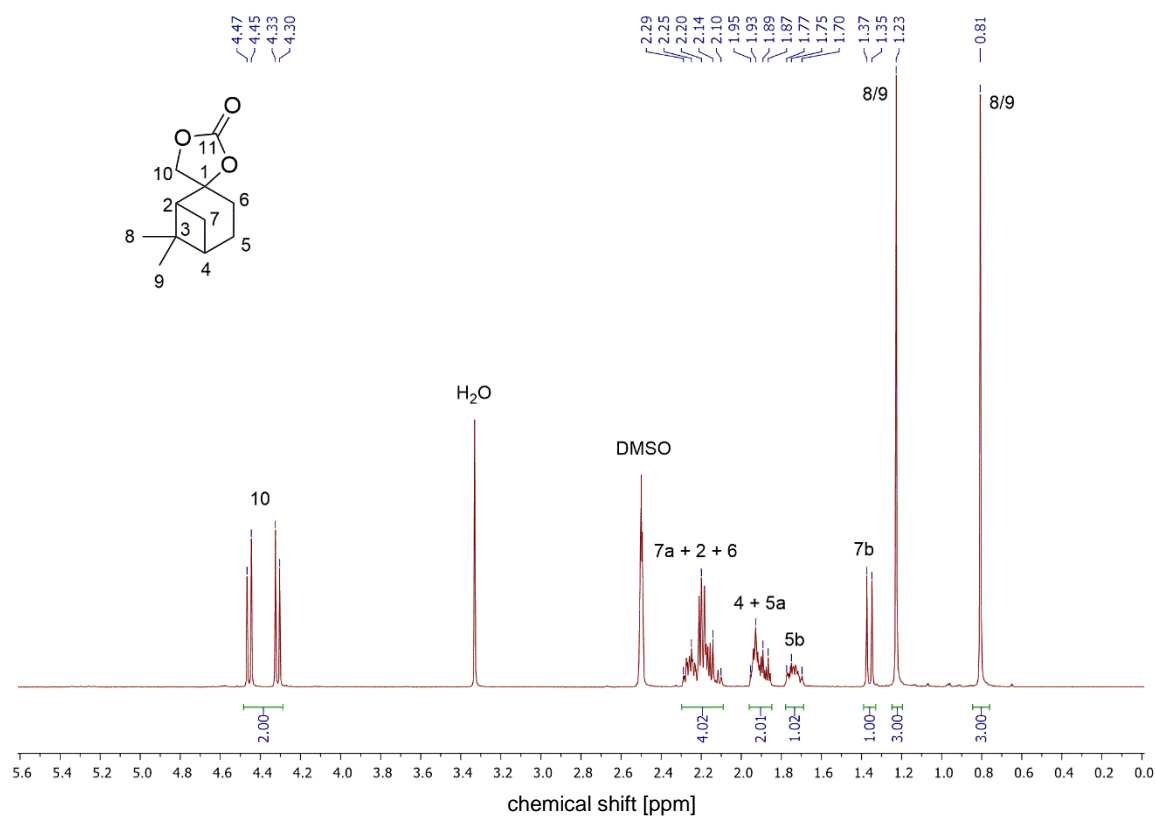


Figure 74: Fully assigned <sup>1</sup>H NMR spectrum of  $\beta$ -pinene carbonate.

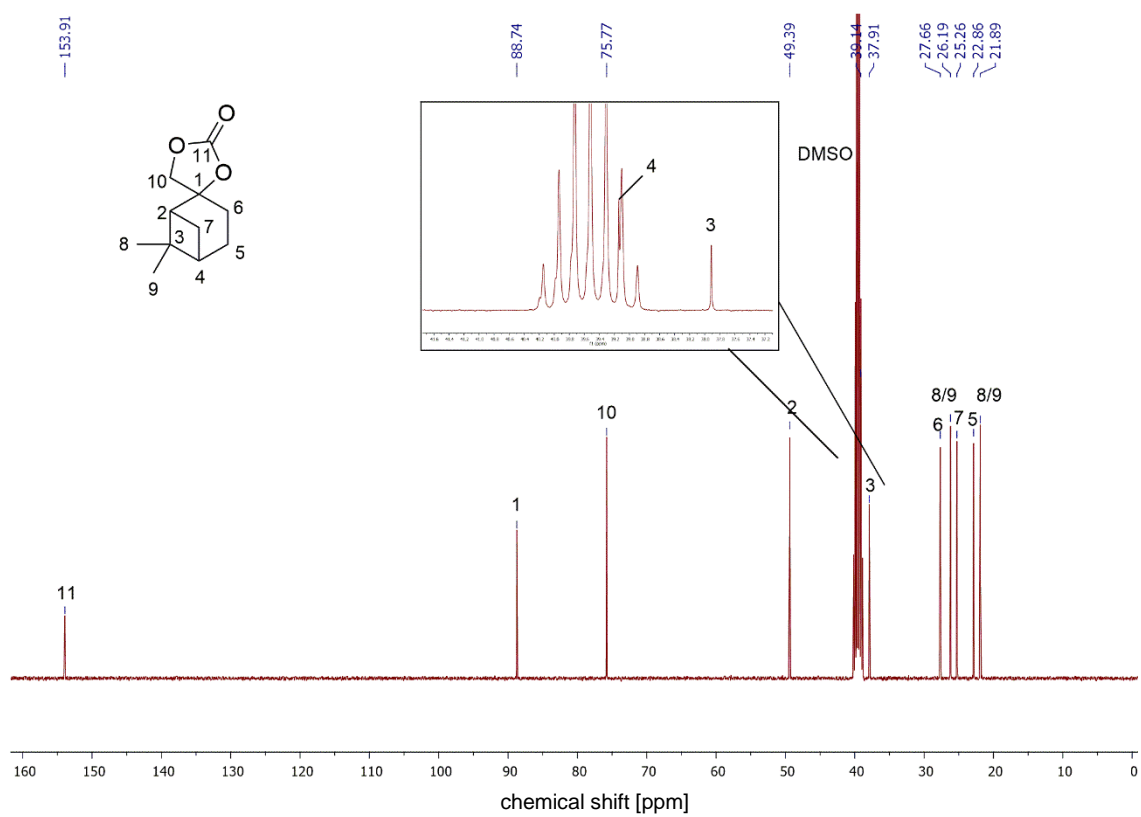


Figure 75: Fully assigned  $^{13}\text{C}$  NMR spectrum of  $\beta$ -pinene carbonate.



### 4.3 Limonene-based Poly(hydroxy urethane)s

Within this chapter, the synthesis of poly(hydroxy urethane)s (PHUs) based on monomers prepared from limonene is described. PHUs can be obtained by step-growth polyaddition of cyclic dicarbonates and diamines and therefore belong to the class of non-isocyanate polyurethanes (NIPUs). Additional relevant methods for synthesising NIPUs are the step-growth polycondensation between linear activated dicarbonates and diamines or similarly between linear activated carbamates and diols, as well as the ring-opening polymerisation of cyclic carbamates.<sup>[280]</sup> Originally, linear polyurethanes are produced by reacting diols with diisocyanates in the presence of a catalyst based on the discovery by Bayer.<sup>[281]</sup> Due to their low cost and diverse application possibilities, polyurethanes account for almost 5 wt% of the worldwide polymer production.<sup>[282]</sup> The growing trend to synthesise polyurethanes without the use of isocyanates stems from the toxicity of isocyanate monomers like methylene diphenyl diisocyanate and toluene diisocyanate, and their synthesis from phosgene, an even more toxic reagent causing environmental hazards.

The most popular synthetic way to synthesise isocyanate-free polyurethanes is the reaction of cyclic dicarbonates and aliphatic amines.<sup>[280]</sup> Among the carbonates, five- and six-membered cyclic dicarbonates have been extensively studied. Six-membered cyclic carbonates have the advantage of higher reactivity than five-membered ones. However, their synthesis generally requires chlorinated carbonylating agents like phosgene or alkyl chloroformates.<sup>[283]</sup> In contrast, five-membered cyclic carbonates can be prepared in a more sustainable way by insertion of CO<sub>2</sub> into epoxides, which can also be present in renewable resources (see Chapter 4.2.1). Additionally, they are the most stable carbonates, which is important for safe storage and shelf-life.<sup>[284]</sup> The reaction route to PHU prepolymers presented in this chapter therefore utilises limonene dioxide as renewable diepoxide for the chemical fixation of CO<sub>2</sub> to obtain fully renewable limonene dicarbonate (see Figure 76). On the other hand, limonene is transformed into a renewable diamine monomer *via* thiol-ene reaction with cysteamine hydrochloride. Both monomers can then be used to synthesise PHUs. However, the reaction between five-membered cyclic carbonates and amines has two drawbacks: first, the low reactivity of the cyclic carbonate aminolysis and second, the low molecular weight of the resulting PHUs.<sup>[284]</sup> To nevertheless transform the obtained oligo-PHUs into useful materials, they can be used as prepolymers for the synthesis of thermosets. Crosslinking of the prepolymers bearing amine end groups can be achieved through the reaction with various renewable monomers having more than two epoxy functionalities, like commercially available epoxidised

soybean oil (ESBO). In that way, the obtained PHU prepolymers are attractive curing agents for renewable epoxy resins.

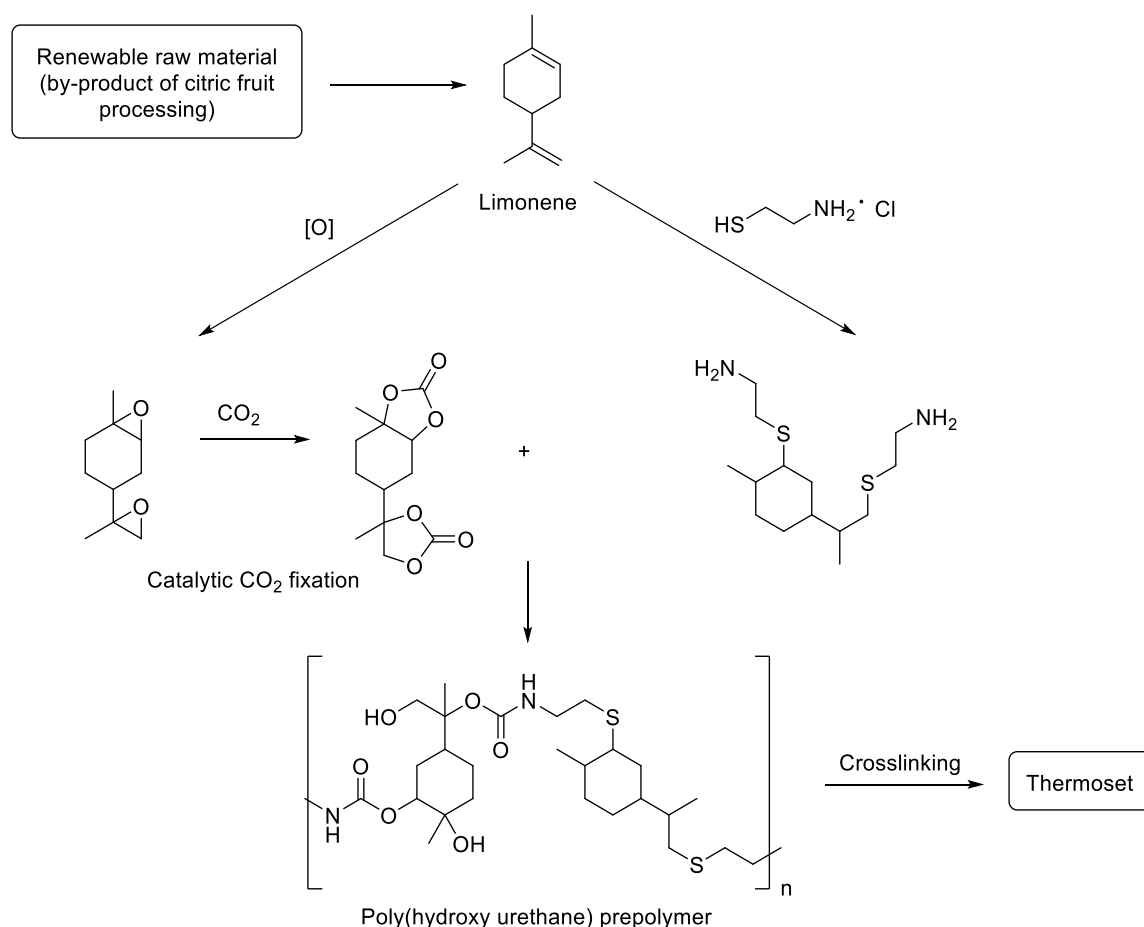


Figure 76: Graphical abstract for the synthesis of poly(hydroxy urethane) prepolymers starting from limonene and further crosslinking to give thermosetting polymers.

### 4.3.1 Monomer Synthesis

#### 4.3.1.1 Cyclic limonene dicarbonate

Starting from limonene, cyclic limonene dicarbonate (LC) can be synthesised in a two-step procedure *via* epoxidation followed by CO<sub>2</sub> insertion (see Figure 77). For the epoxidation of limonene, several oxidation procedures using stoichiometric amounts of organic peroxides *e.g.* peracetic acid or *tert*-butyl hydroperoxide, as oxidising agents are known in the literature.<sup>[285, 286]</sup> Moreover, a procedure using *in situ* generated dimethyl dioxirane by the reaction of acetone and potassium peroxy monosulfate, commercially known under the trade name of Oxone, is able to reach high yields of up to 100% at room temperature in short times (45 min).<sup>[287]</sup> However, those procedures result in stoichiometric amounts of waste, which considerably increases the E factor and makes the reaction less

environmentally benign. In contrast, the use of hydrogen peroxide as oxidising agent only results in water as by-product, which is generally not taken into account for the calculation of the E factor and represents a greener alternative that is economically feasible. Since limonene dioxide (LDO) is used commercially in epoxy resins as reactive diluent, it is produced on industrial scale using hydrogen peroxide as oxidising agent. For the synthesis of limonene dicarbonate from LDO, a commercially available mixture containing two *cis*-(+) and two *trans*-(+) isomers was used.

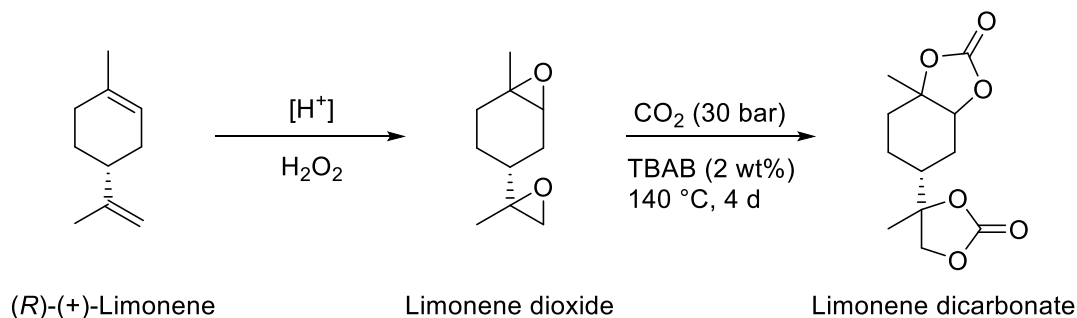


Figure 77: Synthesis route for limonene dicarbonate starting from limonene via epoxidation and subsequent CO<sub>2</sub> insertion.

The transformation of LDO into LC was achieved applying a procedure first published by Mülhaupt *et al.* in 2012<sup>[206]</sup> followed by an improved purification technique reported by the same group in 2017.<sup>[210]</sup> Using LDO as starting material, the carbonation of was performed in bulk under solvent-free conditions. 2 wt% of TBAB were applied as catalyst for a batch size of 100 g of LDO. The reaction was run at 140 °C and 30 bar of CO<sub>2</sub> pressure. After a reaction time of for four days, the crude mixture was allowed to cool down to room temperature and the pressure reactor was slowly depressurised. <sup>1</sup>H NMR spectroscopy indicated full conversion by complete disappearance of the signals belonging to the epoxy groups. However, the formation of olefinic by-products was detected by <sup>1</sup>H NMR spectroscopy showing proton signals visible between 5.6 and 4.7 ppm. The crude product mixture was obtained as highly viscous brown liquid. For the purification of a smaller 1 gram-batches, column chromatography was performed first. However, it was not possible to separate the olefinic by-products from the main product limonene dicarbonate, due to very similar retention times. In contrast, by dilution of the crude reaction mixture with 33 mL EA and addition of 76 mL triethylamine, the pure product precipitated from the crude product mixture. After crystallisation over the weekend, the white solid was filtrated from the mother liquor and washed with very few amounts of EA to obtain a yield of 5% (7.35 g) of a stereoisomerically pure limonene carbonate species, as verified by <sup>1</sup>H and <sup>13</sup>C NMR spectroscopy. In the <sup>1</sup>H NMR spectrum, the CH proton and the CH<sub>2</sub> protons

adjacent to the oxygen atoms are observed at 4.39 ppm and 4.18 ppm, respectively. The  $\text{CH}_2$  protons are observed as two doublets, due to their stereoisomeric difference. The  $^{13}\text{C}$  NMR spectrum proved the formation of two cyclic carbon moieties since two new tertiary carbon peaks with an almost identical chemical shift at 154.20 ppm appeared. Compared to the literature procedure, only one recrystallisation cycle was necessary to result in one specific stereoisomer in a slightly better yield (literature batch size: 1506 g LDO, yield of *trans*-LC: 25.3 g, 1.10%). The yield might be increased by using all stereoisomers instead of only using the *trans*-isomer. However, as reported in the literature, also a blend of two stereoisomers was only obtained in a rather low yield of 18%. Due to the low yield and the high toxicity of triethylamine, the presented purification method is not ideal and needs to be improved to make future applications of LC in polymers and thermosets more sustainable.

#### 4.3.1.2 Limonene-based diamine via thiol-ene reaction

The diamine monomer based on limonene was synthesised following a procedure that was previously established in the Meier group.<sup>[168]</sup> As already shown for the synthesis of limonene-based monomers for polycondensation,<sup>[167]</sup> the thiol-ene reaction of functionalised thiols with both double bonds of limonene is an attractive tool to introduce various functionalities such as hydroxyl, methyl ester or amine groups into the substrate. Thiol-ene reactions have the advantage that the functionalised monomers can be obtained in a one-step procedure with very high atom efficiency directly from the renewable feedstock. For the introduction of an amine functionality, cysteamine hydrochloride was used as thiol component (see Figure 78). Regarding atom efficiency, cysteamine in the pure form is more favourable than the hydrochloride salt. However, cysteamine hydrochloride gave better yields and is more stable, which prevents side reaction and thus the formation of waste. The reaction was performed in ethanol at room temperature and under UV irradiation using DMPA as photo initiator.

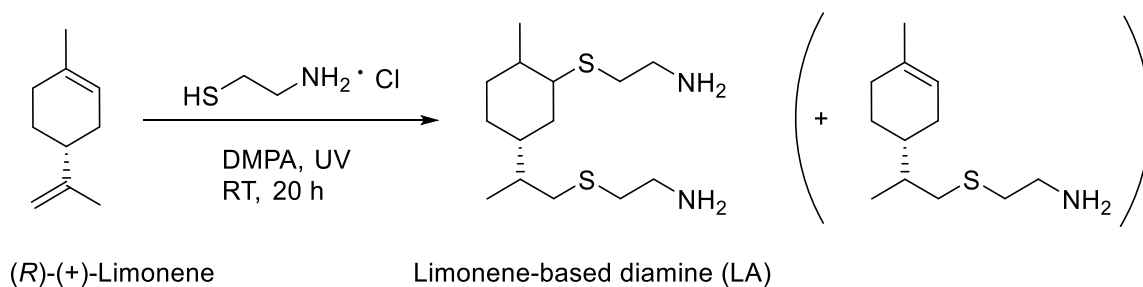


Figure 78: Synthesis of the limonene-based diamine via thiol ene reaction.<sup>[168]</sup>

After 20 h reaction time, the solvent was removed under reduced pressure and the residue was redissolved in dichloromethane. The organic phase was subsequently washed with potassium carbonate solution in water to neutralise the hydrochloride salt and to obtain the free amines. The crude product was purified *via* column chromatography to give the limonene-based diamine (LA) as a slightly yellow viscous liquid in a yield of 56%. Due to the difference in double bond reactivity of the two double bonds in limonene, the monofunctionalised limonene-based amine was observed as by-product (see Figure 78). As reported by Johansson and co-workers, the difference of the reactivity of the two double bonds in limonene is predominantly ascribed to a higher relative energy of the tertiary  $\beta$ -thioether carbon-radical intermediate arising from the thiyl-radical insertion across the endocyclic double bond.<sup>[201]</sup> The effects of steric hindrance are also mentioned to be partially responsible to control the thiyl-radical addition onto the two double bonds. These two effects lead to an about 6.5 times faster thiol-ene coupling reaction at the *exo*-olefinic bond than at the endocyclic one. For that reason, the thiol component cysteamine hydrochloride was used in an excess of 1.5 equivalent per double bond.

Starting from the pure (*R*)-(+)-limonene enantiomer, three additional stereocenters are generated during the reaction and thus  $2^3 = 8$  possible diastereomers can be formed. However, the  $^{13}\text{C}$  spectrum of LA shows only four signals for the carbon atom  $\text{C}^6$  instead of eight different signals (see Figure 79).

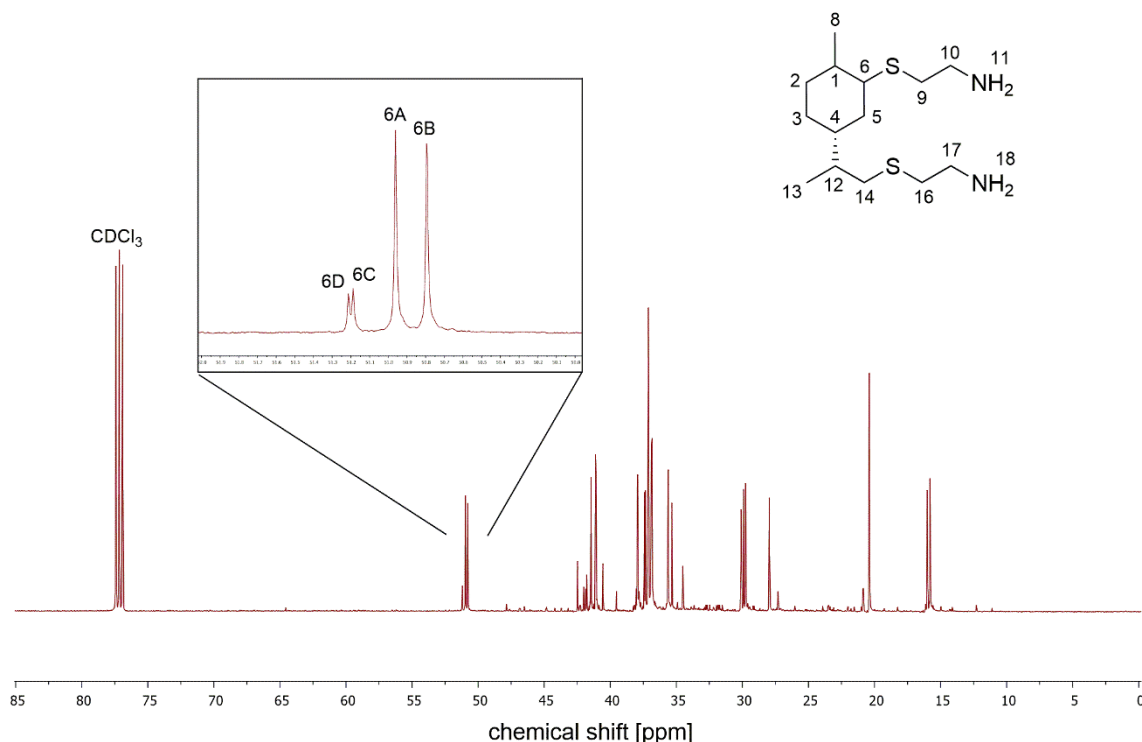


Figure 79:  $^{13}\text{C}$  NMR spectrum of the limonene-based diamine (LA) with a zoom to the region of 52 – 50 ppm showing the signals of the four diastereomers A, B, C and D, belonging to carbon  $\text{C}^6$ .

This finding indicates that the main product of the thiol-ene reaction is a mixture of four different diastereomers, which is in accordance with the literature.<sup>[167, 168]</sup> Due to the four different diastereomers present in the product fraction, complex  $^1\text{H}$  and  $^{13}\text{C}$  NMR spectra were received (see Figure 79 and Figure 80). With the help of 2D NMR techniques, the signals corresponding to the protons at the  $\alpha$ - and  $\beta$ -positions to the thioether were assigned, proving the incorporation of the thiol. The multiplet with a chemical shift of 2.86 – 2.78 ppm belongs to the methylene groups  $\text{CH}_2^{10}$  and  $\text{CH}_2^{17}$ , the multiplet at 2.67 – 2.44 ppm corresponds to the methylene groups  $\text{CH}_2^9$  and  $\text{CH}_2^{16}$ . The protons of the free amines  $\text{NH}_2^{11}$  and  $\text{NH}_2^{18}$  are assigned to the broad signal at 1.58 ppm.

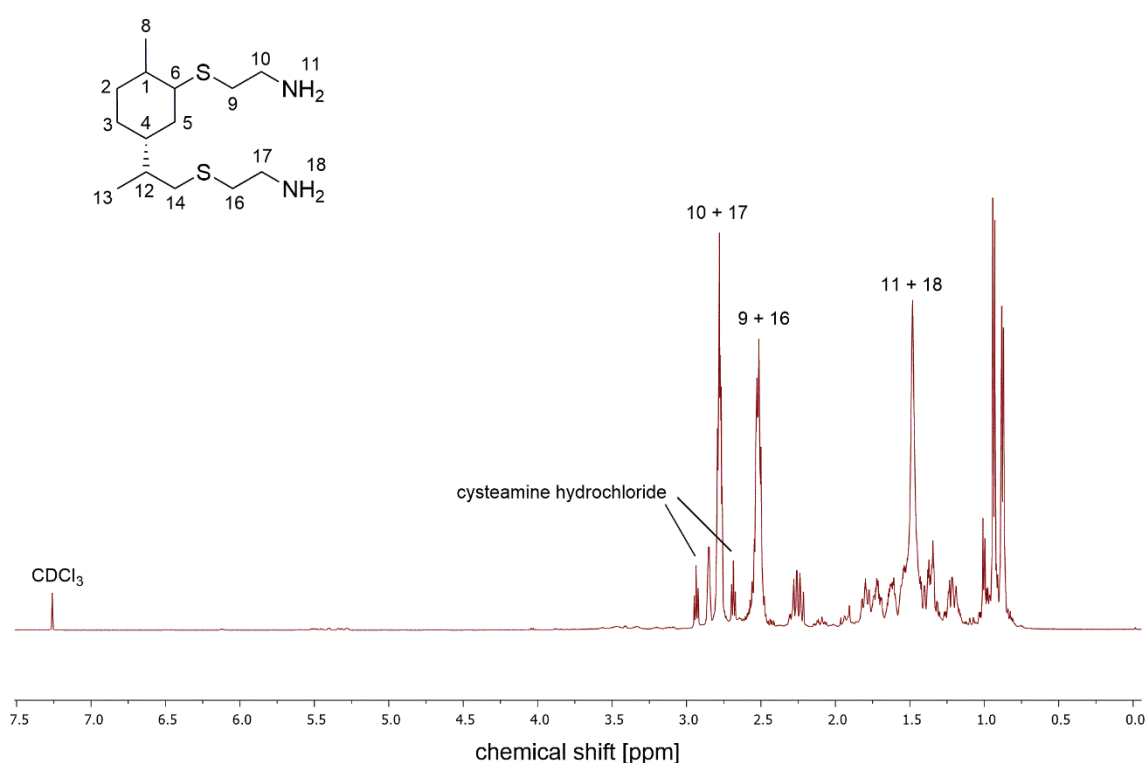


Figure 80:  $^1\text{H}$  NMR spectrum of the limonene-based diamine (LA).

### 4.3.2 Poly(hydroxy urethane) Prepolymer Synthesis

Having the limonene-based cyclic dicarbonate and the limonene-based diamine in hand, the amine-mediated ring-opening of the five-membered cyclic carbonates was investigated as a the next step to obtain poly(hydroxy urethane) prepolymers (see Figure 81). For the synthesis of the poly(hydroxy urethane) prepolymers, various reaction temperatures and catalysts were tested to find suitable reaction conditions. Due to the rather low reactivity of the endocyclic, electron-rich five-membered cyclic carbonate present in LC, elevated temperatures and/or catalysts are necessary to accelerate the

reaction. However, it is generally known that alkylation side reactions increasingly occur at temperatures above 130 °C.<sup>[210]</sup> Thus, the test reactions were conducted at temperatures between 80 and 120 °C. Even if the polymerisation in solvents limits the application range, since solvents are often not suitable at an industrial scale, a protic solvent, *i.e.* ethanol, was evaluated as reaction media for the aminolysis reaction. A model study by Caillol and co-workers showed that the use of protic solvents has a positive influence on both reactivity and conversion of cyclic carbonates during their aminolysis reaction.<sup>[284]</sup> The increased conversion is explained by interactions between the solvent and the polymer that reduce the inter- and intra-molecular hydrogen bonding between the poly(hydroxy urethane) chains and thus increases the mobility of the polymer chains. Moreover, the hydrogen bonds between the oxygen atoms of the cyclic carbonate and the protic solvent result in an increase of the positive partial charge of the carbonyl group. This in turn facilitates the nucleophilic attack of the amine on the cyclic carbonate. Due to its ranking as 'recommended' in the CHEM21 solvent selection guide,<sup>[227]</sup> ethanol (bp: 78 °C) was chosen as a protic solvent for test reactions at 80 °C. Test reactions conducted at 100 °C required higher-boiling DMSO (bp: 189 °C, CHEM21 ranking 'problematic') as aprotic solvent.

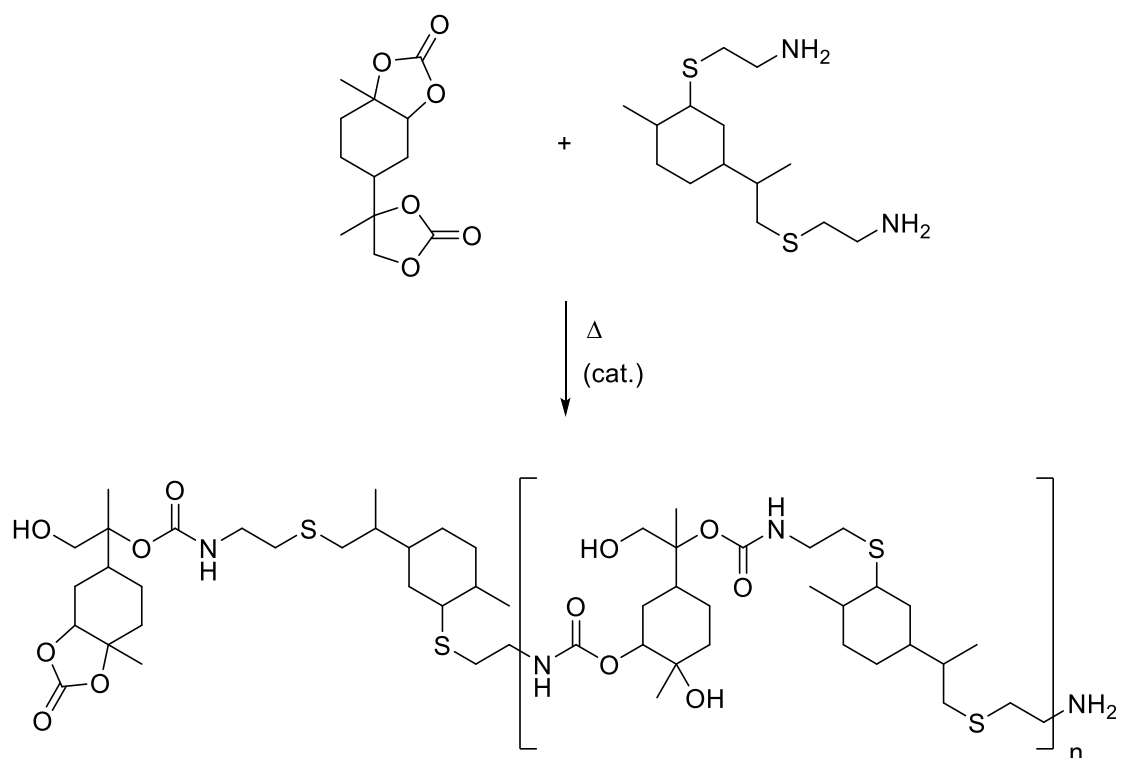


Figure 81: Synthesis of poly(hydroxy urethane) prepolymers from LC and LA at elevated temperatures.

Besides the variation of solvent and temperature, two different catalysts were evaluated for promoting the nucleophilic attack of the amine on the carbonyl group of the cyclic carbonate. The use of a catalyst is generally required due to the low reactivity of five-membered cyclic carbonates. However, in the case of linear primary amines, even at room temperature, the nucleophilicity is sufficient for reacting with the carbonate without the involvement of a catalyst.<sup>[288]</sup> To investigate the influence of a catalyst on the aminolysis reaction, lithium chloride was used as weak Lewis acid and tested for the enhancement of the reactivity of the carbonate function. In addition, TBD was applied as organocatalyst. It is known from literature that TBD can activate both the carbonate and the nucleophile and thus enhances the reaction.<sup>[289, 290]</sup> The screening of the reaction conditions was started by performing the aminolysis reaction on a 0.2 mmol-scale with equimolar amounts of LC and LA at 80 °C for 18 h at ambient atmosphere. Without catalyst, the reaction resulted in a poly(hydroxy urethane) prepolymer with a molecular weight of  $M_n = 1120$  g/mol (PHU1, see Table 11).

Table 11: Screening of the reaction conditions for the synthesis of poly(hydroxy urethane) prepolymers and influence on the molecular weight of the obtained prepolymers. Reaction conditions: LC (50.0 mg, 0.195 mmol), LA (56.7 mg, 0.195 mmol), solvent (1M), catalyst (5 mol%), 18 h.

Prepolymer	Solvent	T [°C]	Catalyst	$M_n$ [g/mol] <sup>a</sup>
PHU1	EtOH	80	-	1120
PHU2	EtOH	80	LiCl	1340
PHU3	EtOH	80	TBD	1250
PHU4	DMSO	100	-	1160
PHU5	DMSO	100	LiCl	1440
PHU6	-	120	-	1650

<sup>a</sup> SEC (System B, DMF, PMMA standards).

The use of 5 mol% lithium chloride as a catalyst increased the molecular weight to  $M_n = 1340$  g/mol (PHU2). Size exclusion chromatography (SEC) analysis comparing PHU1 and PHU2 reveals clear differences in the molar mass distribution (see Figure 82). The signal at 20.8 min corresponding to unreacted LC starting material shows that neither the reaction with catalyst nor the uncatalysed reaction resulted in full LC conversion. However, comparison of the LC signals for both reactions indicates higher conversion for the polymerisation using LiCl as catalyst. Furthermore, the reaction performed with the catalyst resulted in additional oligomeric species with lower retention times (16.0 – 17.5 min) and thus higher molecular weights that are not present in the chromatogram of the uncatalysed reaction, thus proving the effectiveness of the catalyst.



The main products of both reactions are oligomeric species with a retention time of 18.7 min.

Using TBD instead of LiCl as catalyst in ethanol at 80 °C had no significant influence on the molecular weight (PHU3,  $M_n = 1250$  g/mol). In a next step, the reaction temperature was increased to 100 °C and DMSO was used as solvent due to its higher boiling point compared to ethanol. In a first approach, the reaction was conducted without catalyst and resulted in a similarly low  $M_n$  of 1160 g/mol (PHU4) as the uncatalysed aminolysis reaction in ethanol (PHU1,  $M_n = 1120$  g/mol). The addition of LiCl as catalyst again led to an increase of the molecular weight distribution yielding PHU5 with a molecular weight of 1440 g/mol. The obtained molecular weight is in the same range as the molecular weight of the LiCl-catalysed reaction in ethanol at 80°C (PHU2,  $M_n = 1340$  g/mol), indicating that the increase in temperature by 20 K in combination with the change to an aprotic solvent had only very little influence on the reaction.

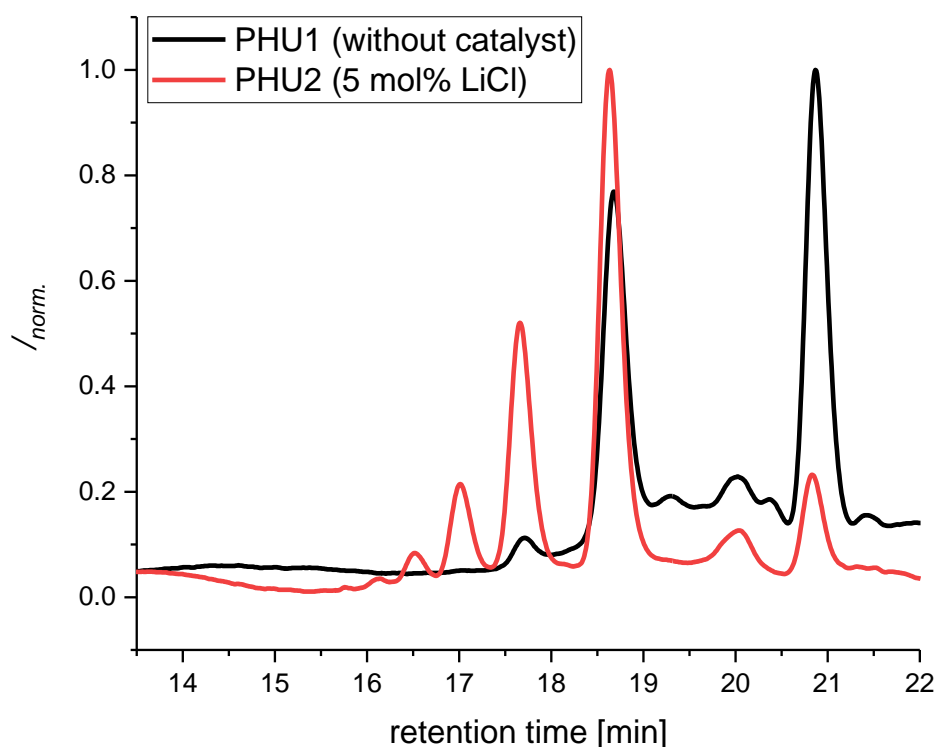


Figure 82: SEC analysis (System A, THF, PMMA standards) of the poly(hydroxy urethane) prepolymers PHU1 and PHU2.

In a last approach, the reaction temperature was increased to 120 °C and the reaction was performed in bulk. Compared to the approaches conducted in solvent, the approach in bulk at a higher temperature resulted in the highest obtained molecular weight of  $M_n = 1650$  g/mol. However, for practical reasons, *i.e.* the preparation of standard solutions of LA, as well as for sustainability considerations and the only small differences that were observed, the following reactions were performed with ethanol as solvent.

In order to investigate the influence of the LC/LA molar ratio on the resulting PHU prepolymers, two different LC/LA ratios, *i.e.* 1:1.1 and 1.1:1 were evaluated. In step-growth polymerisations, the excess of one reactant reduces the number-average value of the degree of polymerisation ( $X_n$ ) for a given monomer conversion,  $p$ , according to the Carothers equation:

$$X_n = \frac{1 + r}{1 + r - 2rp}$$

with  $r$  being the stoichiometric ratio of reactants. Final conversions of cyclocarbonate aminolysis reaction generally remain close to 80%.<sup>[291]</sup> Thus, for a hypothetical conversion of 80% and a monomer ratio of 1:1.1, the number-average value of the degree of polymerisation is 4.2. The reactions with a LC:LA ratio of 1:1.1 (PHU7) and 1.1:1 (PHU8) were conducted on a 50.0 mg scale in a pressure tube to be able to heat the reaction mixture at 100 °C in ethanol for 18 h with 5 mol% of LiCl as catalyst. After the reaction, the solvent was evaporated at reduced pressure and the product was analysed *via* SEC and FT-IR spectroscopy without further purification (see Figure 83).

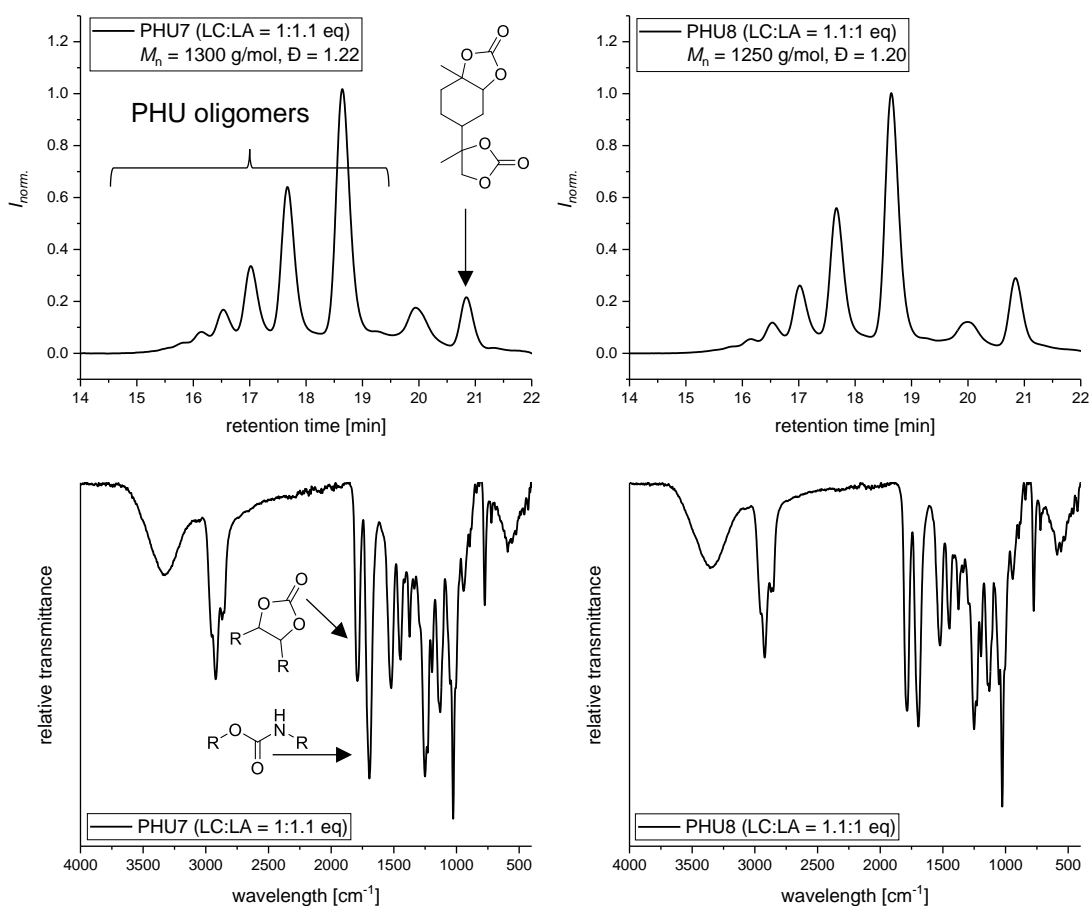


Figure 83: Top: SEC analysis of PHU7 and PHU8 prepared at LC:LA molar ratios of 1:1.1 and 1.1:1, respectively. Bottom: FT-IR spectra of PHU7 and PHU8 showing the characteristic peaks of the carbonate carbonyl band at 1791.5 and 1785.3  $\text{cm}^{-1}$ , respectively, and the carbonyl IR absorption of the urethane group at 1694.8  $\text{cm}^{-1}$ .

SEC analysis showed a very similar molar mass distribution for both polymerisations. Using a 10% excess of the diamine monomer (PHU7) resulted in a molecular weight of  $M_n = 1300 \text{ g/mol}$  and a dispersity of  $D = 1.22$ , while with 10% excess of the dicarbonate monomer (PHU8), a molecular weight of  $M_n = 1250 \text{ g/mol}$  and a dispersity of  $D = 1.20$  was obtained. The SEC chromatograms for both polymerisations show up to five separate oligomeric product species and in both cases the oligomer with the highest retention time of 18.6 min, most likely corresponding to the dimer, is the main product. Again, the signal at 20.8 min belonging to unreacted LC, indicates incomplete conversion. Via integration of the SEC peaks a conversion of around 80% can be estimated. Comparing both peaks corresponding to LC, the polymerisation using the diamine monomer in excess resulted in a smaller amount of unreacted LC. This finding is also reflected in the FT-IR spectra of both polymerisations (see Figure 83). The FT-IR spectra show, in addition to the carbonate

signal at 1791.5 and 1785.3  $\text{cm}^{-1}$ , respectively, the carbonyl IR absorption of the urethane group at 1694.8  $\text{cm}^{-1}$ . Furthermore, the N-H deformation of the urethane group and the hydroxyl groups appear at 3350.7  $\text{cm}^{-1}$ .

To allow for a more detailed analysis of the end groups of the obtained PHU prepolymers, PHU7 (LC:LA = 1:1.1) was analysed by SEC-ESI-MS (see Table 12).

*Table 12: Result of the SEC-ESI-MS analysis of PHU7 showing the calculated masses of each oligomer from monomer to nonamer and the masses that were found in the measurement. Number 1 corresponds to the carbonato telechelic oligomers and number 2 to the amino telechelic ones.*

<b>Oligomer</b>	<b>Calculated</b>	<b>Measured</b>
Monomer 1 (LC)	257.1020 [M+H] <sup>+</sup>	257.1013
Monomer 2 (LA)	291.1923 [M+H] <sup>+</sup>	-
Dimer	547.2870 [M+H] <sup>+</sup>	547.2861
Trimer 1	825.3636 [M+Na] <sup>+</sup>	825.3618
Trimer 2	837.4720 [M+H] <sup>+</sup>	837.4703
Tetramer	1093.5667 [M+H] <sup>+</sup>	1093.5648
Pentamer 1	1371.6434 [M+Na] <sup>+</sup>	1371.6409
Pentamer 2	1383.7518 [M+H] <sup>+</sup>	1383.7512
Hexamer	1639.8465 [M+H] <sup>+</sup>	1639.8470
Heptamer 1	1917.9231 [M+Na] <sup>+</sup>	1917.9248
Heptamer 2	1930.0315 [M+H] <sup>+</sup>	1930.0310
Octamer	2186.1262 [M+H] <sup>+</sup>	2186.1228
Nonamer 1	2464.2028 [M+Na] <sup>+</sup>	-
Nonamer 2	2476.3112 [M+H] <sup>+</sup>	-

Due to an insufficient resolution of the SEC system coupled to the ESI-MS, it was not possible to assign the well-defined signals of the individual oligomers obtained by the previous SEC analysis to their corresponding mass. Analysis of the combined mass spectra at different retention times showed that starting from the mass of the dimer all masses of the following oligomers up to the octamer were present in the analyte. In the case of an uneven number of monomer units, the masses found by ESI-MS include the carbonato telechelic oligomers as well as the amino telechelic ones. This is especially interesting, since the limonene-based diamine monomer was used in an excess of 10%. Possible reasons for unexpected occurrence of unreacted cyclic carbonate end groups are the low reactivity of the endocyclic five-membered cyclic carbonate and the high viscosity of the reaction mixture during the course of the reaction. Exemplarily, a potential

chemical structure of the octamer and its measured isotopic pattern next to the calculated pattern obtained by the program mMass are shown in Figure 84. The high agreement of the isotopic patterns proves the existence of a PHU prepolymer species containing eight monomer units present in the polymerisation product.

PHU octamer:  $[M+H]^+_{\text{calc.}} = 2186.1262$   
 $[M+H]^+_{\text{meas.}} = 2186.1228$

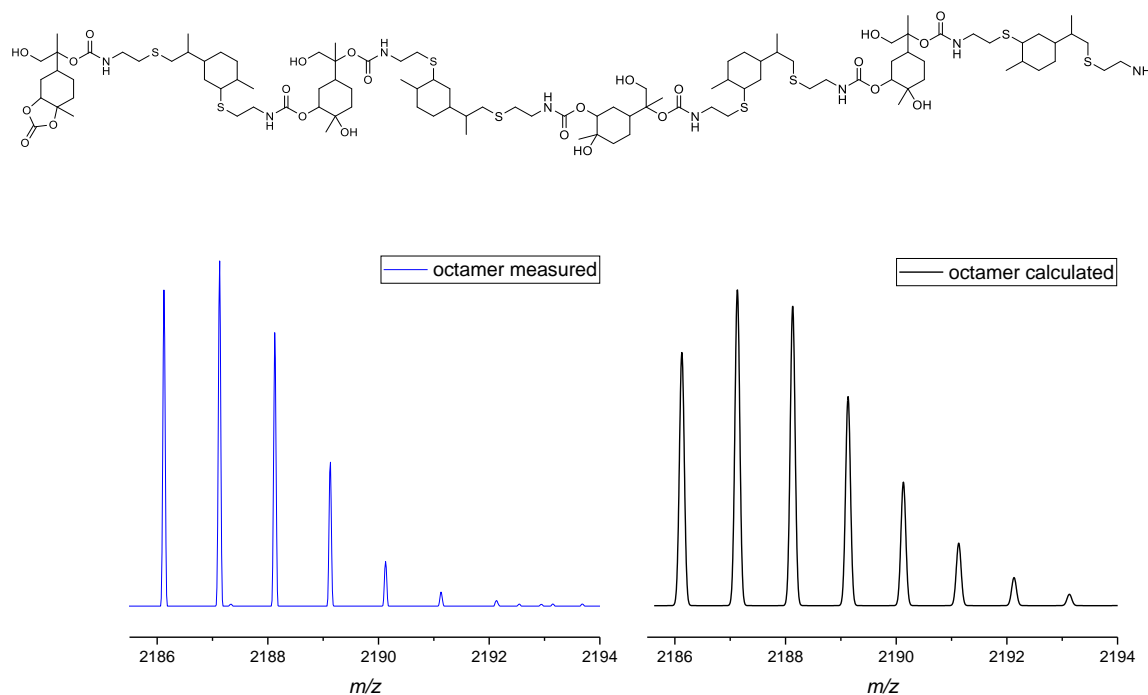


Figure 84: Top: Potential chemical structure of the LC- and LA-based PHU prepolymer species containing eight monomer units. Bottom: Measured isotopic pattern (blue) and calculated isotopic pattern (black) showing high agreement.

To further assess the reactivity of the five-membered cyclic carbonate groups and with the aim to achieve full conversion of LC, 1,10-diaminodecane was applied as sterically less demanding nucleophile for the polymerisation with LC (see Figure 85).

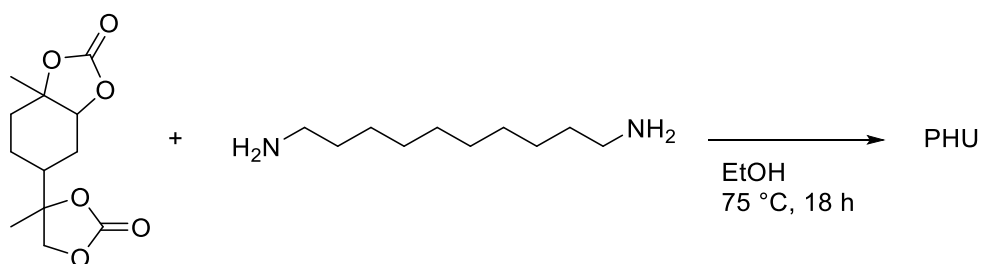


Figure 85: Synthesis of LC-based PHU using 1,10-diaminodecane as amine component. Reaction conditions: LC (50.0 mg, 0.195 mmol, 1 eq), 1,10-diaminodecane (37.0 mg, 0.215 mmol, 1.1 eq), EtOH (1M), 75 °C, 18 h.

The reaction was conducted in ethanol as solvent with a LC:1,10-diaminodecane ratio of 1:1.1 at 75 °C without catalyst. After 18 h, the solvent was evaporated, and the crude product was analysed via SEC (see Figure 86). The only minor peak at 20.8 min indicates that almost full conversion of LC was achieved. The signal at 20.1 min might most probably be assigned to unreacted 1,10-diaminodecane due to its use in excess. Compared to the polymerisations performed with LA instead of 1,10-diaminodecane, the molar mass distribution of the obtained oligomers is similar and shows up to seven separate oligomeric species, from which the presumed dimer, trimer and tetramer account for the largest product fraction. Also, the molecular weight of  $M_n = 1900$  g/mol is in the same range as for the LA-based PHU prepolymers.

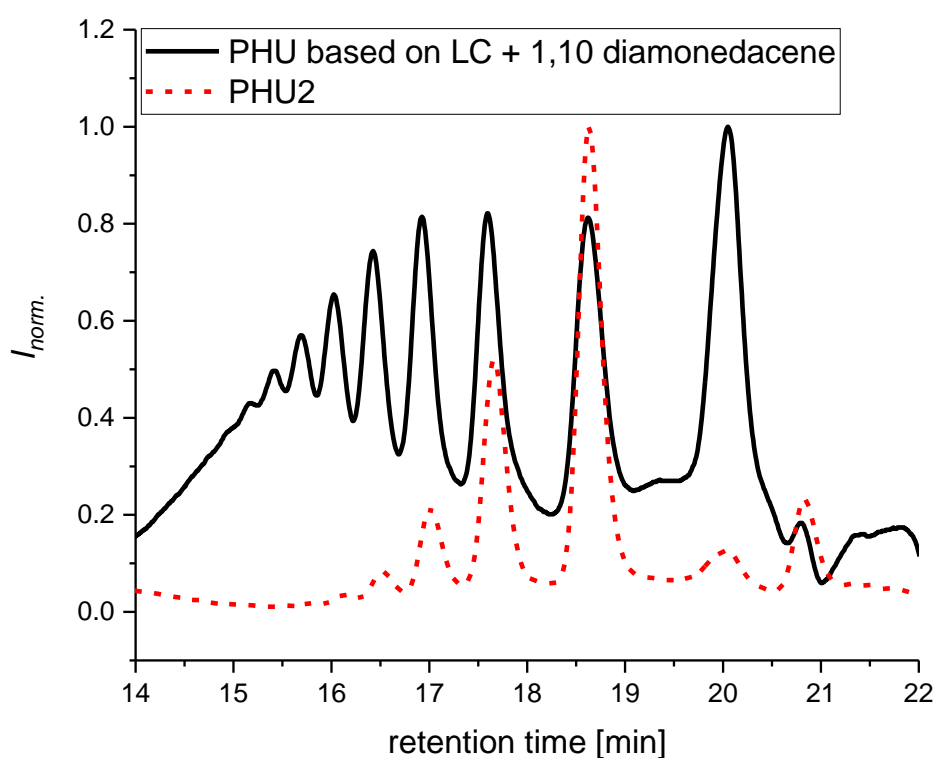


Figure 86: SEC analysis of the PHU obtained from the reaction of LC and 1,10-diaminodecane in comparison to PHU2.

The results of the test reaction showed that the high nucleophilicity of a linear primary amine, such as 1,10-diaminodecane, is able to attack the cyclic carbonates present in LC, resulting in almost full conversion. In contrast, the sterically more demanding LA based on the rigid limonene-carbon skeleton, failed in achieving full conversion of the cyclic carbonate monomer even when a catalyst at higher temperatures was used. However,

high conversion of the cyclic carbonate functionalities is necessary to obtain a large amount of amine terminated PHU prepolymer, which is in turn beneficial for the subsequent application as epoxy hardener. For that reason, the PHU prepolymer subsequently used for the synthesis of epoxy resins was prepared with a LC:LA ratio of 1:1.3. The polymerisation was performed in a pressure tube using 5 mol% of LiCl as catalyst and ethanol as solvent. After heating at 100 °C for 18 h, the solvent was evaporated yielding the crude product as brownish powder. Without further purification, the product was analysed *via* SEC and FT-IR spectroscopy (see Figure 87). The chromatogram obtained by SEC revealed almost full conversion of LC and showed up to four individual oligomer species. The PHU prepolymer was obtained with a molecular weight of  $M_n = 1380$  g/mol and a dispersity of  $\bar{D} = 1.18$ . Analysis of the FT-IR spectrum showed a band with rather low intensity at  $1795.6$   $\text{cm}^{-1}$  characteristic for the carbonate carbonyl functionality which might arise from carbonate terminated prepolymers or small amounts of unreacted starting material. The carbonyl IR absorption band of the urethane group at  $1694.8$   $\text{cm}^{-1}$ , and the N-H deformation of the urethane group and the hydroxyl groups at  $3350.7$   $\text{cm}^{-1}$  prove the successful formation of the poly(hydroxy urethane) prepolymer.

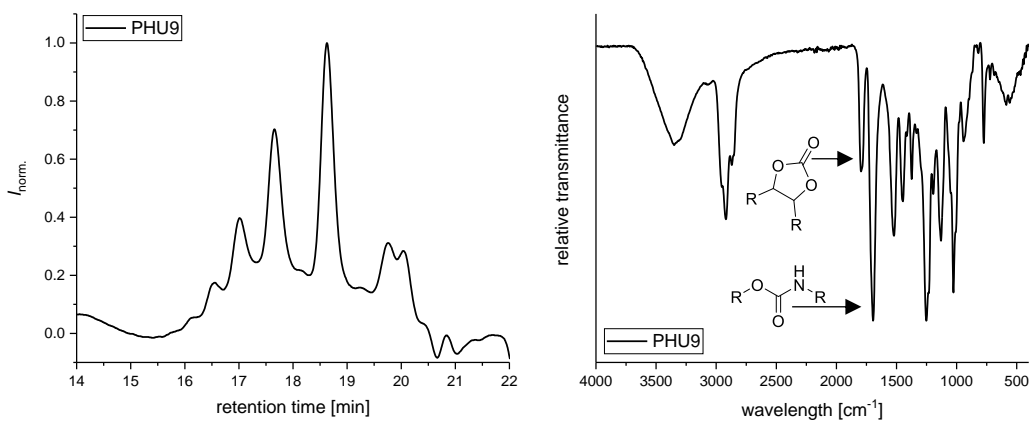


Figure 87: Left: SEC graph of PHU9 showing almost full conversion of LC. Right: FT-IR spectrum of PHU9 showing the characteristic peaks of the carbonate carbonyl band at  $1795.6$   $\text{cm}^{-1}$  and the carbonyl IR absorption of the urethane group at  $1694.8$   $\text{cm}^{-1}$ .

### 4.3.3 Application of PHU Prepolymers as Hardeners for Epoxy Resins

As a next step, the obtained PHU prepolymer PHU9 was assessed as hardener for epoxy resins. In contrast to the synthesis of high molar mass linear PHUs, precise stoichiometry is significantly less important for the preparation of epoxy thermosets. The amine value of

the PHU prepolymer was calculated from the initial LC:LA ratio used for the polymerisation resulting in an amine value of 0.975 mmol/g. Epoxidised soybean oil (ESBO) was chosen as epoxy component. The statistical main component of ESBO is epoxidised linolein, which possesses six epoxy groups per molecule. The commercially available ESBO was analysed *via* FT-IR spectroscopy and  $^1\text{H}$ ,  $^{13}\text{C}$  and 2D NMR spectroscopy (see Figure 88). The IR spectrum shows a characteristic peak at  $822.8\text{ cm}^{-1}$  originating from the epoxy groups. The peak at  $1740.1\text{ cm}^{-1}$  corresponds to the aliphatic C=O stretch of the ester groups. The epoxy content of the ESBO was calculated with the help of the  $^1\text{H}$  NMR data (see Figure 88). The value of the integrals was normalised to the signal of the nine protons belonging to the three methyl groups present at 0.93 – 0.84 ppm. This resulted in a value of 8.63 for the integral of the methylene group protons adjacent to the epoxy groups. The value of the integral corresponds to 4.32 epoxy groups per molecule, which gives an epoxy value of 4.53 mmol/g.



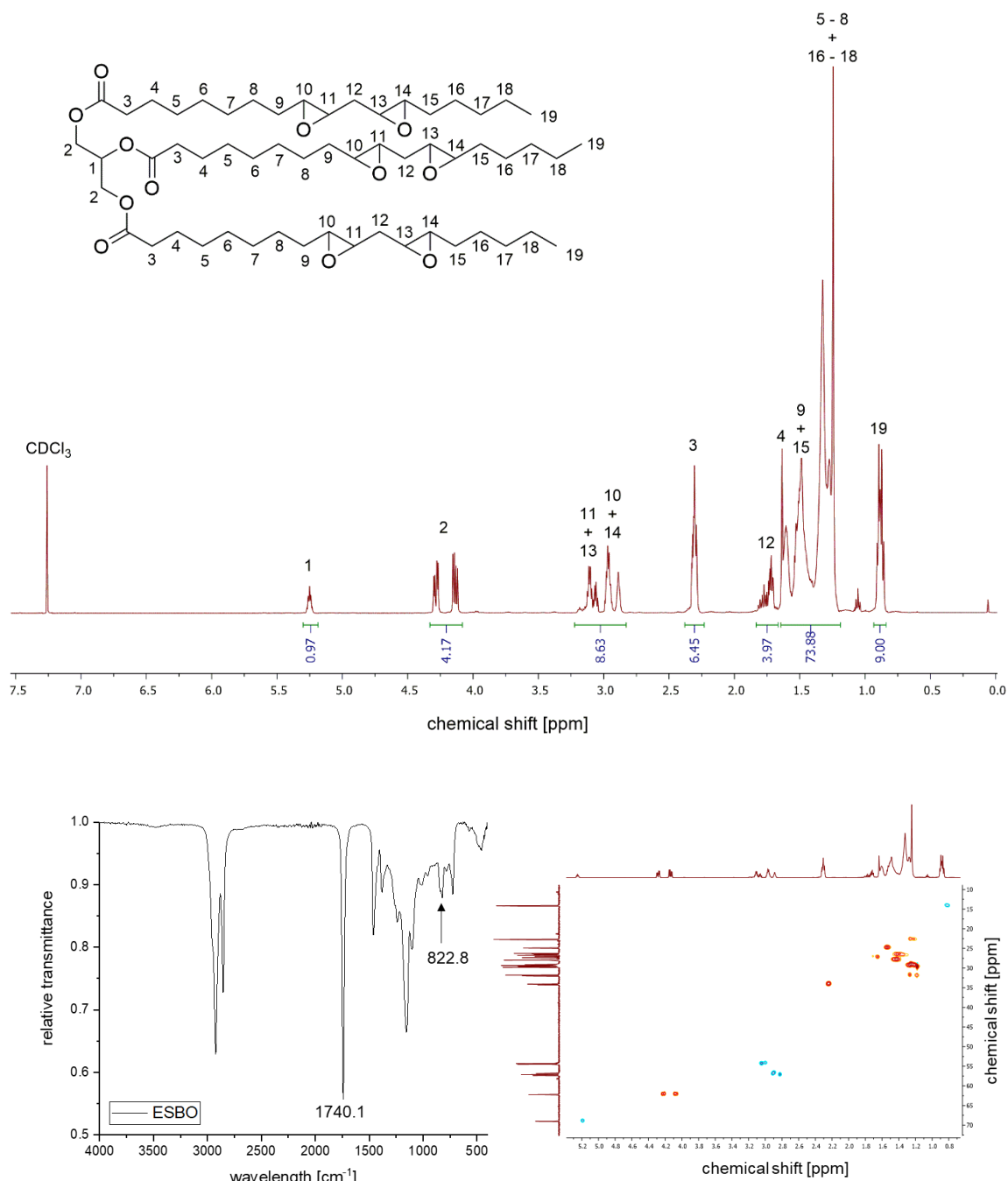


Figure 88: Top: fully assigned  $^1\text{H}$  NMR spectrum of ESBO; bottom: FT-IR spectrum and HSQC spectrum of ESBO.

Since the reaction of primary amines with epoxides results in a hydroxyl group and a secondary amine, which can further react with an epoxide forming an additional hydroxyl group and a tertiary amine, the molar amine to epoxide ratio was chosen to be 1:2 for the subsequent curing reaction. To achieve a homogeneous mixture of the two reactants for the curing reaction, both components were mixed and heated to 70 °C under vigorous

stirring. After a homogeneous mixture was obtained, the mixture was poured into a round silicon mould and heated for 3 h at 140 °C (see Figure 89).

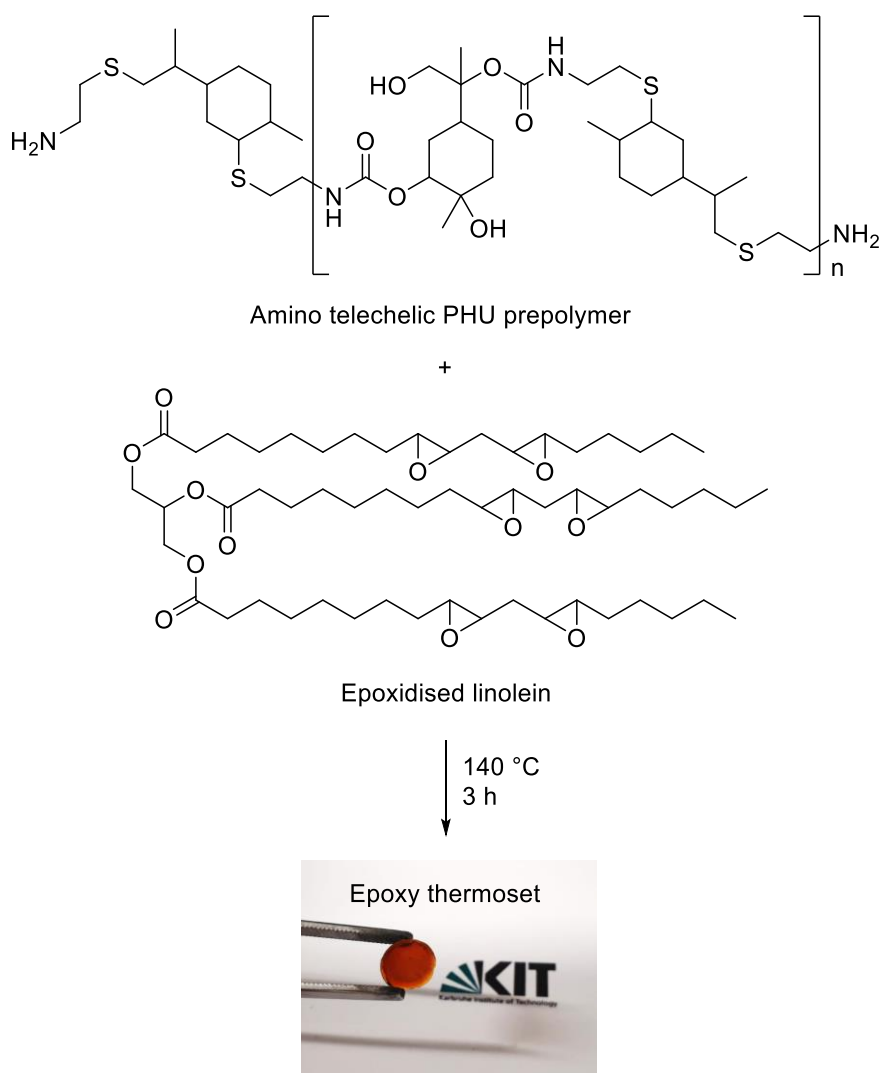


Figure 89: Reaction scheme for the application of the PHU prepolymers as hardener for epoxy thermosets based on epoxidised linolein and photograph of the obtained thermoset.

The curing reaction was further analysed *via* differential scanning calorimetry (DSC). Since thermal gravimetric analysis (TGA) of PHU9 revealed a degradation temperature  $T_{d5\%} = 209$  °C, the curing reaction was analysed from -75 °C to 200 °C by DSC (see Figure 90). In the region between -70 and 10 °C, the melting peaks of the ESBO are visible. The region of 15 to 25 °C shows the glass transition of the PHU prepolymer ( $T_g = 23$  °C). It can be presumed that the enthalpy peak starting at 122 °C corresponds to the reaction between the epoxy groups and the amines. The enthalpy reaches a maximum at 200 °C. However, since the DSC measurement did not allow for higher temperatures, it was not

possible to detect the temperature at the end of the reaction enthalpy peak, which is normally used for a post-curing of the epoxy resin.

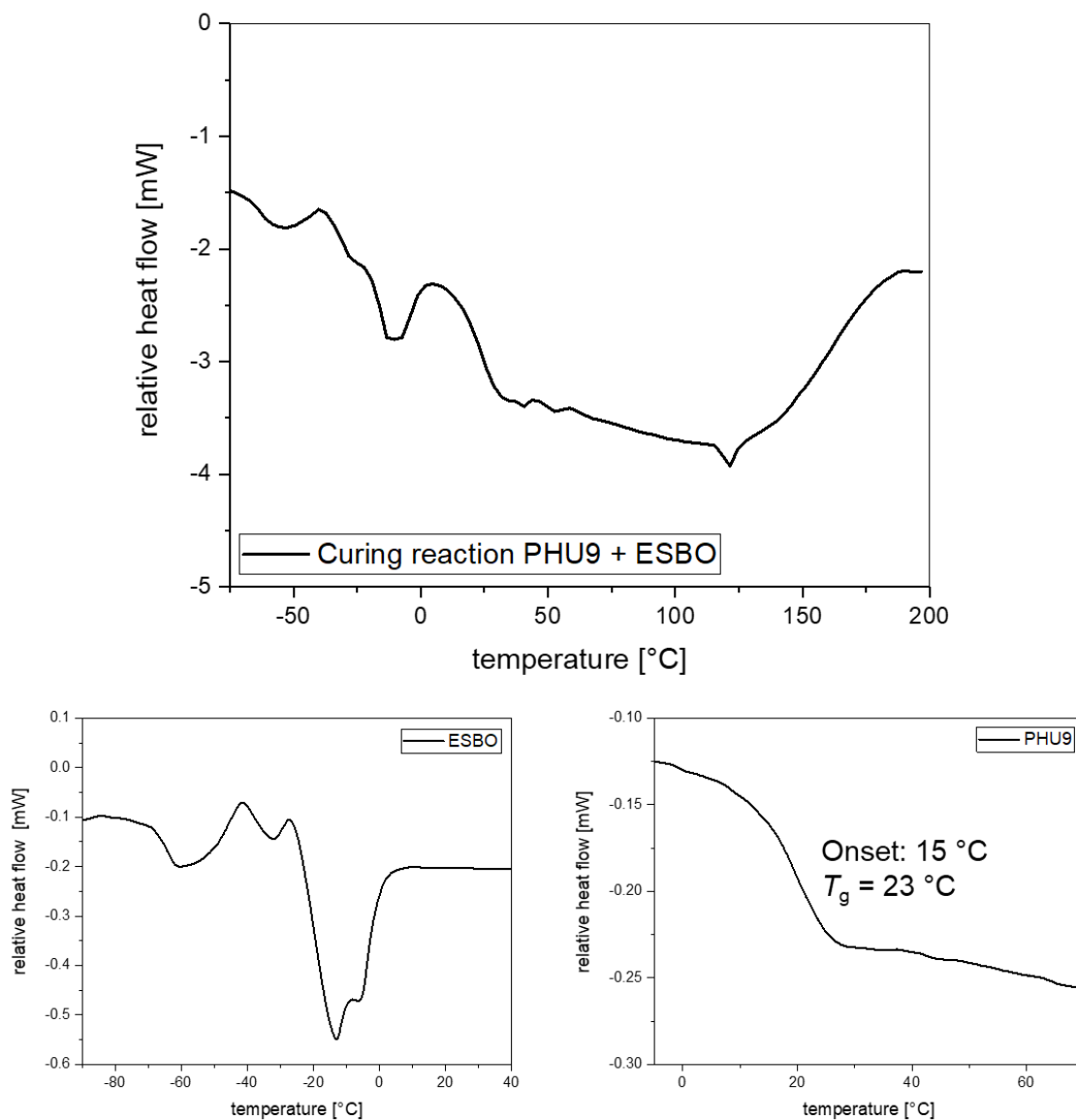


Figure 90: Top: DSC analysis of the curing reaction between PHU9 and ESBO; Bottom: DSC analysis of ESBO (left) and PHU9 (right).

Moreover, the obtained epoxy thermoset was analysed *via*, DSC, TGA and FT-IR. The thermoset showed a glass transition temperature of 29 °C and a thermal stability of  $T_{d\ 5\%} = 237$  °C (see Figure 91).

This first study demonstrated an application for the limonene-based PHU prepolymers. However, further studies are necessary, such as the analysis of the mechanical properties and the swelling properties in order to propose possible applications for the obtained epoxy

resin. Furthermore, it might be promising to investigate the biodegradability which may be induced by the ester groups present in the resin.

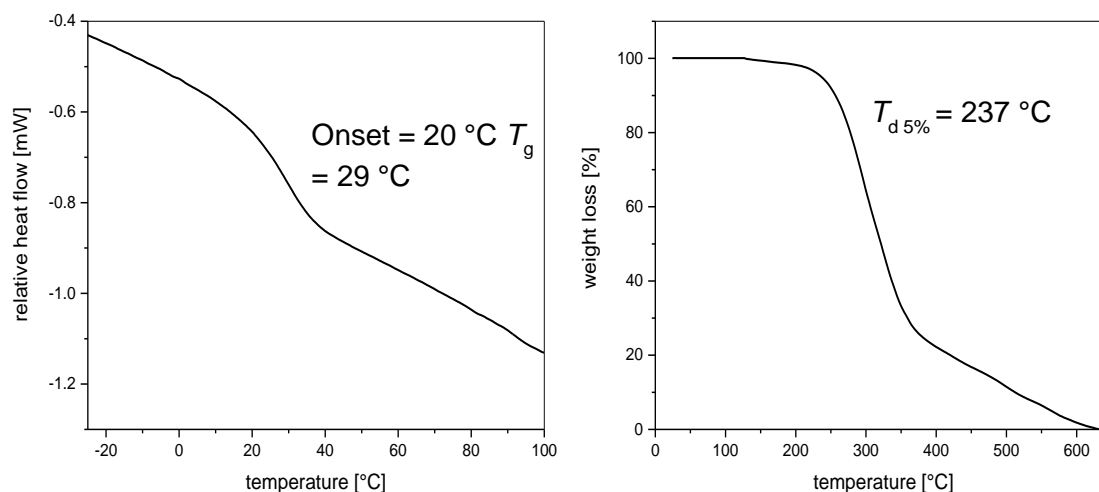


Figure 91: DSC and TGA analysis of the epoxy resin obtained from the curing reaction between PHU9 and ESBO.

In summary, the successful synthesis of two limonene-based AA-monomers bearing either five-membered cyclic carbonate functionalities or amine groups was shown. The monomers were subsequently polymerised to obtain poly(hydroxy urethane) prepolymers that contained all possible oligomeric species up to the octamer as analysed by SEC-ESI-MS measurements. When using the limonene-based diamine in 1.3-fold excess, almost full conversion of limonene dicarbonate was achieved for the polymerisation. Finally, the obtained prepolymer was successfully applied as hardener for the preparation of an epoxy thermoset with epoxidised soybean oil as a proof-of-concept.

## 5 Conclusion and Outlook

The perception that satisfying the increasing needs of our society must not be achieved at the expense of future generations, who should also have the means to satisfy their needs, has triggered the shift towards sustainable chemistry. Developing novel biomass-based chemicals and polymers and innovative technologies, helps to reduce the dependence on depleting fossil resources, to decrease carbon dioxide emission and to promote more environmentally benign materials. In this thesis, three routes for the transformation of terpenes into valuable fine chemicals, monomers and polymers were shown. Besides using renewable resources as starting material, the 12 principles of green chemistry were also followed to design as sustainable synthetic procedures as possible.

In a first approach, Mn(III) acetate was applied for the liquid-phase aerobic oxidation of  $\alpha$ -pinene. Subsequently, the influence of reaction time, solvent, temperature, oxidant flow rate and catalyst concentration on conversion, yield, and selectivity were evaluated. It turned out that high temperatures (130 °C) and high oxidant flow rates (50 mL min<sup>-1</sup>), low catalyst concentrations (0.25 mol%) and a toluene/DMF solvent mixture allowed to achieve the highest conversion (62%) and with the highest yield of pinene oxide (40%, 65% selectivity). Reaction times longer than 6 h did not enhance the formation of pinene oxide, since epoxides tend to isomerise if subjected to such high temperatures for prolonged times. To prevent side reactions, toluene was exchanged by diethyl carbonate, which proved to be inert under the applied conditions and is regarded as a more sustainable solvent. Furthermore, a novel mixed-linker metal-organic framework MIXMIL-53-NH<sub>2</sub>(50)-Mal-Mn was synthesised and structurally characterised. Physisorption experiments showed a high specific surface area, which was maintained after the post-synthetic modification reactions leading to a potentially highly active catalyst. All in all, it could be shown that the metal-organic framework with its immobilised and well-defined manganese(III) complexes featured notable catalytic activity for the oxidation of  $\alpha$ -pinene with molecular oxygen in DEC/DMF applying the aforementioned reaction conditions. The main product, pinene oxide, was obtained in high selectivity, along with smaller amounts of verbenol and verbenone. Compared to the conversion and yield achieved by Mn(III) acetate, the novel MOF catalyst gave similar results, however, the accumulated TON of the MOF catalyst (166) was considerably higher than the TON of the homogeneous catalyst system (23). As indicated by a hot filtration test, the reaction mainly proceeded through a heterogeneous pathway, although an involvement of homogeneous species could not be completely ruled out. Moreover, the constant activity over at least five catalytic

cycles of the Mn-containing MOF proved its recyclability and underlined the stability of the MOF under the applied reaction conditions.

In the second approach, epoxidised  $\alpha$ - and  $\beta$ -pinene were applied as renewable substrates for the synthesis of cyclic and linear carbonates. First, the chemical fixation of CO<sub>2</sub> *via* coupling with  $\alpha$ -pinene oxide was investigated to transform  $\alpha$ -pinene oxide into the corresponding cyclic carbonate. Due to the bulkiness of the bicyclic  $\alpha$ -pinene carbon skeleton, none of the tested catalytic systems was able to achieve the insertion of CO<sub>2</sub> into the epoxide ring, and thus, a new concept was evaluated exploiting the vicinal double bonds present in  $\alpha$ - and  $\beta$ -pinanediol and introducing the carbonyl functionality *via* transesterification with dimethyl carbonate or diallyl carbonate. Therefore,  $\beta$ -pinene was oxidised using commercially available methyltrioxorhenium (MTO) as catalyst and hydrogen peroxide as environmentally benign oxidising agent, as it generates only oxygen and water as waste. The produced water allowed for the *in situ* formation of the desired  $\beta$ -pinanediol as an epoxide ring-opening of the pinene oxide took place with water as the nucleophile. Both,  $\beta$ -pinanediol and the commercially available *cis*- $\alpha$ -pinanediol, were sustainably transformed into the corresponding cyclic carbonates by transesterification with linear carbonates using catalytic amounts of 1,5,7-triazabicyclo[4.4.0]dec-5-ene (TBD) at mild temperatures. An excess amount of linear carbonate allowed to eliminate the need for a solvent. Additionally, the linear carbonate could be easily recycled by distillation, preventing waste formation. The demonstrated procedure for the cyclic carbonate formation based on  $\alpha$ -pinanediol was compared to already existing literature procedures clearly highlighting the environmental benefits of the novel reaction protocol.

In a third approach, limonene was assessed as a raw material for the synthesis of renewable poly(hydroxy urethane)s. After successful synthesis of a limonene-based cyclic dicarbonate *via* CO<sub>2</sub> insertion into the corresponding limonene diepoxide and a limonene-based diamine using thiol-ene chemistry, an environmentally benign reaction protocol for the formation of PHU prepolymers was established using ethanol as solvent at temperatures between 80 and 100 °C. It turned out that the use of a catalyst, *e.g.* lithium chloride, is beneficial for obtaining higher molecular weights at temperatures low enough to prevent side-reactions (*i.e.* <140 °C). The variation of the solvent from aprotic DMSO to protic ethanol had no significant influence on the molecular weight and it appeared that the highest molecular weight was achieved for reactions performed in bulk at 120 °C. Moreover, the obtained PHU prepolymers were analysed *via* SEC-ESI-MS revealing that oligomeric species ranging from two to eight monomer units corresponding to a molecular weight of 2186 g/mol were present in the product. Virtually full conversion of limonene dicarbonate was achieved using the diamine component in 1.3-fold excess. The resulting

prepolymer exhibited a molecular weight of  $M_n = 1,400$  g/mol and a dispersity of  $\mathcal{D} = 1.18$ . As a proof-of-concept, the obtained PHU prepolymer was successfully applied as hardener for an epoxy resin based on soybean oil.

Overall, the presented procedures for the synthesis of  $\alpha$ -pinene oxide, cyclic carbonates from  $\alpha$ - and  $\beta$ -pinene, and PHU prepolymers from functionalised limonene open up novel sustainable routes to renewable fine chemicals and polymers. Regarding future applications of the obtained materials, further investigations of the material properties are necessary and should at least include mechanical properties, swelling properties and biodegradability. In addition, improvements in terms of yields and replacing all steps that contain column chromatographic purification by more environmentally benign and scalable procedures is also necessary to pave the way for upscaling the demonstrated procedures. All in all, this work establishes novel routes towards a sustainable exploitation of renewable resources and their transformation into platform/fine chemicals and polymeric materials.





## 6 Experimental Section

### 6.1 Materials

Ethyl acetate, dichloromethane and cyclohexane were pre-distilled, all other solvents were used without further purification. The following chemicals were used as received from the following: 2-Aminoterephthalic acid (99%, Sigma-Aldrich), terephthalic acid (97%, Sigma-Aldrich), aluminium nitrate nonahydrate (Sigma-Aldrich), *N,N*-dimethylformamide (99.8%, Sigma-Aldrich), maleic anhydride (99%, Sigma-Aldrich), acetonitrile (99.8%, Sigma-Aldrich), ethanol (96%, VWR Chemicals), (+)- $\alpha$ -pinene (98%, Sigma-Aldrich), biphenyl (>99%, Sigma-Aldrich), manganese(III) acetate dihydrate (97%, Sigma-Aldrich), dimethyl carbonate (99%, Acros Organics), diethyl carbonate (Merck Millipore), toluene (99.7% Bernd Kraft),  $\alpha$ -pinene oxide (Sigma-Aldrich, 97%), potassium iodide (Fisher Scientific), triethanolamine (>99%, Sigma-Aldrich), tetrabutylammonium bromide (TBAB, 98%, Sigma-Aldrich), *p*-methoxyphenol (98%, Sigma-Aldrich), *N,N*-dimethylpyridin-4-amine (DMAP, 99%, Alfa Aesar), L-ascorbic acid (99%, Sigma-Aldrich), tetrabutylammonium iodide (TBAI, 98%, abcr GmbH), sodium sulfate (anhydrous, >99%, Bernd Kraft),  $\alpha$ -pinene oxide (>95%, TCI), TLC silica gel F254 (Sigma-Aldrich), Silica gel 60 (0.040 - 0.063, Sigma-Aldrich), cerium(IV) sulfate (99%, Sigma-Aldrich), phosphomolybdic acid hydrate (99%, Sigma-Aldrich), dichloromethane (HPLC grade  $\geq 99.9\%$ , Sigma-Aldrich), 1,8-diazabicyclo[5.4.0]undec-7-ene (DBU, >98%, TCI), hexadecane (99%, Sigma-Aldrich), methyltrioxorhenium (MTO, Re: 71-76%, Sigma-Aldrich), manganese(IV) oxide (>90%, Sigma-Aldrich), (1*R*,2*R*,3*S*,5*R*)-(-)-pinanediol (*cis*- $\alpha$ -pinanediol, 99%, Sigma-Aldrich),  $\beta$ -pinene (99%, Sigma-Aldrich), lipase B (*Candida antarctica* immobilised on Immobead 150, Sigma-Aldrich), *tert*-butanol (99%, Fluka), magnesium sulfate (anhydrous, VWR), sodium sulfite (98%, Merck), magnesium sulfate (anhydrous, 99.5%, Sigma-Aldrich), hydrogen peroxide (30 wt% in H<sub>2</sub>O, Sigma-Aldrich), chloroform-*d* (99.8%, Eurisotop), dimethyl sulfoxide-*d*<sub>6</sub> (99.8%, Eurisotop). Limonene dioxide (mixture of *cis*-(+)) and *trans*-(+)) isomers, 98%, Rheinmetall Nitrochemie), (*R*)-(+)-Limonene (97%, Sigma-Aldrich), cysteamine hydrochloride (>97%, Fluka), 2,2-dimethoxy-2-phenylacetophenone (DMPA, 99%, Sigma-Aldrich), potassium carbonate (99%, Sigma-Aldrich), ninhydrin (95%, ChemPur), 1,10-diaminodecane (97%, Sigma-Aldrich), epoxidised soybean oil (98%, abcr GmbH). Diallyl carbonate was previously synthesised in this group by Charlotte Over. Water, when used in the synthesis, was de-ionised.

## 6.2 Instrumentation

### Powder X-ray diffraction (PXRD)

PXRD measurements were performed using a Bruker D8 Advance. The samples were analysed in the range  $2\Theta = 6 - 50^\circ$  using Cu  $K_\alpha$  radiation. The step width was  $2\Theta = 0.0164^\circ$  with a dwell time of 2 s.

### Nitrogen physisorption (BET)

Nitrogen physisorption was measured using a Belsorp mini II from BEL Japan. The specific surface area was determined using the BET method and the BEL Master software.

### Attenuated total reflection infrared spectroscopy (ATR-IR)

IR data were acquired using either system A or system B:

System A: FT-IR spectrometer Vertex 70 from Bruker Optics equipped with a Golden Gate Single Reflection ATR sample cell from Specac. The data were collected from 4500 to 600  $\text{cm}^{-1}$  and for each spectrum the arithmetic average of 400 measurements was taken.

System B: Bruker Alpha-p instrument in a frequency range from 3998 to 374  $\text{cm}^{-1}$  applying attenuated total reflection (ATR) technology.

### Nuclear Magnetic Resonance (NMR) Spectroscopy

NMR spectra were acquired using either system A or system B:

System A: WB Bruker AVANCE I spectrometer operating at 500 MHz for  $^1\text{H}$ - and 126 MHz for  $^{13}\text{C}$ -measurement.

System B: Bruker Aspect NMR spectrometer operating at 400 MHz for  $^1\text{H}$ - and 101 MHz for  $^{13}\text{C}$ -measurement.

$\text{CDCl}_3$  or  $\text{DMSO-d}_6$  were used as solvents. Chemical shifts are presented in parts per million ( $\delta$ ) relative to the resonance signal at 7.26 ppm ( $^1\text{H}$ ,  $\text{CDCl}_3$ ) and 77.16 ppm ( $^{13}\text{C}$ ,  $\text{CDCl}_3$ ) or 2.50 ppm ( $^1\text{H}$ ,  $\text{DMSO-d}_6$ ) and 39.52 ppm ( $^{13}\text{C}$ ,  $\text{DMSO-d}_6$ ), respectively. Coupling constants ( $J$ ) are reported in Hertz (Hz). All measurements were recorded in a standard fashion at 25  $^\circ\text{C}$ . Full assignment of structures was aided by 2D NMR analysis (COSY, HSQC and HMBC).

### **Atomic absorption spectroscopy (AAS)**

For AAS measurements, a Z-6100 Polarized Zeeman atomic absorption spectrometer from Hitachi was used.

### **Gas chromatography (GC)**

GC measurements were performed either on system A or system B:

System A: GC-2010 Plus instrument from Shimadzu with a nonpolar column (Rxi-5Sil MS, length: 30 m, diameter: 0.25 mm, film thickness: 0.25 mm) and a flame-ionisation detector (FID) was used. The sample was injected and vaporised at 250 °C. The column was heated from 50 to 280 °C at a rate of 10 K min<sup>-1</sup>.

System B: Bruker 430 GC instrument with a capillary column FactorFour™ VF-5ms (30 m × 0.25 mm × 0.25 mm) and an FID.

### **Gas Chromatography-Mass Spectrometry (GC-MS)**

GC-MS (EI) chromatograms were recorded with a Varian 431 GC instrument with a capillary column FactorFour™ VF-5ms (30 m × 0.25 mm × 0.25 mm) and a Varian 210 ion trap mass detector.

### **Thin Layer Chromatography (TLC)**

Thin layer chromatography was carried out on silica gel coated aluminium foil (TLC silica gel F<sub>254</sub>, Sigma-Aldrich). Compounds were visualised by staining with Seebach-solution (mixture of phosphomolybdic acid hydrate, cerium(IV) sulfate, sulfuric acid and water) or ninhydrin solution in ethanol.

### **Size Exclusion Chromatography (SEC)**

SEC analysis was performed either on system A or system B:

System A: Prepolymers were characterised on a Varian 390-LC SEC system equipped with a LC-290 pump (Varian), refractive index detector (24 °C), PL AS RT GPC-autosampler (Polymer laboratories) and a Varian Pro Star column oven Model 510, operating at 40 °C. For separation, two SDV 5 µm linear S columns (8 × 300 mm) and a guard column (8 × 50 mm) supplied by PSS, Germany, were used. Tetrahydrofuran (THF) stabilised with butylated hydroxytoluene (BHT, HPLC-SEC grade) supplied by Sigma

Aldrich was used at a flow rate  $1.0 \text{ mL min}^{-1}$ . Calibration was carried out with linear poly(methyl methacrylate) standards (Agilent) ranging from 875 to 1 677 000 Da. Detection was done by a refractive index detector operating in THF (flow rate  $1.0 \text{ mL min}^{-1}$ ).

System B: DMF–SEC analysis was performed on a TOSOH EcoSEC HLC-8320GPC system equipped with an EcoSEC RI detector and three columns (PSS PFG 5  $\mu\text{m}$ ; Microguard, 100  $\text{\AA}$  and 300  $\text{\AA}$ ) (MW resolving range: 300– $1.0 \times 10^5$  Da) from PSS GmbH. Measurements were carried out at 50  $^\circ\text{C}$  using DMF solvent supplemented with 0.01 M LiBr as mobile phase (isocratic elution,  $0.2 \text{ mL min}^{-1}$ ). A conventional calibration method was created using narrow linear poly(methyl methacrylate) standards. Corrections for flow rate fluctuations were made using toluene as an internal standard. PSS WinGPC Unity software version 7.2 was used to process and analyse the data. Analytes were dissolved in DMF/LiBr solvent ( $2.5 \text{ mg mL}^{-1}$ ) and the resulting solutions filtered with a 0.45  $\mu\text{L}$  teflon filter before analysis.

### **Size Exclusion Chromatography Coupled to Electrospray Ionisation Mass Spectrometry (SEC-ESI-MS)**

Spectra were recorded on a Q Exactive (Orbitrap) mass spectrometer (Thermo Fisher Scientific) equipped with a HESI II probe. The instrument was calibrated in the  $m/z$  range 74–1822 using premixed calibration solutions (Thermo Scientific). A constant spray voltage of 4.6 kV, a dimensionless sheath gas of 8, and a dimensionless auxiliary gas flow rate of 2 were applied. The capillary temperature and the S-lens RF level were set to 320  $^\circ\text{C}$  and 62.0, respectively. The Q Exactive was coupled to an UltiMate 3000 UHPLC System (Dionex, Sunnyvale, CA, USA) consisting of a pump (LPG 3400SD), autosampler (WPS 3000TSL), and a thermostated column department (TCC 3000SD). Separation was performed on two mixed bed size exclusion chromatography columns (Polymer Laboratories, Mesopore 250  $\times$  4.6 mm, particle diameter 3  $\mu\text{m}$ ) with pre-column (Mesopore 50  $\times$  4.6 mm) operating at 30  $^\circ\text{C}$ . THF at a flow rate of  $0.30 \text{ mL min}^{-1}$  was used as eluent. The mass spectrometer was coupled to the column in parallel to a RI-detector (RefractoMax520, ERC, Japan).  $0.27 \text{ mL min}^{-1}$  of the eluent were directed through the RI-detector and  $30 \mu\text{L min}^{-1}$  infused into the electrospray source after postcolumn addition of a 100  $\mu\text{M}$  solution of sodium iodide in methanol at  $20 \mu\text{L min}^{-1}$  by a micro-flow HPLC syringe pump (Teledyne ISCO, Model 100DM). A 20  $\mu\text{L}$  aliquot of a polymer solution with a concentration of  $2 \text{ mg mL}^{-1}$  was injected onto the HPLC system.

### Electron ionisation (EI)

Electron Ionisation (EI) mass spectra were recorded on a Finnigan MAT 95 instrument.

### Differential Scanning Calorimetry (DSC)

The DSC experiments were carried out using a Mettler Toledo DSC star<sup>e</sup> system. The DSC experiments are carried out under nitrogen atmosphere using 40 µl aluminium crucibles and a sample mass of 10 mg. The cured epoxy resin was analysed with the following heating program with two cycles: first heating cycle: 20 °C to 100 °C in 10 K min<sup>-1</sup>; cooling: 100 °C to -40 °C in -10 K min<sup>-1</sup>; second heating cycle: -40 °C to 100 °C in 10 K min<sup>-1</sup>. The PHU prepolymer and ESBO were analysed using the following heating program: first heating cycle: 20 °C to 70 °C in 10 K min<sup>-1</sup>; cooling: 70 °C to -20 °C in -10 K min<sup>-1</sup>; second heating cycle: -20 °C to 70 °C in 10 K min<sup>-1</sup>. The curing reaction of ESBO with the PHU prepolymer was analysed with the following heating program: first heating cycle: 25 °C to 70 °C in 30 K min<sup>-1</sup>; holding at 70 °C for 5 min, cooling: 70 °C to -100 °C in -10 K min<sup>-1</sup>; second heating cycle: -100 °C to 200 °C in 10 K min<sup>-1</sup>. The glass transition temperature ( $T_g$ ) was defined as the midpoint of the change in heat capacity occurring over the transition in the second heating cycle.

### Thermal gravimetric analysis (TGA)

TGA measurements were performed using a Netzsch STA 409C instrument with Al<sub>2</sub>O<sub>3</sub> as a crucible material and reference sample. The samples (15-20 mg) were heated from 25-650 °C with a heating rate of 10 K min<sup>-1</sup> under synthetic air flow.

### Microwave reactor

Microwave-assisted syntheses were performed in a CEM EXPLORER 12 HYBRID microwave reactor using a dynamic program at 150 W. The reaction mixture was pre-stirred with a magnetic stir bar for 30 s at medium speed in glass vessels sealed *with* a PTFE rubber band.

### Pressure reactor

High pressure reactions were performed in a high-pressure laboratory reactor (BR-100) from Berghof products + instruments.

## 6.3 Experimental Procedures

### 6.3.1 Experimental Procedures for Chapter 4.1

#### 6.3.1.1 Synthesis and Characterisation of MIXMIL-53-NH<sub>2</sub>(50)-Mal-Mn<sup>\*</sup>

##### 6.3.1.1.1 Synthesis of MIXMIL-53-NH<sub>2</sub>(50)

MIXMIL-53-NH<sub>2</sub>(50) was synthesised according to a modified procedure of MIL-53(Al)-NH<sub>2</sub>.<sup>[235]</sup> 2-Aminoterephthalic acid (H<sub>2</sub>ABDC, 483 mg, 2.67 mmol, 1.00 eq) and terephthalic acid (H<sub>2</sub>BDC, 444 mg, 2.67 mmol, 1.00 eq) were dissolved in H<sub>2</sub>O (20 mL) and DMF (50 mL) at 90 °C. A solution of Al(NO<sub>3</sub>)<sub>3</sub> × 9 H<sub>2</sub>O (2.00 g, 5.33 mmol, 2.00 eq) in H<sub>2</sub>O (5 mL) was added and the reaction mixture was stirred at 90 °C for 24 h. After filtration, the material was washed with DMF (3 × 25 mL) and H<sub>2</sub>O (1 × 25 mL) and was dried overnight at room temperature and then for 3 days at 130 °C in air.

##### 6.3.1.1.2 Post-synthetic modification of MIXMIL-53-NH<sub>2</sub>(50)

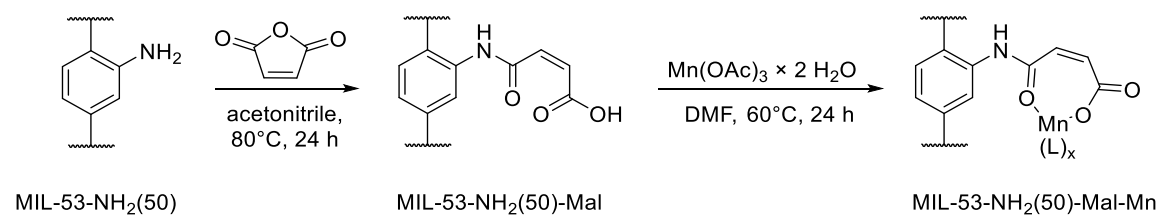


Figure 92: Two-step PSM reaction for the synthesis of MIXMIL-53-NH<sub>2</sub>(50)-Mal-Mn.

MIXMIL-53-NH<sub>2</sub>(50) was modified in a two-step PSM reaction. First step: maleic anhydride (471 mg, 4.80 mmol, 4.00 eq, based on the number of amine groups) was dissolved in acetonitrile (60 mL). MIXMIL-53-NH<sub>2</sub>(50) (517 mg, 2.40 mmol, 1.00 eq) was suspended in the solution and the reaction mixture was heated to 80 °C for 24 h. After filtration, the resulting material was washed with acetonitrile (4 × 20 mL), DMF (1 × 20 mL) and H<sub>2</sub>O (1 × 20 mL). The solid was dried overnight at room temperature and then for 3 days at 130 °C in air. Second step: manganese(III) acetate dihydrate (24.2 mg, 0.09 mmol, 1.00 eq) was dissolved in ethanol (40 mL). MIXMIL-53-NH<sub>2</sub>(50)-Mal (441 mg, 2.50 mmol, 1.00 eq) was suspended in the solution and the reaction mixture was heated to 60 °C for 24 h. After filtration, the resulting material was washed with ethanol (4 × 20 mL). The solid was dried overnight at room temperature and then for 3 days at 130 °C in air.

\* The synthesis and characterisation of MIXMIL-53-NH<sub>2</sub>(50)-Mal-Mn was performed by cooperation partner Ceylan Yildiz at Karlsruhe Institute of Technology (KIT).

### 6.3.1.1.3 Material characterisation of MIXMIL-53-NH<sub>2</sub>(50)-Mal-Mn

PXRD measurements revealed that the structure of MIL-53-NH<sub>2</sub>(50) was retained throughout the whole modification process (see Results and Discussion, Chapter 4.1, Figure 56).

For nitrogen physisorption (BET) the samples were activated for 20 h at 130 °C under vacuum. N<sub>2</sub> physisorption measurements of MIXMIL-53-NH<sub>2</sub>(50)-Mal and MIXMIL-53-NH<sub>2</sub>(50)-Mal-Mn showed a significant decrease of the specific surface area (see Table 9) after modification of MIXMIL-53-NH<sub>2</sub>(50) (see Figure 93).

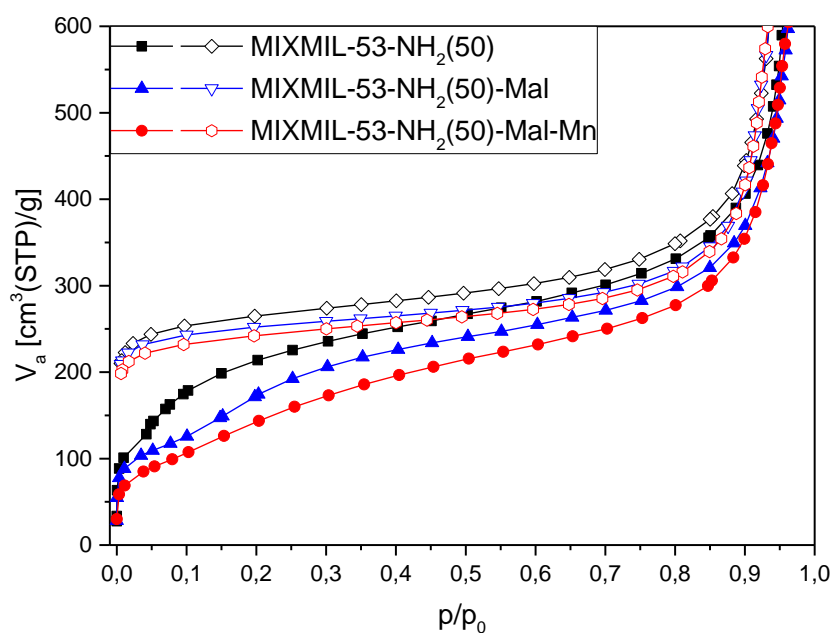


Figure 93: Adsorption (closed symbols) and desorption (open symbols) isotherms of MIXMIL-53-NH<sub>2</sub>(50), MIXMIL-53-NH<sub>2</sub>(50)-Mal and MIXMIL-53-NH<sub>2</sub>(50)-Mal-Mn.

For ATR-IR measurements system A (see Instrumentation, Chapter 6.2) was used.

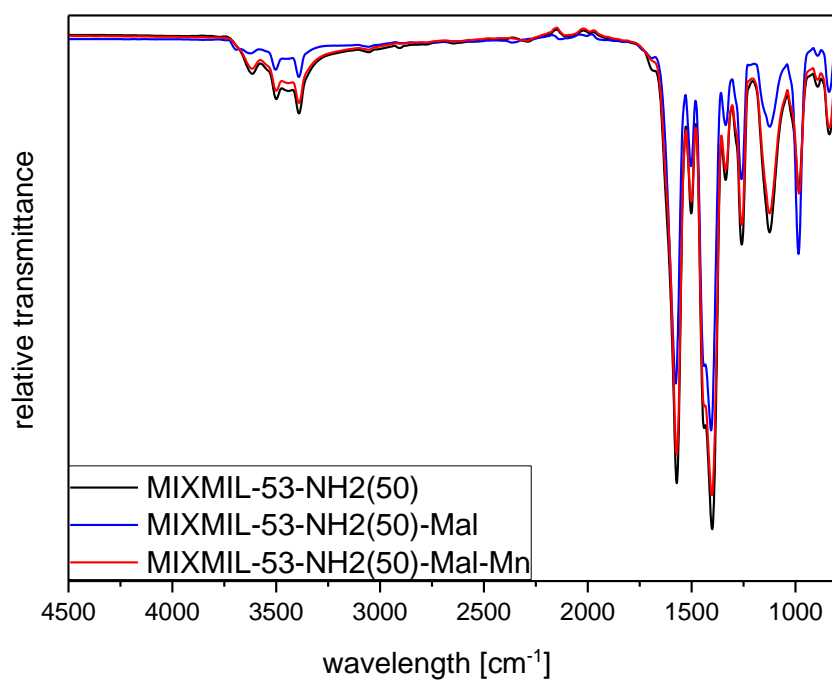


Figure 94: Complete ATR-IR spectra of MIXMIL-53-NH<sub>2</sub>(50), MIXMIL-53-NH<sub>2</sub>(50)-Mal and MIXMIL-53-NH<sub>2</sub>(50)-Mal-Mn.

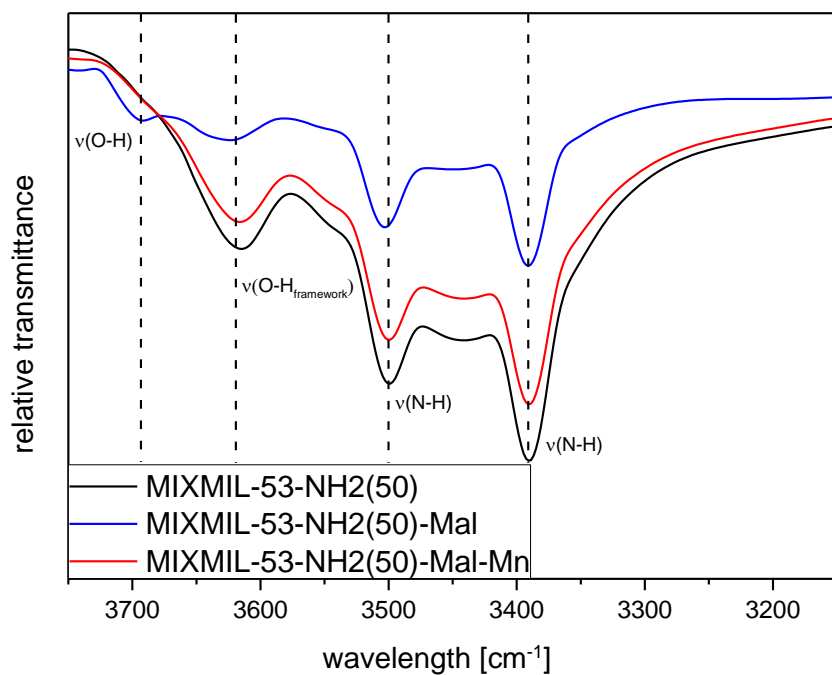


Figure 95: Zoom to O-H and N-H stretching vibrations of ATR-IR spectra of MIXMIL-53-NH<sub>2</sub>(50), MIXMIL-53-NH<sub>2</sub>(50)-Mal and MIXMIL-53-NH<sub>2</sub>(50)-Mal-Mn.



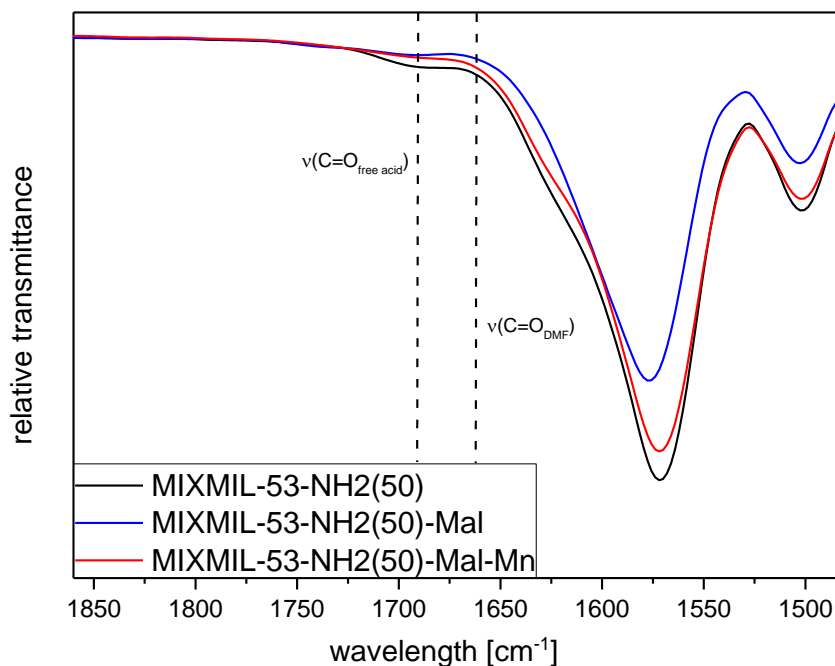


Figure 96: Zoom to expected C=O bands in the ATR-IR spectra of MIXMIL-53-NH<sub>2</sub>(50), MIXMIL-53-NH<sub>2</sub>(50)-Mal and MIXMIL-53-NH<sub>2</sub>(50)-Mal-Mn to exclude free acid or solvent molecules (DMF).

MIXMIL-53-NH<sub>2</sub>(50) (400 MHz, NaOH/D<sub>2</sub>O):  $\delta$  = 7.91 (s, 4H, CH), 7.73 (d, 1H, CH), 7.30 (d, 1H, CH), 7.22 (dd, 1H, CH) ppm.

MIXMIL-53-NH<sub>2</sub>(50)-Mal-Mn (400 MHz, D<sub>2</sub>O):  $\delta$  = 7.92 (s, 4H, CH), 7.75 (d, 1H, CH), 7.31 (s, 1H, CH), 7.23 (d, 1H, CH), 6.56 (s, 1H, CH), 6.06 (s, 1H, CH) ppm.

For AAS measurements the manganese-containing solid frameworks (20 mg) were digested in aqua regia (4 mL) and diluted with distilled water to 25 mL.

### 6.3.1.2 Catalytic test reactions\*

Catalytic test reactions were performed in a 100 mL three-necked flask equipped with a reflux condenser, magnetic stir bar, and gas inlet. The flask was charged with solvent mixture (30 mL, DMF:diethyl carbonate = 10:90),  $\alpha$ -pinene (136 mg, 1.00 mmol, 1.00 eq), catalyst (0.25 mol% Mn) and biphenyl (38.6 mg, 0.25 mmol, 0.25 eq) as internal GC standard. Then, the flask was immersed in an oil bath and kept at 130 °C under vigorous stirring (1000 rpm) for 6 h. Compressed air was continuously fed to the reaction mixture

\* The reaction screening over 24 h and the catalytic test reactions varying the temperature, oxidant flow, DMF to toluene ratio and certain concentrations (0.25, 1.50 and 2.00 mol%) were performed by Yasmin Raupp within the framework of the master thesis.<sup>[214]</sup>

through the gas inlet at 50 mL/min. Reaction temperature, catalyst concentration and flow rate were varied to establish the optimised reaction conditions. Reaction products were identified by GC-MS and quantified by GC techniques. For this, aliquots (200  $\mu$ L) were taken at regular intervals and diluted with ethyl acetate (1.50 mL).

For GC measurements system A was used (see Instrumentation, Chapter 6.2).

#### 6.3.1.2.1 Determination of conversion, yield and selectivity

To determine conversion, selectivity and yield, the gas chromatograph was calibrated. Therefore, five standard solutions containing authentic samples of starting material, products (pinene oxide, verbenone and verbenol) and an internal standard (biphenyl) were prepared and measured. Calibration curves were obtained by plotting the ratio of internal standard peak area to the mass of internal standard in the solution against the ratio of analyte peak area to the mass of analyte. The slope of the calibration lines, received by linear fit, is the response factor  $R_x$ , which takes into account the differences in the detector response between the analyte and the standard:

$$R_x = \frac{A_{is}/m_{is}}{A_x/m_x},$$

with  $A_{is}$ : peak area of the internal standard,  $A_x$ : peak area of the analyte,  $m_{is}$ : mass of the internal standard, and  $m_x$ : mass of the analyte.

Masses then were calculated using the following equation:

$$m_x = \frac{m_{is}}{A_{is}} * A_x * R_x$$

Conversion, yield and selectivity were calculated as follows:

$$conversion = \left( \frac{n_0(\alpha - \text{pinene}) - n(\alpha - \text{pinene})}{n_0(\alpha - \text{pinene})} \right) * 100$$

$$yield = \left( \frac{n(\text{product})}{n_0(\alpha - \text{pinene})} \right) * 100$$

$$selectivity = \left( \frac{yield}{conversion} \right) * 100$$

TONs were calculated using the following equation:

$$TON = \frac{n(\text{product})}{n(\text{catalyst})}$$

$$TOF = \frac{n(\text{product})}{n(\text{catalyst})} / \text{time}$$

#### 6.3.1.2.2 *Recycling experiments*

For recycling experiments, the catalyst was recovered from the reaction mixture by filtration (pore filter, por. 4) after 6 h. Then, the catalyst was washed thoroughly with diethyl carbonate and dried at room temperature. The recycled catalyst was subsequently reused for the next aerobic oxidation of  $\alpha$ -pinene, maintaining the same reaction conditions.

#### 6.3.1.2.3 *Hot filtration test*

For a hot filtration test, the catalyst was removed from the hot reaction mixture after 3 h by filtration (pore filter, por. 4) while the reaction is still ongoing for another 5 h. To follow the reaction progress, GC samples were taken hourly.

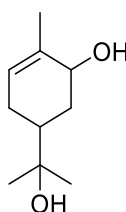
### 6.3.2 Experimental Procedures for Chapter 4.2

For ATR-IR measurements, system B was used (see Instrumentation, Chapter 6.2).

For GC measurements system B was used (see Instrumentation, Chapter 6.2).

In the  $^1\text{H}$  NMR spectra, “a” and “b” differentiates between two protons connected to the same carbon.

#### 6.3.2.1 *Sobrerol (5-(2-hydroxypropan-2-yl)-2-methylcyclohex-2-en-1-ol) via $\alpha$ -pinene oxide hydrolysis in neutral medium*



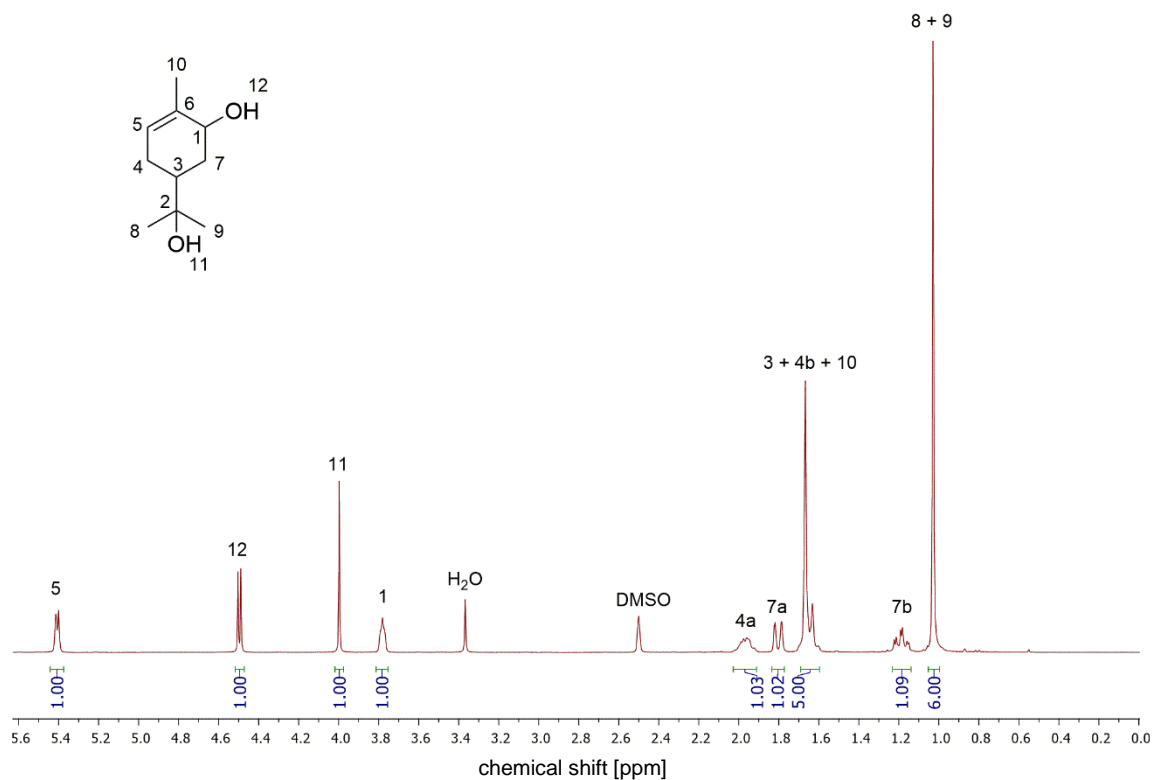
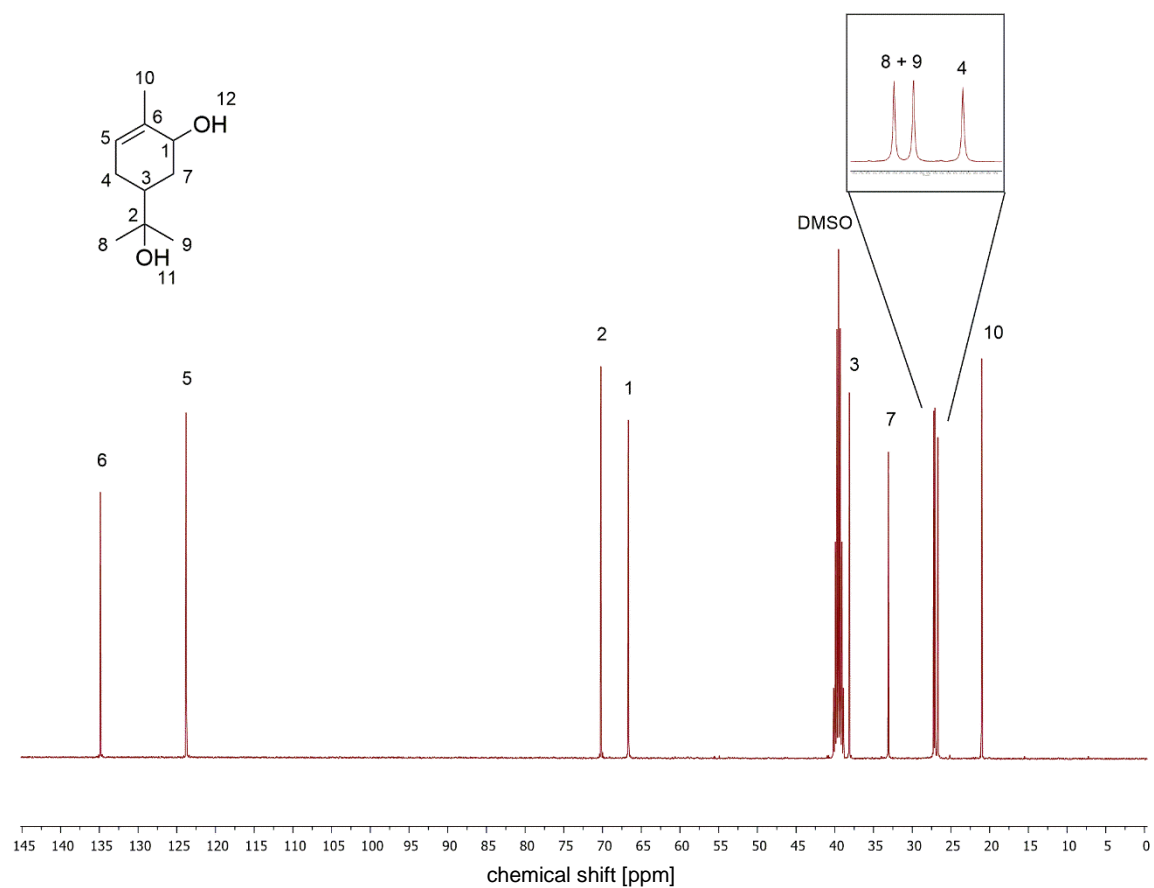
To a solution of  $\alpha$ -pinene oxide (500 mg, 3.28 mmol, 1.00 eq) in 10 mL dioxane, 2 mL water (2.00 g, 111 mmol, 33.8 eq) were added. The reaction mixture was stirred at 90 °C for 24 h and the conversion was monitored by GC. After completion of the reaction, the solvent was evaporated under reduced pressure and the residue dissolved in  $\text{CH}_2\text{Cl}_2$  and dried over sodium sulfate. The crude product was purified *via* column chromatography ( $\text{CH}_2\text{Cl}_2$ :MeOH, 30:1  $\rightarrow$  20:1). The product was obtained as white solid in a yield of 29% (160 mg, 943  $\mu\text{mol}$ ).

**$^1\text{H-NMR}$**  (DMSO- $d_6$ , 400 MHz):  $\delta$  = 5.44 – 5.38 (m, 1H,  $\text{CH}^6$ ), 4.50 (d,  $J$  = 5.8 Hz, 1H,  $\text{OH}^{12}$ ), 4.00 (s, 1H,  $\text{OH}^{11}$ ), 3.81 – 3.75 (m, 1H,  $\text{CH}^1$ ), 2.03 – 1.91 (m, 1H,  $\frac{1}{2}$   $\text{CH}_2^{4a}$ ), 1.84 – 1.77 (m, 1H,  $\frac{1}{2}$   $\text{CH}_2^{7a}$ ), 1.69 – 1.60 (m, 5H,  $\text{CH}^8$ ,  $\frac{1}{2}$   $\text{CH}_2^{4b}$ ,  $\text{CH}_3^{10}$ ), 1.24 – 1.14 (m, 1H,  $\frac{1}{2}$   $\text{CH}_2^{7b}$ ), 1.03 (s, 6H,  $\text{CH}_3^8$ ,  $\text{CH}_3^9$ ) ppm.

**$^{13}\text{C-NMR}$**  (DMSO- $d_6$ , 101 MHz):  $\delta$  (ppm) = 134.88 ( $\text{C}_q^6$ ), 123.79 ( $\text{CH}^5$ ), 70.20 ( $\text{C}_q^2$ ), 66.66 ( $\text{CH}^1$ ), 38.12 ( $\text{CH}^3$ ), 33.08 ( $\text{CH}_2^7$ ), 27.20 ( $\text{CH}_3^{8/9}$ ), 27.06 ( $\text{CH}_3^{8/9}$ ), 26.69 ( $\text{CH}_2^4$ ), 21.02 ( $\text{CH}_3^{10}$ ) ppm.

**HRMS (EI)**  $m/z$ :  $[\text{M}]^+$  calculated for  $[\text{C}_{10}\text{H}_{18}\text{O}_2]^+$ : 170.1307, found 170.1307.

**IR** (ATR platinum diamond):  $\nu/\text{cm}^{-1}$  = 3324.2, 2972.9, 2933.1, 1428.8, 1376.1, 1360.0, 1311.4, 1252.4, 1154.5, 1136.8, 1051.9, 1026.7, 984.3, 959.3, 939.4, 918.1, 861.9, 807.3, 761.5, 661.8, 612.2, 561.0, 500.4, 468.5, 421.6, 405.4.

Figure 97:  $^1\text{H}$  NMR spectrum of sobrerol.Figure 98:  $^{13}\text{C}$  NMR spectrum of sobrerol.

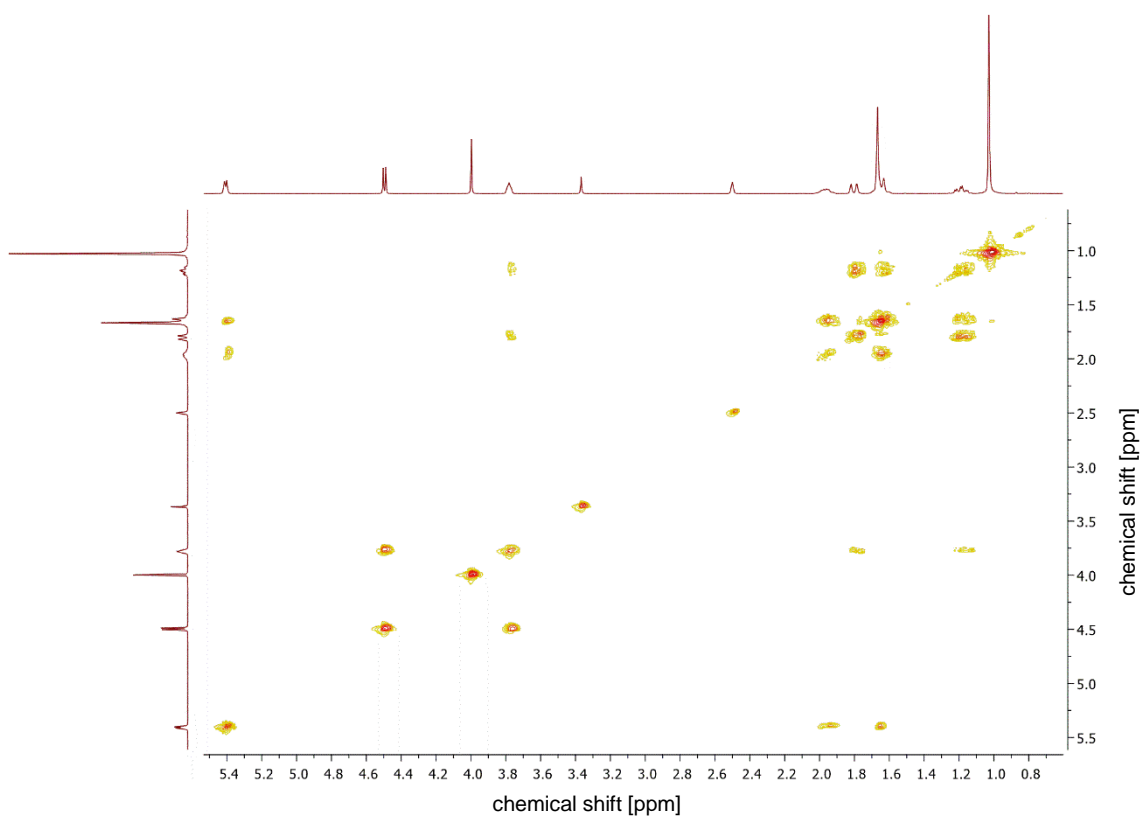


Figure 99: COSY spectrum of sobrerol.

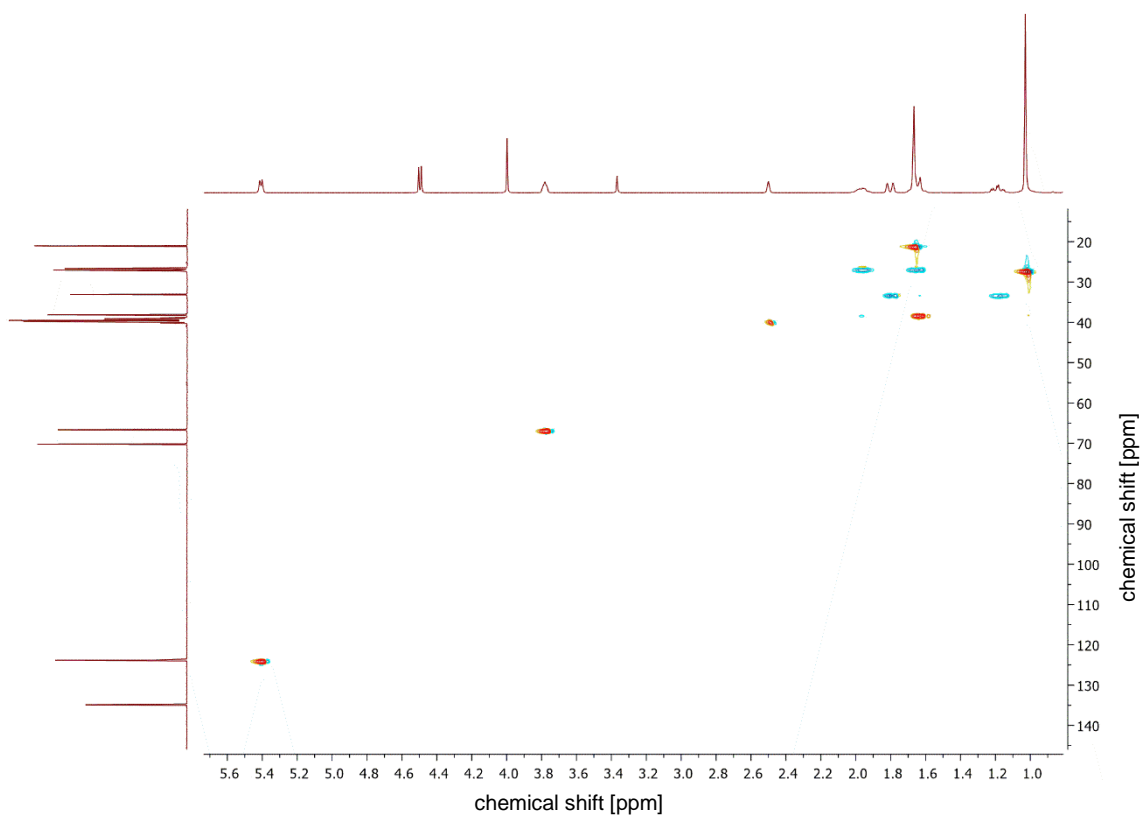


Figure 100: HSQC spectrum of sobrerol.

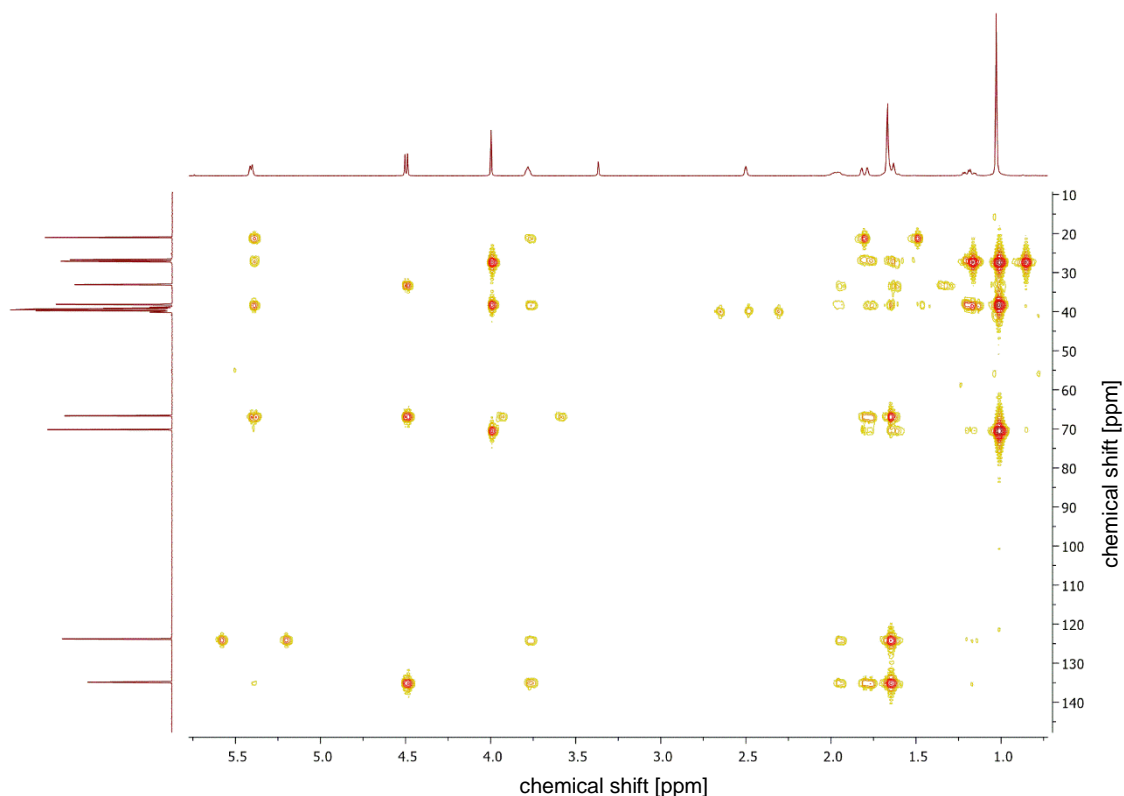
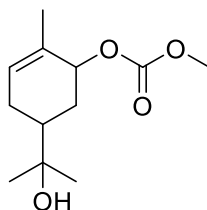


Figure 101: HMBC spectrum of sobrerol.

### 6.3.2.2 5-(2-hydroxypropan-2-yl)-2-methylcyclohex-2-en-1-yl methyl carbonate via *trans*-esterification of sobrerol



To a solution of sobrerol (50.0 mg, 294  $\mu\text{mol}$ , 1.00 eq) in 2.60 mL DMC 5 mol% TBD was added (2.04 mg, 14.7  $\mu\text{mol}$ , 0.05 eq) in a pressure tube. The reaction mixture was then heated to 60  $^{\circ}\text{C}$  for 20 h. After the reaction, DMC was evaporated under reduced pressure and the crude product was purified *via* column chromatography (cyclohexane (CH):ethyl acetate (EA), 10:1  $\rightarrow$  2:1). The product was obtained as white solid in a yield of 84% (56.4 mg, 247  $\mu\text{mol}$ ).

**$^1\text{H-NMR}$**  (DMSO- $d_6$ , 500 MHz):  $\delta$  = 5.73 – 5.68 (m, 1H,  $\text{CH}^{\beta}$ ), 4.96 (s, 1H,  $\text{CH}^{\gamma}$ ), 4.19 (b, 1H,  $\text{OH}^{\gamma}$ ), 3.69 (s, 3H,  $\text{CH}_3^{13}$ ), 2.09 – 1.97 (m, 2H,  $\frac{1}{2} \text{CH}_2^{4a}$ ,  $\frac{1}{2} \text{CH}_2^{7a}$ ), 1.77 – 1.68 (m, 1H,  $\frac{1}{2} \text{CH}_2^{4b}$ ), 1.64 (s, 3H,  $\text{CH}_3^{10}$ ), 1.55 – 1.46 (m, 1H,  $\text{CH}^{\beta}$ ), 1.40 – 1.32 (m, 1H,  $\frac{1}{2} \text{CH}_2^{7b}$ ), 1.04 (s, 1H,  $\text{CH}_3^{8/9}$ ), 1.00 (s, 1H,  $\text{CH}_3^{8/9}$ ) ppm.

<sup>13</sup>C-NMR (DMSO-d<sub>6</sub>, 126 MHz): δ = 155.29 (C<sub>q</sub><sup>12</sup>), 129.67 (C<sub>q</sub><sup>6</sup>), 128.76 (CH<sup>5</sup>), 74.76 (CH<sup>1</sup>), 69.88 (C<sub>q</sub><sup>2</sup>), 54.51 (CH<sub>3</sub><sup>13</sup>), 38.82 (CH<sup>3</sup>), 29.31 (CH<sub>2</sub><sup>7</sup>), 27.62 (CH<sub>3</sub><sup>8/9</sup>), 26.59 (CH<sub>2</sub><sup>4</sup>), 26.17 (CH<sub>3</sub><sup>8/9</sup>), 20.41 (CH<sub>3</sub><sup>10</sup>) ppm.

The NMR spectra are in accordance with the literature.<sup>[292]</sup>

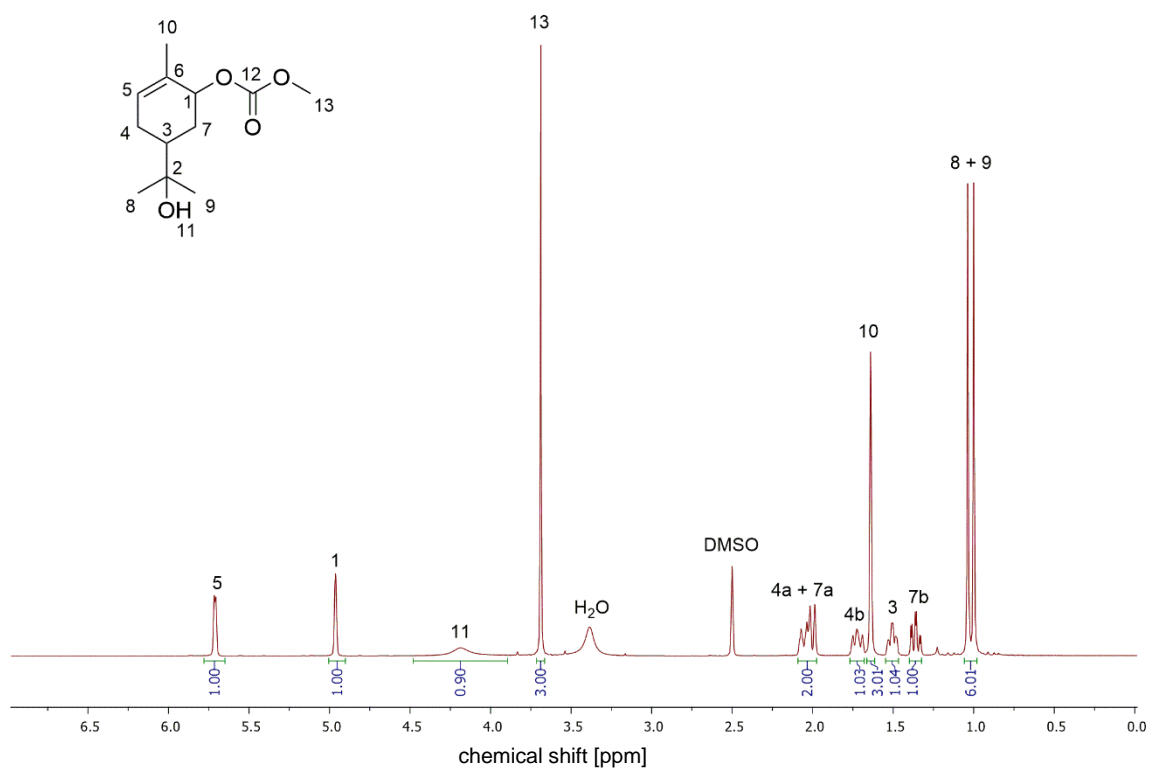


Figure 102: <sup>1</sup>H NMR spectrum of 5-(2-hydroxypropan-2-yl)-2-methylcyclohex-2-en-1-yl methyl carbonate.



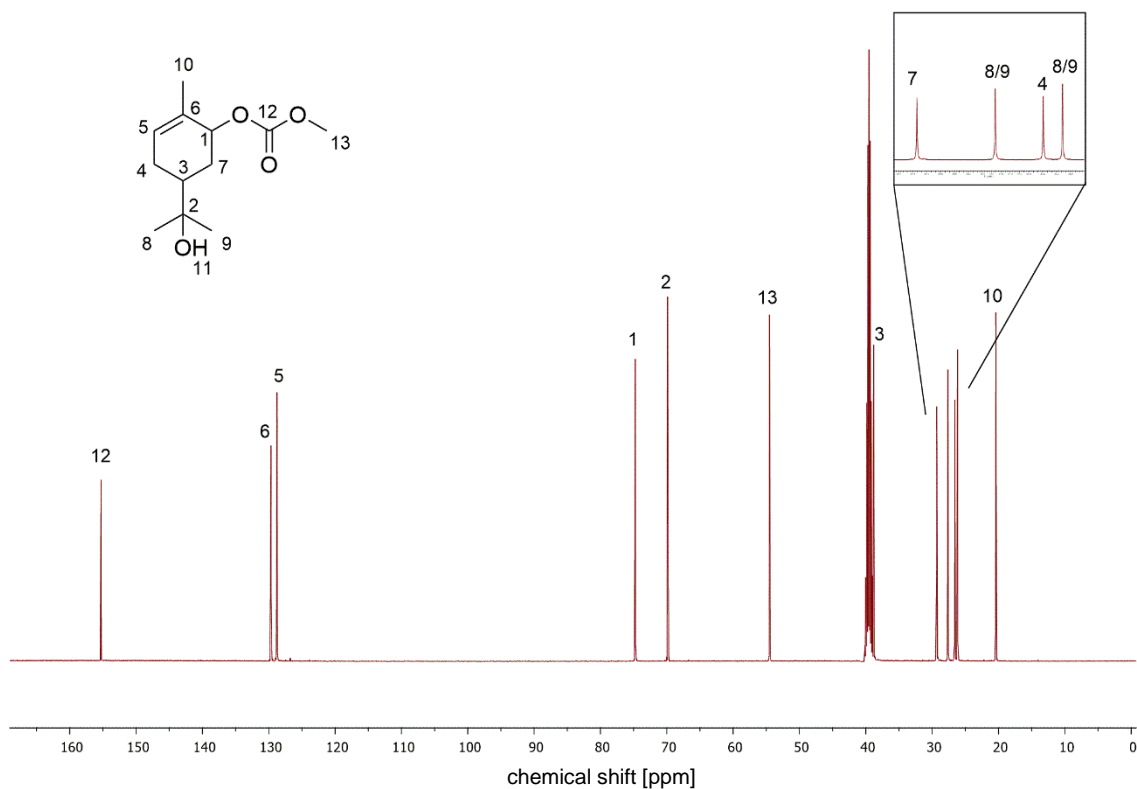


Figure 103:  $^{13}\text{C}$  NMR spectrum of 5-(2-hydroxypropan-2-yl)-2-methylcyclohex-2-en-1-yl methyl carbonate.

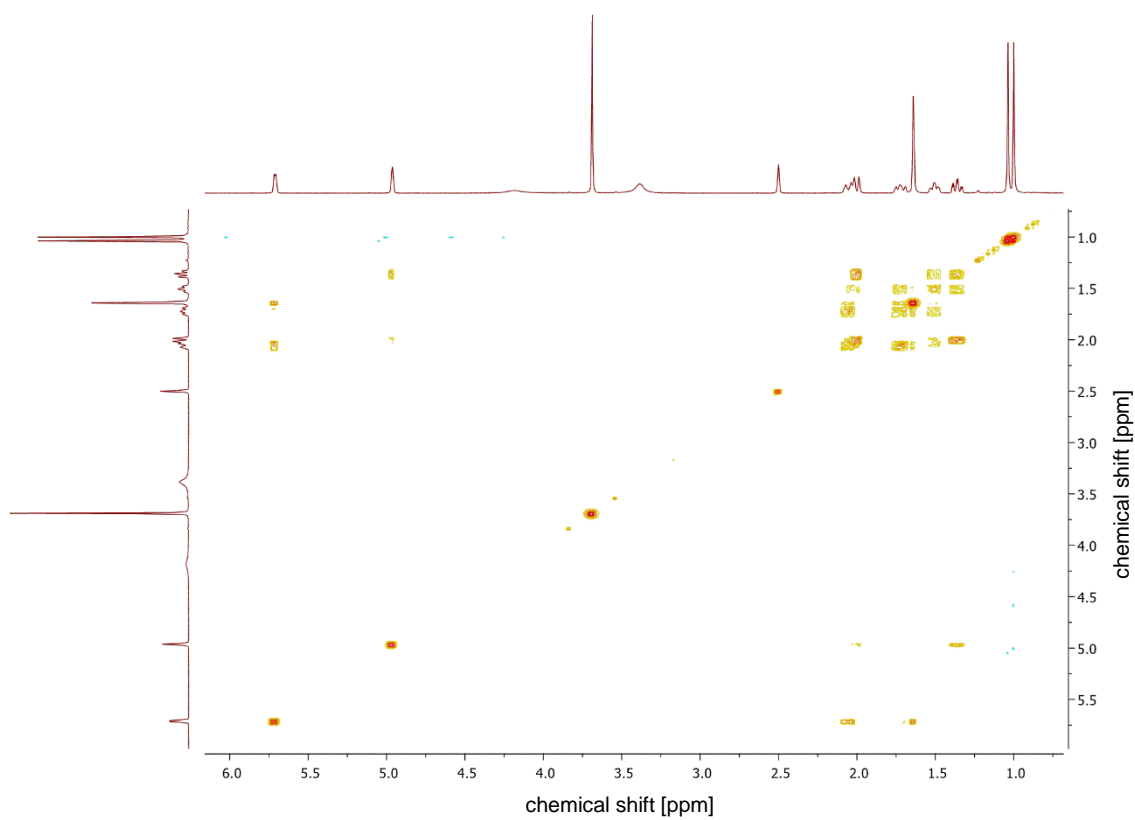


Figure 104: COSY spectrum of 5-(2-hydroxypropan-2-yl)-2-methylcyclohex-2-en-1-yl methyl carbonate.

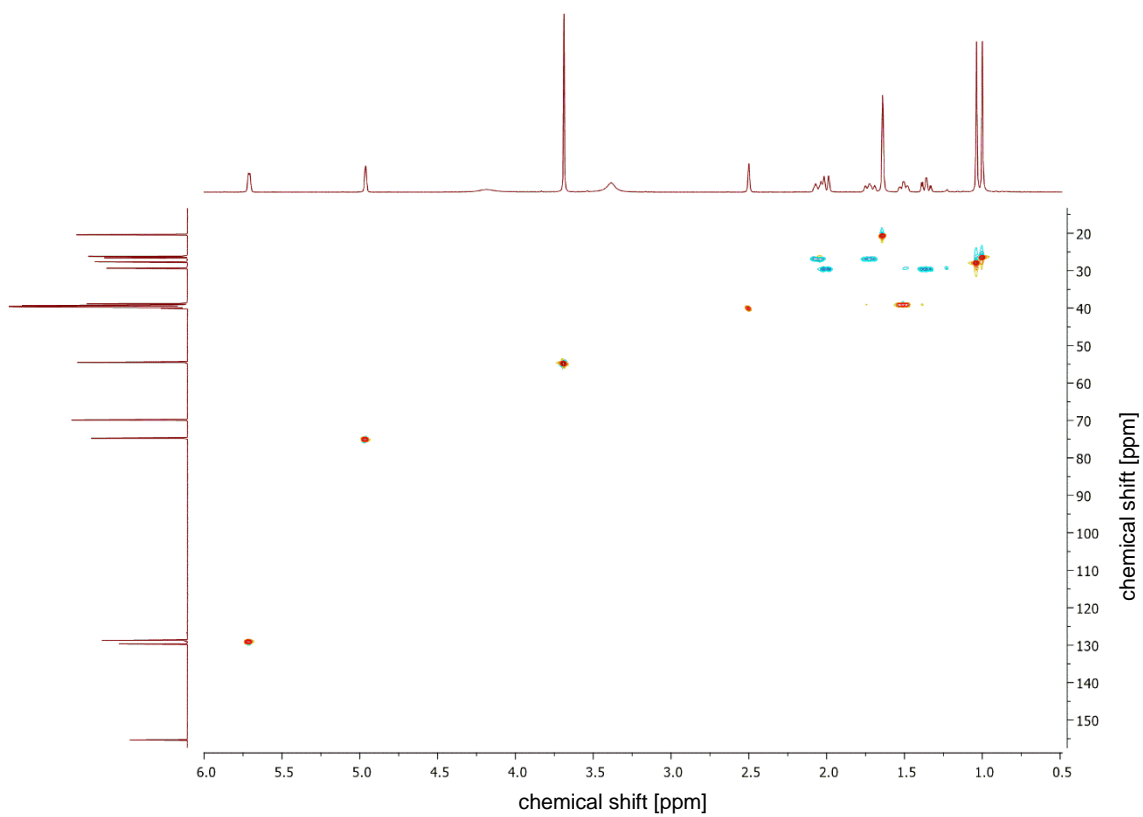


Figure 105: HSQC spectrum of 5-(2-hydroxypropan-2-yl)-2-methylcyclohex-2-en-1-yl methyl carbonate.

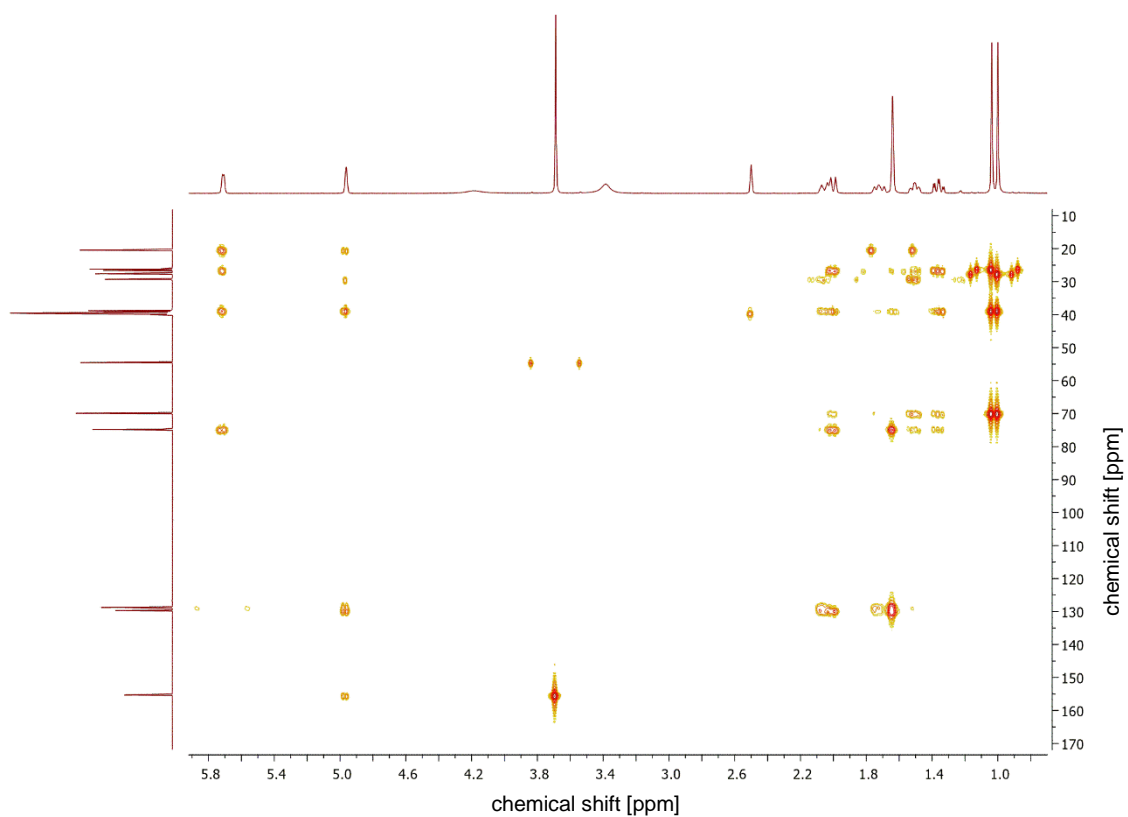
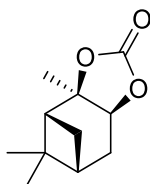


Figure 106: HMBC spectrum of 5-(2-hydroxypropan-2-yl)-2-methylcyclohex-2-en-1-yl methyl carbonate.

6.3.2.3  $\alpha$ -Pinene carbonate ((3aR,4R,6R,7aS)-3a,5,5-trimethylhexahydro-4,6-methanobenzo[d][1,3]dioxol-2-one) via transesterification of *cis*- $\alpha$ -pinanediol with DMC



In a pressure tube, *cis*- $\alpha$ -pinanediol (100 mg, 587  $\mu$ mol, 1.00 eq) and 5 mol% TBD (4.09 mg, 29.4 mmol, 0.05 eq) were dissolved in 1.18 mL DMC. The solution was heated to 60  $^{\circ}$ C for 17 h. Excess DMC was then evaporated under reduced pressure and the residue was diluted with EA. The organic phase was washed with water and dried over sodium sulfate. After evaporation of the solvent under reduced pressure, the pure product was obtained as white solid in a yield of 86% (99.1 mg, 505  $\mu$ mol).

**$^1$ H-NMR** (CDCl<sub>3</sub>, 500 MHz):  $\delta$  = 4.59 – 4.54 (m, 1H, CH<sup>f</sup>), 2.40 – 2.30 (m, 2H,  $\frac{1}{2}$  CH<sub>2</sub><sup>4a</sup>,  $\frac{1}{2}$  CH<sub>2</sub><sup>7a</sup>), 2.18 (t,  $J$  = 5.38 Hz, 1H, CH<sup>l</sup>), 2.07 – 1.96 (m, 2H,  $\frac{1}{2}$  CH<sub>2</sub><sup>4b</sup>, CH<sup>g</sup>), 1.53 (s, 3H, CH<sub>3</sub><sup>10</sup>), 1.31 (s, 3H, CH<sub>3</sub><sup>8/9</sup>), 1.25 (d,  $J$  = 11.5 Hz, 1H,  $\frac{1}{2}$  CH<sub>2</sub><sup>7b</sup>), 0.84 (s, 3H, CH<sub>3</sub><sup>8/9</sup>) ppm.

**$^{13}$ C-NMR** (CDCl<sub>3</sub>, 126 MHz):  $\delta$  = 154.51 (C<sub>q</sub><sup>11</sup>), 87.12 (C<sub>q</sub><sup>6</sup>), 77.30 (CH<sup>5</sup>), 50.16 (CH<sup>1</sup>), 38.74 – 38.72 (2C, C<sub>q</sub><sup>2</sup>, CH<sup>3</sup>), 33.33 (CH<sub>2</sub><sup>4</sup>), 26.93 (CH<sub>3</sub><sup>10</sup>), 26.78 (CH<sub>3</sub><sup>8/9</sup>), 25.96 (CH<sub>2</sub><sup>7</sup>), 23.84 (CH<sub>3</sub><sup>8/9</sup>) ppm.

**HRMS (EI)**  $m/z$ : [M]<sup>+</sup> calculated for [C<sub>11</sub>H<sub>16</sub>O<sub>3</sub>]<sup>+</sup>: 196.1099, found 196.1101.

**IR** (ATR platinum diamond):  $\nu/\text{cm}^{-1}$  = 2946.7, 1787.4, 1482.7, 1384.6, 1363.5, 1337.8, 1276.1, 1256.5, 1211.0, 1141.7, 1122.7, 1107.3, 1078.6, 1043.9, 980.7, 932.9, 908.3, 865.8, 770.3, 700.0, 602.4, 523.9, 460.1.

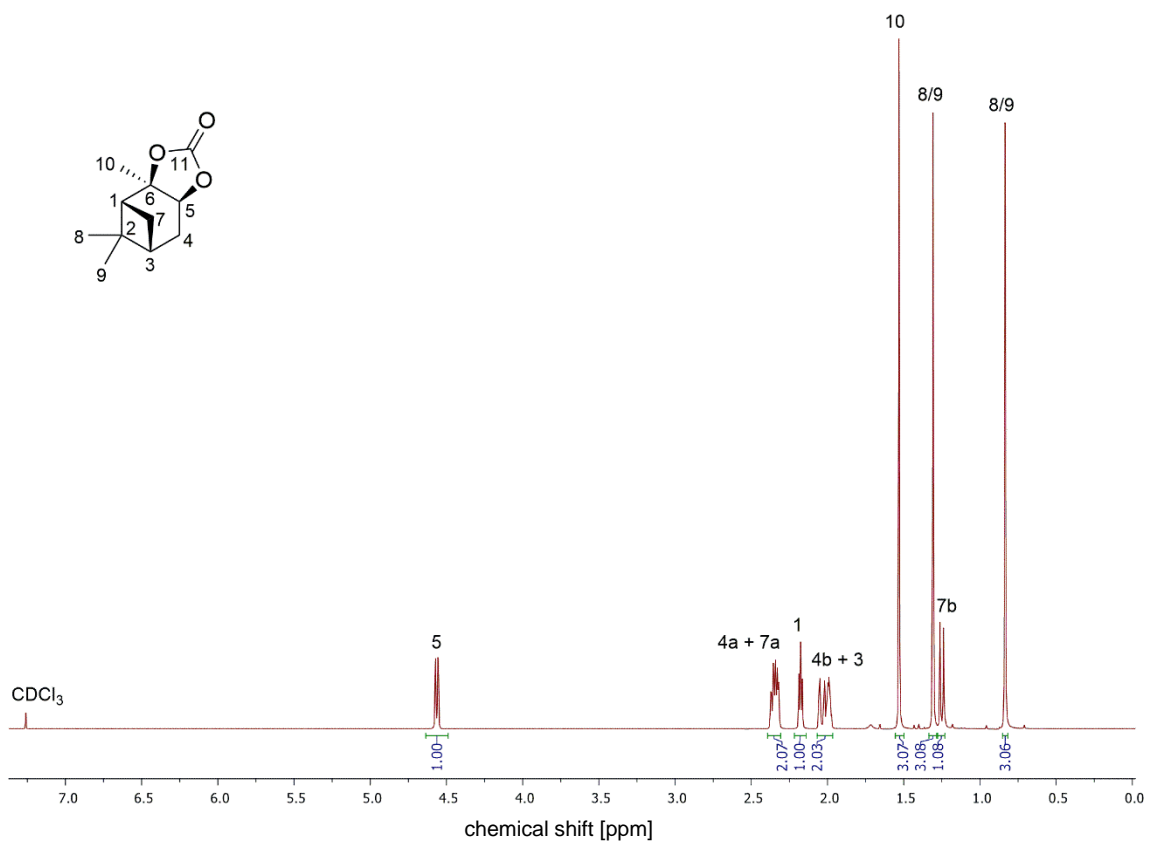


Figure 107:  $^1\text{H}$  NMR spectrum of  $\alpha$ -pinene carbonate.

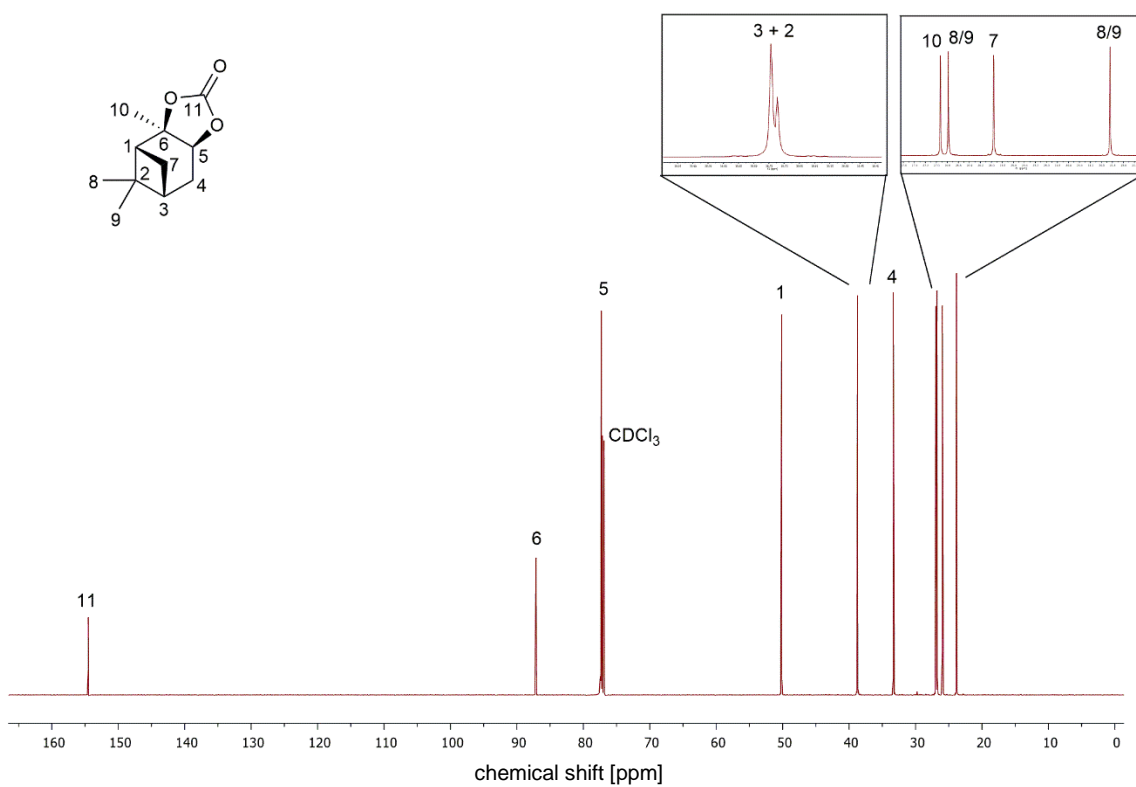


Figure 108:  $^{13}\text{C}$  NMR spectrum of  $\alpha$ -pinene carbonate.

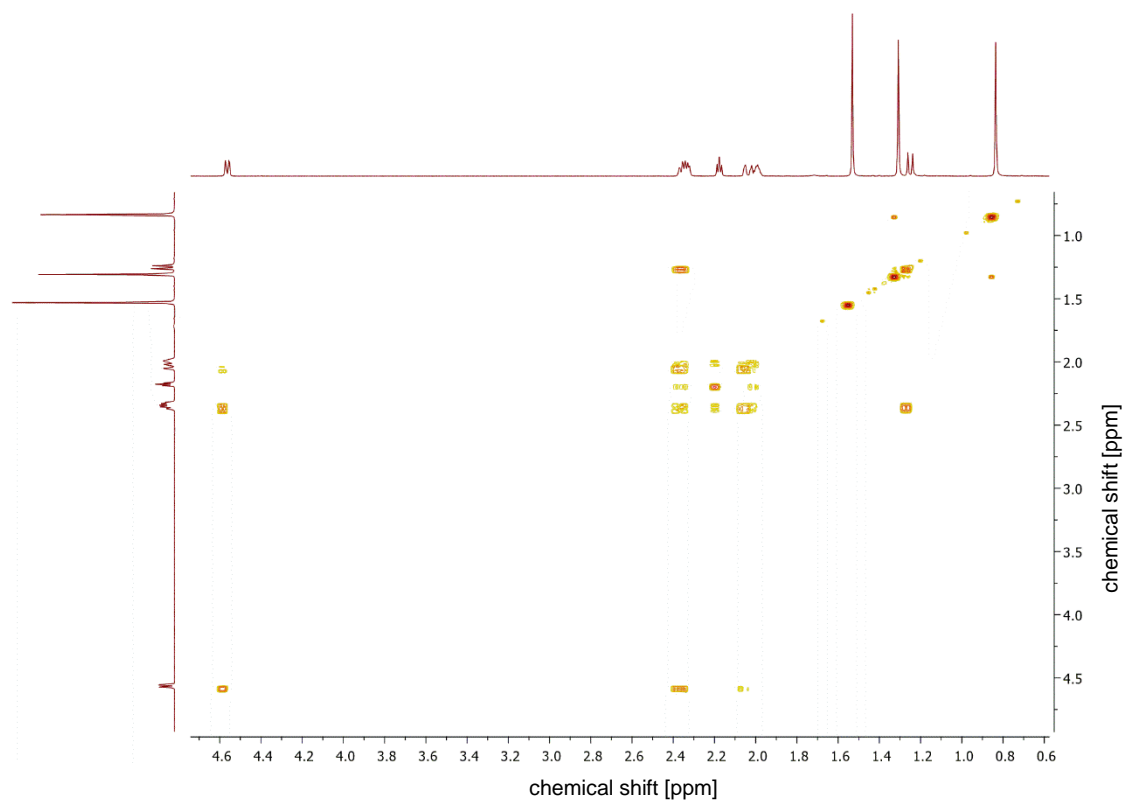


Figure 109: COSY spectrum of  $\alpha$ -pinene carbonate.

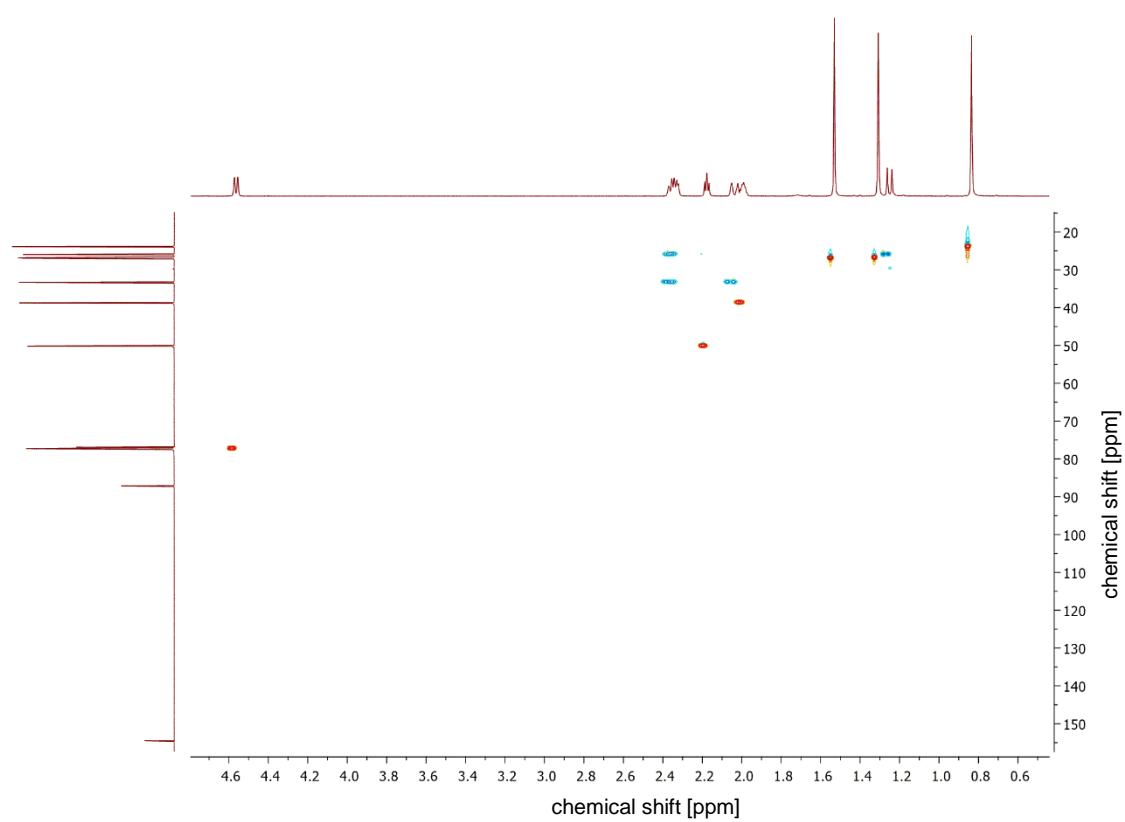


Figure 110: HSQC spectrum of  $\alpha$ -pinene carbonate.

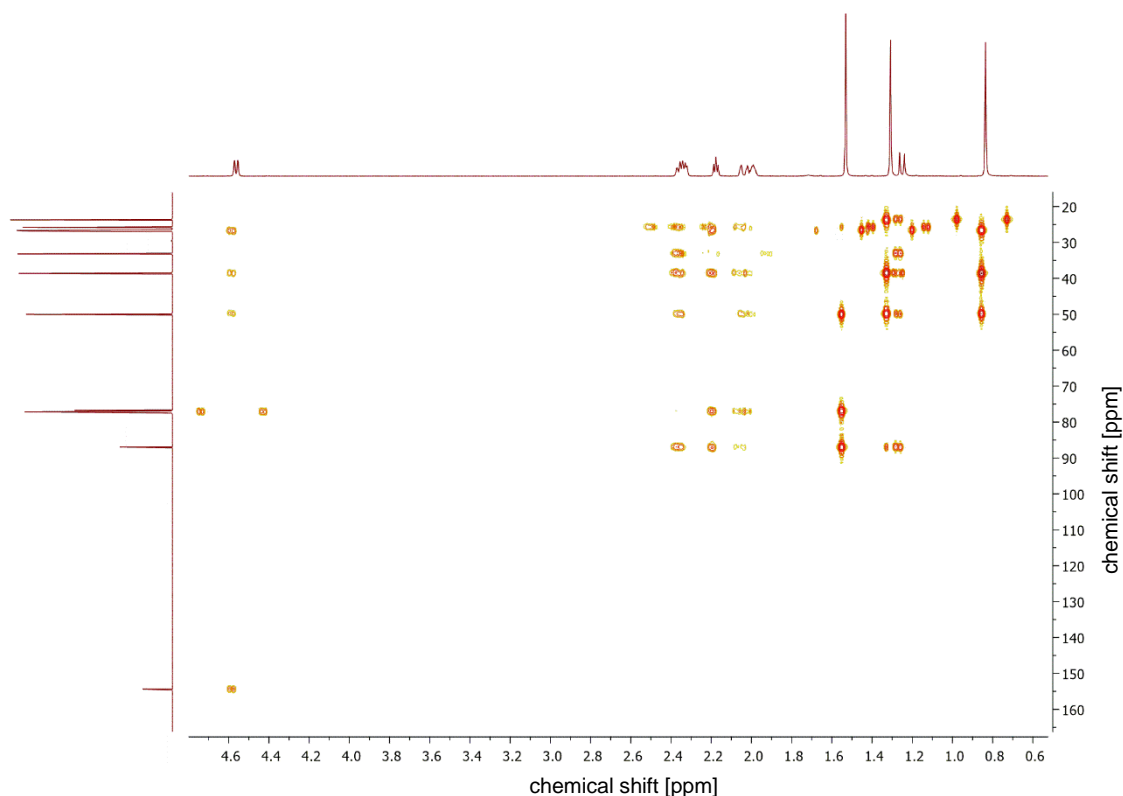
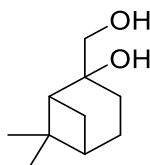


Figure 111: HMBC spectrum of  $\alpha$ -pinene carbonate.

6.3.2.4  $\beta$ -Pinanediol (2-(hydroxymethyl)-6,6-dimethylbicyclo[3.1.1]heptan-2-ol) via MTO-catalysed epoxidation of  $\beta$ -pinene followed by the MTO-catalysed epoxide ring-opening reaction with water\*



The epoxidation of  $\beta$ -pinene followed by *in situ* ring-opening was carried out, analogous to literature.<sup>[277]</sup>

For the preparation of an oxidation solution  $\text{H}_2\text{O}_2$  (30 wt%, 9 mL, 9.99 g, 88.1 mmol, 8.81 eq) was mixed with *tert*-butanol (30 mL) and magnesium sulfate (anhydrous, 6.00 g). The mixture was heated to 30 °C for 2.5 h, filtered and cooled to 5 °C. After MTO (20.0 mg, 80.0  $\mu\text{mol}$ , 0.00800 eq) was dissolved in the oxidation solution,  $\beta$ -pinene was added and the reaction was allowed to heat up to room temperature (1.36 g, 10.0 mmol, 1.00 eq) over night. Then, manganese(IV) oxide was added followed by filtration of the suspension and evaporation of the solvent at reduced pressure. The crude product was purified *via* column

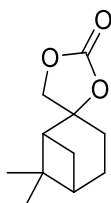
\* The synthesis was carried out by B. Sc. Helene Niess under the lab-supervision of Yasmin Raupp.

chromatography (CH<sub>2</sub>Cl<sub>2</sub>:MeOH, 50:1). Since column chromatography resulted in mixed fractions, the fraction containing two species (a and b) from which one is the desired diol, as verified *via* <sup>13</sup>C NMR, is directly used for the subsequent transesterification with diallyl carbonate (see Chapter 6.3.2.5).

<sup>13</sup>C-NMR (CDCl<sub>3</sub>, 100 MHz): δ = 78.19 (a), 75.58 (b), 69.12 (b), 62.81 (a), 54.88 (a), 48.27 (b), 47.20 (a), 40.56 (b), 38.61 (a), 37.62 (b), 36.28 (a), 30.50 (a), 27.58 (b), 27.00 (b), 26.80 (b), 25.38 (a), 24.68 (b), 23.30 (b), 20.71 (a), 20.19 (a) ppm.

The <sup>13</sup>C-NMR signals of species b are in accordance with the literature.<sup>[279]</sup>

#### 6.3.2.5 β-Pinene carbonate (6,6-dimethylspiro[bicyclo[3.1.1]heptane-2,4'-[1,3]dioxolan]-2'-one) *via* transesterification of β-pinenediol with diallyl carbonate\*



50.0 mg of the mixed fraction of β-pinenediol and another unidentified species obtained from the MTO-catalysed epoxidation and *in situ* ring-opening of β-pinene (see Chapter 6.3.2.4) was dissolved in diallyl carbonate (2.50 mL) and TBD (2.01 mg) was added. The solution was heated to 60 °C at 300 mbar for 7 h. Excess diallyl carbonate was then evaporated under reduced pressure and the residue was purified *via* column chromatography (CH/EA, 1:1) to obtain the pure product as white solid (27.9 mg, 0.142 mmol).

<sup>1</sup>H-NMR (DMSO-d<sub>6</sub>, 500 MHz): δ = 4.39 (2d, *J* = 8.5 Hz, *J* = 8.5 Hz, 2H, CH<sub>2</sub><sup>10</sup>), 2.30 – 2.09 (m, 4H, ½ CH<sub>2</sub><sup>7a</sup>, CH<sup>4</sup>, CH<sub>2</sub><sup>6</sup>), 1.96 – 1.85 (m, 2H, CH<sup>4</sup>, ½ CH<sub>2</sub><sup>5a</sup>), 1.79-1.68 (m, 1H, ½ CH<sub>2</sub><sup>5b</sup>), 1.36 (d, *J* = 10.2 Hz, 1H, ½ CH<sub>2</sub><sup>7b</sup>), 1.23 (s, 3H, CH<sub>3</sub><sup>8/9</sup>), 0.81 (s, 3H, CH<sub>3</sub><sup>8/9</sup>) ppm.

<sup>13</sup>C-NMR (DMSO-d<sub>6</sub>, 126 MHz): δ = 153.91 (C<sub>q</sub><sup>11</sup>), 88.74 (C<sub>q</sub><sup>1</sup>), 75.77 (CH<sub>2</sub><sup>10</sup>), 49.39 (CH<sup>2</sup>), 39.14 (CH<sup>4</sup>), 37.91 (C<sub>q</sub><sup>3</sup>), 27.66 (CH<sub>2</sub><sup>6</sup>), 26.19 (CH<sub>3</sub><sup>8/9</sup>), 25.26 (CH<sub>2</sub><sup>7</sup>), 22.86 (CH<sub>2</sub><sup>5</sup>), 21.89 (CH<sub>3</sub><sup>8/9</sup>) ppm.

Further characterisation data can be found in the literature.<sup>[270]</sup>

\* The synthesis was carried out by B. Sc. Helene Niess under the lab-supervision of Yasmin Raupp.

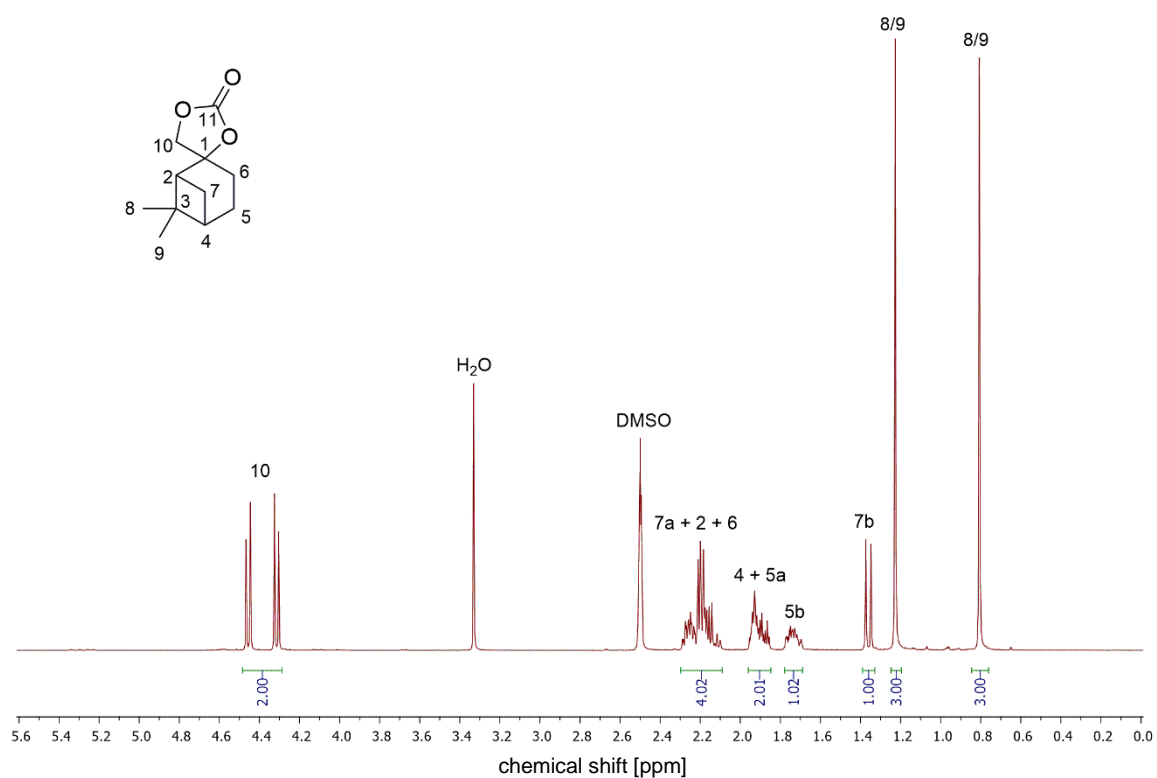


Figure 112:  $^1\text{H}$  NMR spectrum of  $\beta$ -pinene carbonate.

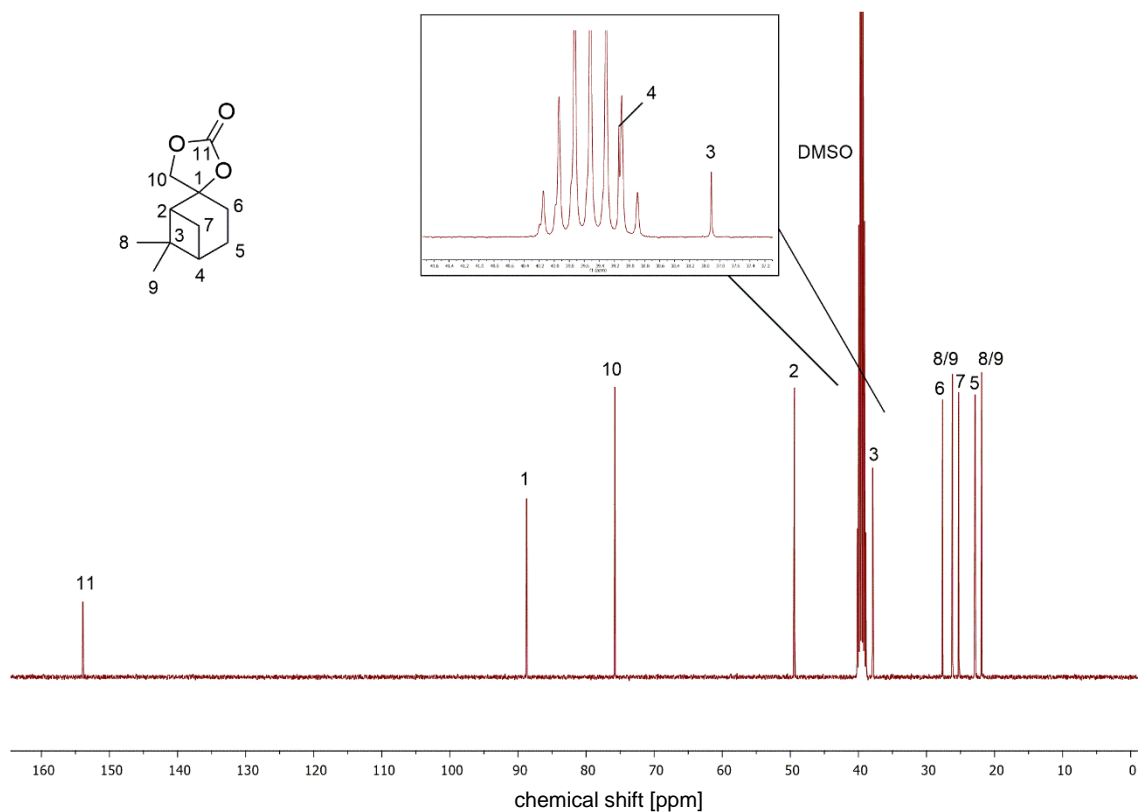


Figure 113:  $^{13}\text{C}$  NMR spectrum of  $\beta$ -pinene carbonate.



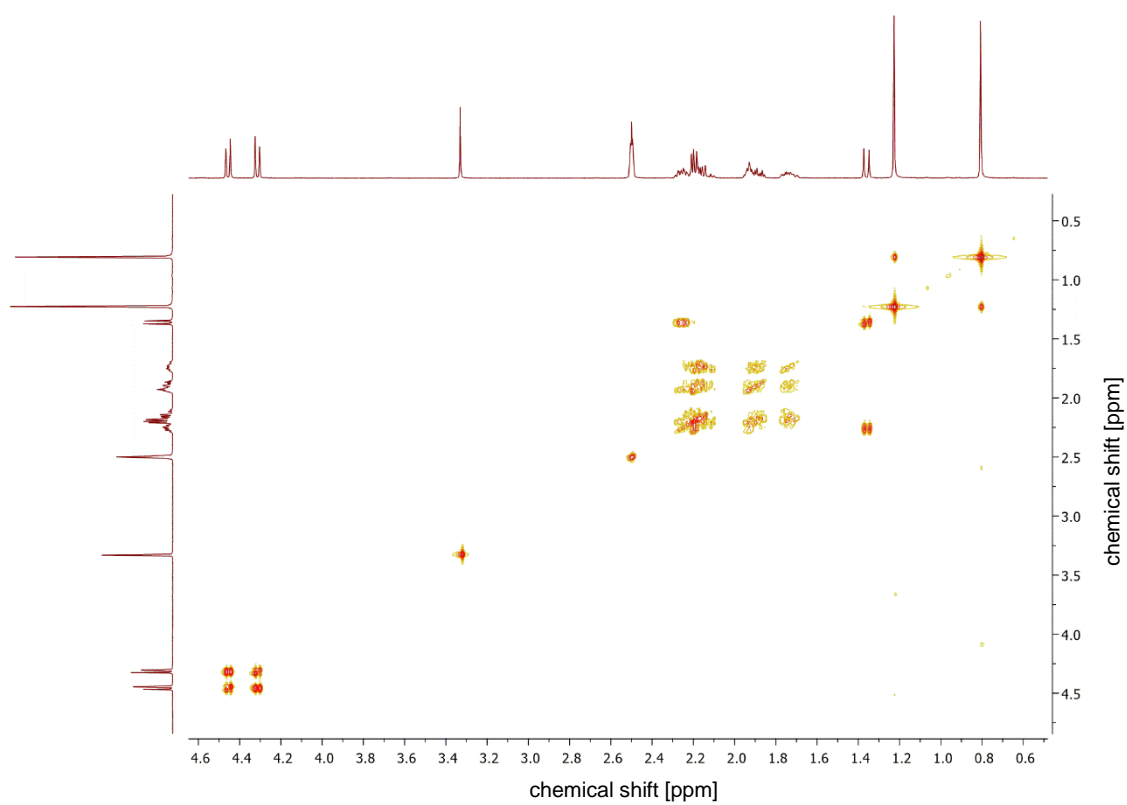


Figure 114: COSY spectrum of  $\beta$ -pinene carbonate.

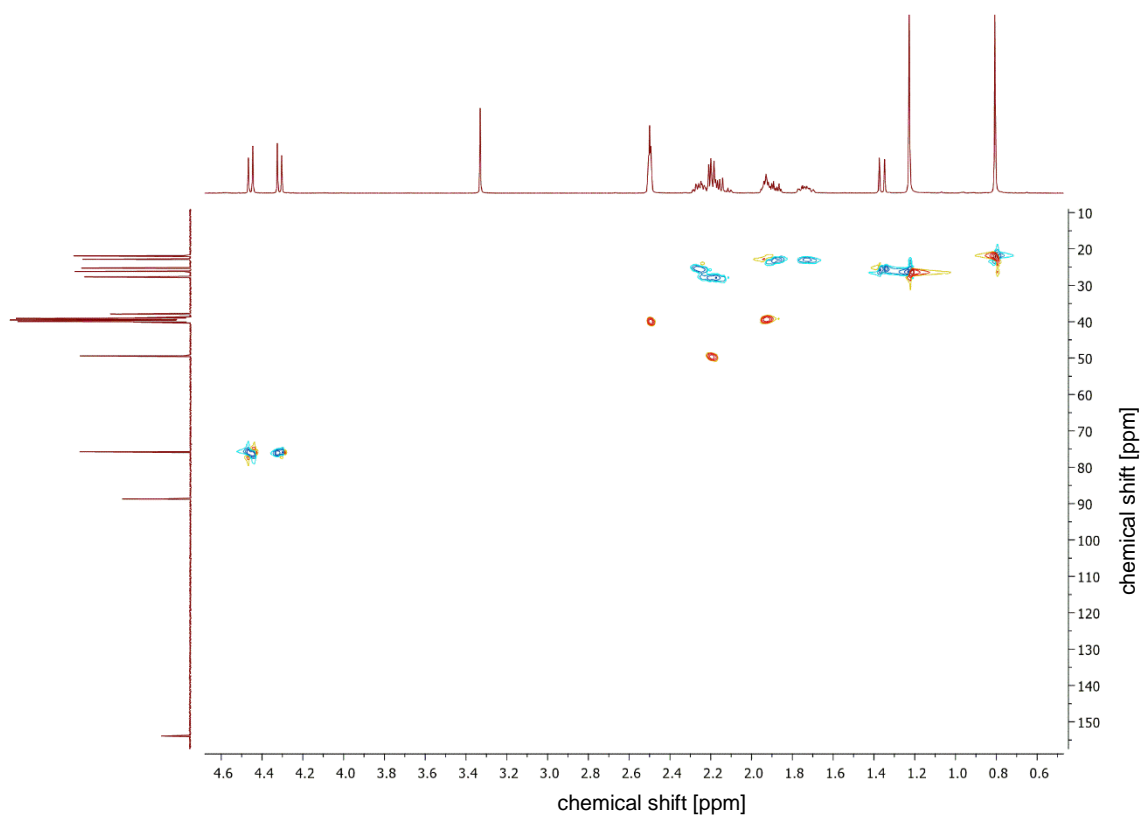


Figure 115: HSQC spectrum of  $\beta$ -pinene carbonate.

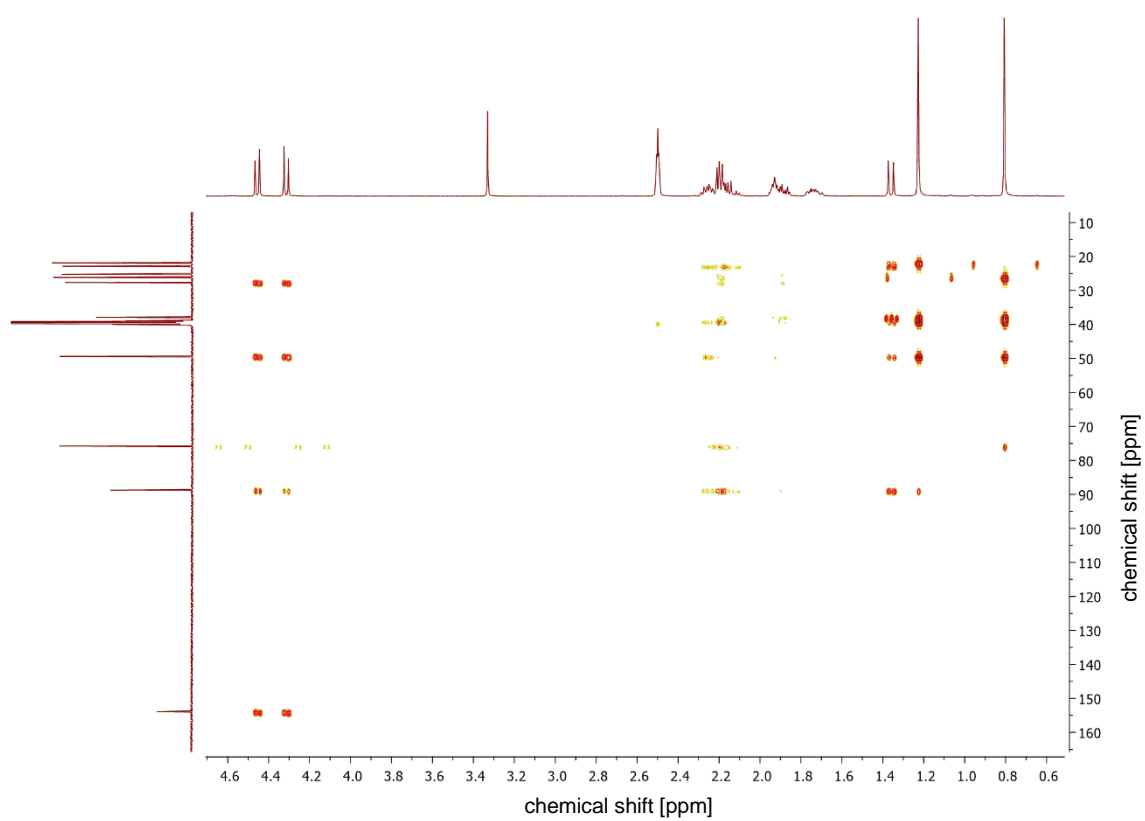
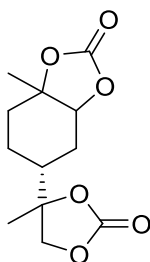


Figure 116: HMBC spectrum of  $\beta$ -pinene carbonate.

### 6.3.3 Experimental Procedures for Chapter 4.3

In the  $^1\text{H}$  NMR spectra, “a” and “b” differentiates between two protons connected to the same carbon.

#### 6.3.3.1 Cyclic limonene dicarbonate (LC, (6*R*)-3*a*-methyl-6-((*R*)-4-methyl-2-oxo-1,3-dioxolan-4-yl)hexahydrobenzo[*d*][1,3]dioxol-2-one) via coupling of $\text{CO}_2$ and limonene dioxide



The carbonation of limonene dioxide was carried out, analogous to literature.<sup>[210]</sup>

A stainless-steel reactor with Teflon inset was charged with limonene dioxide (100 g, 0.594 mol, 1.00 eq), TBAB (2 wt%, 2.00 g, 6.20 mmol, 0.01 eq) and 30 bar  $\text{CO}_2$  pressure. The reaction mixture was stirred and heated to 140 °C for 4 d. After completion of the reaction and cooling to room temperature, the viscous liquid was diluted with EA (33 mL) and triethylamine was added (76 mL). The crude reaction mixture was allowed to crystallise for 72 h before the white precipitate was filtered from the mother liquor and washed with small amounts of EA. The product was obtained as white solid in a yield of 5% (7.35 g, 28.7 mmol).

**$^1\text{H-NMR}$**  ( $\text{CDCl}_3$ , 400 MHz):  $\delta$  = 4.42 – 4.35 (m, 1H,  $\text{CH}^6$ ), 4.18 (2d,  $J$  = 8.7 Hz,  $J$  = 8.7 Hz, 2H,  $\text{CH}_2^{10}$ ), 2.39 – 2.30 (m, 1H,  $\frac{1}{2}$   $\text{CH}_2^{1a}$ ), 2.17 – 2.08 (m, 1H,  $\frac{1}{2}$   $\text{CH}_2^{4a}$ ), 1.84 – 1.71 (m, 2H,  $\frac{1}{2}$   $\text{CH}_2^{2a}$ ,  $\text{CH}^8$ ), 1.68 – 1.58 (m, 1H,  $\frac{1}{2}$   $\text{CH}_2^{1b}$ ), 1.47 (s, 3H,  $\text{CH}_3^{8/9}$ ), 1.46 (s, 3H,  $\text{CH}_3^{8/9}$ ), 1.45 – 1.28 (m, 2H,  $\frac{1}{2}$   $\text{CH}_2^{2b}$ ,  $\frac{1}{2}$   $\text{CH}_2^{4b}$ ) ppm.

**$^{13}\text{C-NMR}$**  ( $\text{CDCl}_3$ , 126 MHz):  $\delta$  = 154.20 ( $\text{C}_q^{11/12}$ ), 154.14 ( $\text{C}_q^{11/12}$ ), 84.75 ( $\text{C}_q^7$ ), 82.07 ( $\text{C}_q^6$ ), 79.57 ( $\text{CH}^5$ ), 73.06 ( $\text{CH}_2^{10}$ ), 40.69 ( $\text{CH}^3$ ), 32.49 ( $\text{CH}_2^1$ ), 29.08 ( $\text{CH}_2^4$ ), 26.05 ( $\text{CH}_3^9$ ), 21.43 ( $\text{CH}_3^8$ ), 20.79 ( $\text{CH}_2^2$ ) ppm.

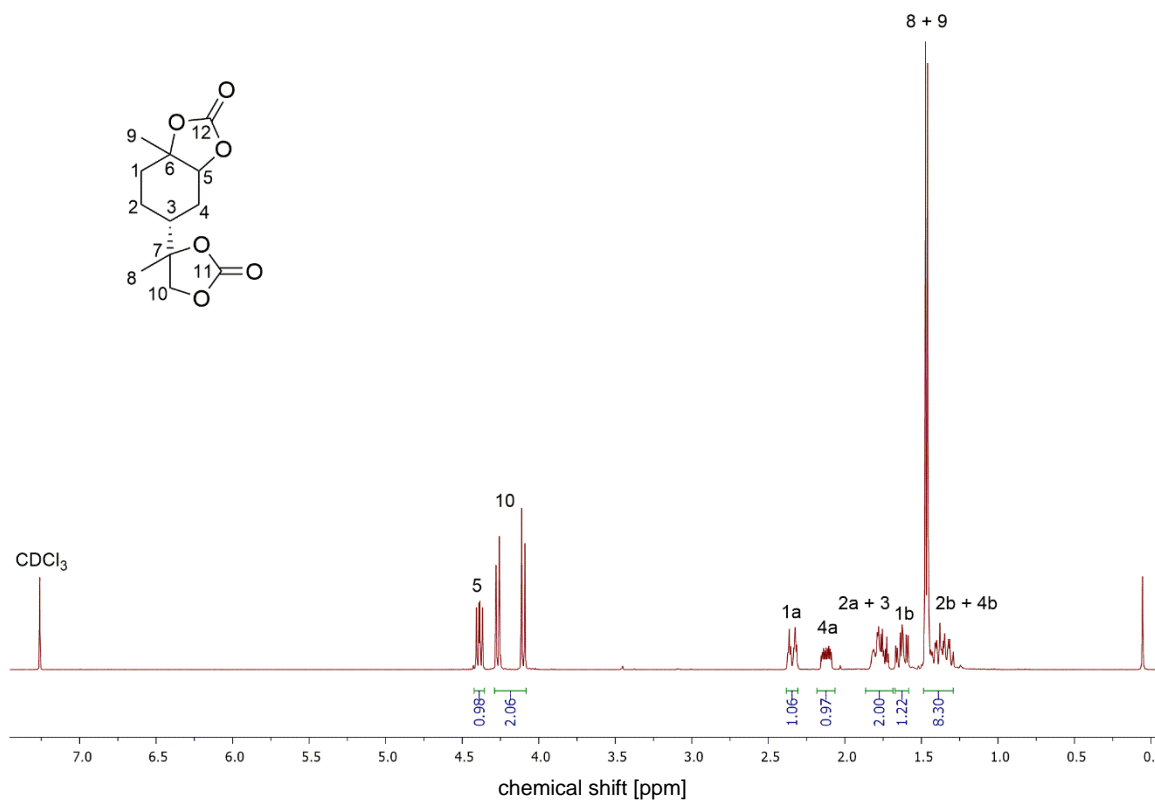


Figure 117:  $^1\text{H}$  NMR spectrum of cyclic limonene dicarbonate.

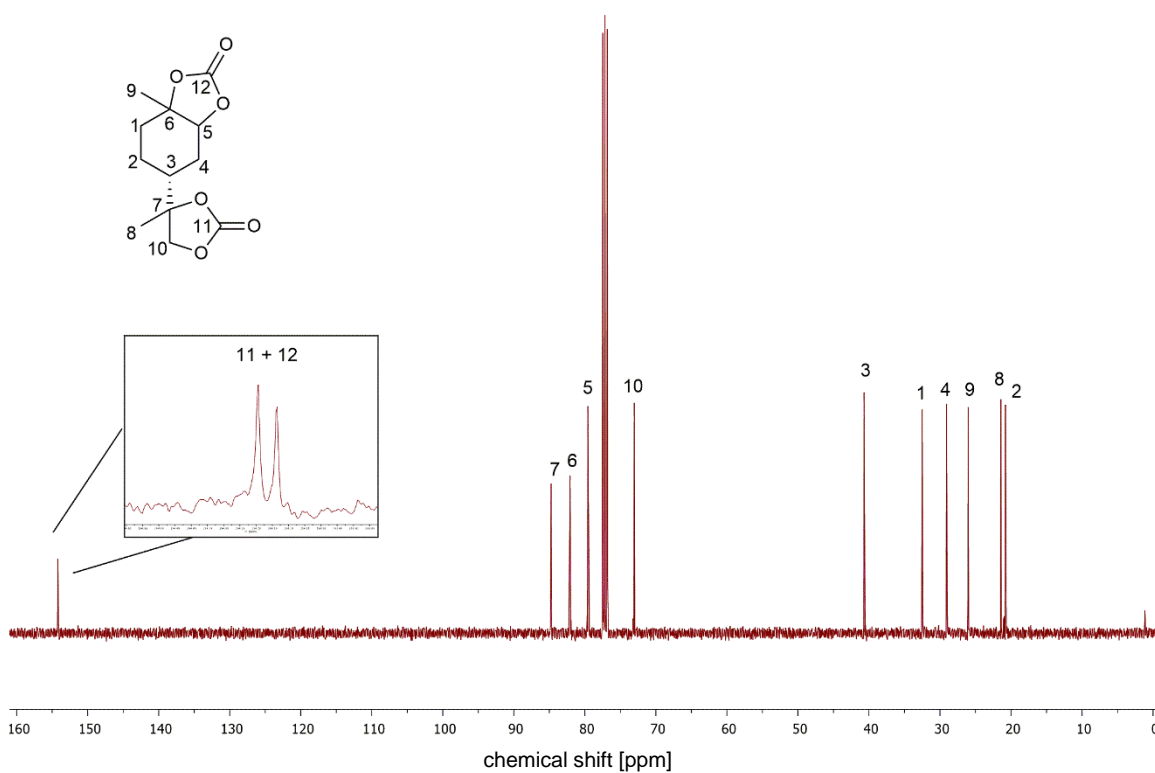


Figure 118:  $^{13}\text{C}$  NMR spectrum of cyclic limonene dicarbonate.

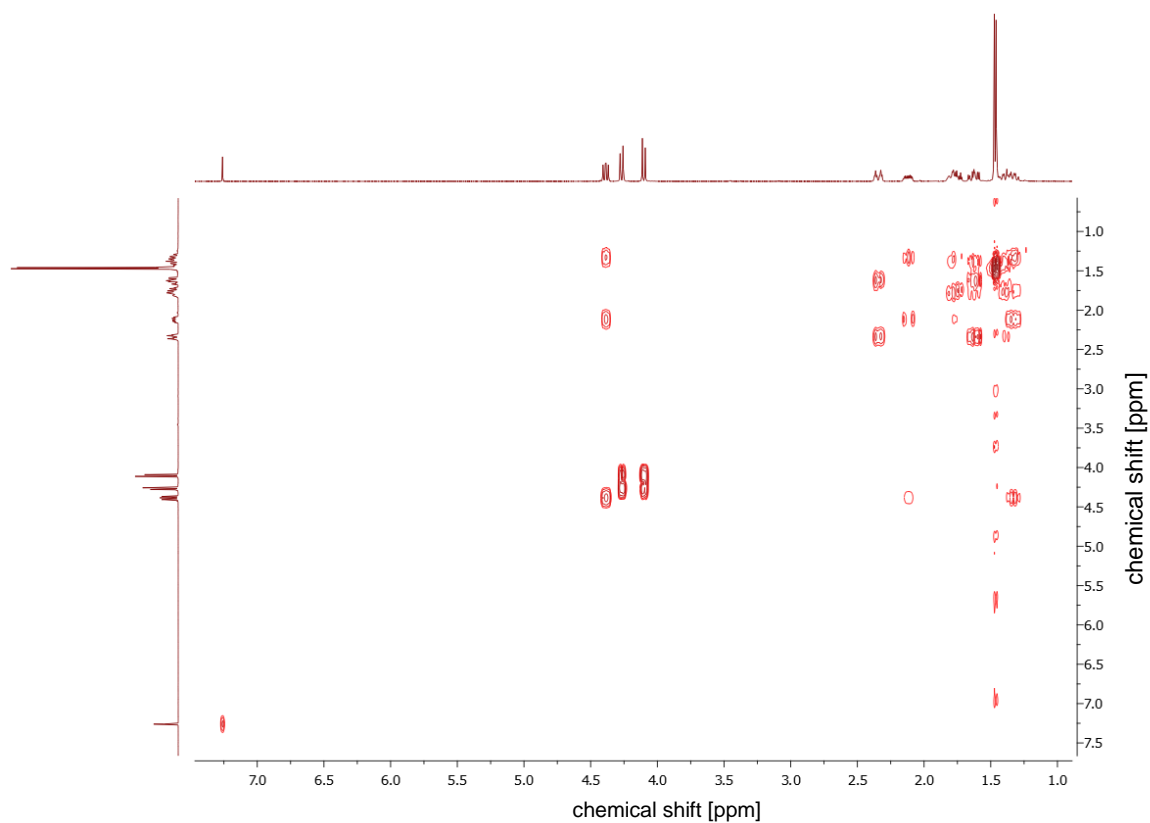


Figure 119: COSY spectrum of cyclic limonene dicarbonate.

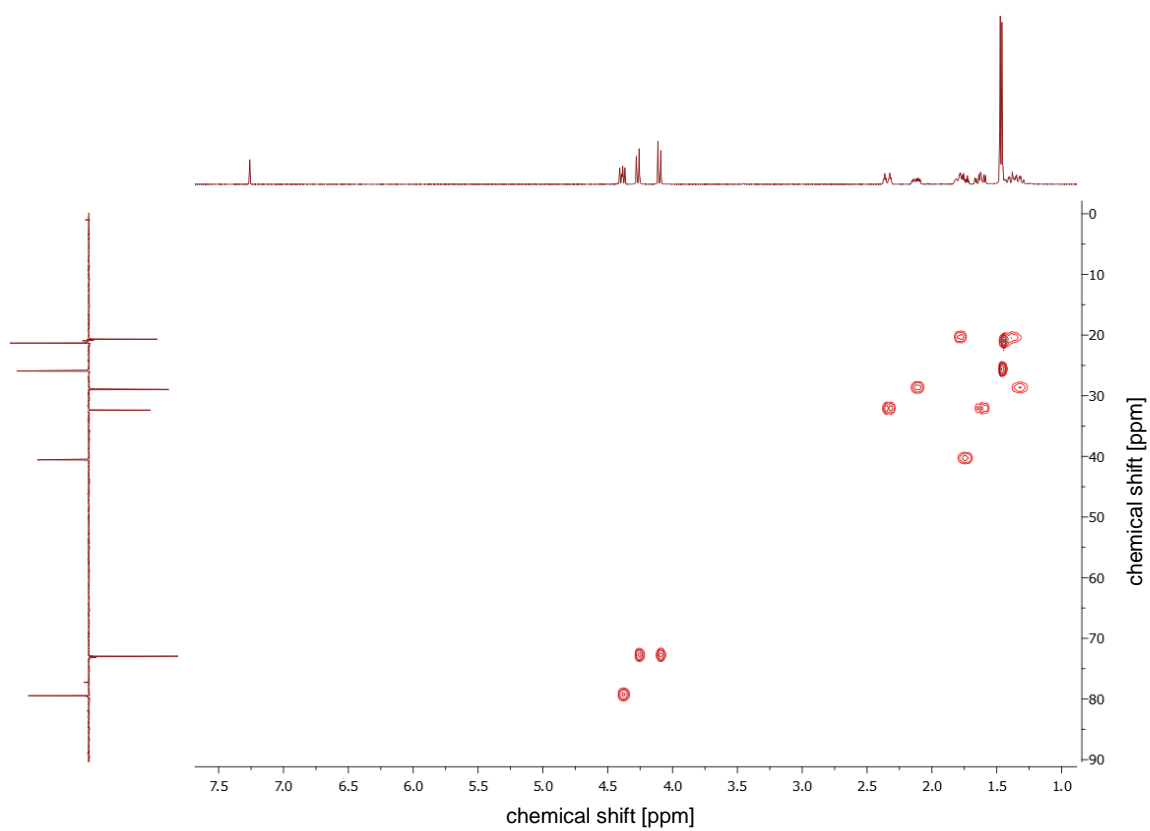


Figure 120: HSQC spectrum of cyclic limonene dicarbonate.

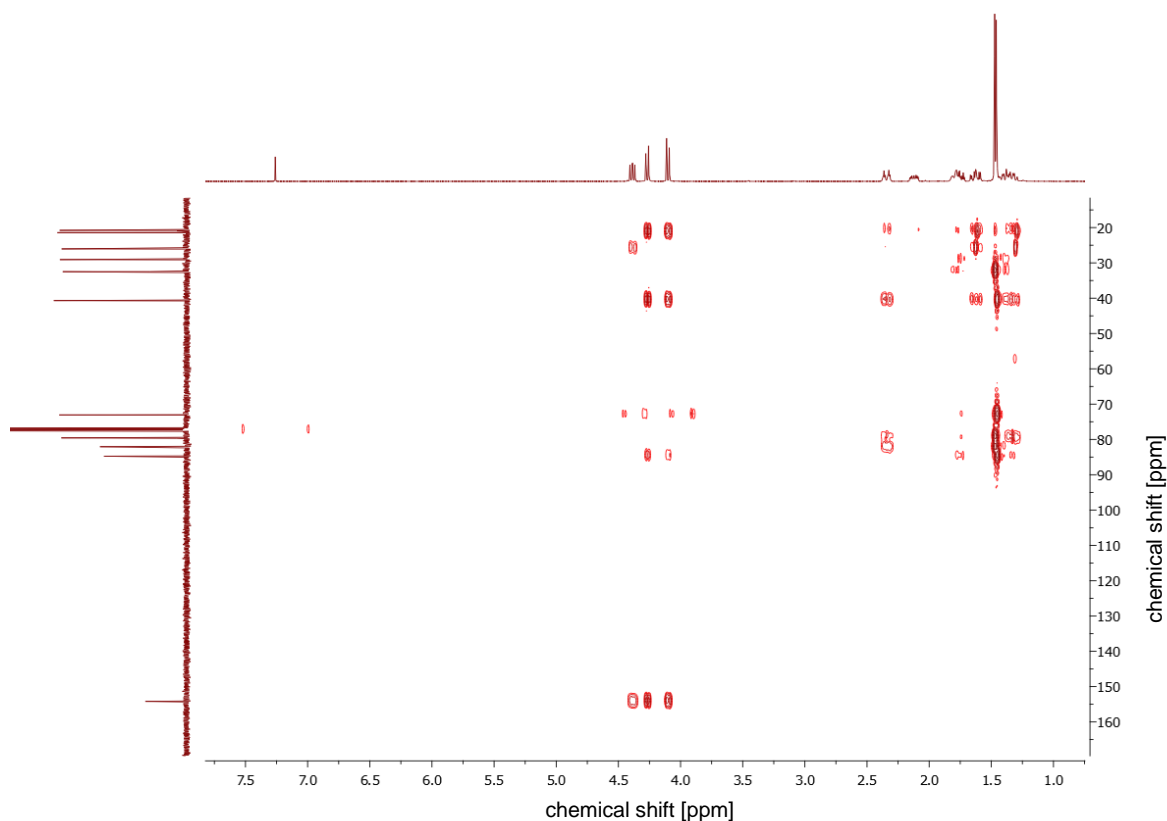
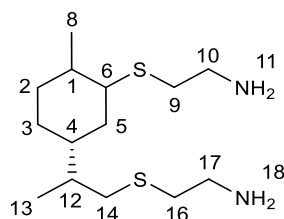


Figure 121: HMBC spectrum of cyclic limonene dicarbonate.

### 6.3.3.2 Limonene-based diamine (2-(((2R)-2-((1R)-3-((2-aminoethyl)thio)-4-methylcyclohexyl)propyl)thio)ethan-1-amine) via thiol ene reaction with cysteamine hydrochloride



The thiol ene reaction of limonene and cysteamine hydrochloride was carried out, analogous to literature.<sup>[168]</sup>

Cysteamine hydrochloride (2.50 g, 22.0 mmol, 3.00 eq) was dissolved in EtOH (30 mL). Then, (*R*)-(+)-limonene (1.00 g, 7.34 mmol, 1.00 eq) and 2,2-dimethoxy-2-phenylacetophenon (DMPA, 94.1 mg, 367  $\mu$ mol, 0.05 eq) were added. The mixture was exposed to a hand-held UV-lamp ( $2 \times 4$  W,  $\lambda = 365$  nm) for 20 h. Then, the solvent was removed under reduced pressure and the mixture was dissolved in dichloromethane. The solution was washed with a  $K_2CO_3$  solution until the pH became 10 and then washed two times with water. The organic layer was dried over anhydrous  $Na_2SO_4$  and the solvent was removed under reduced pressure. The crude product was purified *via* column

chromatography (MeOH:EA, 1:1 → 100% MeOH, TLC was stained with ninhydrin solution in EtOH) to obtain the pure product as yellow viscous liquid in a yield of 56% (1.19 g, 4.11 mmol).

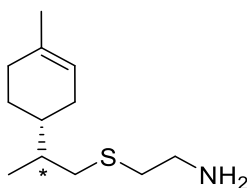
When possible, "A, B, C or D" is used to differentiate between different diastereomers. The two major diastereomers are marked with "A" and "B", and the minor ones with "C" and "D"

**<sup>1</sup>H-NMR** (CDCl<sub>3</sub>, 400 MHz): δ = 2.92 – 2.87 (m, CH<sup>6AB</sup>), 2.86 – 2.78 (m, CH<sub>2</sub><sup>10</sup>, CH<sub>2</sub><sup>17</sup>), 2.67 – 2.44 (m, CH<sub>2</sub><sup>9</sup>, CH<sub>2</sub><sup>16</sup>), 2.38 – 2.21 (m, CH<sub>2</sub><sup>14ABCD</sup>), 2.20 – 2.08 (m, CH<sup>6CD</sup>), 1.99 – 0.85 (m, CH<sub>2</sub><sup>5ABCD</sup>, CH<sup>4ABCD</sup>, CH<sup>1ABCD</sup>, CH<sub>2</sub><sup>3ABCD</sup>, CH<sup>2ABCD</sup>, CH<sub>2</sub><sup>2ABCD</sup>, CH<sub>3</sub><sup>8ABCD</sup>, CH<sub>3</sub><sup>13ABCD</sup>), 1.58 (b, NH<sub>2</sub><sup>18+11</sup>) ppm.

The <sup>1</sup>H NMR spectrum is in accordance with the literature.<sup>[168]</sup>

For <sup>1</sup>H and <sup>13</sup>C spectra see Chapter 4.3.1.2, Figure 80 and Figure 79.

The mono-addition product 2-(((S)-2-((R)-4-methylcyclohex-3-en-1-yl)propyl)thio)ethan-1-amine was obtained as by-product in a yield of 33% (517 mg, 2.42 mmol). The mono-addition product fraction contained two stereoisomers A and B.



**<sup>1</sup>H-NMR** (CDCl<sub>3</sub>, 400 MHz): δ = 5.36 – 5.30 (m, 1H, CH<sup>6</sup>), 2.84 (t, *J* = 6.3 Hz 2H, CH<sub>2</sub><sup>13</sup>), 2.63 – 2.51 (m, 3H, ½ CH<sub>2</sub><sup>10a</sup>, CH<sub>2</sub><sup>12</sup>), 2.38 – 2.28 (m, 1H, ½ CH<sub>2</sub><sup>10b</sup>), 2.05 – 1.84 (m, 3H, CH<sub>2</sub><sup>1</sup>, ½ CH<sub>2</sub><sup>4a</sup>), 1.82 – 1.45 (m, 6H, NH<sub>2</sub><sup>14</sup>, ½ CH<sub>2</sub><sup>4b</sup>, ½ CH<sub>2</sub><sup>2a</sup>, CH<sup>8</sup>, CH<sup>6</sup>), 1.60 (s, 3H, CH<sub>3</sub><sup>7</sup>), 1.34 – 1.14 (m, 1H, ½ CH<sub>2</sub><sup>2b</sup>), 0.94 (dd, *J* = 7.8 Hz, *J* = 6.6 Hz, 3H, CH<sub>3</sub><sup>9</sup>) ppm.

**<sup>13</sup>C-NMR** (CDCl<sub>3</sub>, 101 MHz): δ = 134.08 (C<sub>q</sub><sup>6A</sup>), 134.05 (C<sub>q</sub><sup>6B</sup>), 120.67 (CH<sup>5A</sup>), 120.62 (CH<sup>5B</sup>), 41.18 (CH<sub>2</sub><sup>13</sup>), 37.85 (CH<sup>8A/B</sup>/CH<sup>3A/B</sup>), 37.78 (CH<sup>8A/B</sup>/CH<sup>3A/B</sup>), 37.73 (CH<sup>8A/B</sup>/CH<sup>3A/B</sup>), 37.59 (CH<sup>8A/B</sup>/CH<sup>3A/B</sup>), 37.41 (CH<sub>2</sub><sup>10A</sup>), 37.32 (CH<sub>2</sub><sup>10B</sup>), 36.95 (CH<sub>2</sub><sup>12A</sup>), 36.90 (CH<sub>2</sub><sup>12B</sup>), 30.84 (CH<sub>2</sub><sup>1A</sup>), 30.69 (CH<sub>2</sub><sup>1B</sup>), 29.63 (CH<sub>2</sub><sup>4A</sup>), 27.43 (CH<sub>2</sub><sup>4B</sup>), 27.21 (CH<sub>2</sub><sup>2A</sup>), 25.34 (CH<sub>2</sub><sup>2B</sup>), 23.50 (CH<sub>3</sub><sup>7</sup>), 16.24 (CH<sub>3</sub><sup>9A</sup>), 15.79 (CH<sub>3</sub><sup>9B</sup>) ppm.

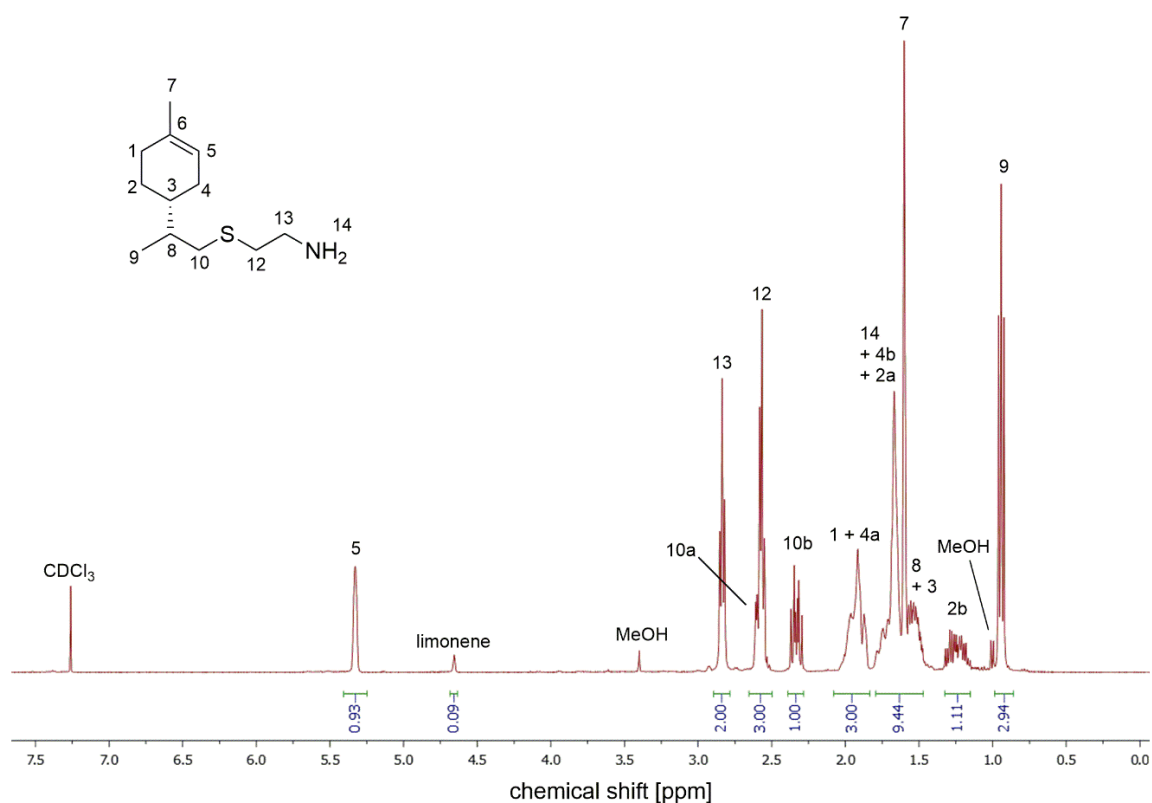


Figure 122:  $^1\text{H}$  NMR spectrum of 2-(((S)-2-((R)-4-methylcyclohex-3-en-1-yl)propyl)thio)ethan-1-amine.

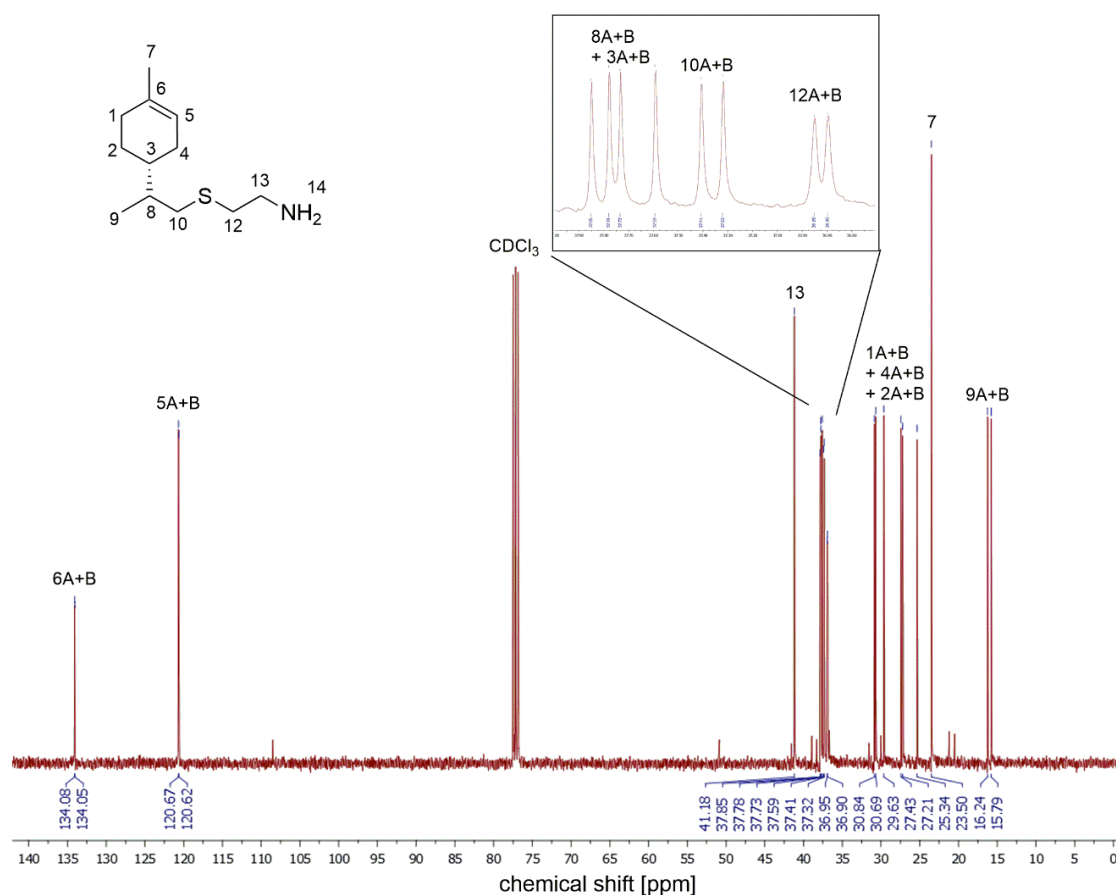


Figure 123:  $^{13}\text{C}$  NMR spectrum of 2-(((S)-2-((R)-4-methylcyclohex-3-en-1-yl)propyl)thio)ethan-1-amine.



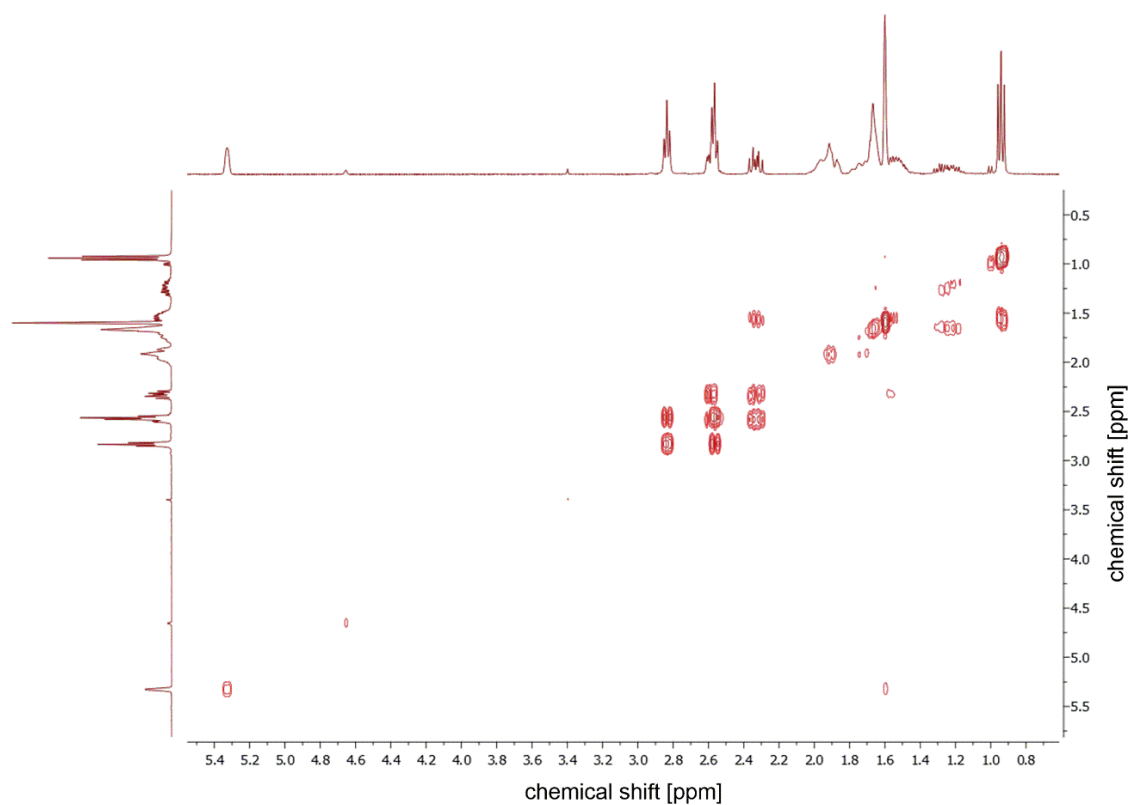


Figure 124: COSY spectrum of 2-(((S)-2-((R)-4-methylcyclohex-3-en-1-yl)propyl)thio)ethan-1-amine.

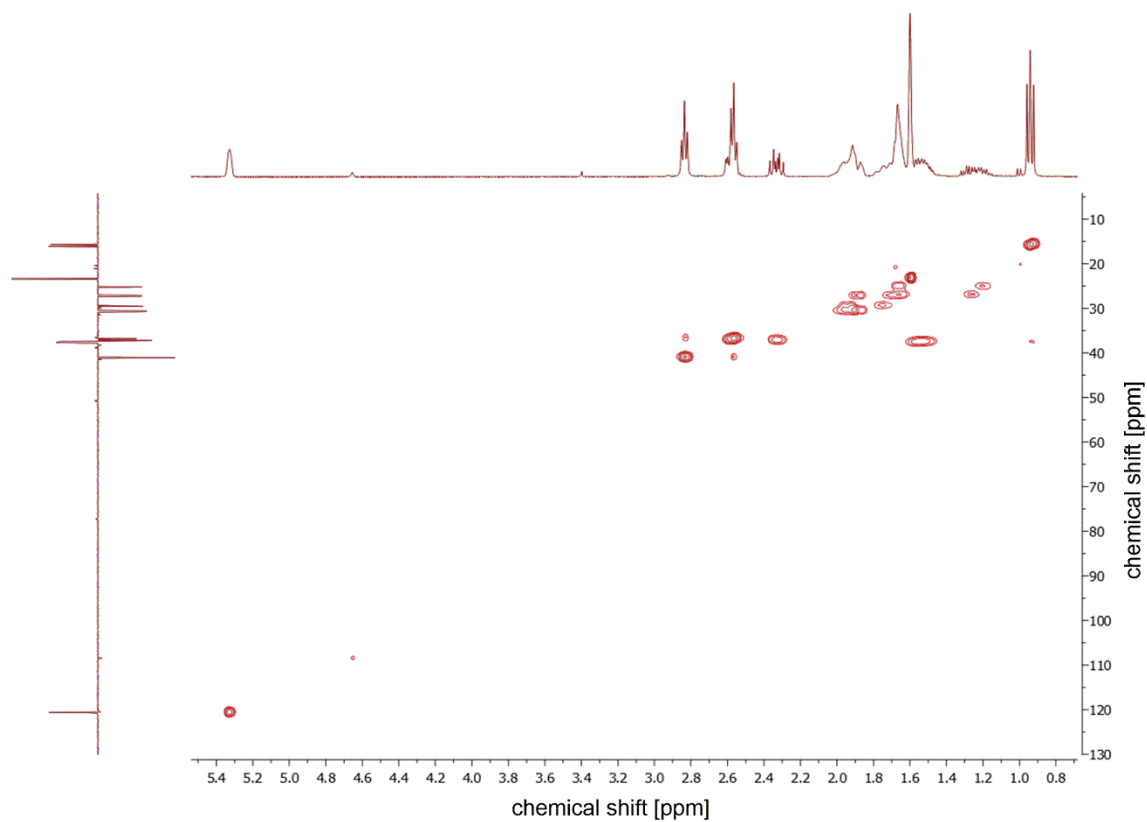


Figure 125: HSQC spectrum of 2-(((S)-2-((R)-4-methylcyclohex-3-en-1-yl)propyl)thio)ethan-1-amine.

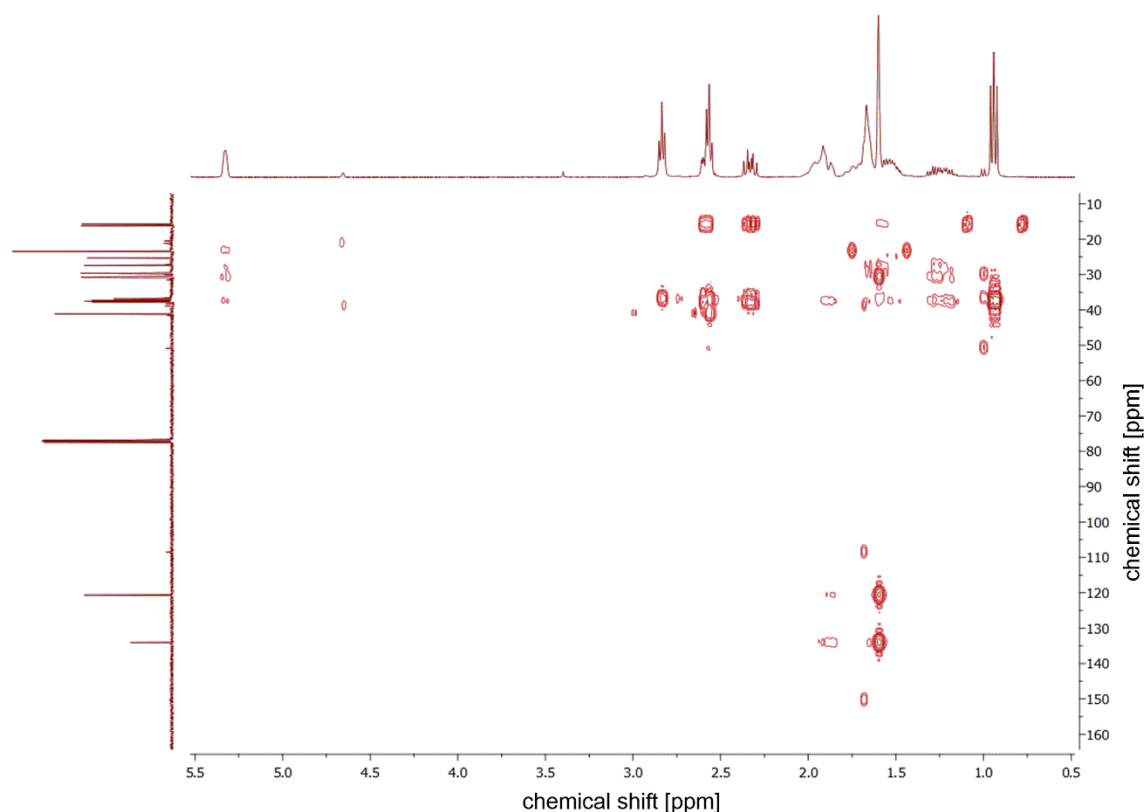
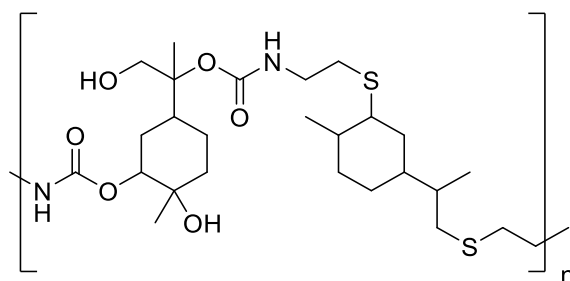


Figure 126: HMBC spectrum of 2-(((S)-2-((R)-4-methylcyclohex-3-en-1-yl)propyl)thio)ethan-1-amine.

### 6.3.3.3 Preparation of LC- and LA- based PHU prepolymers



In a typical experiment (PHU9), LA (600 mg, 2.07 mmol, 1.30 eq) was dissolved in EtOH (2.07 mL, 1M) and the solution was added to LC (40.7 mg, 1.59 mmol, 1.00 eq) in a pressure tube. Then, LiCl (78.9  $\mu$ mol, 3.34 mg, 5 mol%) was added and the suspension was stirred and heated to 100  $^{\circ}$ C for 18 h. The solvent was removed under reduced pressure and the PHU prepolymer was obtained as brownish powder and was analysed *via* SEC and/or FT-IR (ATR).

PHU1: **SEC** (System B, DMF, PMMA standards):  $M_n = 1120$  g/mol,  $M_w = 1480$  g/mol,  $D = 1.32$ .

PHU2: **SEC** (System B, DMF, PMMA standards):  $M_n = 1340$  g/mol,  $M_w = 1930$  g/mol,  $D = 1.44$ .

PHU3: **SEC** (System B, DMF, PMMA standards):  $M_n = 1250$  g/mol,  $M_w = 1730$  g/mol,  $D = 1.39$ .

PHU4: **SEC** (System B, DMF, PMMA standards):  $M_n = 1160$  g/mol,  $M_w = 1490$  g/mol,  $D = 1.28$ .

PHU5: **SEC** (System B, DMF, PMMA standards):  $M_n = 1440$  g/mol,  $M_w = 2250$  g/mol,  $D = 1.57$ .

PHU6: **SEC** (System B, DMF, PMMA standards):  $M_n = 1650$  g/mol,  $M_w = 2620$  g/mol,  $D = 1.59$ .

PHU7: **SEC** (System A, THF, PMMA standards):  $M_n = 1300$  g/mol,  $M_w = 1590$  g/mol,  $D = 1.22$ . **IR** (ATR platinum diamond):  $\nu/\text{cm}^{-1} = 3328.0$  (N-H, O-H), 2953.7, 2920.9 (C-H), 2869.3, 2852.9 (C-H), 1791.5 (C=O, 5mcc), 1694.8 (C=O, urethane), 1522.1, 1448.0, 1374.0, 1252.6, 1230.0, 1195.0, 1131.2, 1051.0, 1026.3 (C-O), 944.1, 894.8, 841.3, 775.5, 722.0, 592.4, 524.5, 427.8.

PHU8: **SEC** (System A, THF, PMMA standards):  $M_n = 1250$  g/mol,  $M_w = 1500$  g/mol,  $D = 1.20$ . **IR** (ATR platinum diamond):  $\nu/\text{cm}^{-1} = 3350.7$  (N-O, O-H), 2951.6, 2920.8 (C-H), 2869.3, 2852.9 (C-H), 1785.3 (C=O, 5mcc), 1694.8 (C=O, urethane), 1522.1, 1448.0, 1376.0, 1250.5, 1230.0, 1195.0, 1141.5, 1129.2, 1053.1, 1026.3 (C-O), 944.12, 894.8, 841.3, 775.45, 722.0, 588.3, 557.4, 425.8.

PHU9: **SEC** (System A, THF, PMMA standards):  $M_n = 1380$  g/mol,  $M_w = 1620$  g/mol,  $D = 1.18$ . **DSC**: Onset = 15 °C,  $T_g = 23$  °C. **TGA**:  $T_{d5\%} = 209$  °C. **IR** (ATR platinum diamond):  $\nu/\text{cm}^{-1} = 3350.7$  (N-H, O-H), 2953.7, 2918.7 (C-H), 2869.3, 2854.9 (C-H), 1795.6 (C=O, 5mcc), 1694.8 (C=O, urethane), 1520.0, 1446.0, 1374.0, 1252.6, 1232.0, 1195.0, 1129.2, 1049.0, 1026.3 (C-O), 942.1, 896.8, 818.6, 773.4, 722.0, 687.0, 586.2, 557.4, 425.8.

For FT-IR spectrum and SEC graph see Chapter 4.3.2, Figure 87.

#### 6.3.3.4 Curing reaction of epoxidised soybean oil (ESBO) with poly(hydroxy urethane) prepolymer (PHU9)

The poly(hydroxy urethane) prepolymer PHU9 (58.1 mg, amine value: 975  $\mu\text{mol/g}$ , 56.7  $\mu\text{mol}$  amine) was mixed with ESBO (25.0 mg, epoxide value: 4.53 mmol/g, 0.113 mmol epoxide) in a v-vial. The mixture was heated to 70 °C and stirred until the prepolymer and the ESBO was melted and a homogeneous mixture was obtained. Then the liquid mixture was poured into a round silicone mould and heated to 140 °C for 3 h

under ambient atmosphere in an oven. After cooling to room temperature, the epoxy resin was removed from the silicon mould and analysed *via* FT-IR spectroscopy, DSC and TGA measurements.

**IR** (ATR platinum diamond):  $\nu/\text{cm}^{-1}$  = 3350.7, 2922.8, 2854.9, 1797.7, 1696.9, 1524.1, 1454.2, 1415.1, 1374.0, 1250.5, 1193.0, 1131.2, 1053.1, 1026.3, 944.1, 866.0, 841.3, 822.8, 773.4, 722.0, 586.2, 427.8.

**DSC:** Onset = 20 °C,  $T_g$  = 29 °C.

**TGA:**  $T_{d\ 5\%}$  = 237 °C.

## 7 Abbreviations

2-MeTHF	2-Methyl tetrahydrofuran
5mcc	5-membered cyclic carbonate
AAS	Atomic absorption spectroscopy
AIBN	Azobisisobutyronitrile
AMMS	$\alpha$ -Methyl- <i>p</i> -methylstyrene
APS	Ammonium persulfate
ATR	Attenuated total reflection
ATRP	Atom transfer radical polymerisation
b	Broad
BDGC	Carbonated 1,4-butanediol diglycidyl ether
BDI	$\beta$ -Diiminate
BET	Nitrogen physisorption
BMI	1,1'-(Methylenedi-4,1-phenylene)bismaleimide
BPA	Bisphenol A
Bp	Boiling point
BQ	Benzoquinone
Cat.	Catalyst
CH	Cyclohexane
CNTs	Carbon nanotubes
Conc.	Concentration
COSY	Correlation spectroscopy
CPD	Cyclopentadienyl
CPME	Cyclopentyl methyl ether
$\bar{D}$	Dispersity
DBU	1,8-Diazabicyclo[5.4.0]undec-7-ene
DCPD	Dicyclopentadiene
dd	Doublet of doublets
DDE	Dichlorodiphenyldichloroethylene
DDT	Dichlorodiphenyltrichloroethane
DEC	Diethyl carbonate
DFT	Density functional theory
DGEBA	Bisphenol A diglycidyl ether
DMAP	<i>N,N</i> -dimethylpyridin-4-amine
DMC	Dimethyl carbonate

DMF	Dimethylformamide
DMPA	2,2-Dimethoxy-2-phenylacetophenone
DMSO-d <sub>6</sub>	Deuterated dimethyl sulfoxide
DSC	Differential scanning calorimetry
EA	Ethyl acetate
EDTA	Ethylenediaminetetraacetic acid
EI	Electron ionisation
EMY	Effective mass yield
ESBO	Epoxidised soybean oil
ESI-MS	Electrospray ionisation mass spectrometry
FDCA	2,5-Furandicarboxylic acid
FID	Flame-ionisation detector
FMF	<i>N</i> -formyl- <i>N</i> -methylformamide
FRP	Free-radical polymerisation
GAC	Green analytical chemistry
GC	Gas chromatography
GC-MS	Gas chromatography-mass spectrometry
GHG	Greenhouse gas
h	Hour
HFIP	Hexafluoroisopropanol
HMBC	Heteronuclear multiple bond correlation
HOSA	Hydroxylamine- <i>O</i> -sulfonic acid
HPLC	High-performance liquid chromatography
HRMS	High resolution mass spectrometry
HSAB	Hard and soft (Lewis) acids and bases
HSQC	Heteronuclear single quantum coherence
HTMA	Hydrogenated terpinene-maleic anhydride
HTME	Hydrogenated terpinene-maleic ester type epoxy resin
Hz	Hertz
IR	Infrared
kDa	Kilo Dalton
LA	Limonene-based diamine
LC	Cyclic limonene dicarbonate
LCA	Life-cycle assessment
LDO	Limonene dioxide
m	Multiplet

---

MAO	Methylaluminoxane
MBL	Methylene butyrolactone
<i>m</i> CPBA	<i>meta</i> -Chloroperoxybenzoic acid
$M_n$	Number average molecular weight
MOF	Metal-organic framework
Mt	Million metric tons
MTO	Methyltrioxorhenium
$M_w$	Weight average molecular weight
NBS	<i>N</i> -bromosuccinimide
NCNTs	Nitrogen-doped carbon nanotubes
NIPU	Non-isocyanate poly(hydroxyurethane)
NMR	Nuclear magnetic resonance
PA	Polyamide
PBAT	Poly(butylene adipate terephthalate)
PBS	Poly(butylene succinate)
PBT	Poly(butylene terephthalate)
PCBs	Polychlorinated biphenyls
PE	Polyethylene
PEF	Poly(ethylene furanoate)
PET	Poly(ethylene terephthalate)
PHA	Polyhydroxyalkanoates
PHU	Poly(hydroxy urethane)
PLA	Poly(lactic acid)
PLDC	Poly(limonene dicarbonate)
PM	Polymenthide
POPs	Persistent organic pollutants
PP	Polypropylene
PPNCI	Bis(triphenylphosphine)iminium chloride
PS	Polystyrene
PSM	Post-synthetic modification
PTFE	Polytetrafluoroethylene
PTM	Pentaerythritol tetrakis(3-mercaptopropionate)
PTT	Polytrimethylene terephthalate
PUR	Polyurethane
PVC	Poly(vinyl chloride)
PXRD	Powder X-ray diffraction

RAFT	Reversible addition-fragmentation chain-transfer
RCM	Ring-closing metathesis
ROCOP	Ring-opening copolymerization
ROMP	Ring-opening metathesis polymerisation
ROP	Ring-opening polymerisation
s	Singlet
SAICM	Strategic Approach to International Chemicals Management
$S_{\text{BET}}$	Specific surface area
SDGs	Sustainable Development Goals
SEC	Size exclusion chromatography
TBAB	Tetrabutylammonium bromide
TBAI	Tetrabutylammonium iodide
TBD	1,5,7-Triazabicyclo[4.4.0]dec-5-en
TBHP	<i>tert</i> -Butyl hydroperoxide
$T_g$	Glass transition temperature
TGA	Thermal gravimetric analysis
$T_m$	Melting temperature
THF	Tetrahydrofuran
TLC	Thin layer chromatography
TMPTMP	Trimethylolpropane tris(3-mercaptopropionate)
TON	Turnover number
TPE	Thermoplastic elastomer
UBA	German Federal Environment Agency (Umweltbundesamt)
US EPA	United States Environmental Protection Agency
UV	Ultraviolet
WCED	World Commission on Environment and Development
WHO	World Health Organisation
wt%	Weight percent



## 8 List of Figures

Figure 1: The relationship of sustainability, sustainable chemistry, green engineering, green technology and green chemistry. <sup>[7]</sup> .....	10
Figure 2: Relative quantities of organic raw materials used by the chemical industry in Germany in 2017. <sup>[37]</sup> .....	13
Figure 3: Global bio-based/biodegradable plastics production capacity by material in 2018. <sup>[42]</sup> .....	15
Figure 4: Options for replacing petrochemicals as raw material for polymer synthesis. Adopted from reference <sup>[12]</sup> .....	17
Figure 5: Global production, use, and fate of polymer resins, synthetic fibres, and additives (1950 to 2015; in Mt). This figure is reprinted from R. Geyer, J. R. Jambeck, K. L. Law, <i>Sci. Adv.</i> 2017; 3: e1700782, which is licensed under the terms of the Creative Commons Attribution Licence. <sup>[50]</sup> .....	18
Figure 6: Cumulative plastic waste generation and disposal (in Mt). This figure is reprinted from R. Geyer, J. R. Jambeck, K. L. Law, <i>Sci. Adv.</i> 2017; 3: e1700782, which is licensed under the terms of the Creative Commons Attribution Licence. <sup>[50]</sup> .....	19
Figure 7: Schematic illustration of plastic biodegradation. This figure is reprinted from R. Wei, W. Zimmermann, <i>Microbial biotechnology</i> , 2017, 10, 1308-1322, which is licensed under the terms of the Creative Commons Attribution Licence. <sup>[56]</sup> .....	21
Figure 8: Classical and new routes to citral. <sup>[33]</sup> .....	22
Figure 9: Diagram of criticality of elements according to A. J. Hunt et. al., <i>Element Recovery and Sustainability</i> , The Royal Society of Chemistry, Cambridge, 2013. <sup>[64]</sup> .....	23
Figure 10: Isoprene unit and examples of terpenes and terpenoids with varying number of carbon atoms. ....	25
Figure 11: Structures of the most common monoterpenes found in turpentine. <sup>[76]</sup> .....	26
Figure 12: Overview of valuable compounds obtained from $\alpha$ - and $\beta$ -pinene, adopted from reference <sup>[72]</sup> .....	28
Figure 13: Industrial $\alpha$ -terpineol synthesis via the hydration of $\alpha$ -pinene. <sup>[87]</sup> .....	29
Figure 14: Possible pathways and products resulting from dehydroisomerisation of $\alpha$ -pinene. ....	30
Figure 15: Main products observed during the thermal oxidation of $\alpha$ -pinene. <sup>[95]</sup> .....	31
Figure 16: Four different oxidation sites (denoted a – d) in $\alpha$ -pinene and the resulting resonance-stabilised radicals formed upon abstraction of an hydrogen atom at the a- and d-sites (top and bottom, respectively). <sup>[95]</sup> .....	32
Figure 17: Epoxidation of $\alpha$ -pinene under autoxidation conditions. <sup>[95]</sup> .....	32

Figure 18: Addition of molecular oxygen to a radical adduct; a reaction that can potentially compete with the epoxidation shown in Figure 17. <sup>[95]</sup> .....	33
Figure 19: Proposed fate of the $R_{(a)}-O\cdot$ radicals. <sup>[95]</sup> .....	33
Figure 20: Proposed reaction pathways of the NCNT-catalysed oxidation of $\alpha$ -pinene. <sup>[96]</sup> .....	34
Figure 21: Compounds obtained from isomerisation of $\alpha$ -pinene. <sup>[72]</sup> .....	37
Figure 22: Cationic polymerisation of $\beta$ -pinene: A) General mechanism catalysed by $AlCl_3$ , <sup>[120]</sup> B) Proposed mechanism using $H_2O/AlCl_3OPh_2$ as initiating system. <sup>[122]</sup> ..	39
Figure 23: Two proposed mechanisms for the polymerisation of $\alpha$ -pinene. <sup>[118]</sup> .....	41
Figure 24: Copolymers obtained by sequence-regulated radical copolymerisation of limonene and functionalised maleimide derivatives. <sup>[138]</sup> .....	42
Figure 25: Two polymerisation procedures for the synthesis of polymyrcene: A) Emulsion polymerisation, <sup>[140]</sup> B) RAFT polymerisation. <sup>[141]</sup> .....	43
Figure 26: Synthesis of PAMMS-PMYR-PAMMS triblock copolymer by sequential anionic polymerisation of $\alpha$ -methyl-p-methylstyrene (AMMS) and myrcene (MYR) and subsequent coupling with dichlorodimethylsilane. <sup>[142]</sup> .....	44
Figure 27: Selective ring-opening radical polymerisation of $\alpha$ -pinene-derived pinocarvone. <sup>[144]</sup> .....	45
Figure 28: Synthesis of acrylate and methacrylate monomers based on various terpenes followed by free-radical polymerisation. <sup>[145]</sup> .....	46
Figure 29: Catalytic C-H oxidation/coupling of $\beta$ -pinene with methacrylic acid in a one-step procedure. <sup>[145]</sup> .....	46
Figure 30: Tandem synthesis of aliphatic polyesters from epoxides and anhydrides. Salen-complexes are efficient catalysts for the cyclisation of dicarboxylic acids and the subsequent polymerisation of the resulting anhydride with epoxides. <sup>[148]</sup> .....	47
Figure 31: Cyclic anhydride comonomers: The first three were obtained by reacting 1,3-cyclohexadiene, $\alpha$ -phellandrene and $\alpha$ -terpinene, respectively, with maleic anhydride in a Diels-Alder reaction. The fourth was obtained by catalytic hydrogenation of the third one. <sup>[150]</sup> .....	48
Figure 32: Copolymerisation of trans- and cis-(R)-limonene oxide and $CO_2$ using $\beta$ -diiminate zinc acetate complexes as catalyst. <sup>[152]</sup> .....	49
Figure 33: A) Stereoselective synthesis of trans-limonene oxide via the corresponding trans-bromohydrin and subsequent ring-closing by the addition of a base; B) O-Methylation of OH-impurities with sodium hydride and methyl iodide. <sup>[44]</sup> .....	50
Figure 34: Structural elements of the co-polymers derived from limonene oxide and $\alpha$ -pinene oxide with 1,2-epoxydecane. <sup>[160]</sup> .....	52
Figure 35: General mechanism of thiol-ene additions. <sup>[166]</sup> .....	53

Figure 36: A) Monomer synthesis via diadditions or mono- and subsequent diadditions of thiols to limonene; B) resulting monomers; C) homopolymerisation of heterodifunctional monomers a and b, respectively, and co-polymerisation of difunctional monomers c and d (yielding oligomers). <sup>[167]</sup> .....	54
Figure 37: Synthesis of limonene-derived diamine and dicarbamate monomers for the synthesis of A) polyamides; and B) polyurethanes. <sup>[168]</sup> .....	55
Figure 38: Synthesis of a limonene-based dithiol monomer and subsequent co-polymerisation with a castor oil-derived diene via thiol-ene reaction. <sup>[170]</sup> .....	56
Figure 39: A) Synthesis of terephthalic acid from limonene; B) Butanediol synthesis from succinic acid; and terephthalate polyester synthesis. <sup>[172]</sup> .....	57
Figure 40: Ring-closing metathesis of myrcene to 3-methylenecyclopentene and subsequent cationic polymerisation with <i>i</i> -BuOCH(Cl)Me/Lewis Acid/Et <sub>2</sub> O in toluene. <sup>[173]</sup> .....	57
Figure 41: Retrosynthesis of dihydrocarvone and synthesis of dihydrocarvone-based lactones followed by polymerisation to polydihydrocarvide and polycarvomenthide. <sup>[175, 176]</sup> .....	59
Figure 42: Synthesis of menthone from menthol followed by Baeyer-Villiger oxidation to give menthide and polymerisation of menthide using a defined Zn alkoxide catalyst. <sup>[177]</sup> .....	59
Figure 43: Menthone-based synthesis of lactams a and b, via oxime, or direct and regioselective synthesis of lactam b with hydroxylamine-O-sulfonic acid (HOSA) followed by ROP. <sup>[187]</sup> .....	61
Figure 44: Formula of menthane diamine and terpene diphenol that can be used as hardeners for epoxy resins and formula of the C-alkylated product of 1-naphthol and limonene that can be transformed into an epoxy resin. ....	63
Figure 45: Synthesis of polyols and polyurethanes from hydrogenated terpinene-maleic ester type epoxy resin (HTME). <sup>[198]</sup> .....	64
Figure 46: A) Synthesis route for the limonene-terminated precursors. Bidirectional grey arrows denote thiol-ene coupling between multifunctional thiols and macromonomers. B) Network formation based on equimolar amounts of multifunctional groups. <sup>[200]</sup> .....	65
Figure 47: Conversion of limonene dioxide to limonene dicarbonate. <sup>[206]</sup> .....	67
Figure 48: Coupling of terpene-based epoxides with CO <sub>2</sub> catalysed by Al(aminotriphenolate) complexes and product scope. <sup>[207]</sup> .....	67
Figure 49: Synthesis of fully bio-based NIPU thermosets from carbonated pentaerythritol glycidyl ether/limonene dicarbonate blends cured with 1,5-diaminopentane and synthesis of thermoplastic NIPU copolymers via prepolymers based on limonene dicarbonate and Priamine 1074 with subsequent chain extension by using carbonated 1,4-butanediol diglycidyl ether. <sup>[210]</sup> .....	68

- Figure 50: Graphical abstract for the aerobic oxidation of  $\alpha$ -pinene catalysed by homogeneous and MOF-based Mn catalysts yielding pinene oxide as main product and verbenone and verbenol as side-products..... 76
- Figure 51: Conversion, yield and selectivity of aerobic  $\alpha$ -pinene oxidation catalysed by Mn(III) acetate. Reaction conditions:  $\alpha$ -pinene (1.00 mmol), catalyst (1.00 mol% Mn), toluene/DMF (50:50, 30 mL), compressed air (50 mL min<sup>-1</sup>), 130 °C..... 77
- Figure 52: Autoxidation of DMF: a: thermal oxidation of DMF including the epoxidation of alkenes in DMF and the formation of N-formyl-N-methylformamide (FMF); b: metal ion-catalysed oxidation of DMF.<sup>[223]</sup> ..... 78
- Figure 53: Dependency of reaction temperature on conversion and yield. Reaction conditions:  $\alpha$ -pinene (1.00 mmol), Mn(III) acetate (1.00 mol%), toluene/DMF (90:10, 30 mL), compressed air (50 mL min<sup>-1</sup>). ..... 80
- Figure 54: Influence of air flow rate on conversion and yield for the catalytic oxidation of  $\alpha$ -pinene. Reaction conditions:  $\alpha$ -pinene (1.00 mmol), catalyst (0.500 mol% Mn), toluene/DMF (90:10, 30 mL), compressed air (flow as indicated), 130 °C, 6 h. .... 81
- Figure 55: Synthesis procedure for MIXMIL-53-NH<sub>2</sub>(50) and subsequent two-step post-synthetic modification to immobilise manganese complexes..... 84
- Figure 56: XRD patterns of simulated MIL-53(Al) and MIXMIL-53(Al)-NH<sub>2</sub>(50)-Mal-Mn. 85
- Figure 57: Catalytic oxidation of  $\alpha$ -pinene by MIXMIL-53-NH<sub>2</sub>(50)-Mal-Mn resulting in pinene oxide, verbenone and verbenol as the main products (conversion: 31%, selectivities: 54, 8 and 3%, respectively). Reaction conditions:  $\alpha$ -pinene (1.00 mmol), MIXMIL-53-NH<sub>2</sub>(50)-Mal-Mn (0.500 mol% Mn), DEC/DMF (90:10, 30 mL), compressed air (50 mL min<sup>-1</sup>), 130 °C, 6 h. .... 86
- Figure 58: Conversion and yield of aerobic  $\alpha$ -pinene oxidation catalysed by MIXMIL-53-NH<sub>2</sub>(50)-Mal-Mn and homogeneous Mn(III) acetate, respectively. Reaction conditions:  $\alpha$ -pinene (1.00 mmol), catalyst (0.500 mol% Mn), DEC/DMF (90:10, 30 mL), compressed air (50 mL min<sup>-1</sup>), 130 °C. .... 87
- Figure 59: Catalytic performance of MIXMIL-53-NH<sub>2</sub>(50)-Mal-Mn in five cycles of  $\alpha$ -pinene epoxidation. Reaction conditions:  $\alpha$ -pinene (1.00 mmol), MIXMIL-53-NH<sub>2</sub>(50)-Mal-Mn (0.500 mol% Mn), DEC/DMF (90:10, 30 mL), compressed air (50 mL min<sup>-1</sup>), 130 °C, 6 h. .... 88
- Figure 60: Comparison of conversion and yield of  $\alpha$ -pinene epoxidation with and without catalyst removal after 3 h (as indicated by vertical line). Reaction conditions:  $\alpha$ -pinene (1.00 mmol), MIXMIL-53-NH<sub>2</sub>(50)-Mal-Mn (0.500 mol% Mn), DEC/DMF (90:10, 30 mL), compressed air (50 mL min<sup>-1</sup>), 130 °C. .... 89
- Figure 61: Synthesis routes for the production of linear carbonates exemplified by dimethyl carbonate. A) via phosgene; B) by catalytic oxidative carbonylation of methanol, C) by CO<sub>2</sub> insertion into oxirane; D) dehydrative condensation of methanol and CO<sub>2</sub>; and E) by transesterification of urea with methanol. .... 91
- Figure 62: Reactivity of dimethyl carbonate according to the HSAB theory: transesterification (left) and alkylation (right).<sup>[257]</sup> ..... 92

Figure 63: Synthetic routes to five-membered cyclic carbonates and various fields of application.....	92
Figure 64: Proposed reaction mechanism for the synthesis of five-membered cyclic carbonates via direct chemical fixation of CO <sub>2</sub> with epoxides. <sup>[266]</sup> .....	93
Figure 65: Theoretical coupling reaction between $\alpha$ -pinene oxide and CO <sub>2</sub> yielding $\alpha$ -pinene cyclic carbonate.....	94
Figure 66: Literature procedures for the coupling reaction between epoxides and CO <sub>2</sub> . A) Werner and Tenhumberg; <sup>[267]</sup> B) Mülhaupt et al.; <sup>[210]</sup> C) Shi et al. <sup>[268]</sup> and D) D'Elia et al. <sup>[269]</sup> .....	95
Figure 67: GC chromatograms of $\alpha$ -pinene oxide hydrolysis under neutral conditions. A: $t = 0$ h, B: crude reaction mixture under basic conditions after 24 h. C: crude reaction mixture in acidic medium after 24 h. D: crude reaction mixture in neutral medium after 24 h, E: pure product after purification via column chromatography. Reaction conditions: B: $\alpha$ -pinene oxide (100 mg), water (1.00 mL), dioxane (5.00 mL), 1M-sodium hydroxide solution (0.9 mL), 115 °C, 24 h. Reaction conditions C: $\alpha$ -pinene oxide (100 mg), water (1.00 mL), H <sub>2</sub> SO <sub>4</sub> (0.03 mL), dioxane (5.00 mL), RT, 24 h. D: $\alpha$ -pinene oxide (100 mg), water (1.00 mL), dioxane (5.00 mL), 115 °C, 24 h.....	99
Figure 68: Proposed reaction mechanism for the acid-catalysed synthesis of sobrerol from $\alpha$ -pinene oxide. <sup>[273]</sup> .....	100
Figure 69: Transesterification of sobrerol with DMC showing both theoretically possible products. ....	101
Figure 70: TBD-catalysed transesterification of cis- $\alpha$ -pinanediol with DMC yielding $\alpha$ -pinene carbonate. ....	101
Figure 71: MTO-catalysed epoxidation of $\beta$ -pinene followed by the MTO-catalysed epoxide ring-opening reaction with water yielding $\beta$ -pinanediol. ....	104
Figure 72: GC chromatograms of the MTO catalysed epoxidation and ring-opening reaction of $\beta$ -pinene. Bottom: crude reaction mixture. Top: fraction containing two species after column chromatography.....	105
Figure 73: Transesterification reaction of $\beta$ -pinanediol showing all theoretically possible products. ....	106
Figure 74: Fully assigned <sup>1</sup> H NMR spectrum of $\beta$ -pinene carbonate.....	107
Figure 75: Fully assigned <sup>13</sup> C NMR spectrum of $\beta$ -pinene carbonate. ....	108
Figure 76: Graphical abstract for the synthesis of poly(hydroxy urethane) prepolymers starting from limonene and further crosslinking to give thermosetting polymers. ..	110
Figure 77: Synthesis route for limonene dicarbonate starting from limonene via epoxidation and subsequent CO <sub>2</sub> insertion.....	111
Figure 78: Synthesis of the limonene-based diamine via thiol ene reaction. <sup>[168]</sup> .....	112

- Figure 79:  $^{13}\text{C}$  NMR spectrum of the limonene-based diamine (LA) with a zoom to the region of 52 – 50 ppm showing the signals of the four diastereomers A, B, C and D, belonging to carbon  $\text{C}^6$ ..... 113
- Figure 80:  $^1\text{H}$  NMR spectrum of the limonene-based diamine (LA). ..... 114
- Figure 81: Synthesis of poly(hydroxy urethane) prepolymers from LC and LA at elevated temperatures..... 115
- Figure 82: SEC analysis (System A, THF, PMMA standards) of the poly(hydroxy urethane) prepolymers PHU1 and PHU2. .... 117
- Figure 83: Top: SEC analysis of PHU7 and PHU8 prepared at LC:LA molar ratios of 1:1.1 and 1.1:1, respectively. Bottom: FT-IR spectra of PHU7 and PHU8 showing the characteristic peaks of the carbonate carbonyl band at 1791.5 and 1785.3  $\text{cm}^{-1}$ , respectively, and the carbonyl IR absorption of the urethane group at 1694.8  $\text{cm}^{-1}$ . ..... 119
- Figure 84: Top: Potential chemical structure of the LC- and LA-based PHU prepolymer species containing eight monomer units. Bottom: Measured isotopic pattern (blue) and calculated isotopic pattern (black) showing high agreement..... 121
- Figure 85: Synthesis of LC-based PHU using 1,10-diaminodecane as amine component. Reaction conditions: LC (50.0 mg, 0.195 mmol, 1 eq), 1,10-diaminodecane (37.0 mg, 0.215 mmol, 1.1 eq), EtOH (1M), 75 °C, 18 h..... 121
- Figure 86: SEC analysis of the PHU obtained from the reaction of LC and 1,10-diaminodecane in comparison to PHU2. .... 122
- Figure 87: Left: SEC graph of PHU9 showing almost full conversion of LC. Right: FT-IR spectrum of PHU9 showing the characteristic peaks of the carbonate carbonyl band at 1795.6  $\text{cm}^{-1}$  and the carbonyl IR absorption of the urethane group at 1694.8  $\text{cm}^{-1}$ . ..... 123
- Figure 88: Top: fully assigned  $^1\text{H}$  NMR spectrum of ESBO; bottom: FT-IR spectrum and HSQC spectrum of ESBO. .... 125
- Figure 89: Reaction scheme for the application of the PHU prepolymers as hardener for epoxy thermosets based on epoxidised linolein and photograph of the obtained thermoset..... 126
- Figure 90: Top: DSC analysis of the curing reaction between PHU9 and ESBO; Bottom: DSC analysis of ESBO (left) and PHU9 (right). ..... 127
- Figure 91: DSC and TGA analysis of the epoxy resin obtained from the curing reaction between PHU9 and ESBO. .... 128
- Figure 92: Two-step PSM reaction for the synthesis of MIXMIL-53-NH<sub>2</sub>(50)-Mal-Mn. . 138
- Figure 93: Adsorption (closed symbols) and desorption (open symbols) isotherms of MIXMIL-53-NH<sub>2</sub>(50), MIXMIL-53-NH<sub>2</sub>(50)-Mal and MIXMIL-53-NH<sub>2</sub>(50)-Mal-Mn.. 139
- Figure 94: Complete ATR-IR spectra of MIXMIL-53-NH<sub>2</sub>(50), MIXMIL-53-NH<sub>2</sub>(50)-Mal and MIXMIL-53-NH<sub>2</sub>(50)-Mal-Mn..... 140

---

Figure 95: Zoom to O-H and N-H stretching vibrations of ATR-IR spectra of MIXMIL-53-NH <sub>2</sub> (50), MIXMIL-53-NH <sub>2</sub> (50)-Mal and MIXMIL-53-NH <sub>2</sub> (50)-Mal-Mn. ....	140
Figure 96: Zoom to expected C=O bands in the ATR-IR spectra of MIXMIL-53-NH <sub>2</sub> (50), MIXMIL-53-NH <sub>2</sub> (50)-Mal and MIXMIL-53-NH <sub>2</sub> (50)-Mal-Mn to exclude free acid or solvent molecules (DMF).....	141
Figure 97: <sup>1</sup> H NMR spectrum of sobrerol. ....	145
Figure 98: <sup>13</sup> C NMR spectrum of sobrerol.....	145
Figure 99: COSY spectrum of sobrerol.....	146
Figure 100: HSQC spectrum of sobrerol.....	146
Figure 101: HMBC spectrum of sobrerol. ....	147
Figure 102: <sup>1</sup> H NMR spectrum of 5-(2-hydroxypropan-2-yl)-2-methylcyclohex-2-en-1-yl methyl carbonate.....	148
Figure 103: <sup>13</sup> C NMR spectrum of 5-(2-hydroxypropan-2-yl)-2-methylcyclohex-2-en-1-yl methyl carbonate.....	149
Figure 104: COSY spectrum of 5-(2-hydroxypropan-2-yl)-2-methylcyclohex-2-en-1-yl methyl carbonate.....	149
Figure 105: HSQC spectrum of 5-(2-hydroxypropan-2-yl)-2-methylcyclohex-2-en-1-yl methyl carbonate.....	150
Figure 106: HMBC spectrum of 5-(2-hydroxypropan-2-yl)-2-methylcyclohex-2-en-1-yl methyl carbonate.....	150
Figure 107: <sup>1</sup> H NMR spectrum of α-pinene carbonate. ....	152
Figure 108: <sup>13</sup> C NMR spectrum of α-pinene carbonate. ....	152
Figure 109: COSY spectrum of α-pinene carbonate. ....	153
Figure 110: HSQC spectrum of α-pinene carbonate.....	153
Figure 111: HMBC spectrum of α-pinene carbonate.....	154
Figure 112: <sup>1</sup> H NMR spectrum of β-pinene carbonate. ....	156
Figure 113: <sup>13</sup> C NMR spectrum of β-pinene carbonate. ....	156
Figure 114: COSY spectrum of β-pinene carbonate. ....	157
Figure 115: HSQC spectrum of β-pinene carbonate.....	157
Figure 116: HMBC spectrum of β-pinene carbonate.....	158
Figure 117: <sup>1</sup> H NMR spectrum of cyclic limonene dicarbonate. ....	160
Figure 118: <sup>13</sup> C NMR spectrum of cyclic limonene dicarbonate. ....	160

<i>Figure 119: COSY spectrum of cyclic limonene dicarbonate.</i> .....	161
<i>Figure 120: HSQC spectrum of cyclic limonene dicarbonate.</i> .....	161
<i>Figure 121: HMBC spectrum of cyclic limonene dicarbonate.</i> .....	162
<i>Figure 122: <sup>1</sup>H NMR spectrum of 2-(((S)-2-((R)-4-methylcyclohex-3-en-1-yl)propyl)thio)ethan-1-amine.</i> .....	164
<i>Figure 123: <sup>13</sup>C NMR spectrum of 2-(((S)-2-((R)-4-methylcyclohex-3-en-1-yl)propyl)thio)ethan-1-amine.</i> .....	164
<i>Figure 124: COSY spectrum of 2-(((S)-2-((R)-4-methylcyclohex-3-en-1-yl)propyl)thio)ethan-1-amine.</i> .....	165
<i>Figure 125: HSQC spectrum of 2-(((S)-2-((R)-4-methylcyclohex-3-en-1-yl)propyl)thio)ethan-1-amine.</i> .....	165
<i>Figure 126: HMBC spectrum of 2-(((S)-2-((R)-4-methylcyclohex-3-en-1-yl)propyl)thio)ethan-1-amine.</i> .....	166



## 9 List of Tables

Table 1: The 12 principles of green chemistry proposed by Anastas and Warner. <sup>[22]</sup> .....	5
Table 2: The 12 principles of green chemistry written in the form of a mnemonic: PRODUCTIVELY. <sup>[23]</sup> .....	6
Table 3: The 12 principles of green analytical chemistry proposed by Gałuszka, Migaszewski and Namieśnik. <sup>[24]</sup> .....	7
Table 4: The 12 principles of green engineering proposed by Anastas and Zimmerman. <sup>[26]</sup> .....	8
Table 5: E factors in the chemical industry. <sup>[33]</sup> .....	11
Table 6: Some terpenes and the plants they can be isolated from. <sup>[73]</sup> .....	26
Table 7: Effect of catalyst concentration on conversion and selectivity. Reaction conditions: $\alpha$ -pinene (1.00 mmol), Mn(III) acetate (as indicated), toluene/DMF (90:10, 30 mL), compressed air (50 mL min <sup>-1</sup> ), 130 °C, 6 h.....	79
Table 8: Solvent effect in the aerobic epoxidation of $\alpha$ -pinene. Reaction conditions: $\alpha$ -pinene (1.00 mmol), Mn(III) acetate (1.00 mol%), solvent (30 mL), compressed air (50 mL min <sup>-1</sup> ), 130 °C, 6 h.....	83
Table 9: Specific surface areas and micropore volumes of modified MIL-53(Al) materials obtained from nitrogen physisorption measurements. Mn content of MIXMIL-53-NH <sub>2</sub> (50)-Mal-Mn determined by AAS measurements. ....	86
Table 10: Comparison of literature procedures and the new procedure for the synthesis of $\alpha$ -pinene carbonate. ....	103
Table 11: Screening of the reaction conditions for the synthesis of poly(hydroxy urethane) prepolymers and influence on the molecular weight of the obtained prepolymers. Reaction conditions: LC (50.0 mg, 0.195 mmol), LA (56.7 mg, 0.195 mmol), solvent (1M), catalyst (5 mol%), 18 h.....	116
Table 12: Result of the SEC-ESI-MS analysis of PHU7 showing the calculated masses of each oligomer from monomer to nonamer and the masses that were found in the measurement. Number 1 corresponds to the carbonato telechelic oligomers and number 2 to the amino telechelic ones. ....	120



## 10 Bibliography

- [1] H. C. von Carlowitz, *Sylvicultura oeconomica*, Braun, Leipzig, **1732**.
- [2] World Commission on Environment and Development (WCED), *Our Common Future*, Oxford University Press, Oxford, **1987**.
- [3] W. Steffen, P. J. Crutzen, J. R. McNeill, *Ambio* **2007**, *36*, 614-622.
- [4] J. Rockström, W. Steffen, K. Noone, Å. Persson, F. S. Chapin, E. F. Lambin, T. M. Lenton, M. Scheffer, C. Folke, H. J. Schellnhuber, B. Nykvist, C. A. de Wit, T. Hughes, S. van der Leeuw, H. Rodhe, S. Sörlin, P. K. Snyder, R. Costanza, U. Svedin, M. Falkenmark, L. Karlberg, R. W. Corell, V. J. Fabry, J. Hansen, B. Walker, D. Liverman, K. Richardson, P. Crutzen, J. A. Foley, *Nature* **2009**, *461*, 472-475.
- [5] W. Steffen, R. A. Sanderson, P. D. Tyson, J. Jäger, P. A. Matson, B. Moore III, F. Oldfield, K. Richardson, H.-J. Schellnhuber, B. L. Turner, *Global change and the earth system: a planet under pressure*, Springer Science & Business Media, Berlin - Heidelberg - New York, **2006**.
- [6] United Nations (**2019**), Sustainable Development Goals, retrieved November 1, 2019, from <https://unstats.un.org/sdgs/>
- [7] K. Kümmerer, J. Clark, in *Sustainability Science: An Introduction* (Eds.: H. Heinrichs, P. Martens, G. Michelsen, A. Wiek), Springer Netherlands, Dordrecht, **2016**, 43-59.
- [8] SAICM UN Environment Programme (**2019**), Strategic Approach to International Chemicals Management, retrieved November 1, 2019, from <http://www.saicm.org/Home/tabid/5410/language/en-US/Default.aspx>
- [9] International Energy Agency, *Energy Technology Perspectives 2017: Catalysing Energy Technology Transformations*, IEA Publications, **2017**.
- [10] T. C. Carole Ferguson, James Smyth, CDP UK, *Catalyst for change: Which chemical companies are prepared for the low carbon transition? Executive Summary*, **2017**.
- [11] United Nations Framework Convention on Climate Change, The Paris Agreement (**2019**), retrieved November 1, 2019, from <https://unfccc.int/process-and-meetings/the-paris-agreement/the-paris-agreement>
- [12] Y. Zhu, C. Romain, C. K. Williams, *Nature* **2016**, *540*, 354.
- [13] I. T. Horváth, *Chem. Rev.* **2018**, *118*, 369-371.
- [14] R. Carson, *Silent spring*, Houghton Mifflin Harcourt, New York, **2002**.

- [15] Secretariat of the Stockholm Convention (**2008**), retrieved November 3, 2019, from <http://chm.pops.int/>
- [16] Umweltbundesamt (**2017**), Dioxine, retrieved November 3, 2019, from <https://www.umweltbundesamt.de/themen/chemikalien/dioxine#textpart-6>
- [17] I. T. Horváth, P. T. Anastas, *Chem. Rev.* **2007**, *107*, 2169-2173.
- [18] P. T. Anastas, *Green Chemistry: Theory and Practice*, Oxford University Press, Oxford, **1998**.
- [19] United States Environmental Protection Agency (**2017**), Basics of Green Chemistry, retrieved August 28, 2019, from <https://www.epa.gov/greenchemistry/basics-green-chemistry#definition>
- [20] A. S. Cannon, J. C. Warner, *New Solut.* **2011**, *21*, 499-517.
- [21] P. T. Anastas, L. G. Heine, T. C. Williamson, *Green Chemical Syntheses and Processes*, ACS Symposium Series, American Chemical Society, Washington, DC, **2000**.
- [22] P. T. Anastas, N. Eghbali, *Chem. Soc. Rev.* **2010**, *39*, 301-312.
- [23] S. L. Tang, R. L. Smith, M. Poliakoff, *Green Chem.* **2005**, *7*, 761-762.
- [24] A. Gałuszka, Z. Migaszewski, J. Namieśnik, *Trends Anal. Chem.* **2013**, *50*, 78-84.
- [25] P. T. Anastas, *Crit. Rev. Anal. Chem.* **1999**, *29*, 167-175.
- [26] P. T. Anastas, J. B. Zimmerman, *Environ. Sci. & Technol.* **2003**, *37*, 94A-101A.
- [27] K. Kümmerer, *Angew. Chem. Int. Ed.* **2017**, *56*, 16420-16421.
- [28] IPEN/WECF (**2017**), Beyond 2020: Green chemistry and sustainable chemistry, retrieved August 28, 2019, from <http://www.wecf.eu/download/2017/01-January/Beyond2020Greenchemistryandsustainablechemistry.pdf>
- [29] ISC3 - International Sustainable Chemistry Collaborative Centre (**2018**), Sustainable Chemistry, retrieved August 28, 2019, from <https://www.isc3.org/en/home.html>
- [30] P. Anastas, in *Abstract of Papers of the American Chemical Society, Vol. 228*, **2004**, U765-U765.
- [31] P. Schwager, N. Decker, I. Kaltenegger, *Curr. Opin. Green and Sustainable Chem.* **2016**, *1*, 18-21.
- [32] R. A. Sheldon, *Green Chem.* **2007**, *9*, 1273-1283.
- [33] R. A. Sheldon, I. Arends, U. Hanefeld, *Green chemistry and catalysis*, Wiley-VCH, Weinheim, **2007**.
- [34] B. M. Trost, *Science* **1991**, *254*, 1471-1477.
- [35] T. Hudlicky, D. A. Frey, L. Koroniak, C. D. Claeboe, L. E. Brammer Jr, *Green Chem.* **1999**, *1*, 57-59.

- [36] R. Horne, T. Grant, K. Verghese, *Life cycle assessment: principles, practice and prospects*, Csiro Publishing, Collingwood, Australia, **2009**.
- [37] Fachagentur Nachwachsende Rohstoffe e. V. (**2019**), Anbau und Verwendung nachwachsender Rohstoffe in Deutschland, retrieved August 30, 2019, from <http://www.fnr-server.de/ftp/pdf/berichte/22004416.pdf>
- [38] K. Aleklett, *Peeking at Peak Oil*, Springer Science+Business Media, New York, **2012**.
- [39] Umweltbundesamt (**2018**), Primärenergieimporte und Versorgungssicherheit, retrieved August 31, 2019, from [https://www.umweltbundesamt.de/sites/default/files/medien/384/bilder/dateien/3\\_t\\_ab\\_primaerenergieimp-versorgungssich\\_2019-02-26.pdf](https://www.umweltbundesamt.de/sites/default/files/medien/384/bilder/dateien/3_t_ab_primaerenergieimp-versorgungssich_2019-02-26.pdf)
- [40] C. Graves, S. D. Ebbesen, M. Mogensen, K. S. Lackner, *Renewable Sustainable Energy Rev.* **2011**, 15, 1-23.
- [41] N. Qureshi, D. B. Hodge, A. Vertès, *Biorefineries: Integrated biochemical processes for liquid biofuels*, Elsevier, Amsterdam - Oxford - Waltham, **2014**.
- [42] PlasticsEurope (**2018**), Plastics - the Facts 2018, retrieved September 1, 2019, from [https://www.plasticseurope.org/application/files/6315/4510/9658/Plastics\\_the\\_facts\\_2018\\_AF\\_web.pdf](https://www.plasticseurope.org/application/files/6315/4510/9658/Plastics_the_facts_2018_AF_web.pdf)
- [43] S. H. Lee, A. Cyriac, J. Y. Jeon, B. Y. Lee, *Polym. Chem.* **2012**, 3, 1215-1220.
- [44] O. Hauenstein, M. Reiter, S. Agarwal, B. Rieger, A. Greiner, *Green Chem.* **2016**, 18, 760-770.
- [45] M. A. Meier, J. O. Metzger, U. S. Schubert, *Chem. Soc. Rev.* **2007**, 36, 1788-1802.
- [46] L. Maisonneuve, T. Lebarbé, E. Grau, H. Cramail, *Polym. Chem.* **2013**, 4, 5472-5517.
- [47] B. Braun, J. R. Dorgan, L. O. Hollingsworth, *Biomacromolecules* **2012**, 13, 2013-2019.
- [48] J. O. Metzger, A. Hüttermann, *Naturwissenschaften* **2009**, 96, 279-288.
- [49] R. Mülhaupt, *Chimia* **1996**, 50, 191-198.
- [50] R. Geyer, J. R. Jambeck, K. L. Law, *Sci. Adv.* **2017**, 3, e1700782.
- [51] C. J. Moore, *Environ. Res.* **2008**, 108, 131-139.
- [52] J. G. B. Derraik, *Mar. Pollut. Bull.* **2002**, 44, 842-852.
- [53] E. L. Teuten, J. M. Saquing, D. R. Knappe, M. A. Barlaz, S. Jonsson, A. Björn, S. J. Rowland, R. C. Thompson, T. S. Galloway, R. Yamashita, *Philosophical Transactions of the Royal Society B: Biological Sciences* **2009**, 364, 2027-2045.
- [54] Y. Mato, T. Isobe, H. Takada, H. Kanehiro, C. Ohtake, T. Kaminuma, *Environ. Sci. Technol.* **2001**, 35, 318-324.

- [55] A. Künkel, J. Becker, L. Börger, J. Hamprecht, S. Koltzenburg, R. Loos, M. B. Schick, K. Schlegel, C. Sinkel, G. Skupin, *Ullmann's Encyclopedia of Industrial Chemistry* **2000**, 1-29.
- [56] R. Wei, W. Zimmermann, *Microb. Biotechnol.* **2017**, *10*, 1308-1322.
- [57] N. Lucas, C. Bienaime, C. Belloy, M. Queneudec, F. Silvestre, J.-E. Nava-Saucedo, *Chemosphere* **2008**, *73*, 429-442.
- [58] X. Wang, X. Guo, Y. Yang, S. Tao, B. Xing, *Environ. Sci. Technol.* **2011**, *45*, 2124-2130.
- [59] I. Chorkendorff, J. W. Niemantsverdriet, *Concepts of modern catalysis and kinetics*, Wiley-VCH, Weinheim, **2007**.
- [60] J. A. Moulijn, P. W. van Leeuwen, R. A. van Santen, *Catalysis: an integrated approach to homogeneous, heterogeneous and industrial catalysis, Vol. 79*, Elsevier, Amsterdam, **1993**.
- [61] R. A. Sheldon, J. K. Kochi, *Metal-catalyzed oxidations of organic compounds: mechanistic principles and synthetic methodology including biochemical processes*, Academic Press, New York, **1981**.
- [62] A. Chauvel, B. Delmon, W. F. Hölderich, *Appl. Catal., A* **1994**, *115*, 173-217.
- [63] D. R. Lide, *CRC handbook of chemistry and physics, Internet Version* **2005**, 14-17.
- [64] A. J. Hunt (Ed.), *Element Recovery and Sustainability*, The Royal Society of Chemistry, Cambridge, **2013**.
- [65] M. North, *Sustainable Catalysis: With Non-endangered Metals, Part 1*, Royal Society of Chemistry, Cambridge, **2015**.
- [66] A. J. Hunt, A. S. Matharu, A. H. King, J. H. Clark, *Green Chem.* **2015**, *17*, 1949-1950.
- [67] E. Breitmaier, *Terpenes: Flavors, Fragrances, Pharmaca, Pheromones*, Wiley-VCH, Weinheim, **2006**.
- [68] G. P. Moss, P. A. S. Smith, D. Tavernier, in *Pure Appl. Chem.* **1995**, 1307.
- [69] L. Ružička, in *Pure Appl. Chem.* **1963**, 493.
- [70] L. Ružička, *Experientia* **1953**, *9*, 357-367.
- [71] A. Kekulé, *Lehrbuch der organischen Chemie., Vol. 2*, Verlag von Ferdinand Enke, Erlangen, **1866**.
- [72] A. Corma, S. Iborra, A. Velty, *Chem. Rev.* **2007**, *107*, 2411-2502.
- [73] J. L. F. Monteiro, C. O. Veloso, *Top. Catal.* **2004**, *27*, 169-180.
- [74] A. Gandini, T. M. Lacerda, *Prog. Polym. Sci.* **2015**, *48*, 1-39.
- [75] R. Ciriminna, M. Lomeli-Rodriguez, P. D. Cara, J. A. Lopez-Sanchez, M. Pagliaro, *Chem. Commun.* **2014**, *50*, 15288-15296.
- [76] A. Gandini, *Green Chem.* **2011**, *13*, 1061-1083.

- [77] A. Pandey, R. Höfer, M. Taherzadeh, M. Nampoothiri, C. Larroche, *Industrial biorefineries and white biotechnology*, Elsevier, Amsterdam - Oxford - Waltham, **2015**.
- [78] A. M. Balu, V. Budarin, P. S. Shuttleworth, L. A. Pfaltzgraff, K. Waldron, R. Luque, J. H. Clark, *ChemSusChem* **2012**, *5*, 1694-1697.
- [79] W. Schwab, C. Fuchs, F.-C. Huang, *Eur. J. Lipid Sci. Technol.* **2013**, *115*, 3-8.
- [80] K. A. Swift, *Top. Catal.* **2004**, *27*, 143-155.
- [81] N. Ravasio, F. Zaccheria, M. Guidotti, R. Psaro, *Top. Catal.* **2004**, *27*, 157-168.
- [82] A. Severino, J. Vital, L. Lobo, *Stud. Surf. Sci. Catal.* **1993**, *78*, 685-692.
- [83] I. L. Simakova, Y. S. Solkina, B. L. Moroz, O. A. Simakova, S. I. Reshetnikov, I. P. Prosvirin, V. I. Bukhtiyarov, V. N. Parmon, D. Y. Murzin, *Appl. Catal., A* **2010**, *385*, 136-143.
- [84] C. Volzone, O. Masini, N. Comelli, L. Grzona, E. Ponzi, M. Ponzi, *Mater. Chem. Phys.* **2005**, *93*, 296-300.
- [85] A. I. Allahverdiev, S. Irandoust, B. Andersson, D. Y. Murzin, *Appl. Catal., A* **2000**, *198*, 197-206.
- [86] S. Findik, G. Gündüz, *J. Am. Oil Chem. Soc.* **1997**, *74*, 1145-1151.
- [87] H. Surburg, J. Panten, *Common fragrance and flavor materials: preparation, properties and uses*, Wiley-VCH, Weinheim, **2016**.
- [88] A. Stanislaus, L. Yeddanapalli, *Can. J. Chem.* **1972**, *50*, 113-118.
- [89] V. Krishnasamy, *Aust. J. Chem.* **1980**, *33*, 1313-1321.
- [90] D. Buhl, D. Roberge, W. Hölderich, *Appl. Catal., A* **1999**, *188*, 287-299.
- [91] D. M. Roberge, D. Buhl, J. P. M. Niederer, W. F. Hölderich, *Appl. Catal., A* **2001**, *215*, 111-124.
- [92] E. F. Murphy, T. Mallat, A. Baiker, *Catal. Today* **2000**, *57*, 115-126.
- [93] H. Mimoun, *Chimia* **1996**, *50*, 620-625.
- [94] P. A. Wender, T. P. Mucciario, *J. Am. Chem. Soc.* **1992**, *114*, 5878-5879.
- [95] U. Neuenschwander, F. Guignard, I. Hermans, *ChemSusChem* **2010**, *3*, 75-84.
- [96] Y. Cao, Y. Li, H. Yu, F. Peng, H. Wang, *Catal. Sci. Technol.* **2015**, *5*, 3935-3944.
- [97] L. Menini, M. J. da Silva, M. F. Lelis, J. D. Fabris, R. M. Lago, E. V. Gusevskaya, *Appl. Catal., A* **2004**, *269*, 117-121.
- [98] A. Mouret, L. Leclercq, A. Mühlbauer, V. Nardello-Rataj, *Green Chem.* **2014**, *16*, 269-278.
- [99] T. Mukaiyama, T. Yamada, *Bull. Chem. Soc. Jpn.* **1995**, *68*, 17-35.
- [100] M. K. Lajunen, T. Maunula, A. M. Koskinen, *Tetrahedron* **2000**, *56*, 8167-8171.

- [101] N. V. Maksimchuk, K. A. Kovalenko, S. S. Arzumanov, Y. A. Chesalov, M. S. Melgunov, A. G. Stepanov, V. P. Fedin, O. A. Kholdeeva, *Inorg. Chem.* **2010**, *49*, 2920-2930.
- [102] P. A. Robles-Dutenhefner, B. B. Brandão, L. F. De Sousa, E. V. Gusevskaya, *Appl. Catal., A* **2011**, *399*, 172-178.
- [103] I. Y. Skobelev, A. B. Sorokin, K. A. Kovalenko, V. P. Fedin, O. A. Kholdeeva, *J. Catal.* **2013**, *298*, 61-69.
- [104] O. A. Kholdeeva, I. Y. Skobelev, I. D. Ivanchikova, K. A. Kovalenko, V. P. Fedin, A. B. Sorokin, *Catal. Today* **2014**, *238*, 54-61.
- [105] R. A. Sheldon, M. Wallau, I. W. Arends, U. Schuchardt, *Acc. Chem. Res.* **1998**, *31*, 485-493.
- [106] A. S. Demir, M. Emrullahoglu, *Curr. Org. Synth.* **2007**, *4*, 321-350.
- [107] J. Gilmore, J. Mellor, *J. Chem. Soc. C* **1971**, 2355-2357.
- [108] B. B. Snider, *Chem. Rev.* **1996**, *96*, 339-364.
- [109] B. B. Snider, L. Han, C. Xie, *J. Org. Chem.* **1997**, *62*, 6978-6984.
- [110] K. Ravikumar, F. Barbier, J.-P. Bégué, D. Bonnet-Delpon, *Tetrahedron* **1998**, *54*, 7457-7464.
- [111] T. K. Shing, Y.-Y. Yeung, P. L. Su, *Org. Lett.* **2006**, *8*, 3149-3151.
- [112] R. Raja, G. Sankar, J. M. Thomas, *Chem. Commun.* **1999**, 829-830.
- [113] M. N. Timofeeva, V. N. Panchenko, A. A. Abel, N. A. Khan, I. Ahmed, A. B. Ayupov, K. P. Volcho, S. H. Jhung, *J. Catal.* **2014**, *311*, 114-120.
- [114] J. B. Lewis, G. W. Hedrick, *J. Org. Chem.* **1965**, *30*, 4271-4275.
- [115] F. Vermoortele, R. Ameloot, L. Alaerts, R. Matthessen, B. Carlier, E. V. R. Fernandez, J. Gascon, F. Kapteijn, D. E. De Vos, *J. Mater. Chem.* **2012**, *22*, 10313-10321.
- [116] W. Hölderich, J. Röseler, G. Heitmann, A. Liebens, *Catal. Today* **1997**, *37*, 353-366.
- [117] A. Liebens, C. Mahaim, W. Hölderich, *Stud. Surf. Sci. Catal.* **1997**, *108*, 587-594.
- [118] M. R. Thomsett, T. E. Storr, O. R. Monaghan, R. A. Stockman, S. M. Howdle, *Green Materials* **2016**, *4*, 115-134.
- [119] A. J. D. Silvestre, A. Gandini, in *Monomers, Polymers and Composites from Renewable Resources* (Eds.: M. N. Belgacem, A. Gandini), Elsevier, Amsterdam, **2008**, pp. 17-38.
- [120] W. J. Roberts, A. R. Day, *J. Am. Chem. Soc.* **1950**, *72*, 1226-1230.
- [121] J. Lu, M. Kamigaito, M. Sawamoto, T. Higashimura, Y.-X. Deng, *Macromolecules* **1997**, *30*, 27-31.
- [122] N. A. Kukhta, I. V. Vasilenko, S. V. Kostjuk, *Green Chem.* **2011**, *13*, 2362-2364.



- [123] P. Yu, A. L. Li, H. Liang, J. Lu, *J. Polym. Sci. Part A: Polym. Chem.* **2007**, *45*, 3739-3746.
- [124] K. Satoh, H. Sugiyama, M. Kamigaito, *Green Chem.* **2006**, *8*, 878-882.
- [125] K. Satoh, A. Nakahara, K. Mukunoki, H. Sugiyama, H. Saito, M. Kamigaito, *Polym. Chem.* **2014**, *5*, 3222-3230.
- [126] T. Higashimura, J. Lu, M. Kamigaito, M. Sawamoto, Y. X. Deng, *Macromolecular Chem. Phys.* **1992**, *193*, 2311-2321.
- [127] J. Lu, M. Kamigaito, M. Sawamoto, T. Higashimura, Y. X. Deng, *J. Appl. Polym. Sci.* **1996**, *61*, 1011-1016.
- [128] M. Modena, R. Bates, C. Marvel, *J. Polym. Sci. Part A: General Papers* **1965**, *3*, 949-960.
- [129] F. J. B. Brum, F. N. Laux, M. M. C. Forte, *Des. Monomers Polym.* **2013**, *16*, 291-301.
- [130] A. M. Ramos, L. S. Lobo, J. M. Bordado, *Macromol Symp.* 1998, *127*, 43-50.
- [131] A. M. Adur, F. Williams, *J. Polym. Sci., Polym. Lett. Ed.:(United States)* **1981**, *19*.
- [132] S. Sharma, A. Srivastava, *Journal of Macromolecular Science, Part A* **2003**, *40*, 593-603.
- [133] S. Sharma, A. Srivastava, *Indian J. Chem. Technol.* **2005**, *12*, 62-67.
- [134] S. Sharma, A. Srivastava, *Polym.-Plast. Technol. Eng.* **2003**, *42*, 485-502.
- [135] S. Sharma, A. Srivastava, *Eur. Polym. J.* **2004**, *40*, 2235-2240.
- [136] S. Sharma, A. Srivastava, *Des. Monomers Polym.* **2006**, *9*, 503-516.
- [137] K. Satoh, M. Matsuda, K. Nagai, M. Kamigaito, *J. Am. Chem. Soc.* **2010**, *132*, 10003-10005.
- [138] M. Matsuda, K. Satoh, M. Kamigaito, *Macromolecules* **2013**, *46*, 5473-5482.
- [139] A. Behr, L. Johnen, *ChemSusChem* **2009**, *2*, 1072-1095.
- [140] P. Sarkar, A. K. Bhowmick, *RSC Adv.* **2014**, *4*, 61343-61354.
- [141] J. Hilschmann, G. Kali, *Eur. Polym. J.* **2015**, *73*, 363-373.
- [142] J. M. Bolton, M. A. Hillmyer, T. R. Hoye, *ACS Macro Lett.* **2014**, *3*, 717-720.
- [143] P. Horrillo-Martínez, M.-A. Virolleaud, C. Jaekel, *ChemCatChem* **2010**, *2*, 175-181.
- [144] H. Miyaji, K. Satoh, M. Kamigaito, *Angew. Chem. Int. Ed.* **2016**, *55*, 1372-1376.
- [145] M. Sainz, J. Souto, D. Regentova, M. Johansson, S. Timhagen, D. J. Irvine, P. Buijssen, C. Koning, R. Stockman, S. M. Howdle, *Polym. Chem.* **2016**, *7*, 2882-2887.
- [146] R. C. Jeske, A. M. DiCiccio, G. W. Coates, *J. Am. Chem. Soc.* **2007**, *129*, 11330-11331.
- [147] D. R. Moore, M. Cheng, E. B. Lobkovsky, G. W. Coates, *J. Am. Chem. Soc.* **2003**, *125*, 11911-11924.

- [148] C. Robert, F. de Montigny, C. M. Thomas, *Nat. Commun.* **2011**, *2*, 586.
- [149] E. H. Nejad, A. Paoniasari, C. G. van Melis, C. E. Koning, R. Duchateau, *Macromolecules* **2013**, *46*, 631-637.
- [150] N. J. Van Zee, G. W. Coates, *Angew. Chem. Int. Ed.* **2015**, *54*, 2665-2668.
- [151] M. Cheng, E. B. Lobkovsky, G. W. Coates, *J. Am. Chem. Soc.* **1998**, *120*, 11018-11019.
- [152] C. M. Byrne, S. D. Allen, E. B. Lobkovsky, G. W. Coates, *J. Am. Chem. Soc.* **2004**, *126*, 11404-11405.
- [153] K. Gurudutt, S. Rao, P. Srinivas, *Flavour Fragr. J.* **1992**, *7*, 343-345.
- [154] O. Hauenstein, S. Agarwal, A. Greiner, *Nat. Commun.* **2016**, *7*, 11862.
- [155] N. Kindermann, À. Cristòfol, A. W. Kleij, *ACS Catalysis* **2017**, *7*, 3860-3863.
- [156] C. Li, R. J. Sablong, C. E. Koning, *Angew. Chem.* **2016**, *128*, 11744-11748.
- [157] C. Martín, A. W. Kleij, *Macromolecules* **2016**, *49*, 6285-6295.
- [158] T. Stößer, C. Li, J. Unruangsri, P. K. Saini, R. J. Sablong, M. A. Meier, C. K. Williams, C. Koning, *Polym. Chem.* **2017**, *8*, 6099-6105.
- [159] F. Auriemma, C. De Rosa, M. R. Di Caprio, R. Di Girolamo, W. C. Ellis, G. W. Coates, *Angew. Chem. Int. Ed.* **2015**, *54*, 1215-1218.
- [160] H. J. Park, C. Y. Ryu, J. V. Crivello, *J. Polym. Sci. Part A: Polym. Chem.* **2013**, *51*, 109-117.
- [161] T. Posner, *Berichte der deutschen chemischen Gesellschaft* **1905**, *38*, 646-657.
- [162] M. Firdaus, *Asian J. Org. Chem.* **2017**, *6*, 1702-1714.
- [163] H. C. Kolb, M. Finn, K. B. Sharpless, *Angew. Chem. Int. Ed.* **2001**, *40*, 2004-2021.
- [164] U. Biermann, W. Butte, R. Koch, P. A. Fokou, O. Türünç, M. A. R. Meier, J. O. Metzger, *Chem. Eur. J.* **2012**, *18*, 8201-8207.
- [165] C. Chatgililoglu, A. Altieri, H. Fischer, *J. Am. Chem. Soc.* **2002**, *124*, 12816-12823.
- [166] K. W. E. Sy Piecco, A. M. Aboelenen, J. R. Pyle, J. R. Vicente, D. Gautam, J. Chen, *ACS Omega* **2018**, *3*, 14327-14332.
- [167] M. Firdaus, L. Montero de Espinosa, M. A. Meier, *Macromolecules* **2011**, *44*, 7253-7262.
- [168] M. Firdaus, M. A. Meier, *Green Chem.* **2013**, *15*, 370-380.
- [169] C. Marvel, L. E. Olson, *J. Polym. Sci.* **1957**, *26*, 23-28.
- [170] M. Firdaus, M. A. Meier, U. Biermann, J. O. Metzger, *Eur. J. Lipid Sci. Technol.* **2014**, *116*, 31-36.
- [171] S. Khan, Z. Wang, R. Wang, L. Zhang, *Mate. Sci. Eng. C* **2016**, *67*, 554-560.
- [172] M. Colonna, C. Berti, M. Fiorini, E. Binassi, M. Mazzacurati, M. Vannini, S. Karanam, *Green Chem.* **2011**, *13*, 2543-2548.

- [173] S. Kobayashi, C. Lu, T. R. Hoye, M. A. Hillmyer, *J. Am. Chem. Soc.* **2009**, *131*, 7960-7961.
- [174] C. C. C. R. de Carvalho, M. M. R. da Fonseca, *Food Chem.* **2006**, *95*, 413-422.
- [175] J. R. Lowe, W. B. Tolman, M. A. Hillmyer, *Biomacromolecules* **2009**, *10*, 2003-2008.
- [176] J. R. Lowe, M. T. Martello, W. B. Tolman, M. A. Hillmyer, *Polym. Chem.* **2011**, *2*, 702-708.
- [177] D. Zhang, M. A. Hillmyer, W. B. Tolman, *Biomacromolecules* **2005**, *6*, 2091-2095.
- [178] M. A. Hillmyer, W. B. Tolman, *Acc. Chem. Res.* **2014**, *47*, 2390-2396.
- [179] C. L. Wanamaker, L. E. O'Leary, N. A. Lynd, M. A. Hillmyer, W. B. Tolman, *Biomacromolecules* **2007**, *8*, 3634-3640.
- [180] J. Shin, M. T. Martello, M. Shrestha, J. E. Wissinger, W. B. Tolman, M. A. Hillmyer, *Macromolecules* **2010**, *44*, 87-94.
- [181] J. Shin, Y. Lee, W. B. Tolman, M. A. Hillmyer, *Biomacromolecules* **2012**, *13*, 3833-3840.
- [182] M. Imoto, H. Sakurai, T. Kono, *J. Polym. Sci.* **1961**, *50*, 467-473.
- [183] J. Kondelíková, J. Šejba, Z. Černý, J. Králíček, *Macromol. Rapid. Commun.* **1980**, *1*, 35-39.
- [184] J. Kondelíková, J. Šejba, J. Králíček, Z. Smrčková, *Die Angewandte Makromolekulare Chemie* **1980**, *88*, 103-111.
- [185] N. Komatsu, S. Simizu, T. Sugita, *Synth. Commun.* **1992**, *22*, 277-279.
- [186] M. Winnacker, S. Vagin, V. Auer, B. Rieger, *Macromol. Chem. Phys.* **2014**, *215*, 1654-1660.
- [187] M. Winnacker, A. Tischner, M. Neumeier, B. Rieger, *RSC Advances* **2015**, *5*, 77699-77705.
- [188] M. Winnacker, M. Neumeier, X. Zhang, C. M. Papadakis, B. Rieger, *Macromol. Rapid Commun.* **2016**, *37*, 851-857.
- [189] K. Horie, M. Barón, R. B. Fox, J. He, M. Hess, J. Kahovec, T. Kitayama, P. Kubisa, E. Maréchal, W. Mormann, R. F. T. Stepto, D. Tabak, J. Vohlídal, E. S. Wilks, W. J. Work, *Pure Appl. Chem.* **2004**, *76*, 889.
- [190] R. Auvergne, S. Caillol, G. David, B. Boutevin, J.-P. Pascault, *Chem. Rev.* **2014**, *114*, 1082-1115.
- [191] J. M. Delancey, M. D. Cavazza, M. G. Rendos, C. J. Ulisse, S. G. Palumbo, R. T. Mathers, *J. Polym. Sci. Part A: Polym. Chem.* **2011**, *49*, 3719-3727.
- [192] C. H. Mckeever, R. N. Washburne, *Process for the preparation of methane diamine*, U.S. Patent Nr. 2,955,138, **1960**.
- [193] Y. Xin, H. Uyama, *J. Polym. Res.* **2012**, *19*, 15.

- [194] K. Xu, M. Chen, K. Zhang, J. Hu, *Polymer* **2004**, *45*, 1133-1140.
- [195] M. Shibata, M. Asano, *J. Appl. Polym. Sci.* **2013**, *129*, 301-309.
- [196] B. Sibaja, J. Sargent, M. L. Auad, *J. Appl. Polym. Sci.* **2014**, *131*.
- [197] P. A. Wilbon, F. Chu, C. Tang, *Macromol. Rapid Commun.* **2013**, *34*, 8-37.
- [198] J. Zhang, *Rosin-based chemicals and polymers*, Smithers Rapra, Shawbury, **2012**.
- [199] G. M. Wu, Z. W. Kong, H. Huang, J. Chen, F. X. Chu, *J. Appl. Polym. Sci.* **2009**, *113*, 2894-2901.
- [200] M. Claudino, J.-M. Mathevet, M. Jonsson, M. Johansson, *Polym. Chem.* **2014**, *5*, 3245-3260.
- [201] M. Claudino, M. Jonsson, M. Johansson, *RSC Adv.* **2013**, *3*, 11021-11034.
- [202] M. Claudino, M. Jonsson, M. Johansson, *RSC Adv.* **2014**, *4*, 10317-10329.
- [203] K. Hearon, L. D. Nash, J. N. Rodriguez, A. T. Lonnecker, J. E. Raymond, T. S. Wilson, K. L. Wooley, D. J. Maitland, *Adv. Mat.* **2014**, *26*, 1552-1558.
- [204] J. Yan, S. Ariyasivam, D. Weerasinghe, J. He, B. Chisholm, Z. Chen, D. Webster, *Polym. Int.* **2012**, *61*, 602-608.
- [205] H. Morinaga, M. Sakamoto, *Tetrahedron Lett.* **2017**, *58*, 2438-2440.
- [206] M. Bähr, A. Bitto, R. Mülhaupt, *Green Chem.* **2012**, *14*, 1447-1454.
- [207] G. Fiorani, M. Stuck, C. Martín, M. M. Belmonte, E. Martin, E. C. Escudero-Adán, A. W. Kleij, *ChemSusChem* **2016**, *9*, 1304-1311.
- [208] C. J. Whiteoak, N. Kielland, V. Laserna, F. Castro-Gómez, E. Martin, E. C. Escudero-Adán, C. Bo, A. W. Kleij, *Chem. - Eur. J.* **2014**, *20*, 2264-2275.
- [209] C. J. Whiteoak, N. Kielland, V. Laserna, E. C. Escudero-Adán, E. Martin, A. W. Kleij, *J. Am. Chem. Soc.* **2013**, *135*, 1228-1231.
- [210] V. Schimpf, B. S. Ritter, P. Weis, K. Parison, R. Mülhaupt, *Macromolecules* **2017**, *50*, 944-955.
- [211] EC-European Commission, *Closing the loop – An EU action plan for the circular economy*, Brüssel, **2015**.
- [212] A. Llevot, P. K. Dannecker, M. von Czapiewski, L. C. Over, Z. Soeyler, M. A. Meier, *Chem. - Eur. J.* **2016**, *22*, 11510-11521.
- [213] Y. S. Raupp, C. Yildiz, W. Kleist, M. A. Meier, *Appl. Catal., A* **2017**, *546*, 1-6.
- [214] Y. S. Raupp, Master thesis, Karlsruhe Institute of Technology (KIT) (Karlsruhe), **2016**.
- [215] M. Salavati-Niasari, S. Abdolmohammadi, M. Oftadeh, *J. Coord. Chem.* **2008**, *61*, 2837-2851.
- [216] M. V. Patil, M. K. Yadav, R. V. Jasra, *J. Mol. Catal. A: Chem.* **2007**, *277*, 72-80.
- [217] M. L. Kantam, B. P. C. Rao, R. S. Reddy, N. Sekhar, B. Sreedhar, B. Choudary, *J. Mol. Catal. A: Chem.* **2007**, *272*, 1-5.

- [218] Q. Tang, Q. Zhang, H. Wu, Y. Wang, *J. Catal.* **2005**, *230*, 384-397.
- [219] Q. Tang, Y. Wang, J. Liang, P. Wang, Q. Zhang, H. Wan, *Chem. Commun.* **2004**, 440-441.
- [220] K. M. Jinka, J. Sebastian, R. V. Jasra, *J. Mol. Catal. A: Chem.* **2007**, *274*, 33-41.
- [221] T. Mallat, A. Baiker, *Catal. Sci. Technol.* **2011**, *1*, 1572-1583.
- [222] M. J. Beier, W. Kleist, M. T. Wharmby, R. Kissner, B. Kimmerle, P. A. Wright, J. D. Grunwaldt, A. Baiker, *Chem. - Eur. J.* **2012**, *18*, 887-898.
- [223] Z. Opre, T. Mallat, A. Baiker, *J. Catal.* **2007**, *245*, 482-486.
- [224] P. Timmanagoudar, G. Hiremath, S. Nandibewoor, *J. Indian Chem. Soc.* **1997**, *74*, 296-298.
- [225] A. Bhunia, M. A. Gotthardt, M. Yadav, M. T. Gamer, A. Eichhöfer, W. Kleist, P. W. Roesky, *Chem. - Eur. J.* **2013**, *19*, 1986-1995.
- [226] K. Guillois, S. Mangematin, A. Tuel, V. Caps, *Catal. Today* **2013**, *203*, 111-115.
- [227] D. Prat, A. Wells, J. Hayler, H. Sneddon, C. R. McElroy, S. Abou-Shehada, P. J. Dunn, *Green Chem.* **2016**, *18*, 288-296.
- [228] I. Arends, R. Sheldon, *Appl. Catal., A* **2001**, *212*, 175-187.
- [229] S. Proch, J. Herrmannsdörfer, R. Kempe, C. Kern, A. Jess, L. Seyfarth, J. Senker, *Chem. - Eur. J.* **2008**, *14*, 8204-8212.
- [230] F. Carson, S. Agrawal, M. Gustafsson, A. Bartoszewicz, F. Moraga, X. Zou, B. Martín-Matute, *Chem. - Eur. J.* **2012**, *18*, 15337-15344.
- [231] F. X. L. i Xamena, A. Abad, A. Corma, H. Garcia, *J. Catal.* **2007**, *250*, 294-298.
- [232] K. Brown, S. Zolezzi, P. Aguirre, D. Venegas-Yazigi, V. Paredes-García, R. Baggio, M. A. Novak, E. Spodine, *Dalton Trans.* **2009**, 1422-1427.
- [233] K. Leus, I. Muylaert, M. Vandichel, G. B. Marin, M. Waroquier, V. Van Speybroeck, P. Van Der Voort, *Chem. Commun.* **2010**, *46*, 5085-5087.
- [234] M. A. Gotthardt, A. Beilmann, R. Schoch, J. Engelke, W. Kleist, *RSC Adv.* **2013**, *3*, 10676-10679.
- [235] M. A. Gotthardt, R. Schoch, T. S. Brunner, M. Bauer, W. Kleist, *ChemPlusChem* **2015**, *80*, 188-195.
- [236] T. Loiseau, C. Serre, C. Huguenard, G. Fink, F. Taulelle, M. Henry, T. Bataille, G. Férey, *Chem. - Eur. J.* **2004**, *10*, 1373-1382.
- [237] H. Blattmann, M. Fleischer, M. Bähr, R. Mülhaupt, *Macromol. Rapid Commun.* **2014**, *35*, 1238-1254.
- [238] Y. Li, K. Junge, M. Beller, *ChemCatChem* **2013**, *5*, 1072-1074.
- [239] L. F. S. Souza, P. R. R. Ferreira, J. L. de Medeiros, R. M. B. Alves, O. Q. F. Araújo, *ACS Sustainable Chem. Eng.* **2014**, *2*, 62-69.

- [240] V. Laserna, G. Fiorani, C. J. Whiteoak, E. Martin, E. Escudero-Adán, A. W. Kleij, *Angew. Chem. Int. Ed.* **2014**, *53*, 10416-10419.
- [241] B. Wang, S. Yang, L. Min, Y. Gu, Y. Zhang, X. Wu, L. Zhang, E. H. M. Elageed, S. Wu, G. Gao, *Adv. Synth. Catal.* **2014**, *356*, 3125-3134.
- [242] M. Fleischer, H. Blattmann, R. Mülhaupt, *Green Chem.* **2013**, *15*, 934-942.
- [243] V. Besse, F. Camara, C. Voirin, R. Auvergne, S. Caillol, B. Boutevin, *Polym. Chem.* **2013**, *4*, 4545-4561.
- [244] M. S. Kathalewar, P. B. Joshi, A. S. Sabnis, V. C. Malshe, *RSC Adv.* **2013**, *3*, 4110-4129.
- [245] M. Bähr, R. Mülhaupt, *Green Chem.* **2012**, *14*, 483-489.
- [246] M. Philipp, R. Bernhard, H. A. Gasteiger, B. Rieger, *J. Electrochem. Soc.* **2015**, *162*, A1319-A1326.
- [247] L. Zhang, Y. Luo, Z. Hou, Z. He, W. Eli, *J. Am. Oil Chem. Soc.* **2014**, *91*, 143-150.
- [248] A. Kowalewicz, M. Wojtyniak, *Proceedings of the institution of mechanical engineers, Part D: Journal of automobile engineering* **2005**, *219*, 103-125.
- [249] T. Sakakura, K. Kohno, *Chem. Commun.* **2009**, 1312-1330.
- [250] A.-A. G. Shaikh, S. Sivaram, *Chem. Rev.* **1996**, *96*, 951-976.
- [251] B. Schaffner, F. Schaffner, S. P. Verevkin, A. Borner, *Chem. Rev.* **2010**, *110*, 4554-4581.
- [252] P. Tundo, M. Selva, *Acc. Chem. Res.* **2002**, *35*, 706-716.
- [253] P. Tundo, M. Musolino, F. Aricò, *Green Chem.* **2018**, *20*, 28-85.
- [254] M. North, R. Pasquale, C. Young, *Green Chem.* **2010**, *12*, 1514-1539.
- [255] M. Wang, N. Zhao, Wei, Y. Sun, *Ind. Eng. Chem. Res.* **2005**, *44*, 7596-7599.
- [256] P. Tundo, *Pure Appl. Chem.* **2012**, *84*, 411-423.
- [257] P. Tundo, L. Rossi, A. Loris, *J. Org. Chem.* **2005**, *70*, 2219-2224.
- [258] J. H. Clements, *Ind. Eng. Chem. Res.* **2003**, *42*, 663-674.
- [259] M. Taherimehr, J. P. C. C. Sertã, A. W. Kleij, C. J. Whiteoak, P. P. Pescarmona, *ChemSusChem* **2015**, *8*, 1034-1042.
- [260] W. Desens, C. Kohrt, M. Frank, T. Werner, *ChemSusChem* **2015**, *8*, 3815-3822.
- [261] R. Lindner, M. L. Lejkowski, S. Lavy, P. Deglmann, K. T. Wiss, S. Zarbakhsh, L. Meyer, M. Limbach, *ChemCatChem* **2014**, *6*, 618-625.
- [262] M. E. Wilhelm, M. H. Anthofer, M. Cokoja, I. I. E. Markovits, W. A. Herrmann, F. E. Kühn, *ChemSusChem* **2014**, *7*, 1357-1360.
- [263] H. Büttner, J. Steinbauer, T. Werner, *ChemSusChem* **2015**, *8*, 2655-2669.
- [264] C. Kohrt, T. Werner, *ChemSusChem* **2015**, *8*, 2031-2034.
- [265] A.-L. Girard, N. Simon, M. Zanatta, S. Marmitt, P. Gonçalves, J. Dupont, *Green Chem.* **2014**, *16*, 2815-2825.

- [266] T. Yu, R. G. Weiss, *Green Chem.* **2012**, *14*, 209-216.
- [267] T. Werner, N. Tenhumberg, *J. CO<sub>2</sub> Util.* **2014**, *7*, 39-45.
- [268] Y. M. Shen, W. L. Duan, M. Shi, *Eur. J. Org. Chem.* **2004**, *2004*, 3080-3089.
- [269] S. Arayachukiat, C. Kongtes, A. Barthel, S. V. C. Vummaleti, A. Poater, S. Wannakao, L. Cavallo, V. D'Elia, *ACS Sustainable Chem. Eng.* **2017**, *5*, 6392-6397.
- [270] J. M. Coxon, E. Dansted, M. P. Hartshorn, K. E. Richards, *Tetrahedron* **1969**, *25*, 3307-3312.
- [271] M. Peña-López, H. Neumann, M. Beller, *Eur. J. Org. Chem.* **2016**, *2016*, 3721-3727.
- [272] Y. Zhu, G. Wu, X. Zhu, Y. Ma, X. Zhao, Y. Li, Y. Yuan, J. Yang, S. Yu, F. Shao, M. Lei, *J. Med. Chem.* **2010**, *53*, 8619-8626.
- [273] D. B. Bleier, M. J. Elrod, *J. Phys. Chem. A* **2013**, *117*, 4223-4232.
- [274] R. C. Pratt, B. G. Lohmeijer, D. A. Long, R. M. Waymouth, J. L. Hedrick, *J. Am. Chem. Soc.* **2006**, *128*, 4556-4557.
- [275] P.-K. Dannecker, M. A. Meier, *Sci. Rep.* **2019**, *9*, 9858.
- [276] E. R. Baral, J. H. Lee, J. G. Kim, *J. Org. Chem.* **2018**, *83*, 11768-11776.
- [277] W. A. Herrmann, R. W. Fischer, D. W. Marz, *Angew. Chem.* **1991**, *103*, 1706-1709.
- [278] A. L. de Villa, D. E. De Vos, C. C. de Montes, P. A. Jacobs, *Tetrahedron Lett.* **1998**, *39*, 8521-8524.
- [279] A. Wang, H. Jiang, *J. Org. Chem.* **2010**, *75*, 2321-2326.
- [280] H. Sardon, A. Pascual, D. Mecerreyes, D. Taton, H. Cramail, J. L. Hedrick, *Macromolecules* **2015**, *48*, 3153-3165.
- [281] D. Chattopadhyay, D. C. Webster, *Prog. Polym. Sci.* **2009**, *34*, 1068-1133.
- [282] H.-W. Engels, H.-G. Pirkl, R. Albers, R. W. Albach, J. Krause, A. Hoffmann, H. Casselmann, J. Dormish, *Angew. Chem. Int. Ed.* **2013**, *52*, 9422-9441.
- [283] A. Bossion, R. H. Aguirresarobe, L. Irusta, D. Taton, H. Cramail, E. Grau, D. Mecerreyes, C. Su, G. Liu, A. J. Müller, H. Sardon, *Macromolecules* **2018**, *51*, 5556-5566.
- [284] A. Cornille, M. Blain, R. Auvergne, B. Andrioletti, B. Boutevin, S. Caillol, *Polym. Chem.* **2017**, *8*, 592-604.
- [285] T. J. Terry, T. D. P. Stack, *J. Am. Chem. Soc.* **2008**, *130*, 4945-4953.
- [286] N. Afzali, S. Tangestaninejad, M. Moghadam, V. Mirkhani, A. Mechler, I. Mohammadpoor-Baltork, R. Kardanpour, F. Zadehahmadi, *Appl. Organomet. Chem.* **2018**, *32*, e3958.
- [287] L. Charbonneau, X. Foster, D. Zhao, S. Kaliaguine, *ACS Sustain. Chem. Eng.* **2018**, *6*, 5115-5121.

- [288] M. Blain, L. Jean-Gerard, R. Auvergne, D. Benazet, S. Caillol, B. Andrioletti, *Green Chem.* **2014**, *16*, 4286-4291.
- [289] R. H. Lambeth, T. J. Henderson, *Polymer* **2013**, *54*, 5568-5573.
- [290] M. K. Kiesewetter, M. D. Scholten, N. Kirn, R. L. Weber, J. L. Hedrick, R. M. Waymouth, *J. Org. Chem.* **2009**, *74*, 9490-9496.
- [291] M. Blain, A. Cornille, B. Boutevin, R. Auvergne, D. Benazet, B. Andrioletti, S. Caillol, *J. Appl. Polym. Sci.* **2017**, *134*, 44958.
- [292] H.-S. Um, J. Min, T. An, J. Choi, C. Lee, *Org. Chem. Front.* **2018**, *5*, 2158-2162.



# 11 Appendix

## 11.1 Publications

- (2) *Aerobic oxidation of  $\alpha$ -pinene catalyzed by homogeneous and MOF-based Mn catalysts*, Yasmin S. Raupp, Ceylan Yildiz, Wolfgang Kleist, Michael A. R. Meier, *Appl. Catal. A: General*, **2017**, 546, 1–6.
- (1) *Modified poly( $\epsilon$ -caprolactone)s: An efficient and renewable access via Thia-Michael addition and Baeyer–Villiger oxidation*, Matthias Winkler, Yasmin S. Raupp, Lenz A. M. Köhl, Hanna E. Wagner, and Michael A. R. Meier, *Macromolecules*, **2014**, 47, 2842–2846.

## 11.2 Conference Contributions

### Oral Presentations

- (3) *Catalytic aerobic oxidation of terpenes and follow-up chemistry towards renewable poly(hydroxy urethane)s*, 4<sup>th</sup> Conference on Green and Sustainable Chemistry of the European Chemical Society, September 22<sup>nd</sup> – 25<sup>th</sup>, 2019, Tarragona, Spain.
- (2) *Catalytic aerobic oxidation of terpenes and follow-up chemistry towards renewable poly(hydroxy urethane)s*, 7<sup>th</sup> International Conference on Biobased and Biodegradable Polymers, June 17<sup>th</sup> – 19<sup>th</sup>, 2019, Stockholm, Sweden.
- (1) *Aerobic oxidation of  $\alpha$ -pinene catalyzed by Mn(III)*, 4<sup>th</sup> International Symposium on Green Chemistry, May 16<sup>th</sup> – 19<sup>th</sup>, 2017, La Rochelle, France.

### Poster Presentations

- (6) *Aerobic oxidation of  $\alpha$ -pinene catalyzed by homogeneous and MOF-based Mn catalysts*, 4<sup>th</sup> Conference on Green and Sustainable Chemistry of the European Chemical Society, September 22<sup>nd</sup> – 25<sup>th</sup>, 2019, Tarragona, Spain.
- (5) *Aerobic oxidation of  $\alpha$ -pinene catalyzed by homogeneous and MOF-based Mn catalysts*, Annual meeting of the Gesellschaft Deutscher Chemiker (GDCh)-

division Sustainable Chemistry, September 17<sup>th</sup> – 19<sup>th</sup>, 2018, Aachen, Germany. (Poster prize)

- (4) *Aerobic oxidation of  $\alpha$ -pinene catalyzed by homogeneous and MOF-based Mn catalysts*, 3<sup>rd</sup> Green & Sustainable Chemistry Conference, May 13<sup>rd</sup> – 16<sup>th</sup>, 2018, Berlin, Germany.
- (3) *Eco-friendly aerobic oxidation of  $\alpha$ -pinene catalyzed by homogeneous and heterogeneous Mn catalysts*, 9<sup>th</sup> Workshop on Fats and Oils as Renewable Feedstock for the Chemical Industry, March 19<sup>th</sup> – 21<sup>st</sup>, 2017, Karlsruhe, Germany.
- (2) *Aerobic oxidation of  $\alpha$ -pinene using Mn(III) acetate*, Annual meeting of the Gesellschaft Deutscher Chemiker (GDCh)-division Sustainable Chemistry, September 19<sup>th</sup> – 21<sup>st</sup>, 2016, Karlsruhe, Germany.
- (1) *Modified poly( $\epsilon$ -caprolactone)s: An efficient and renewable access via Thia-Michael addition and Baeyer–Villiger oxidation*, 8<sup>th</sup> Workshop on Fats and Oils as Renewable Feedstock for the Chemical Industry, March 29<sup>th</sup> – 31<sup>st</sup>, 2015, Karlsruhe, Germany.





## Acknowledgements

An dieser Stelle möchte ich mich bei all den Personen bedanken, die mich während meiner Promotion unterstützt haben und die dazu beigetragen haben, dass die vergangenen drei Jahre zu einer wunderschönen und unvergesslichen Zeit wurden.

Mein besonderer Dank geht an Mike für das entgegengebrachte Vertrauen und die angenehme Arbeitsatmosphäre. Vielen Dank, dass deine Tür immer für uns alle offensteht und wir uns mit allen Fragen und Anliegen an dich wenden können. Danke auch, dass du die zahlreichen Grouptrips, Ausflüge, spannenden Konferenzen und meinen Auslandsaufenthalt in Stockholm ermöglicht hast, die diese Zeit zu etwas ganz Besonderem gemacht haben.

I would like to thank the whole Meier group, actual and former members, for the great working atmosphere and all the enjoyable time we spend together during group activities, BBQs after work, active breaks, and many trips and conferences. Thank you all for being more than just group members but friends!

Katha, ohne dich wäre die Zeit der Promotion und auch schon das Studium davor nicht halb so schön und spannend gewesen. Ich danke dir für all die wunderbaren Dinge und Erfahrungen, die wir zusammen erlebt und gemacht haben. Danke für deine immerwährende Unterstützung und unsere Freundschaft! Pia, mein Terpen- und Konferenz-Buddy, dir möchte ich für die großartige Unterstützung und Motivation bei allen Herausforderungen rund um die Terpene danken, für die wunderbare Zeit bei den Konferenzen in Berlin, Stockholm und Tarragona und für die vielen guten Gespräche in den Cafépausen wie auch bei den gemeinsamen Nähabenden. Danke auch an meine ehemaligen und aktuellen Laborkollegen Patrick, Rebekka, Charlotte, Rieke, Philipp und Kevin, für die schöne Zeit in 408. Ein herzlicher Dank gilt auch allen anderen Gruppenmitgliedern Ben, Marc, Eren, Luca, Maxi, Dani, Roman, Michi, Juli, Dennis, Dafni, Philip, Audrey, Baptiste, Kenny, Gregor, Stefan, Wiebke, Andi, Maike, Barbara, Susanne, Ansgar und Matthias. Thanks to all of you for the fun times and the unique support. Danke an die fleißigen Korrekturleser, Katha, Dafni, Pia, Philipp, Kevin und Philip für eure Mühe und die Korrekturvorschläge. Außerdem möchte ich mich bedanken bei Becci, für deinen Einsatz innerhalb und außerhalb der Labore. Auch bei Pinar möchte ich mich für die liebe Unterstützung bei allem Organisatorischen bedanken. Danke auch an Moritz, Helene und Annika, für eure tatkräftige Unterstützung und die Zusammenarbeit während euren Bachelorarbeiten. Bei Prof. Barner-Kowollik und dem CBK Masse Team möchte ich mich für den Zugang zum SEC-ESI-MS Equipment bedanken.

I would like to thank Mats Johansson for giving me the opportunity to come to KTH and work with the Ytgruppen. Thanks to the whole group for making me feel very welcome, for the nice and enjoyable working atmosphere and for all your support, which I truly appreciated. Thank you, Karin, Eva, Linda, Michael, Per-Olof, Haris, Samer, Yanmiao, Wissam, Viktor, Heba, Marcus, Tahani, Mads, Arne, Jamie, Sarah, Dan, Calvin, Deniz, Niklas, Tobias, Carmen and Joakim. A very special thanks goes to Rosella, Tijana, Jakob, Lynn, Karen and Ludvig. Thank you for all the great activities during the weekends and the unforgettable time we spend together. I am beyond grateful for all the shared experiences, and I hope our friendship will continue.

Bei meinen Freunden außerhalb des Labors, insbesondere Leonie und Hannah, möchte ich mich für die großartige Freundschaft und unsere gemeinsamen Unternehmungen bedanken.

Zuletzt gilt mein größter Dank meiner Familie, die mir stets Rückhalt gibt und mich unendlich unterstützt und stärkt.